Universidade de Aveiro Departamento de Química
2014

Carla Maria Dias Marques de Oliveira

Vias de degradação oxidativa de vinho

Pathways of oxidative degradation of wine

Universidade de Aveiro Departamento de Química
2014

Carla Maria Dias Marques de Oliveira

Vias de degradação oxidativa de vinho

Pathways of oxidative degradation of wine

Tese apresentada à Universidade de Aveiro para cumprimento dos requisitos necessários à obtenção do grau de Doutor em Química, realizada sob a orientação científica do Doutor Artur Manuel Soares da Silva, professor catedrático do Departamento de Química da Universidade de Aveiro e com a coorientação do Doutor António César da Silva Ferreira, professor auxiliar da Escola Superior de Biotecnologia da Universidade Católica Portuguesa do Porto.

Apoio financeiro do POCTI no âmbito do III Quadro Comunitário de Apoio.

Apoio financeiro da FCT e do FSE no âmbito do III Quadro Comunitário de Apoio.

POCTI
Programa Operacional
Ciência Tecnologia Inovação
MINISTÉRIO DA CIÊNCIA E DO ENSINO SUPERIOR

FCT
Fundação para a Ciência e a Tecnologia
MINISTÉRIO DA EDUCAÇÃO E CIÊNCIA

Dedico este trabalho à minha família pelo incansável apoio.

o júri

Presidente

Doutor João Manuel Nunes Torrão, Professor Catedrático da Universidade de Aveiro.

Vogais

Doutor Jorge Manuel Rodrigues Ricardo da Silva, Professor Catedrático do Instituto Superior de Agronomia da Universidade de Lisboa.

Doutor Victor Manuel Pereira Freitas, Professor Catedrático da Faculdade de Ciências da Universidade do Porto.

Doutor Artur Manuel Soares da Silva, Professor Catedrático da Universidade de Aveiro. (Orientador)

Doutora Maria Paula do Amaral Alegria Guedes de Pinho, Investigadora Auxiliar da Faculdade de Farmácia da Universidade do Porto.

Doutor José Sousa Câmara, Professor Auxiliar da Universidade da Madeira.

Doutor António César da Silva Ferreira, Professor Auxiliar Convidado da Escola Superior de Biotecnologia da Universidade Católica Portuguesa. (Coorientador)

Doutor António de Sousa Barros, Investigador Auxiliar da Universidade de Aveiro.

agradecimentos

Ao Professor Doutor Artur Silva, orientador desta dissertação, o meu sincero reconhecimento pelos ensinamentos e incentivos que me transmitiu. Agradeço ainda a disponibilidade dispensada ao longo de todo o desenvolvimento deste trabalho.

Ao Doutor António César Ferreira, coorientador desta dissertação, o meu sincero agradecimento pelos ensinamentos, incentivos e pela amizade demonstrada ao longo deste trabalho.

Ao Doutor António Barros, o meu sincero reconhecimento pelos ensinamentos que me transmitiu, e pela disponibilidade dispensada ao longo deste trabalho.

À Universidade de Aveiro e à Escola Superior de Biotecnologia pela disponibilização dos meios necessários à execução experimental deste trabalho.

À Ana Rita Monforte e à Carla Teixeira pelo companheirismo, prontidão e amizade demonstrada ao longo desta dissertação.

Ao Doutor Carlos Lima da Faculdade de Ciências da Universidade do Porto pelo contributo prestado na obtenção dos parâmetros cinéticos.

Um agradecimento especial à minha colega Sónia Santos, pelo contributo prestado na obtenção dos espectros de LC-MS.

Aos meus pais e irmãs. Obrigada pela vossa presença constante, pela vossa preocupação e pelo vosso apoio.

Ao João, pelo teu apoio em todos os momentos.

palavras-chave

Vinho branco; vinho do Porto tinto; degradação; oxidação; Reação de Maillard; compostos odorantes; mecanismos moleculares

resumo

As alterações aromáticas e/ou cromáticas dos vinhos resultam da combinação e interligação de diferentes mecanismos reacionais. Entre estes, o fenómeno de oxidação e a reação de Maillard destacam-se com especial relevância, devido ao elevado impacto na qualidade sensorial dos vinhos e consequentemente no tempo de "vida de prateleira" dos mesmos.

O objetivo desta tese é conseguir uma visão global e interligada das principais vias reacionais relacionadas com a degradação do vinho. A identificação de reações, bem como de mediadores envolvidos nas alterações aromáticas e cromáticas dos vinhos, será avaliada com base em diferentes tipos de deteção.

Este trabalho inclui dois tipos de abordagem: Em primeiro lugar é utilizada uma abordagem "não direcionada", através de voltametria cíclica e deteção por fotodíodos, que permite uma visão ampla do sistema e a anotação de compostos alvo relacionados com a degradação do vinho. Em segundo lugar é utilizada uma abordagem "direcionada", pela qual a identificação e quantificação dos diferentes compostos são realizadas através de diferentes detetores (HPLC-UV/Vis, LC-MS, GC-MS, e FID). Dois padrões de degradação serão usados neste estudo: vinhos gerados por introdução de O_2 e temperatura, e soluções sintéticas para a validação de alguns mecanismos reacionais.

Os resultados demonstram claramente uma interligação de mecanismos de oxidação e escurecimento do vinho a nível molecular. A presença de oxigénio em combinação com a temperatura teve um efeito sinérgico sobre na formação de diversos compostos odorantes. Os resultados deste trabalho poderão ser traduzidos para o ambiente de produção e/ou armazenamento de vinho pela modelação dos compostos analisados. As condições de temperatura e oxigénio poderão ser calculadas e a taxa e a extensão de cada reação poderá ser utilizada na sua modelação.

keywords

White wine; red Port wine; degradation; oxidation; Maillard reaction; key odorant compounds; molecular mechanisms

abstract

The production of color/flavor compounds in wine is the result of different interrelated mechanism reactions. Among these, the oxidation phenomenon and the Maillard reaction stands out with particular relevance due to their large impact on the sensory quality of wines and consequently on the product shelf-life.

The aim of this thesis is to achieve a global vision of wine degradation mechanisms. The identification of mediators' reactions involved in oxidative browning and aromatic degradation will be attempted based on different detectors.

Two approaches are implemented in this work: a "non-target" approach by which relevant analytical tools will be used to merge the information of cyclic voltammetry and Diode-Array (DAD) detectors, allowing a broader overview of the system and the note of interesting compounds, and a "target" approach by which the identification and quantification of the different compounds related to the wine degradation process will be performed using different detectors (HPLC-UV/Vis, LC-MS, GC-MS, and FID). Two different patterns of degradation will be used in this study: wines generated by O_2 and temperature perturbations, and synthetic solutions with relevant wine constituents for mechanisms validation.

Results clearly demonstrate a "convolution" of chemical mechanisms. The presence of oxygen combined with temperature had a synergistic effect on the formation of several key odorant compounds.The results of this work could be translated to the wine-making and wine-storage environment from the modelling of the analysed compounds.

Pathways of oxidative degradation of wine

1. Chapter 1 - Preamble 22
1.1. Scope and motivation 22
1.2. Aim, strategy and outline 24
1.3. References 26
2. Chapter 2 - A review of wine browning and aromatic degradation 28
2.1. Oxidative degradation mechanisms in food and beverages 28
2.2. Phenolic reactions 29
2.2.1. Occurrence of phenolics in wine 29
2.2.2. Phenolic reactions in wine 35
2.2.2.1. Enzymatic degradation 35
2.2.2.2. Non-enzymatic degradation 39
2.3. Maillard reaction and "Strecker degradation" 45
2.3.1. Occurrence of Maillard reactions and "Strecker degradation" in wine 45
2.3.2. Maillard reactions 46
2.3.2.1. Degradation of DFG [N-(1-deoxy-D-fructose-1-yl)glycine] 49
2.3.2.2. Formation of organic acids and parent sugars 51
2.3.2.3. Different formation pathways of "Strecker aldehydes" 53
i. From amino acids through oxidizing agents 54
ii. From amino acids through temperature 55
iii. From amino acids through α-dicarbonyl compounds 55
iv. From direct formation through Amadori compounds 56
v. From amino acids through α-keto acids 58
vi. From amino acids through quinones 59
2.4. Sugar reactions - Caramelization 61
2.4.1. Occurrence of sugars in wine 61
2.4.2. Sugar reactions 61
2.5. Oxygen and ROS in wine 62
2.5.1. Occurrence of oxygen and ROS in wine 62
2.5.2. Oxygen and ROS reactions in wine 63

2.6. Preventing of browning and aromatic degradation in wine: use of antioxidants 67
2.6.1. Sulfur dioxide in wine 67
2.6.2. Ascorbic acid in wine 70
2.7. References 73
3. Chapter 3 - Material and Methods 91
3.1. Wine characterization 91
3.2. Experimental isothermal storage forced aging protocol 93
3.2.1. White wine 93
3.2.2. Red Port wine 94
3.3. Oxygen measurements 94
3.3.1. White wine 94
3.3.2. Red Port wine 95
3.4. Generating of ROS (Reactive Oxygen Species) 95
3.5. Cyclic voltammetry 95
3.5.1. Introduction to electroanalytical methods - cyclic voltammetry 95
3.5.2. Study of glass carbon electrode 96
3.5.3. Effect of dilutions 97
3.5.4. Repeatability of carbon electrode 99
3.6. HPLC with diode array detection (DAD) 100
3.6.1. Screening of low molecular weight phenolic compounds 100
3.6.2. Quantification of 3-deoxyglucosone (3DG) 102
3.7. HPLC with refractive index (RI) detection 105
3.8. HPLC with fluorescence detection 105
3.8.1. Amino acids 105
3.8.2. α-Ketoacids (β-phenylpyruvic acid) 108
3.9. LC-MS: non-volatiles analysis 109
3.10. GC-MS: volatiles analysis 111
3.10.1. Liquid-liquid extraction 112
3.10.2. Solid Phase Micro Extraction (SPME) extraction 114
3.11. GC-FID acetaldehyde analysis 114
3.11.1. Direct injection 114
3.11.2. SPME extraction 114

3.12. Analyses of Cu and Fe 115
3.13. Folin-Ciocalteu (FC) Index 116
3.14. SO_2 determination 116
3.15. pH determination 116
3.16. Multivariate analysis 116
3.17. Chemicals 117
3.18. References 118
4. Chapter 4 - Role of oxygen in wine 120
4.1. Oxygen uptake of white and red Port wines under four different temperatures and two oxygen regimes 120
4.2. Oxygen uptake of white and red Port wines in the presence of a chelating agent cocktail (EDTA + phenanthroline) 123
4.3. Relation between oxygen uptake and phenolic composition of wines 127
4.3.1. Phenolic composition of wines versus oxygen uptake 127
4.3.2. Oxygen uptake of phenolic compounds in wine-model solutions 129
4.4. Quantification of key intermediaries' of oxygen reactions in wine 131
4.4.1. Quantification of sulfur dioxide in white wine 131
4.4.2. Quantification of aldehydes in white and red Port wines 132
4.4.3. Quantification of heterocyclic acetals in white and red Port wines 137
4.5. Influence of iron and copper on sulfur dioxide oxidation and acetaldehyde formation in the presence of gallic acid 139
4.6. Study of quinones reactions with wine nucleophiles in wine-model solutions by cyclic voltammetry 142
4.7. Conclusions 150
4.8. References 152
5. Chapter 5 - Role of phenolics degradation in wine 158
5.1. Introduction to wine phenolics degradation monitoring 158
5.2. Voltammetric analysis of phenolic compounds 159
5.2.1. Effect of phenolic compounds addition in model wine solutions 159
5.2.2. Effect of pH on phenolic compounds voltammetric signals in model wine solutions 162
5.2.3. Voltammetric curve pattern in white and red Port wines 163

5.2.4. Effect of temperature on voltammetric signals in white and red Port wines. 166
5.2.5. Effect of oxygen on voltammetric signals in white and red Port wines 168
5.2.6. Correlation between phenolic composition and voltammetric signals in white and red Port wines 170
5.3. Diode-Array Detector (DAD) analysis of phenolic compounds 172
5.3.1. Analysis of particular relevant wavelengths on phenolics composition changes 172
5.3.2. Analysis of the overall array surface of phenolics composition changes 178
5.3.3. Identification of phenolic compounds in white and red Port wines 185
5.3.4. Quantification of relevant phenolic compounds in white and red Port wines 189
5.4. Kinetic modeling of anthocyanins oxidation in Port wines 194
5.5. Conclusions 199
5.6. References 201
6. Chapter 6 - Role of Maillard degradation in wine 208
6.1. Introduction to wine Maillard degradation 208
6.2. Quantification of key intermediaries' of Maillard reaction 208
6.2.1. Quantification of sugars in white and red Port wines 211
6.2.2. Quantification of amino acids in white and red Port wines 212
6.2.3. Quantification of 3-deoxyosone (3DG) 219
6.2.3.1. Quantification of 3-deoxyosone (3DG) in white and red Port wines 219
6.2.3.2. Quantification of 3-deoxyosone (3DG) in model wine solutions. Comparison of 3DG formation between glucose and fructose 223
6.3. Quantification of compounds chemically linked with Maillard-like reactions 225
6.3.1. Quantification of furan derivatives 225
6.3.1.1. Quantification of furan derivatives in white and red Port wines 226
6.3.1.2. Quantification of furan derivatives in model wine solutions. Comparison of 2-furfural, 5-(hydroxymethyl)furfural, and 5-methylfurfural formation from glucose, fructose or 3DG 231
6.3.2. Quantification of enolic compounds in white and red Port wines 232
6.3.3. Quantification of "Strecker aldehydes" in white and red Port wines 236
6.4. Approach to "Strecker mechanism" in wine: quinones - key intermediaries' on wine oxidation as "Strecker degradation reagents" 239

6.5. Conclusions 246
6.6. References 248
7. Chapter 7 - Conclusions and future work 258
7.1. Conclusions 258
7.2. Future work 261
8. Appendix 262
8.1. Data 262
8.2. Expressions 266

List of Figures

Figure 1.1. Different interaction reactions of color/flavor compounds. 23
Figure 1.2. Work strategy for the study of the pathways of oxidative browning and aromatic degradation of wine.. 25
Figure 2.1. Flavane structure. 30
Figure 2.2a. Most common flavonoid compounds in wine. 31
Figure 2.2b. Most common non-flavonoid compounds in wine. 32
Figure 2.3. Tyrosinase-catalyzed oxidation of tyrosine results in precursors of melanin. .. 36
Figure 2.4. Laccase-catalyzed oxidation of 1,4-dihydroxybenzene to para-quinone. 36
Figure 2.5. Enzymatic browning process in grape must (Li et al., 2008). 38
Figure 2.6. First and second electron reduction of the 1,2-benzoquinone/catechol system (Danilewicz, 2003). 39
Figure 2.7. Oxidation of (+)-catechin in wine (Danilewicz, 2003). 40
Figure 2.8. Regeneration of oligomers by reaction between two semi-quinones or a quinone and a phenol (Singleton, 1987). 41
Figure 2.9a. Mechanisms of acetaldehyde- and glyoxylic acid-mediated polymerization of flavanols (Fulcrand et al., 2006). 43
Figure 2.9b. Mechanisms of acetaldehyde- and glyoxylic acid-mediated polymerization of flavanols and anthocyanins (Sousa et al., 2010) 44
Figure 2.10. Maillard reaction scheme adapted from Hodge (1953) 47
Figure 2.11. Maillard reaction scheme adapted from Tressl et al., (1995). AMP (Advanced Maillard Products); 1DG or 1DH (1-deoxy-2,3-diketose); 3DG or 3DH (3-deoxyaldolose); 4DG or 4DH (4-deoxy-2,3-diketose). 49
Figure 2.12. Degradation of the Amadori product through enolization pathway. 50
Figure 2.13. Degradation of the Amadori product through retro-aldol pathway. Adapted from Martins et al., 2003a. 51
Figure 2.14. Organic acids formation and parent sugars from primary thermal degradation products. Adapted from Ginz et al., 2000. 52
Figure 2.15. Comparison of “Strecker degradation” and Amadori rearrangement (Yaylayan, 2003). 54

Figure 2.16. Formation of “Strecker aldehydes” from oxidative decarboxylation of amino acids. 54
Figure 2.17. Formation of “Strecker aldehydes” from thermal decarbonylation of amino acids. 55
Figure 2.18. Formation of “Strecker aldehydes” from α-dicarbonyl assisted oxidative decarboxylation of amino acids. 56
Figure 2.19. Formation of Strecker aldehyde directly from Amadori rearrangement product. Pathway A proposed by Cremer and others (2000). 56
Figure 2.20. Formation of Strecker aldehyde directly from Amadori rearrangement product. Pathway B proposed by Hofmann and Schieberle (2000). 57
Figure 2.21. Formation of Strecker acids from Strecker degradation. Adapted from Hofmann et al. (2000). 58
Figure 2.22. Formation of “Strecker aldehydes” through α-keto-acids. 59
Figure 2.23. Proposed Michael addition reaction of *ortho*-quinones with α-amino acids to produce the “Strecker aldehydes”. Adapted from Rizzi, 2006. 60
Figure 2.24. Proposed catalytic action of iron and copper ions in the oxidation of catechols to produce ortho-quinones and hydrogen peroxide (Danilewicz et al., 2008). 63
Figure 2.25. Fenton reaction. 63
Figure 2.26. Oxygen reduction (Waterhouse and Laurie, 2006). 64
Figure 2.27. Reacting of ethanol and L-tartaric acid with hydrogen peroxide in association with ferrous ions (Danilewicz, 2003). 66
Figure 2.28. The proposed degradation of the tartaric acid via Fenton chemistry mechanisms (Clark et al., 2008). 67
Figure 2.29. The scavenging of hydrogen peroxide formed by the oxidation of catechols by SO_2, so preventing oxidation of ethanol by the Fenton reaction (Danilewicz, 2007). 69
Figure 2.30. The interaction of bisulfite with hydrogen peroxide and quinones following catechol oxidation (Danilewicz et al., 2008). 70
Figure 3.1. White wine forced aging protocol. 93
Figure 3.2. Red Port wine forced aging protocol. 94
Figure 3.3. Voltammetric apparatus. 97
Figure 3.4a. Voltammetric curves addressing white wines dilutions. 98

Figure 3.4b. PCA scores plot: First principal component as a function of dilution-fold for white wine. 98
Figure 3.5a. Voltammetric curves addressing red Port wines dilutions.. 99
Figure 3.5b. PCA scores plot: First principal component as a function of dilution-fold for red Port wine..... 99
Figure 3.6. UV quinoxalines chromatograms of white wine (top) and red Port wine (bottom) recorded at 317 nm. 103
Figure 3.7. MS^n fragmentation pathway of the respective quinoxaline of 3DG standard. 104
Figure 3.8. Fluorescence chromatograms of amino acids derivatives recorded at λext. 356 nm and λemis. 445 nm. 107
Figure 3.9. CG-MS chromatograms of white wine (top) and red Port wine (bottom). 112
Figure 4.1. Oxidation mechanism occurring in wines. 120
Figure 4.2. Oxygen depletion of the white wine samples kept at 20, 30, 40 and 50ºC, and for the red Port wine samples kept at 20, 30, 35 and 40ºC, with treatment I. 121
Figure 4.3. Arrhenius plot for both white and red Port wines in treatment I. 122
Figure 4.4. Oxygen depletion of white wine under the addition of a chelating agent cocktail (EDTA + phenanthroline) at two different temperatures (20 and 40ºC). 126
Figure 4.5. Oxygen depletion of red Port wine under the addition of a chelating agent cocktail (EDTA + phenanthroline) at two different temperatures (20 and 40ºC). 126
Figure 4.6. Oxygen depletion of the phenolic compounds: catechin, para-coumaric acid, gallic acid, caffeic acid, syringic acid, and ferulic acid. 130
Figure 4.7. Free sulfur dioxide of the samples kept at 20, 30, 40 and 50ºC, with both oxygen treatments: treatment I and treatment II (N=2). 132
Figure 4.8. Bound sulfur dioxide of the samples kept at 20, 30, 40 and 50ºC, with both oxygen treatments: treatment I and treatment II (N=2). 132
Figure 4.9. Evolution of acetaldehyde, during the white wine forced aging protocol, under respectively no oxygen addition (treatment I) and oxygen addition (treatment II). 134
Figure 4.10. Evolution of acetaldehyde, during the red Port wine forced aging protocol, under respectively no oxygen addition (treatment I) and oxygen addition (treatment II). 135
Figure 4.11. Evolution of benzaldehyde, during the white wine forced aging protocol, under respectively no oxygen addition (treatment I) and oxygen addition (treatment II). 135

Figure 4.12. Evolution of benzaldehyde, during the red Port wine forced aging protocol, under respectively no oxygen addition (treatment I) and oxygen addition (treatment II). 135
Figure 4.13. Acetalization of acetaldehyde (ethanal) in wine. 138
Figure 4.14. Formation of the heterocyclic acetals for the white wine forced aging protocols, at respectively 20ºC and 40ºC. (i) *cis*-5-hydroxy-2-methyl-1,3-dioxane; (ii) *trans*-5-hydroxy-2-methyl-1,3-dioxane; (iii) *cis*-4-hydroxymethyl-2-methyl-1,3-dioxolane; (iv) *trans*-4-hydroxymethyl-2-methyl-1,3-dioxolane; I - no oxygen addition; II - oxygen addition. 139
Figure 4.15. Formation of the heterocyclic acetals for the red Port wine forced aging protocol, at respectively 20ºC and 40ºC. (i) *cis*-5-hydroxy-2-methyl-1,3-dioxane; (ii) *trans*-5-hydroxy-2-methyl-1,3-dioxane; (iii) *cis*-4-hydroxymethyl-2-methyl-1,3-dioxolane; (iv) *trans*-4-hydroxymethyl-2-methyl-1,3-dioxolane; I - no oxygen addition; II - oxygen addition. 139
Figure 4.16. Sulfur dioxide oxidation in a wine-model system with gallic acid, sulfur dioxide and transition metal ions (N=2). 141
Figure 4.17. Acetaldehyde formation in a wine-model system with gallic acid, sulfur dioxide and transition metal ions (N=2). 142
Figure 4.18. Structures of thiol derivatives present in wines. 144
Figure 4.19. Cyclic voltammograms taken at a 3 mm glassy carbon electrode at 100 mV/s of a): 0.6 mM gallic acid in the absence (blue curve) and in the presence of (black curve) of 2.4 mM Phe, and in the presence of (red curve) of 2.4 mM Met; b): 0.6 mM caffeic acid in the absence (blue curve) and in the presence of (black curve) of 2.4 mM Phe, and in the presence of (red curve) of 2.4 mM Met; and c): 0.6 mM (+)-catechin in the absence (blue curve) and in the presence of (black curve) of 2.4 mM Phe, and in the presence of (red curve) of 2.4 mM Met. 145
Figure 4.20. Cyclic voltammograms taken at a 3 mm glassy carbon electrode at 100 mV/s of a): 0.6 mM gallic acid in the absence (blue curve) and in the presence of (black curve) of 2.4 mM 2FMT, in the presence of (red curve) of 2.4 mM 3SH, and in the presence of (green curve) of 2.4 mM 4MSP; b): 0.6 mM caffeic acid in the absence (blue curve) and in the presence of (black curve) of 2.4 mM 2FMT, in the presence of (red curve) of 2.4 mM 3SH, and in the presence of (green curve) of 2.4 mM 4MSP; and c): 0.6 mM (+)-catechin in the absence (blue curve) and in the presence of (black curve) of 2.4 mM 2FMT, in the

presence of (red curve) of 2.4 mM 3SH, and in the presence of (green curve) of 2.4 mM 4MSP. 145
Figure 4.21. Cyclic voltammograms taken at a 3 mm glassy carbon electrode at 100 mV/s of a): 0.6 mM gallic acid in the absence (blue curve) and in the presence of (black curve) of 2.4 mM AA, and in the presence of (red curve) of 2.4 mM SO_2; b): 0.6 mM caffeic acid in the absence (blue curve) and in the presence of (black curve) of 2.4 mM AA, and in the presence of (red curve) of 2.4 mM SO_2; and c): 0.6 mM (+)-catechin in the absence (blue curve) and in the presence of (black curve) of 2.4 mM AA, and in the presence of (red curve) of 2.4 mM SO_2. 146
Figure 5.1. Oxidation curves of phenolics combinations (Table 5.1 codes) in a model wine solution. 161
Figure 5.2. Relationship between PC1 scores and phenolics concentration. 161
Figure 5.3. Cyclic voltammetric curves for white wine samples kept at 20 and 50ºC, for treatment I and II, during the 42 days of storage. Samples were used undiluted. 165
Figure 5.4. Cyclic voltammetric curves for red Port wine samples kept at 20 and 40ºC, for treatment I and II, during the 63 days of storage. Samples were used diluted 20x. 165
Figure 5.5. Scores scatter plot (PC1 vs PC2) of white wine voltammetric oxidation signals for oxygen treatment I (no supplemented oxygen addition) and corresponding PC1 loadings. Components 1 and 2 account for 100% of the total variance. 166
Figure 5.6. Scores scatter plot (PC1 vs PC2) of white wine voltammetric oxidation signals for oxygen treatment II (oxygen addition every sampling point) and corresponding PC1 loadings. Components 1 and 2 account for 99% of the total variance. 167
Figure 5.7. Scores scatter plot (PC1 vs PC2) of red Port wine voltammetric oxidation signals for oxygen treatment I (no supplemented oxygen addition) and corresponding PC1 loadings. Components 1 and 2 account for 94% of the total variance. 167
Figure 5.8. Scores scatter plot (PC1 vs PC2) of red Port wine voltammetric oxidation signals for oxygen treatment II (oxygen addition every sampling point) and corresponding PC1 loadings. Components 1 and 2 account for 95% of the total variance. 168
Figure 5.9. Relationship between white wine voltammetric oxidation signals and the consumed oxygen during the 42 days of storage. RMSE = 2.32 mg/L (LVs=5). 169
Figure 5.10. Relationship between red Port wine voltammetric oxidation signals and the consumed oxygen during the 63 days of storage. RMSE = 4.53 mg/L (LVs=5). 169

Figure 5.11. Representation of current intensities at the two anodic peak potentials Ep,a (0.45 and 0.85 V) versus the total phenolic content evaluated by the FC index. 170
Figure 5.12. Representation of current intensities at the tree anodic peak potentials: a) Ep,a (0.55 V); and b) (0.35 and 0.75 V) versus the total phenolic content evaluated by the FC index. 171
Figure 5.13. Array surface interpretation of white wine samples kept at 20 and 50ºC, for treatment I, during the 42 days of storage. 173
Figure 5.14. Array surface interpretation of white wine samples kept at 20 and 50ºC, for treatment II, during the 42 days of storage. 173
Figure 5.15. Array surface interpretation of red Port wine samples kept at 20 and 40ºC, for treatment I, during the 63 days of storage. 174
Figure 5.16. Array surface interpretation of red Port wine samples kept at 20 and 40ºC, for treatment II, during the 63 days of storage. 174
Figure 5.17. Chromatogram of white wines, P1_20ºC and P6_50ºC_O_2 at 280 nm. 175
Figure 5.18. Chromatogram of white wines, P1_20ºC and P6_50ºC_O_2 at 320 nm. 176
Figure 5.19. Chromatogram of red Port wines, P1_20ºC and P9_40ºC_O_2 at 280 nm. 176
Figure 5.20. Chromatogram of red Port wines, P1_20ºC and P9_40ºC_O_2 at 320 nm. 177
Figure 5.21. Chromatogram of red Port wines, P1_20ºC and P9_40ºC_O_2 at 528 nm. 177
Figure 5.22. Scores scatter scatter plot (PC1 vs PC2) of the overall array surface (212 at 600 nm) with different applied temperature regimes (20, 30, 40 and 50ºC) during the degradation process (P1, P2, P3, P4, P5 and P6) of white wine. Components 1 and 2 account for 89% of the total variance. 180
Figure 5.23. White wine surf loadings of plot 1 (PC 1) combining HPLC chromatographic data and the correspondent absorption (DAD) to each wavelength scan. 180
Figure 5.24. Scores scatter plot (PC1 vs PC2) of phenolics content of the overall array surface (212 at 600 nm) with different applied temperature regimes (20, 30, 35 and 40ºC) during the oxidation process (P2, P4 and P9) of red Port wine. Components 1 and 2 account for 96% of the total variance. 182
Figure 5.25. Red Port wine surf loadings of plot 1 (PC 1) combining HPLC chromatographic data and the correspondent absorption (DAD) to each wavelength scan. 182

Figure 5.26. Phenolics formation or depletion during the forced aging protocols in white wines. I - no oxygen addition; II - oxygen addition. Data in appendix of this thesis. 189
Figure 5.27. Phenolics formation or depletion during the forced aging protocols in red Port wines. I - no oxygen addition; II - oxygen addition. Data in appendix of this thesis. 190
Figure 5.28. Arrhenius plot for delphinidin-3-glucoside (Dp-3G) and petunidin-3-glucoside (Pt-3G) depletion 197
Figure 5.29. Arrhenius plot for peonidin-3-glucoside (Pn-3G) and malvidin-3-glucoside (Mv-3G) depletion 197
Figure 5.30. Arrhenius plot for malvidin-3-*O*-acetylglucoside (Mv-3acG) and malvidin-3-*O*-coumaroylglucoside (Mv-3cmG) depletion 198
Figure 6.1. A compressive scheme of degradation of the Amadori product from a sugar (aldose) and an amino compound. 210
Figure 6.2. Representative structures of Maillard derivative compounds from deoxyosones (i: from 1,2-enolization.; ii and iii: from 2,3-enolization), and iv: other pathways. 211
Figure 6.3. Amino acids content of both white and red Port untreated wines (P0). 214
Figure 6.4. Amino acids depletion during the forced aging protocols in white wines (mg/L/day). I - no oxygen addition; II - oxygen addition. Data in appendix. 214
Figure 6.5. Amino acids depletion during the forced aging protocols in red Port wines (mg/L/day). I - no oxygen addition; II - oxygen addition. Data in appendix. 215
Figure 6.6. Evolution of glutamic acid, during the white wine forced aging protocol, under respectively no oxygen addition (treatment I) and oxygen addition (treatment II). 215
Figure 6.7. Evolution of glutamic acid, during the Port wine forced aging protocol, under respectively no oxygen addition (treatment I) and oxygen addition (treatment II). 216
Figure 6.8. Proposed mechanism for degradation of glutamic acid in wines. Adapted from Ferreia, 1997. 217
Figure 6.9. Methionine oxidation to the sulfoxide and then to the sulfone. 218
Figure 6.10. Evolution of 3-deoxyosone (3DG) for oxygen treatments I and II, at 40ºC, for respectively, white and red Port wines forced aging protocols (N = 2). 221
Figure 6.11. Compressive scheme of 3DG formation and depletion in wine. 221
Figure 6.12. Amino acids content of the applied wine-model system. 224
Figure 6.13. 3DG quantification in a wine-model system. 224

Figure 6.14. Furan derivatives formation or depletion (furfuryl alcohol) during the forced aging protocol of white wines. I - no oxygen addition; II - oxygen addition. Data in appendix. 229
Figure 6.15. Furan derivatives formation or depletion (furfuryl alcohol) during the forced aging protocol of red Port wines. I - no oxygen addition; II - oxygen addition. Data in appendix. 229
Figure 6.16. Evolution of 2-furfural, during the white wine forced aging protocol, under respectively no oxygen addition (treatment I) and oxygen addition (treatment II). 230
Figure 6.17. Evolution of 2-furfural, during the red Port wine forced aging protocol, under respectively no oxygen addition (treatment I) and oxygen addition (treatment II). 230
Figure 6.18. Evolution of 5-(hydroxymethyl)furfural, during the white wine forced aging protocol, under respectively no oxygen addition (treatment I) and oxygen addition (treatment II). 230
Figure 6.19. Evolution of 5-(hydroxymethyl)furfural, during the red Port wine forced aging protocol, under respectively no oxygen addition (treatment I) and oxygen addition (treatment II). 231
Figure 6.20. 2-Furfural, HMF, and 5-methylfurfural quantification in a wine-model system (N=2). Data in appendix. 232
Figure 6.21. Evolution of sotolon [3-hydroxy-4,5-dimethylfuran-2(5*H*)-one], during the red Port wine forced aging protocol, under respectively no oxygen addition (treatment I) and oxygen addition (treatment II). 234
Figure 6.22. Evolution of maltol (3-hydroxy-2-methyl-4*H*-pyran-4-one), during the red Port wine forced aging protocol, under respectively no oxygen addition (treatment I) and oxygen addition (treatment II). 235
Figure 6.23. Evolution of 5-hydroxymaltol (3,5-dihydroxy-2-methylpyran-4-one; DMP), during the red Port wine forced aging protocol, under respectively no oxygen addition (treatment I) and oxygen addition (treatment II). 235
Figure 6.24. Evolution of pantolactone [4,5-dihydro-3-hydroxy-4,4-dimethyl-2(3*H*)-furanone], during the white wine forced aging protocol, under respectively no oxygen addition (treatment I) and oxygen addition (treatment II). 236

Figure 6.25. Evolution of pantolactone [4,5-dihydro-3-hydroxy-4,4-dimethyl-2(3*H*)-furanone], during the red Port wine forced aging protocol, under respectively no oxygen addition (treatment I) and oxygen addition (treatment II). 236
Figure 6.26. Evolution of phenylacetaldehyde, during the white wine forced aging protocol, under respectively no oxygen addition (treatment I) and oxygen addition (treatment II). 238
Figure 6.27. Evolution of phenylacetaldehyde, during the red Port wine forced aging protocol, under respectively no oxygen addition (treatment I) and oxygen addition (treatment II). 238
Figure 6.28. Evolution of methional, during the white wine forced aging protocol, under respectively no oxygen addition (treatment I) and oxygen addition (treatment II). 239
Figure 6.29. Wine-model system used for the study of "Strecker aldehydes". 241
Figure 6.30. Evolution of phenylacetaldehyde and methional under the wine-model system used for the study of "Strecker aldehydes" (N=2). 241
Figure 6.31. Formation of Strecker aldehydes from *ortho*-quinones assisted decarboxylation/deamination of amino acids. 244
Figure 6.32. MS/MS fragments of phenylpyruvic acid. 244
Figure 6.33a. MS/MS fragments occurred for gallic acid quionone products with phenylalanine. 245
Figure 6.33b. MS/MS fragments occurred for caffeic acid quionone products with phenylalanine. 245
Figure 7.1. Pathways of different interaction reactions of color/flavor compounds. 258

List of Tables

Table 2.1. Phenolic compounds in both red and white wine (De Beer et al., 2002). 34
Table 2.2. Phenolic compounds in both red and white wine with aging (Waterhouse, 2002). 35
Table 3.1. Phenolic compounds present in both white and red Port wines (N=2). 92
Table 3.2. Analytical parameters for the quantification of low molecular weight phenolic compounds for white wines. RSD (%) = 2.5 (N=8). 101

Table 3.3. Analytical parameters for the quantification of low molecular weight phenolic compounds for red Port wines. RSD (%) = 2.5 (N=8). 102
Table 3.4. Analytical parameters of the working method for the quantification of 3DG. 104
Table 3.5. Analytical parameters for the quantification of glucose, fructose, and ethanol (N=8). 105
Table 3.6. Analytical parameters for the quantification of amino acids (N=8). 108
Table 3.7. LC-MS data of phenolic compounds. 110
Table 3.8. Analytical parameters for the quantification of phenolic compounds by LC-MS (N=8). 111
Table 3.9. Analytical parameters for the quantification of volatile compounds by GC-MS (N=8). 113
Table 3.10. Analytical parameters of the working method for the quantification of acetaldehyde. 115
Table 4.1. Kinetic parameters of oxygen depletion in wine, given by Arrhenius equation. 122
Table 4.2. Overall consumed oxygen in moles per liter at the different storage temperatures. 123
Table 4.3. Uptake of dissolved oxygen in moles of O_2 per liter per second (mol/L·s), under saturated oxygen conditions. 127
Table 4.4. Relationship between gallic acid and wines oxygen consumption. 131
Table 4.5. Vanillin and syringaldehyde formation rates during the forced aging protocols in both white and red Port wines. 136
Table 4.6. Evaluation of the anodic and cathodic peak potentials at pH 3.6, of the studied polyphenols [Ep,a - anodic peak potential (V); Ep,c - cathodic peak potential (V)], as well the anodic and cathodic peak currents at pH 3.6 [Ip,a - anodic peak current (A); Ip,c - cathodic peak current (A)] during the cyclic voltammetry experiment. 147
Table 5.1. Combinations of phenolic compounds concentrations normally present in wines. 160
Table 5.2. Anodic and cathodic peak potentials at pH 3.2 and pH 3.6, of the studied polyphenols. 162
Table 5.3. Anodic and cathodic peak currents at pH 3.2 and pH 3.6, of the studied polyphenols. 163

Table 5.4. White wine retention time's identification based on loadings values of PC 1. 181
Table 5.5. Red Port wine retention time's identification based on loadings values of PC 1. 183
Table 5.6. White wine compounds identification based on DAD and/or LC-MS. 186
Table 5.7. Red Port wine compounds identification based on DAD and/or LC-MS. 187
Table 5.8a. Evolution of anthocyanins under treatment I (no oxygen addition). 191
Table 5.8b. Evolution of anthocyanins under treatment II (oxygen addition). 191
Table 5.9. Kinetic parameters of anthocyanins hydrolysis reaction in Port wine.. 198
Table 6.1. Sugar content of the analysed wines. 212
Table 6.2. 3DG quantification in white wines from different vintages (between 3 and 18 years old) (N= 2). 222
Table 6.3. 3DG quantification in red Port wines from different vintages (between 2 and 78 years old) (N=2). 222
Table 6.4. Analysed sets used for the 2-furfural, HMF, and 5-methylfurfural quantification in a wine-model system. 232
Table 6.5. Mass-selected precursor ions (negative mode) of the proposed Michael addition reaction products of *ortho*-quinones with phenylalanine (adapted from Rizzi, 2006). 243
Table 6.6. Mass-selected precursor ions (negative mode) of the proposed Strecker aldehyde reaction products formation through assisted *ortho*-quinones (adapted from Strecker, 1862). 244

List of abbreviations

1DG - 1-deoxyosone

1DH - 1-deoxy-2,3-diketose

2FMT - furan-2-ylmethanethiol

3DG - 3-deoxyosone

3DH - 3-deoxyaldolose

3SH - 3-sulfanylhexan-1-ol

4DG - 4-deoxyosone

4DH - 4-deoxy-2,3-diketose

4-MeC - 4-methylcatechol

4MSP - 4-methyl-4-sulfanylpentan-2-one

AMP - advanced Maillard products

AR - Amadori rearrangement

BA - benzenesulfinic acid

HHMFone - 4-hydroxy-2-(hydroxymethyl)-5-methylfuran-3(*2H*)-one

HMF - 5-(hydroxymethyl)furfural

DFG - *N*-(1-deoxy-D-fructose-1-yl)-glycine

DDMP - 2,3-dihydro-3,5-dihydroxy-6-methyl-*4H*-pyran-4-one

DMHF - furaneol

DMP - 5-hydroxymaltol

TFA - trifluoroacetic acid

TMP - tetramethylpyrazine

NC-IUBMB - *Nomenclature Committee of the International Union of Biochemistry and Molecular Biology*

Dp-3G - delphinidin-3-glucoside

Mv-3acG - malvidin-3-*O*-acetylglucoside

Mv-3cmG - malvidin-3-*O*-coumaroylglucoside

Mv-3G - malvidin-3-glucoside

Pn-3G - peonidin-3-glucoside

Pt-3G - petunidin-3-glucoside

GRP - grape reaction product

GSH - glutathione

Asp - aspartic acid

Glu - glutamic acid

Cys - cystein

Asn - asparagine

Ser - serine

Gln - glutamine

Thr - threonine

Arg - arginine

Ala -alanine

Tyr - tyrosine

Val - valine

Met - methionine

Phe - phenylalanine

Ile - isoleucine

Leu - leucine

OPA - *ortho*-phthalaldehyde

IDA - iminodiacetic acid

API - atmospheric pressure ionization

ESI - electrospray ionization

LCD - liquid crystal display

EI - electron impact

ESR - electron spin resonance

FC - Folin-Ciocalteu

GAE - gallic acid equivalents

EDTA - ethylenediaminetetraacetic acid

RID - rich information detector

DAD - diode array detector

HPLC - high performance liquide chromatography

GC - gas chromatography

FID - flame ionization detector

PDA - photodiode array

C18 - octadecyl carbon chain bonded silica

USA - United States of America

UV - ultraviolet

RI - refractive index

MS - mass spectrometry

GC-MS - gas chromatography coupled with mass spectrometry

LC-MS - liquid chromatography coupled with mass spectrometry

PTFE - polytetrafluoroethylene

PVPP - polyvinyl polypyrrolidone

FDA - food and drug administration

DVB/CAR/PDMS - divinylbenzene/carboxen/polydimethylsiloxane

SPME - solid phase micro extraction

SD - Strecker degradation

NMR - nuclear magnetic resonance

MS^2 - tandem mass spectrometry

MS^n - multi-stage mass spectrometry

CID - collision-induced dissociation

MVA - multivariate analysis

LOD - limit of detection

LOQ - limit of quantification

LVs - levels

R^2 - coefficient of determination

R - coefficient of correlation

RSD - coefficient of variation

^{13}C-labeled - labeled carbon atom

2D - bidimensional

RMSE - root mean square error

PSt3 - planar oxygen sensitive spots

PCA - principle component analysis

PLSR - partial least squares regression

PC1 - first principal component

PC2 - second principal component

LOOH - lipid peroxide

$RO^{\bullet}$ - alkoxyl radical

$ROO^{\bullet}$ - peroxyl rdical

ROS - reactive oxygen species

POD - peroxidases

PPO - polyphenoloxidases

Q - quinone

Q4MeC - 4-methyl-1,2-benzoquinone

$Q^{\bullet-}$ - semi-quinone radical

$QH^{\bullet}$ - protonated specie for the semi-quinone radical

Q^{2-} - dianion of quinone

QH_2 - protonated specie for the dianion of quinone

Ep,a - anodic peak potential

Ep,c - cathodic peak potential

Emid - potential midway between Ep,a and Ep,c peak potentials

ΔEp - peak potential separation

Sa - anodic peak area

Sc - cathodic peak area

Ip,a - anodic peak current

Ip,c - cathodic peak current

pK - dissociation constants

pKa - acid dissociation constant

m/z - mass to charge ratio (mass spectrometry)

M - molar

λemis. - maximun emission wavelength

λext. - maximum excitation wavelength

n - number of determinations

i - number of samples

j - number of variables of each analysis

k - number of principal components

l - number of scans

m - number of absorption values

S - vector

Q - matrix

T - scores matrix

P - loadings matrix

E.C. 1 - oxidoreductases

E.C. 1.10.3 - oxidoreductases that use oxygen as electron acceptor

E.C. 1.10.3.1 - tyrosinase or catechol oxidase

E.C. 1.10.3.2 - laccase

E.C. 1.10.3.4 - *ortho*-aminophenol oxidase

E.C. 1.11.1 - peroxidases

E.C. 1.11.1.13 - manganese peroxidase

E.C. 1.11.1.14 - diarylpropane peroxidase

E.C. 1.11.1.7 - horseradish

E.C. 1.14 - monooxygenases

E.C. 1.14.18.1 - monophenol monooxygenase

1. Chapter 1 - Preamble

1.1. Scope and motivation

The main non-enzymatic reactions occurring during wines processing or storage are the Maillard reaction and oxidation or reactions with reactive oxygen species (ROS), leading to browning and aroma/flavor formation.

Oxygen management is one of the most challenging tasks in wine making. Starting from the initial juice to the maturation process, several critical steps, relating to the oxygen exposure, can be found, where the quantities of oxygen supplied will have a major impact on the organoleptic characteristics of the finished product.

It has been demonstrated that some key odorants play a critical role in the perceived oxidized character of wines (Silva Ferreira et al., 2003a, Silva Ferreira et al., 2003b). Nevertheless, the mechanisms for these key odorants formation are not fully understood; only that temperature and mainly oxygen have a synergistic impact on their formation (Silva Ferreira et al., 2002).

Molecular oxygen (triplet state) needs to be activated to singlet state to become reactive and then be reduced to water taking electrons in a stepwise manner. In wines, this process requires reducing species with catechol-like structure and, most important, the presence of transition metal ions, such as iron or copper, which will act as electron pumps during the entire mechanism. The reactivity of reactive oxygen species (ROS) increases dramatically, from molecular oxygen (singlet state), hydroperoxyl radical ($HO_2^{\bullet}$), hydrogen peroxide (H_2O_2), to the most lethal (problematic) radical form, the hydroxyl radical ($HO^{\bullet}$). This species, produced by the Fenton reaction, reacts in a non-selective manner with all organic molecules present in the matrix. According to the respective reduction potentials and concentrations, several wine constituents, including antioxidants, will be consumed at different stages of the global oxidation process.

Reactions of reactive oxygen species (ROS) with phenolics, alcohols, organic acids, even sugars, can interact with Maillard reaction ("Strecker degradation"). Figure 1.1 represents hypothetic interaction reactions of color/flavor compounds generation. In addition, "Strecker degradation" has been suggested to play a switching role in directing the Maillard reaction towards aromagenic rather than chromogenic pathways (Yaylayan,

2003). However, "Strecker degradation" of amino acids is not only produced by α-dicarbonyl or α-hydroxycarbonyl compounds formed by carbohydrate thermal degradation (Maillard reaction) (Granvogl et al., 2012). Carbonyl compounds are produced after wine alcoholic and malolatic fermentation, but can also be formed by the oxidation reaction of the hydroxyl radical ($HO^{\bullet}$) with organic acids or lipid-derived degradation (Hidalgo and Zamora, 2004). In the same way, the quinones produced by phenolics oxidation (Rizzi, 2006, Rizzi, 2008) have also been described as significant producers of "Strecker aldehydes", although this route has not been yet fully understood. All these assignments suggest that the production of color/flavor compounds may be the result of different interrelated reactions. For these reasons, the mechanisms suggested for key color/flavor formation through temperature and oxygen must be evaluated.

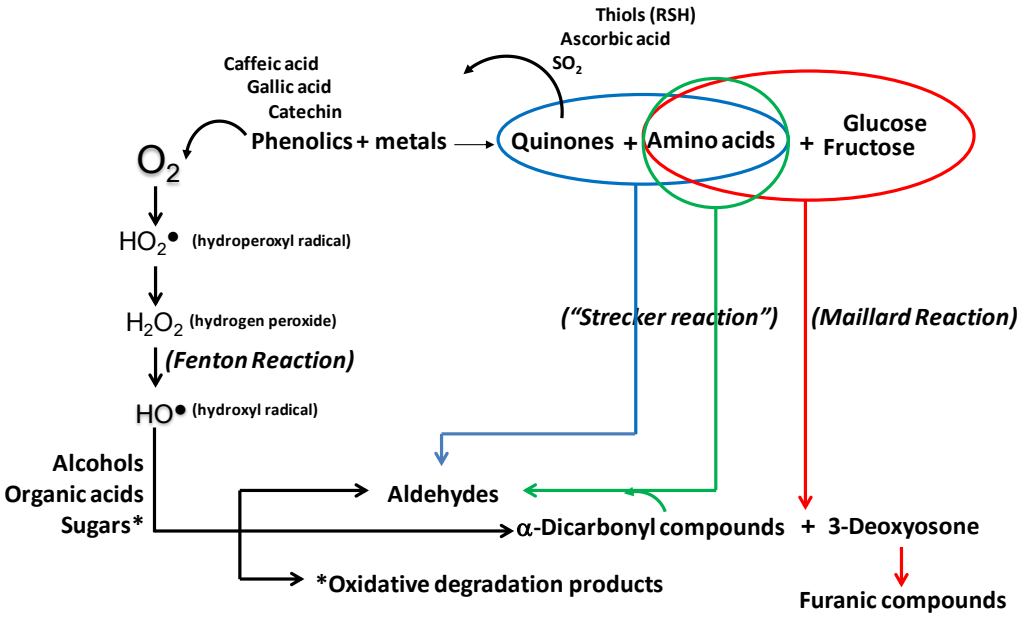

Figure 1.1. Different interaction reactions of color/flavor compounds.

In this thesis two different wines, a *dry white wine* and a *sweet red Port wine* were used for the proposed study. These two wines have different concentrations on the main substrates for the degradation reactions. Port wine is a fortified wine, which involves the addition of natural grape spirit to the fermenting juice. Fermentations are relatively short, about two days, and are intentionally interrupted at a point when approximately half of the grapes natural sugar has been converted into alcohol, resulting in a wine containing about 18-20%

of alcohol, and higher levels of sugars (40 to 130 g/L). In this way, this wine is a sweet wine where sugars are readily available for Maillard reactions. However, dry wine have residual reducing sugars (1 to 3 g/L) that may also participate in these reactions, and therefore can be used for the study. Port wine has also different contents in compounds coming from the fermentative process (amino acids, alcohols, organic acids, etc). Likewise, using different grape varietals, white grapes for the dry white wine and red grapes for the sweet Port wine, originates dissimilar concentrations in phenolic compounds.

1.2. Aim, strategy and outline

The ***aim*** of this thesis is to achieve a new vision of wine oxidative mechanisms. The complexity of the mechanisms involved in oxidative browning and aromatic degradation is not yet fully understood, and the identification of mediators' reactions and their characterization needs to be done. Additionally, with this study we wish to demonstrate an intricate interaction among chemical mechanisms.

For this purpose, we developed a ***strategy*** capable to classify the "*degradation status*" of wines based on different detectors in order to monitoring and characterize the degradation pathways. Figure 1.2 represents the work strategy for the study of the mechanisms of oxidative browning and aromatic degradation of wine.

In order to extract the necessary chemical information to attain our goal, two approaches will be implemented in this work: a "non-target" approach by which relevant analytical tools will be used to merge the information of cyclic voltammetry and Diode-Array (DAD) detectors, allowing a broader overview of the system and the note of interesting compounds, and a "target" approach by which the identification and quantification of the different compounds related to the mechanisms of browning and aromatic degradation process will be performed using different detectors (HPLC-DAD, LC-MS, GC-MS, and FID) (Figure 1.2). Two different patterns of degradation will be used in this study: wines generated by perturbations (O_2 and temperature); and synthetic solutions with relevant wine constituents for mechanisms validation (Figure 1.2).

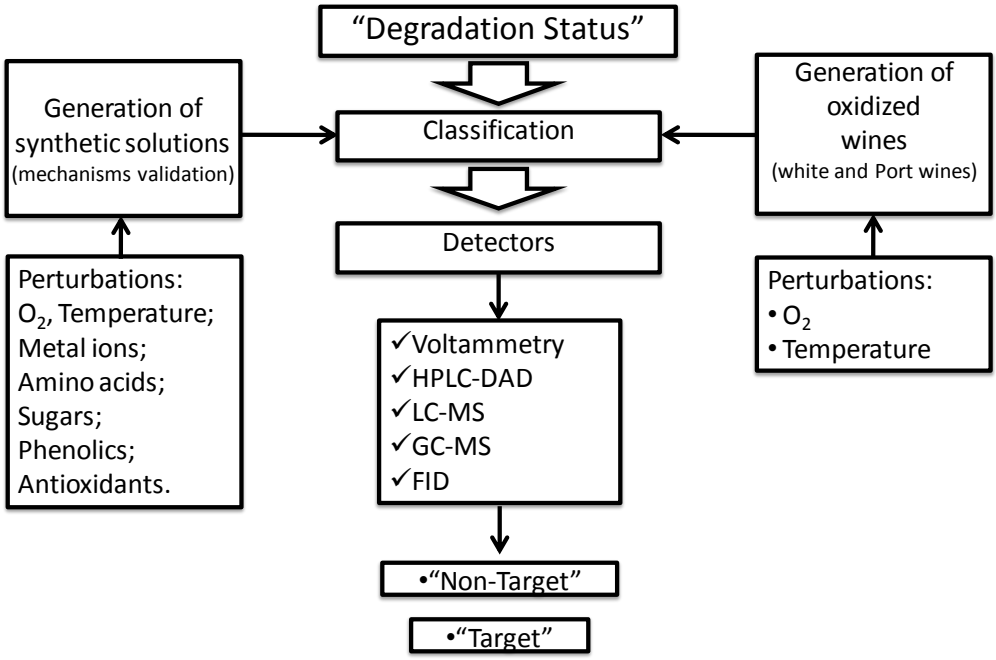

Figure 1.2. Work strategy for the study of the pathways of oxidative browning and aromatic degradation of wine.

This thesis ***outline*** is organized into seven chapters. The first chapter (Introduction) begins with a presentation of the thesis motivation, establishes the aim and briefly describes the strategy outlined.

The second chapter is dedicated to a review of the state of the art of wine browning and aromatic degradation, which include: oxidative degradation mechanisms in food and beverages, phenolic reactions, Maillard reactions, oxygen and ROS reactions in wine, and how to mitigate the browning and aromatic degradation in wine.

The third chapter is the material and methods applied and/or developed in this thesis.

The following tree chapters (4, 5 and 6) are related with the obtained results. In chapter four we study the role of oxygen in wine, by the observation of the oxygen uptake of both white and red Port wines under four different temperatures, two oxygen regimes, and the application of chelating agents. Likewise, the quantification of key intermediaries' of oxygen reactions in wine was assessed. The study of quinones' reactions with wine antioxidants, in wine-model solutions by cyclic voltammetry, was also achieved in this chapter. In chapter five we study the role of phenolics degradation in wine. As this class of compounds is electroactive, cyclic voltammetry was used in order to monitor and classify the degradation process in both "non-target" and "target" approaches. This chapter include

an introduction to wine phenolics degradation monitoring, voltammetric analysis of phenolic compounds, Diode-Array Detector (DAD) analysis of phenolic compounds, and a kinetic modeling of anthocyanins oxidation in Port wines. In chapter six we study the role of Maillard degradation in wine. This chapter include an introduction to wine Maillard degradation, the quantification of key intermediaries' of Maillard reaction, the quantification of compounds chemically linked with Maillard-like reactions, and an approach to "Strecker mechanism" in wine: quinones as key intermediaries' on wine oxidation as "Strecker degradation reagents". Finally, chapter seven reflects the major achievements summary and suggest future approaches for wine analysis.

1.3. References

Granvogl, M., Beksan, E. & Schieberle, P. (2012). New insights into the formation of aroma-active Strecker aldehydes from 3-oxazolines as transient intermediates. *Journal of Agricultural and Food Chemistry, 60,* 6312-6322.

Hidalgo, F. J., & Zamora, R. (2004). Strecker-type degradation produced by the lipid oxidation products 4,5-epoxy-2-alkenals. *Journal of Agricultural and Food Chemistry, 52,* 7126-7131.

Rizzi, G. P. (2006). Formation of strecker aldehydes from polyphenol-derived quinones and α-amino acids in a nonenzymic model system. *Journal of Agricultural and Food Chemistry, 54,* 1893-1897.

Rizzi, G. P. (2008). The strecker degradation of amino acids: Newer avenues for flavor formation. *Food Reviews International, 24,* 416-435.

Silva Ferreira, A. C., Guedes Pinho, P, Rodrigues, P., Hogg, T. (2002). Kinetics of oxidative degradation of wines and how they are effected by selected technological parameters *Journal of Agricultural and Food Chemistry, 50,* 5919-5924.

Silva Ferreira, A. C., Barbe, J. C., Bertrand, A. (2003a). 3-Hydroxy-4,5-dimethyl-2(5H) furanone: a key odorant of the typical aroma of oxidative aged port wine. *Journal of Agricultural and Food Chemistry, 51*, 4356-4363.

Silva Ferreira, A. C., Hogg, T., Guedes de Pinho, P. (2003b). Identification of key-odorants related to the typical aroma of oxidation-spoiled wines. *Journal of Agricultural and Food Chemistry, 51*, 1373-1376.

Yaylayan, V. A. (2003). Recent advances in the chemistry of Strecker degradation and Amadori rearrangement: implications to aroma and colour formation. (Review). *Food Science Technology Research, 9*, 1-6.

2. Chapter 2 - A review of wine browning and aromatic degradation

2.1. Oxidative degradation mechanisms in food and beverages

The main non-enzymatic reactions occurring during food and beverages processing or storage are the degradation of polyphenols, Maillard reaction, sugars caramelization, and oxidation and/or reactions with reactive oxygen species (ROS), leading to browning and aroma/flavor formation. Along with these reactions, degradation of ascorbic acid is also a relevant source of browning and aroma/flavor in food and beverages. All these reactions lead to browning. However, the resulting color and aroma/flavor is not always recognized to be damaging the quality. The degradation of polyphenols, Maillard reaction, and sugars caramelization, in some processed food products like tea, coffee, cocoa, raisins, baked bread or cakes, toasted cereals, cooked meat, and even in some beverages, could be desirable. In fact, compounds coming from Maillard reaction have shown appreciable antioxidant activity. Nevertheless, this last reaction can also induce negative changes in color during storage, as well negative changes in aroma/flavor during processing and storage, along with loss of palatability and digestibility, and related toxicity or mutagenicity. Reactions of oxygen and ROS with food components produce undesirable volatile compounds, damage of essential nutrients, and changes in the functionalities of proteins, lipids and carbohydrates, along with the formation of carcinogen compounds. However, in a small extent, oxygen reactions could also induce some positive color or aroma/flavors improving the complexity of food and beverages.

2.2. Phenolic reactions

Phenolic compounds are responsible for major organoleptic characteristics of plant-derived foods and beverages, particularly color and taste properties. They are also reported to contribute to the health benefits associated with consumption of diets rich in fruits and vegetables or plant-derived beverages (such as tea and wine). Polyphenols are reactive compounds, which can be degraded and polymerized through both enzymatic and non-enzymatic reactions during food and beverage processing and storage. Enzymatic oxidation is ubiquitous in plant-derived foods. The resulting browning is usually damaging the quality, particularly in postharvest storage of fresh fruits or juice, but may be desirable for some processed food products like tea, coffee, cocoa, and raisins (Cheynier, 2005). Chemical reactions occur simultaneously as enzymatic reactions, and progressively become relevant as the enzymatic activity decrease (Cheynier, 2005).

2.2.1. Occurrence of phenolics in wine

Wine polyphenolic substances are usually subdivided into two groups: flavonoids and non-flavonoid compounds. The flavonoids have a common core, the flavane nucleus, consisting of two benzene rings (A and B) linked by an oxygen-containing pyran ring (C) ($C_6C_3C_6$) (Figure 2.1). Differences in the degree of oxidation of the heterocyclic ring (C) and hydroxylation/methoxylation of the three rings results in a large family of structures with essential differences in physicochemical properties and stability. The most common wine flavonoid compounds are flavonols (kaempferol, quercetin, and myricetin), flavan-3-ols (catechin, epicatechin, and tannins), and anthocyanins (cyanidin-3-glucoside, peonidin-3-glucoside, delphinidin-3-glucoside, petunidin-3-glucoside, and malvidin-3-glucoside) (Figure 2.2a). The concentration of flavonoids in wine are strongly affected by the winemaking practices such as pressing and maceration that affect the degree of extraction from skins and especially from seeds which are rich in flavan-3-ol units. Flavan-3-ols are found in the solid parts of the berry (seed, skin and stem) in monomeric, oligomeric, or polymeric forms. The latter two forms are also known as proanthocyanidins or condensed tannins. While seed tannins are oligomers and polymers composed of the monomeric flavan-3-ols (+)-catechin, (-)-epicatechin, and (-)-epicatechin gallate (Prieur et al., 1994)

(Figure 2.2a), skin tannins also contain (-)-epigallocatechin and trace amounts of (+)-gallocatechin and (-)-epigallocatechin gallate (Escribano-Bailón et al., 1995, Souquet et al., 1996) (Figure 2.2a). The seeds contain higher concentrations of monomeric, oligomeric, and polymeric flavan-3-ols than the skins (Sun et al., 1999, De Freitas et al., 2000). Levels of proanthocyanidins or condensed tannins are between 1 g/L and 4 g/L in red wines (Ribéreau-Gayon et al., 2000), while in white wine, levels are in the range of 100 mg/L and highly dependent on pressing techniques (Ribéreau-Gayon et al., 2000). Concerning the sensorial properties of these compounds, monomeric catechins are bitter, while polymers are essentially astringents (Peleg et al., 1999).

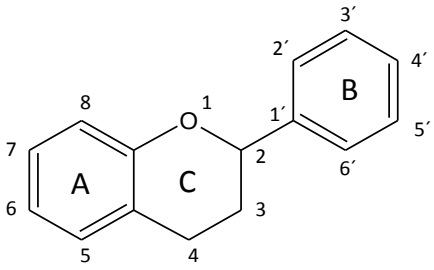

Figure 2.1. Flavane structure.

Non-flavonoid compounds are mainly derivatives of benzoic acid and of cinnamic acid (Figure 2.2b). Another class of non-flavonoids in grape includes the stilbenes and stilbene glycosides, *trans*-resveratrol being the best known example (Figure 2.2b). A different class of non-flavonoids is the hydrolysable tannins. In wine, these compounds are derived from oak and their levels are near 100 mg/L for white wines aged for about 6 months in barrel, while red wines will have levels in the range of 250 mg/L, after aging two or more years (Quinn and Singleton, 1985). Hydrolysable tannins are esters of gallic acid (gallotannins) and ellagic acid (ellagitannins) with glucose or related sugars.

(a) Flavonoids

Flavonols

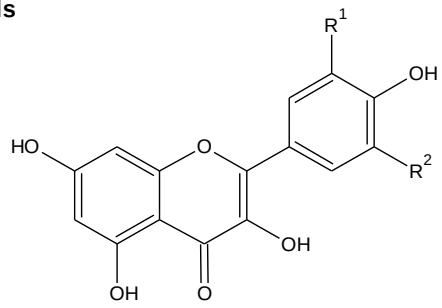

Kaempferol (R^1=R^2=H)
Quercetin (R^1=OH, R^2=H)
Myricetin (R^1=R^2=OH)

Flavan-3-ols

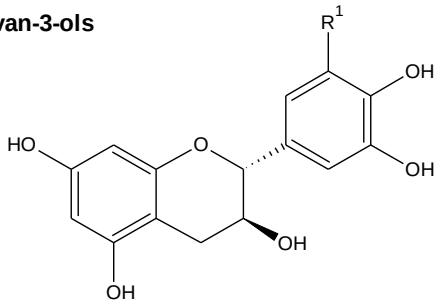

(+)-Catechin (R^1=H)
(+)-Gallocatechin (R^1=OH)

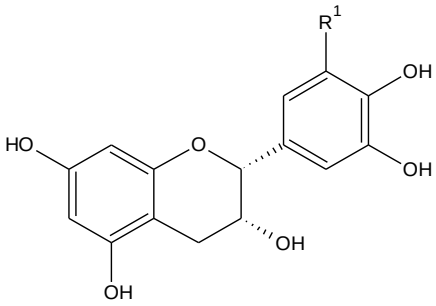

(-)-Epicatechin (R^1=H)
(-)-Epigallocatechin (R^1=OH)

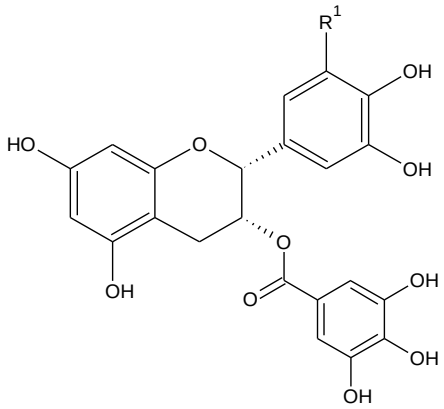

(-)-Epicatechin gallate (R^1=H)
(-)-Epigallocatechin gallate (R^1=OH)

Anthocyanins

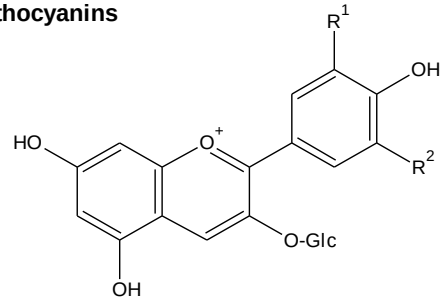

Cyanidin 3-glucoside (R^1=OH, R^2=H)
Peonidin 3-glucoside (R^1=OCH_3, R^2=H)
Delphinidin 3-glucoside (R^1=R^2=OH)
Petunidin 3-glucoside (R^1=OH, R^2=OCH_3)
Malvidin 3-glucoside (R^1=R^2=OCH_3)

Figure 2.2a. Most common flavonoid compounds in wine.

(b) Non - Flavonoids

Derivatives of benzoic and cinnamic acid

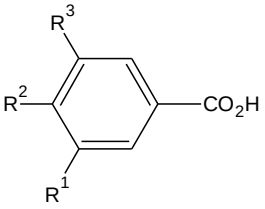

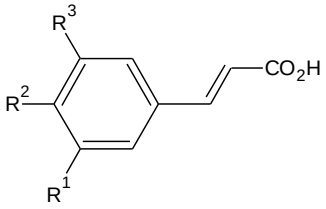

	R^1	R^2	R^3	
Benzoic acid	H	H	H	**Cinnamic acid**
***p*-Hydroxybenzoic acid**	H	OH	H	***p*-Coumaric acid**
Protocatechuic acid	OH	OH	H	**Caffeic acid**
Vanillic acid	OCH_3	OH	H	**Ferulic acid**
Gallic acid	OH	OH	OH	
Syringic acid	OCH_3	OH	OCH_3	**Sinapic acid**

Stilbenes

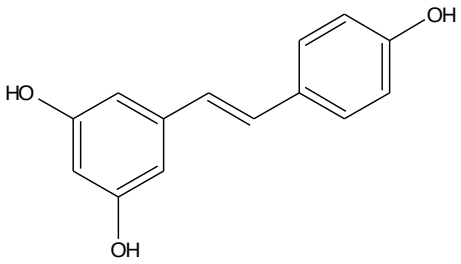

***trans*-Resveratrol**

Volatile Phenols

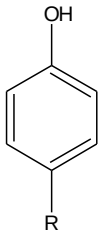

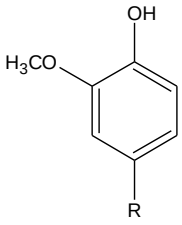

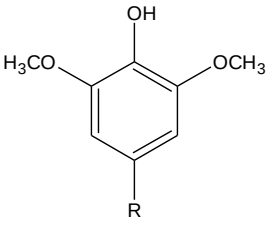

Ethylphenol (R=CH_2CH_3)
Vinylphenol (R=$CHCH_2$)

4-Guaiacol (R=H)
4-Methylguaiacol (R=CH_3)
4-Ethylguaiacol (R=CH_2CH_3)
4-Vinylguaiacol (R=$CHCH_2$)

Syringol (R=H)
5-Methylsyringol (R=CH_3)

Figure 2.2b. Most common non-flavonoid compounds in wine.

The average phenolic composition of red and white wines is significantly different (Table 2.1) (De Beer et al., 2002). Red wines contain polyphenols at a higher concentration (1 to 5 g/L) than white wines (0.2 to 0.5 g/L), particularly much higher levels of flavan-3-ols and proanthocyanidins. In addition, during aging these values could also change (Table 2.2) (Waterhouse, 2002). The main reason for this is that white wines are mostly made by quickly pressing the juice away from the grape solids, while red wines are made by fermenting the juice in the presence of the grape solids (skin and seeds). Since the skins and seeds contain most of the polyphenols, red wine is a more concentrated whole berry extract, while white wine is a less concentrated juice product (Waterhouse, 2002, De Beer et al., 2002).

Table 2.1. Phenolic compounds in both red and white wine (De Beer et al., 2002).

Phenolic group/Compound	White wine (mg/L)	Red wine (mg/L)
Non-flavonoids	***160-260***	***240-500***
Hydroxybenzoic acids:		
para-hydroxybenzoic acid	nd	20.0
protocatechuic acid	nd	88.0
gallic acid	2.8-11.0	3.1-320
syringic acid	nd	4.9-18.0
total gallates	6.8-7.0	38.6-58.7
Hydroxycinnamic acids:		
caffeic acid	1.5-5.2	4.7-18.0
para-coumaric acid	1.0-3.2	0.9-22.0
ferulic acid	nd	2.9-19.0
Hydroxycinnamic esters:		
monocaffeoyl tartaric acid	3.0-7.0	13.4-178
monocumaroyl tartaric acid	0-1.8	21.0-137
Stilbenes:		
trans-resveratrol	0-0.1	0.1-3.2
Flavonoids	***25-30***	***750-1060***
Flavan-3-ols:		
(+)-catechin	12.0-46.0	15.3-390
(-)-epicatechin	1.5-46.0	9.2-62
Flavonols:		
quercetin	0-1.2	0.5-28.5
myricetin	0-0.3	0-64.5
kaempferol	0-0.1	0.1-6.0
rutin	0-0.9	0-31.7
Anthocyanins:		
delphinidin-3-glucoside	nd	39.4-469
cyanidin-3-glucoside	nd	0-38.0
petunidin 3-glucoside	nd	18.0-24.0
malvidin-3-glucoside	nd	0-206
malvidin-3-*O*-acetylglucoside	nd	13.2-129
malvidin-3-*O*-coumaroylglucoside	nd	8.3-44.0
Total Polyphenols	***96-331***	***700-4059***

Table 2.2. Phenolic compounds in both red and white wine with aging (Waterhouse, 2002).

Phenol Class	White Wine		Red Wine	
Flavonoids	Young	Aged	Young	Aged
Flavan-3-ols	25	15	200	100
Proanthocyanidins and condensed tannins	20	25	750	1000
Flavonols	_	_	100	100
Anthocyanins	_	_	400	90
Others	_	_	50	75
Total (mg/L)	**45**	**40**	**1500**	**1365**
Non-Flavonoids				
Derivatives of cinnamic acid	154	130	165	60
Derivatives of benzoic acid	10	15	60	60
Hydrolyzable tannins (from oak)	0	100	0	250
Stilbenes (resveratrol)	0.5	0.5	7	7
Total (mg/L)	**164.5**	**245.5**	**232**	**377**
Total all phenols (mg/L)	**209.5**	**285.5**	**1732**	**1742**

Young means new wine, less than six months of age, not having been aged or fermented in oak barrels. Aged implies about one year for white wine, about two years for red wine and some oak barrel aging (or other oak contact).

2.2.2. Phenolic reactions in wine

2.2.2.1. Enzymatic degradation

In wine, enzymatic browning occurs mostly in grape must. A likely mechanism for the oxidation of phenolic compounds involves hydroxylation to the *ortho*-position of an existing hydroxyl group of the phenolic substrate (monophenol oxidase activity), and oxidation of *ortho*-dihydroxybenzenes to *ortho*-benzoquinones (diphenol oxidase activity). Several classes of enzymes can catalyze these reactions. According to the *Nomenclature Committee of the International Union of Biochemistry and Molecular Biology* (NC-IUBMB), these enzymes are part of the E.C. 1 class of oxidoreductases. The three main classes of enzymes that catalyze the oxidation of phenolic compounds are the oxidoreductases that use oxygen as electron acceptor (E.C. 1.10.3), the monophenol monooxygenase (E.C. 1.14.18.1), and the peroxidases (E.C. 1.11.1).

The E.C. 1.10.3 subclass includes enzymes that use catechols or related compounds as electron donors and oxygen as electron acceptor, leading to the oxidized donor and water. Members include catechol oxidase (E.C. 1.10.3.1), laccase (E.C. 1.10.3.2), and *ortho*-aminophenol oxidase (E.C. 1.10.3.4). Catechol oxidase is also known as diphenoloxidase, phenoloxidase, polyphenoloxidase, *ortho*-diphenolase, phenolase and tyrosinase, whereas, laccase is also known as *para*-diphenoloxidase. Many of these names are also used in reference to a different enzyme, monophenol monooxygenase (E.C. 1.14.18.1). E.C. 1.14 classes of monooxygenases contain enzymes acting on paired donors, with the incorporation or reduction of molecular oxygen. Monophenol monooxygenase (E.C. 1.14.18.1) catalyzes the same reactions as catechol oxidase (E.C. 1.10.3.1) if only catechols are available as substrate.

The phenol oxidizing enzyme tyrosinase has two types of activity: (i) phenol *ortho*-hydroxylase (cresolase) activity, whereby a monophenol is converted into a catechol via the incorporation of oxygen, and (ii) catecholase activity, whereby the catechol is oxidized to the brown pigment melanin (Figure 2.3) (Sánchez-Ferrer et al., 1995). Laccase catalyzes the oxidation of *para*-hydroquinones to *para*-benzoquinones (Figure 2.4).

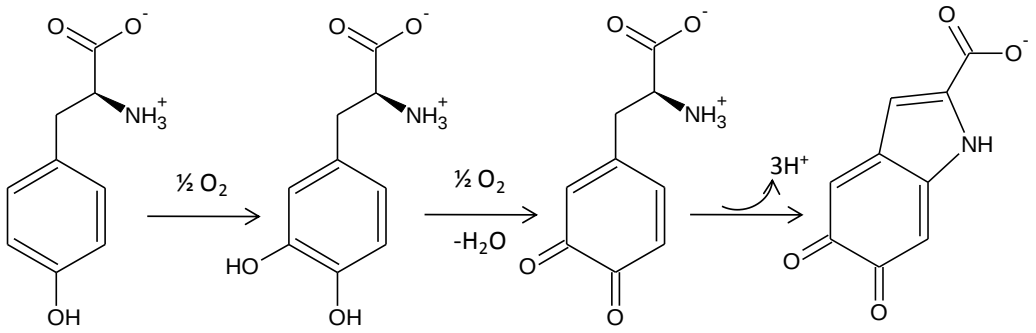

Figure 2.3. Tyrosinase-catalyzed oxidation of tyrosine results in precursors of melanin.

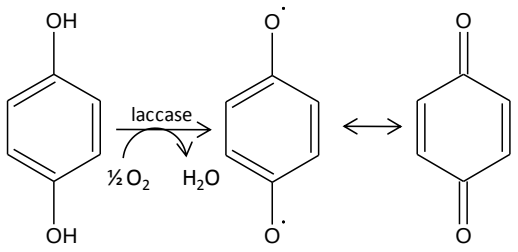

Figure 2.4. Laccase-catalyzed oxidation of 1,4-dihydroxybenzene to *para*-quinone.

The E.C. 1.11.1 subclass contains the peroxidases, which use hydrogen peroxide (H_2O_2) as electron acceptor to oxidize the donor, thereby forming the oxidized donor and water. Members include horseradish peroxidase (E.C. 1.11.1.7) also known as guaiacol peroxidase and scopoletin peroxidase, manganese peroxidase (E.C. 1.11.1.13) and diarylpropane peroxidase (E.C. 1.11.1.14). All three classes are hemoproteins. Mechanistically, hydrogen peroxide oxidizes the active site of the peroxidase enzyme, and upon substrate binding in the active site, the substrate becomes oxidized and the enzyme returns to its reduced state. Peroxidases are encoded by a large multi-gene family, which has complicated the study of individual peroxidase enzymes (Wilfred and Ralph, 2006).

The most important oxidoreductases responsible for browning during grape processing are polyphenoloxidases (PPO), namely, catechol oxidase or tyrosinase (E.C. 1.10.3.1) and laccase (E.C. 1.10.3.2), and peroxidases (POD), namely, horseradish peroxidase (E.C. 1.11.1.7) (Whitaker and Lee, 1995, Li et al., 2008). PPO is a Cu-containing enzyme, while POD is a Fe-containing enzyme. Tyrosinase, is naturally produced in grape berry and can catalyze the oxidation of monophenols and catechols (Singleton, 1987, Li et al., 2008). Laccase is produced by molds and are able to oxidize a great number of substrates, especially 1,2- and 1,4-dihydroxybenzene. Moreover, the browning caused by POD seems to be insignificant in fruits although some researchers found that it did increase the degradation of phenols when coexisting with PPO (Robards et al., 1999).

In grape must, enzymatic browning (Figure 2.5) is largely related with the content of hydroxycinnamates such as caffeoyltartaric acid (caftaric acid) and *para*-coumaroyltartaric acid (coutaric acid) (Cheynier et al., 1986), and is promoted by flavan-3-ols (Cheynier et al., 1995). When grapes are crushed, polyphenoloxidases (PPO) are released, and rapidly oxidize the hydroxycinnamates to benzoquinones. Meanwhile, the benzoquinones produced by enzymatic oxidation will undergo further reactions, according to their redox properties and electronic affinities (Robards et al., 1999). Being oxidants, quinones can oxidize substances which have a lower potential such as polyphenols and ascorbic acid as well as SO_2. The quinone is then reduced back to its original catechol. As electrophiles, they can also react with nucleophiles like amino derivatives (Kutyrev and Moskva, 1991).

In must oxidation, the initial oxygen uptake by *ortho*-dihydroxybenzenes is slowed by addition of thiols like cysteine (Cys) or glutathione (GSH) (Cheynier and Van Hulst, 1988). When caftaric acid is oxidised to its corresponding quinone by tyrosinase, GSH will

quickly react with the quinone forming a colorless product called grape reaction product (GRP; 2-*S*-glutathionyl caftaric acid), which is no longer a substrate for further oxidation by tyrosinase (Salgues et al., 1986, Singleton and Cilliers, 1995). Therefore, the formation of GRP is believed to limit the must browning and depends on the relative amounts of GSH. Analysis of aged bottled wines shows that GRP is slowly hydrolyzed to the GSH-caffeic acid derivative (the tartrate ester is hydrolyzed) (Cheynier et al., 1986). The specific brown products are not well characterized, but it appears that the hydroxycinnamate quinones react with flavan-3-ols to form colored products (Rigaud et al., 1991, Cheynier et al., 1995).

SO_2 inhibits tyrosinase (Dubernet and Ribéreau-Gayon, 1973) and prevent the production of GRP, which will maintain a high level of free hydroxycinnamates with high browning potential. Moreover, unlike tyrosinase, laccase will readily oxidise GRP. GRP was shown to be oxidized by laccase from *Botrytis cinerea* to the corresponding *ortho*-quinone with substitution of the latter by glutathione. When no glutathione is available, polymerization of the quinones led to browning of the juice (Salgues et al., 1986). It is accepted that tyrosinase is more sensitive to SO_2, while laccase is more resistant to SO_2 and has a wider substrate oxidation spectrum (Du Toit et al., 2006). In general, not all the enzymatic oxidation occurring in white grape must is detrimental. White must hyperoxygenation decreases the browning potential of wine in two ways: by the tyrosinase disappearance and by the depletion of oxidizable polyphenols during the oxidation reactions. These results in wines with low polyphenol concentrations and high GRP content, which are more stable than those made from non-oxidized juice, where the high polyphenols contents are maintained with a high browning potential (Li et al., 2008). However, during red wine processing the impact of enzymatic oxidation is limited (Cheynier et al., 2000).

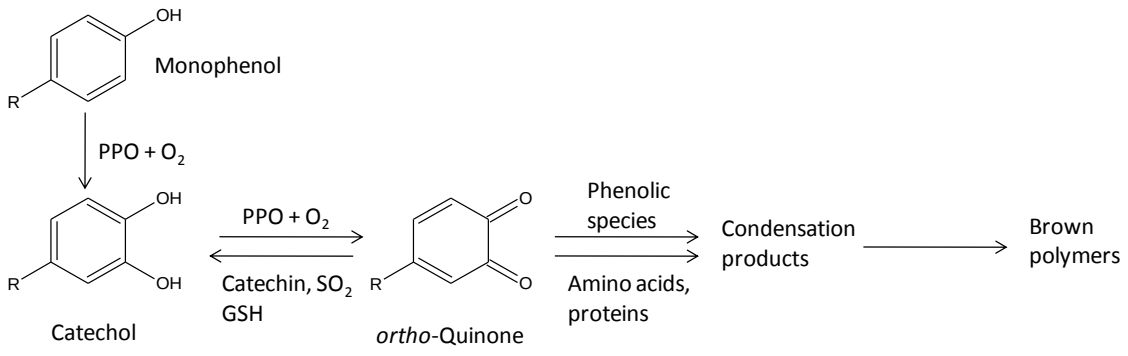

Figure 2.5. Enzymatic browning process in grape must (Li et al., 2008).

2.2.2.2. Non-enzymatic degradation

Phenolics chemical reactions have been particularly studied in wine (Cheynier, 2005), where these reactions include mainly oxidations and/or polymerizations. Polyphenols are the most readily oxidized wine constituents.

Phenols are oxidized to quinones in a sequential transference of two hydrogen atoms (Danilewicz, 2003). Following convention, the process is described in reverse to achieve reduction potentials. The first step is the one-electron reduction of the quinone (Q) to the semi-quinone radical ($Q^{\bullet-}$). The corresponding protonated specie ($QH^{\bullet}$) is a highly electron-deficient system and, at pH wine conditions, the semi-quinone is 90-99% protonated. The second step is the reduction of the semi-quinone radical ($Q^{\bullet-}$) to the dianion (Q^{2-}) almost totally in its protonated form QH_2 (pK_1 = 9.45 and pK_2 = 12.8), at wine conditions (Figure 2.6). Under normal wine conditions there is a slow rate of phenolic oxidation reactions. On the other hand, electrons are rapidly transfer from phenols to semi-quinones at pH 7 (Danilewicz, 2003), and in alkaline conditions there is a quicker oxygen consumption in wine (Singleton et al., 1979). Moreover, phenolic compounds under high pH conditions can react directly with oxygen. The weakly acidic nature of phenolic compounds (pKa = 9-10) allows them to form phenolate anions that react directly with oxygen (Waterhouse and Laurie, 2006).

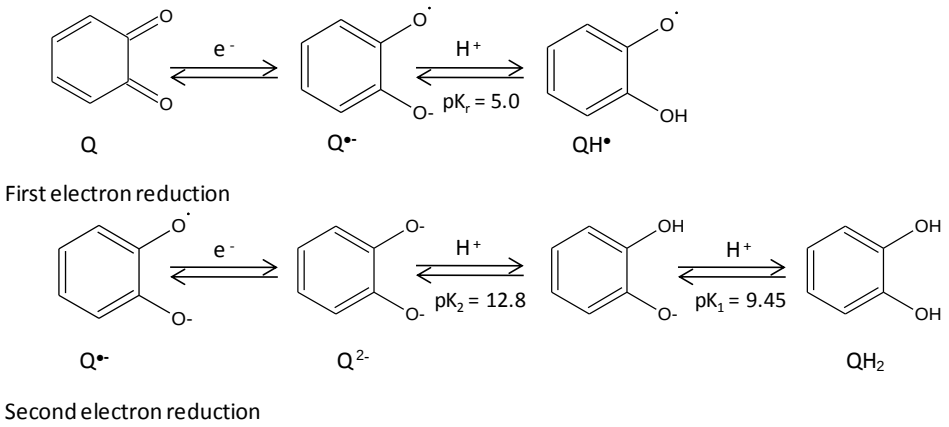

Figure 2.6. First and second electron reduction of the 1,2-benzoquinone/catechol system (Danilewicz, 2003).

During the non-enzymatic phenolics oxidation, the oxidative processes is favored by the oxidation of polyphenols containing an *ortho*-dihydroxybenzene derivative (a catechol moiety) or a 1,2,3-trihydroxybenzene derivative (a galloyl group), such as (+)-catechin / (-)-epicatechin, gallocatechin, gallic acid and its esters, and caffeic acid, which are the most readily oxidized wine constituents (Singleton, 1987, Singleton, 2000, Kilmartin et al., 2001, Danilewicz, 2003, Li et al., 2008). These substrates are sequentially oxidized to semi-quinone radicals and benzoquinones while oxygen is reduced to hydrogen peroxide, and the whole process is mediated by the redox cycle of Fe^{3+}/Fe^{2+} (Figure 2.7) (Danilewicz, 2003, Danilewicz, et al., 2008). Further compounds with more isolated phenolic groups such as malvidin, the major colored anthocyanin in red wines, *para*-coumaric acid and resveratrol are oxidized at higher potentials (Kilmartin et al., 2001).

The quinones formed from the oxidation of polyphenols, as the primary products, are unstable and may undergo further reactions. Quinones can spontaneously combine with nucleophilic compounds (including some phenols, thiols and amino compounds) due to their high electrophilic character. Furthermore, the produced dimers or polymers may rearrange their structure through an enol-like conversion reaction to form new dihydroxybenzene moieties (Figure 2.8) (Li et al., 2008). Moreover, these dimers or polymers in coupled oxidation reactions have lower redox potentials than their initial phenols and are much more easily oxidized (Singleton, 1987, Li et al., 2008). Consequently, it is proposed that oxidation of these products results in an acceleration of the polymerization process (Boulton et al., 2001, Zhai et al., 2001).

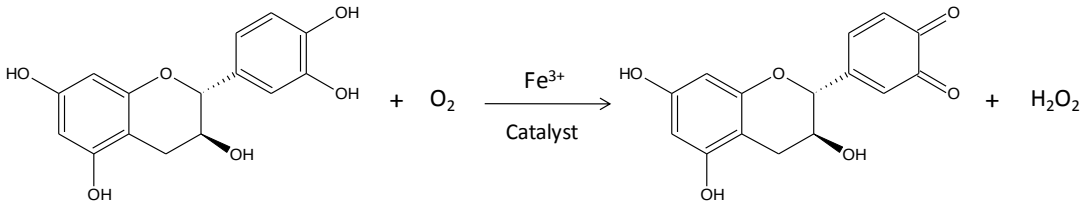

Figure 2.7. Oxidation of (+)-catechin in wine (Danilewicz, 2003).

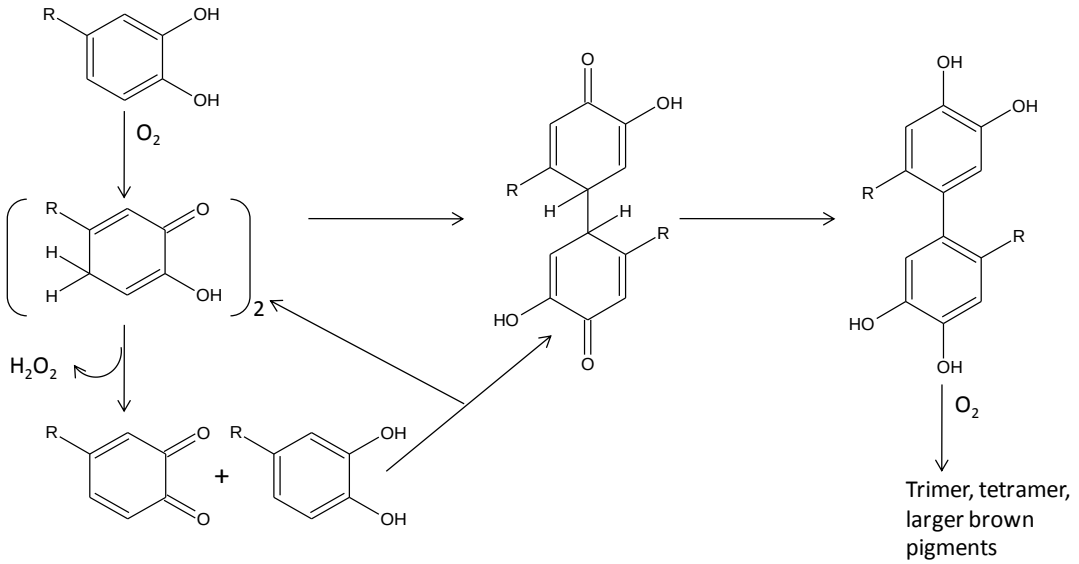

Figure 2.8. Regeneration of oligomers by reaction between two semi-quinones or a quinone and a phenol (Singleton, 1987).

Some of the established effects of O_2 additions to red wine include a decrease in the phenolic compounds such as (+)-catechin, (-)-epicatechin, quercetin, caffeic acid and anthocyanins, and an increase in red polymeric pigments improving the wine color density (Castellari et al., 2000). It is established that oxygenation could improve the evolution of red wines during aging, along with decreasing on astringency (Gambuti et al., 2013), but also deplete the amount of some monomer and oligomeric phenolic compounds related with health benefits (Castellari et al., 2000). Equally, several recent reports on the effects of micro-oxygenation in red wines have confirmed the loss of monomeric anthocyanins and other polyphenols, along with the formation of polymeric pigments, resistant to sulfur dioxide (SO_2) bleaching, often with an increase in wine color density (Tao et al., 2007, De Beer et al., 2008).

During aging, aldehydes and mostly acetaldehyde, resulting essentially from ethanol oxidation, are important intermediates in the chemical transformations occurring in red wine, leading to color and flavor changes. Additional changes in red wine pigments include the formation of methylmethine-anthocyanin-catechin compounds and pyranoanthocyanin-catechin compounds mediated by acetaldehyde released during wine oxidation processes (Timberlake and Bridle, 1976, Francia-Aricha et al., 1997, Mateus et al., 2002). In fact, one of the first reactions described in red wines was the polymerization reaction between anthocyanins and flavanols (catechins and condensed tannins) mediated

by acetaldehyde (Timberlake and Bridle, 1976, Rivas-Gonzalo et al., 1995, Lee et al., 2004). Acetaldehyde may also cross-link flavanols yielding methylmethine-linked flavanol adducts (Danilewicz, 2003, Cheynier, 2005, Fulcrand et al., 2006).

The reaction of acetaldehyde with flavonoids is believed to start with the protonation of acetaldehyde to a carbocation under acidic conditions, followed by a nucleophillic addition of the nucleophilic position C-8 and less likely C-6 of the phloroglucinol ring of the flavanol to the formed carbocation (Figure 2.9a, 2.9b). After losing a water molecule, the ethanol adduct forms a new carbocation intermediate that is attacked by another flavanol unit (Figure 2.9a) or a anthocyanin (Figure 2.9b) to yield a methylmethine-linked flavanol adduct (Figure 2.9a) or a methylmethine-linked anthocyanin-flavanol adduct (Figure 2.9b). The reaction may begin again from the newly formed dimers leading to polymers. Acetaldehyde may also mediate the self-condensation of anthocyanins leading to the formation of oligomeric methylmethine-linked anthocyanins (Atanasova et al., 2002, Salas et al., 2005), and also reacts directly with malvidin-3-*O*-glucoside to produce vitisin-B (Bakker and Timberlake, 1997).

The methylmethine-linked flavanol adducts generated with acetaldehyde are not stable and cleave into vinylflavanol oligomers (Figure 2.9a (1)) (Francia-Aricha et al., 1997, Francia-Aricha et al., 1998, Es-Safi et al., 1999a, Fulcrand et al., 1997, Fulcrand et al., 2006). These vinylflavanols can further react with malvidin-3-*O*-glucoside and carboxypyrano-malvidin-3-*O*-glucoside (vitisin A) to produce pyranoanthocyanins-flavanols (orange color) (Cruz et al., 2008) and vinylpyranoanthocyanin-catechins (portisins, blue color) pigments, respectively (Mateus et al., 2003).

Some others aldehydes present is wines such as glyoxylic acid, resulting from the tartaric acid oxidation, furfural and 5-(hydroxymethyl)furfural (HMF), which are both sugar degradation products (by caramelization or Maillard reaction) formed during the processing and storage of wine, react directly with flavanols leading to the formation of yellow-orange xanthylium compounds (Es-Safi et al., 2000). The reaction mechanism resembles an acetaldehyde-induced condensation. However, the colorless dimer would form yellow pigments by a dehydration follow by an oxidation process (Figure 2.9a (2)). Furthermore, furfural and methylfurfural have also shown to react directly with malvidin-3-glucoside leading to the formation of anthocyanin-furanic aldehyde adducts (Sousa et al.,

2010). The acetaldehyde-mediated condensation was found to occur more generally than with glyoxylic acid, furfural, and HMF (Es-Safi et al., 2002).

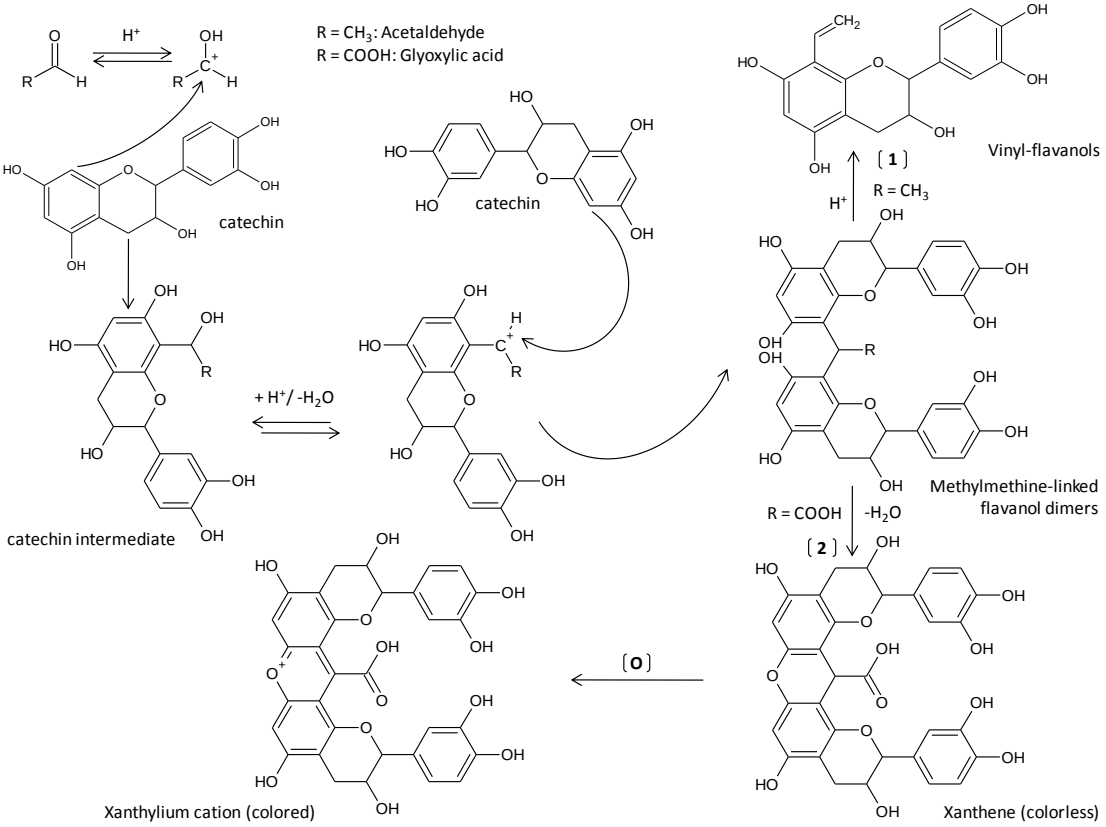

Figure 2.9a. Mechanisms of acetaldehyde- and glyoxylic acid-mediated polymerization of flavanols (Fulcrand et al., 2006).

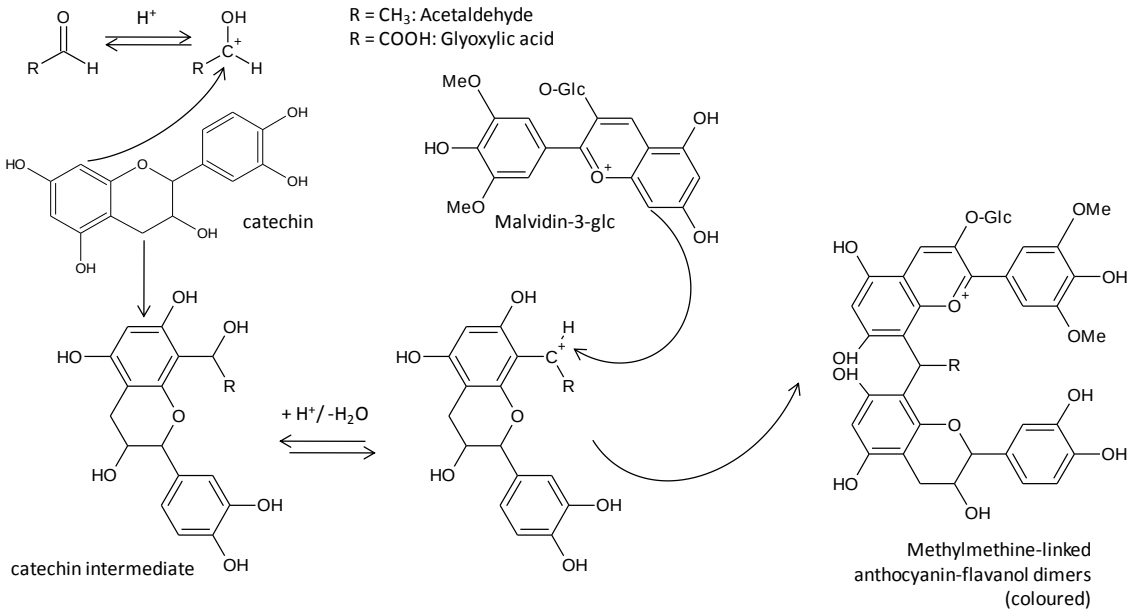

Figure 2.9b. Mechanisms of acetaldehyde- and glyoxylic acid-mediated polymerization of flavanols and anthocyanins (Sousa et al., 2010).

White wines contain lower levels of polyphenols, mainly hydroxycinnamic acids (Betes-Saura et al., 1996), but these remain very important for oxidation related issues in wine browning and losses of varietal aroma. The low concentrations of flavonoids such as catechin and quercetin glycosides remain important, particularly for wine browning and are more prevalent in musts exposed to longer skin contact times and harder pressing conditions (Singleton, 1987). Tests on browning rates with different wines have shown variable results with respect to the importance of phenolic content, SO_2 level, pH, and metal ions content (Simpson, 1982).

2.3. Maillard reaction and "Strecker degradation"

2.3.1. Occurrence of Maillard reactions and "Strecker degradation" in wine

Maillard reaction occurs in food and beverages during processing and cooking, even during storage, and proceeds well at 50ºC, at a favored pH of 4 to 7. Although the Maillard reaction has been found in beer and other foods, there is little supportive evidence for its occurrence in wine (Main, 1992, Zoecklein et al., 1995). However, because wine contains the necessary Maillard reaction substrates such as amino acids, proteins, and reducing sugars, the possibility of its occurrence should not be overlooked. After alcoholic and malolactic fermentations in wine, dicarbonyl compounds are obtained, which are susceptible of participating in Maillard reaction (Pripis-Nicolau et al., 2000). Recent studies indicates a number of volatile compounds chemically linked with Maillard-like reactions between sugars and amino acids in wine model systems (low pH, aqueous medium, and low temperature), such as glucose with alanine, arginine and proline (Kroh 1994), or carbonyl and α-dicarbonyl compounds with amino acids (Pripis-Nicolau et al., 2000, Marchand et al., 2002, De Revel et al., 2004, Marchand et al., 2011). Moreover, the influence of this reaction in the aroma of sweet fortified wines (Cutzach et al., 1999) and the production of Amadori compounds in Japanese white wines have already been described (Hashiba, 1978). Several by-products of Maillard reaction are identical or similar to some produced in degradation reactions catalysed by acids or bases. More recently, several Maillard-like compounds have been identified in a typical aroma or aging aromas of champagne wines (Keim et al., 2002, Tominaga et al., 2003) and fortified wines (Keim et al., 2002, Câmara et al., 2006, Silva Ferreira et al., 2006, Oliveira e Silva et al., 2008).

The "Strecker degradation" of amino acids is described as a result of the Maillard reaction and involves the interaction of sugar-derived α-dicarbonyl compounds with free amino acids to form an aldehyde (Shonberg and Moubacher, 1952). This reaction has supported evidence that occurs in wine (Pripis-Nicolau et al., 2000, Escudero et al., 2000a, Escudero et al., 2000b Marchand et al., 2000, Keim, et al., 2002, Escudero et al., 2002, Silva Ferreira et al., 2002). Typically, α-dicarbonyl compounds, such as glyoxal, pyruvaldehyde, butane-2,3-dione, and others, are reported as "Strecker degradation" reagents but, in principle, any dicarbonyl compound with extended conjugation can be used (Rizzi, 2006, Rizzi, 2008).

The latter structural category can be extended to include *ortho*-quinones, formed during the oxidation process of wine phenolic compounds.

2.3.2. Maillard reactions

The reaction between sugars and amino groups was first described in 1908 by two Englishmen, Ling and Malting, who considered color formation in beer. In 1912, a French chemist Louis Camille Maillard named this reaction "*Maillard reaction*", who considered a browning reaction between a reducing sugar (hexose or pentose) and a compound possessing a free amino group (amino acid or protein). Despite not being the first to report the reaction, Maillard was the first to realize the significance of the reaction in areas as diverse as plant pathology, geology and medicine. "*Strecker degradation*" is a "sub-reaction" category in the Maillard reaction where the amino acid, in the presence of α-dicarbonyl compounds, is decarboxylated and deaminated forming an aldehyde with one carbon atom less than the former amino acid known as "Strecker aldehyde". Strecker's pathway is not the major color producing reaction, but it is responsible for the origin of off-flavors usually associated with Maillard browning. The Maillard reaction has an important role in foods and beverages. For as long as food has been cooked, the Maillard reaction has played an important role in improving the appearance and taste of foods. Furthermore, it has been a central and major challenge in food industry, because the Maillard reaction is related to aroma, taste and color, particularly in traditional processes such as the roasting of coffee and cocoa, the baking of bread and cakes, the toasting of cereals, and the cooking of meat (Fors, 1983, Friedman, 1996). The general types of products and consequences of this reaction include: insoluble brown pigmented products, "melanoidins", which have variable structures, molecular weights and nitrogen content; volatile compounds that contribute to the aroma associated with many cooked foods; flavored compounds, often bitter substances; reducing compounds that may help prevent oxidative deterioration, increasing the stability (shelf-life) of the food (Yanagimoto et al., 2004); the formation of mutagenic compounds; and the loss of (essential) amino acids.

The first clear scheme of Maillard reaction was put by Hodge in 1953 (Figure 2.10). It states that in an early stage, a reducing sugar (aldose, like glucose; or ketose, like fructose) condenses with a compound possessing a free amino group (of an amino acid or amine) to

give a condensation product, *N*-substituted glycosylamine, which rearranges to form an aminoketose, the Amadori rearrangement product 1-amino-1-deoxyketose (ARP) (Figure 2.10). If fructose reacts in a corresponding way with an amino acid or an amine, an aminoaldose called a Heyns rearrangement product (2-amino-2-deoxyaldose) is formed. The subsequent degradation of the Amadori product is dependent on the pH of the system. This reaction usually requires heat.

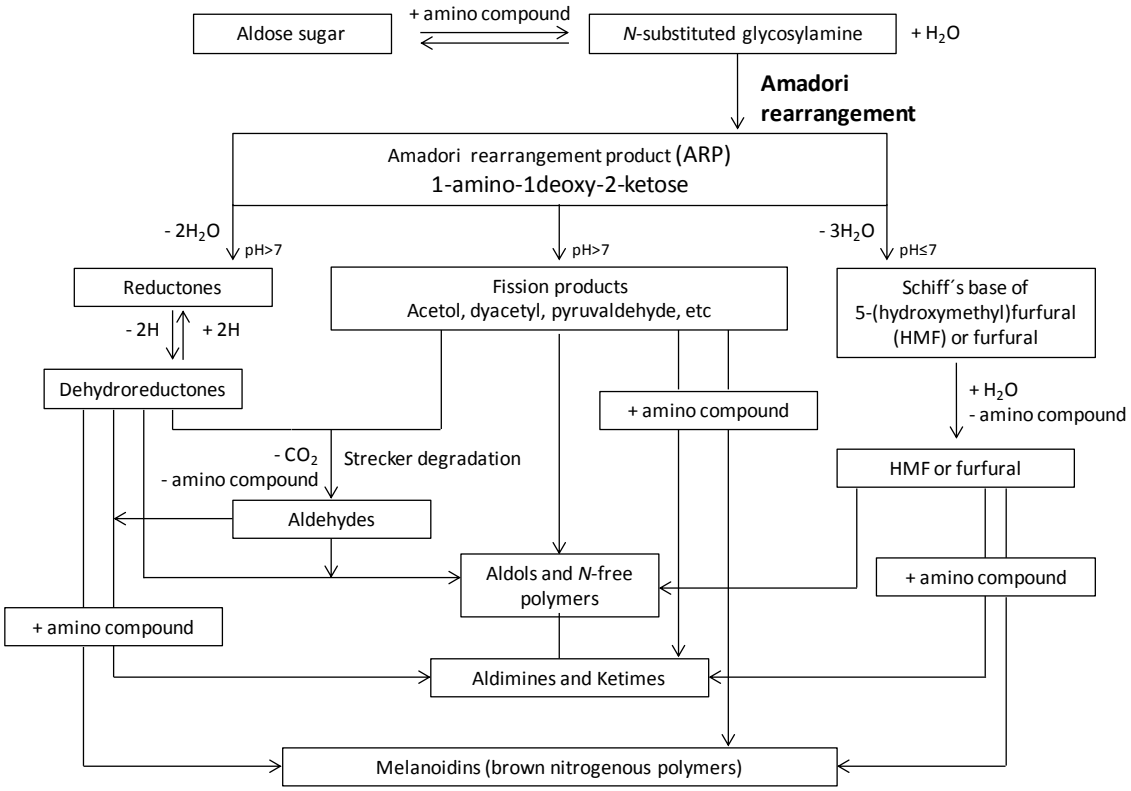

Figure 2.10. Maillard reaction scheme adapted from Hodge (1953).

At pH 7 or below, it undergoes mainly 1,2-enolization with the formation of 5-(hydroxymethyl)furfural (HMF) (when hexoses are involved) or furfural (when pentoses are involved). At pH >7 the degradation of the Amadori compound is thought to involve mainly 2,3-enolization, where reductones HHMFone [4-hydroxy-2-(hydroxymethyl)-5-methylfuran-3(*2H*)-one], when hexoses are involved, or norfuraneol [(4-hydroxy-5-methylfuran-3(*2H*)-one)], when pentoses are involved, and a variety of fission products are formed (Figure 2.10).

All these compounds are highly reactive and take part in further reactions. Carbonyl groups can condense with free amino groups, which results in the incorporation of nitrogen into the reaction products. Dicarbonyl compounds will react with amino acids with the formation of aldehydes and α-amino ketones. This reaction is known as the "Strecker degradation" (SD). In an advanced stage, a range of reactions takes place, which ultimately, lead to the formation of brown nitrogenous polymers and copolymers, known as melanoidins.

In the first comprehensive reaction scheme of Hodge (Figure 2.10), the ARP played a central role. It was the main intermediate formed in the early stage of the Maillard reaction from which all the flavor and color compounds would be formed. However, because of the development of improved analytical techniques, new important intermediates, not reported by Hodge, have been recognized and described by Tressl and others 1995 (Figure 2.11). This can be seen as the modern revised scheme of Hodge. The main difference was that 3-deoxyosones or 3-deoxyaldoloses (3DH in Figure 2.11) were reported to be the most important intermediate in color formation, formed through an intermediate prior to the ARP. Along with enolization reactions, the Amadori product and its dicarbonyl derivatives can undergo concurrently retro-aldol reactions producing more reactive C2, C3, C4 and C5 sugar fragments. Retro-aldol reactions become more important at higher pH values. Huyghues-Despointes and Yaylayan (1996) confirmed that under basic conditions ARP could generate acetic acid and methyglyoxal (pyruvaldehyde) and other lower sugars in addition to free amino acid. As a result, high pH is suggested to be the main pathway to flavor formation (Figure 2.11). In addition to retro-aldol reactions, model studies have indicated that reductions in Maillard systems can be effected by three pathways: through hydride transfer from formic acid; through cyclic dimerization of α-hydroxycarbonyl compounds followed by electrocyclic ring opening to produce oxidation/reduction products; and by disproportionation of enediols with α-dicarbonyl compounds through double proton transfer (Huyghues-Despointes and Yaylayan, 1996).

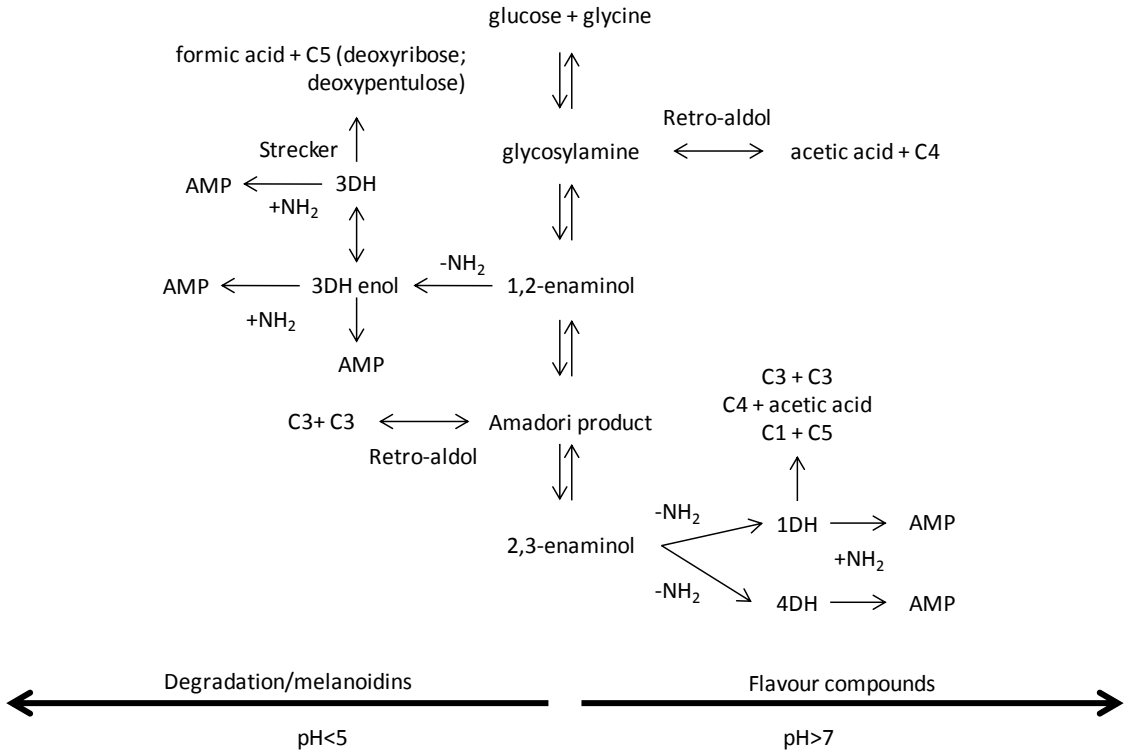

Figure 2.11. Maillard reaction scheme adapted from Tressl et al., (1995). AMP (Advanced Maillard Products); 1DG or 1DH (1-deoxy-2,3-diketose); 3DG or 3DH (3-deoxyaldolose); 4DG or 4DH (4-deoxy-2,3-diketose).

2.3.2.1. Degradation of DFG [N-(1-deoxy-D-fructose-1-yl)glycine]

Figure 2.12 represents a compressive scheme of degradation of the Amadori product from a sugar (glucose) and glycine. Two possible degradation pathways of DFG [*N*-(1-deoxy-D-fructose-1-yl)glycine] are the enolization pathway (Figure 2.12) and the retro-aldolization pathway (Figure 2.13). Through enolization, the amino-enol intermediates (1,2-eneaminol and 2,3-eneaminol) can lead to either 3-deoxyosone (A: 3-deoxyglucosone; 3DG) from 1,2-eneaminol, and 1-deoxyosone (B: 1-deoxyglucosone; 1DG) or 4-deoxyosone (C: 4-deoxyglucosone; 4DG) from 2,3-eneaminol (Figure 2.12). At lower pH, 1,2-enolization is believed to be favored and therefore a higher yield of 3DG is expected. On the other hand as the pH increases to neutral/alkaline values, 2,3-enolization is believed to be favored and therefore 1DG or 4DG should be present in higher amounts (Figure 2.12). Then, cyclization/condensation of 3- and 1-deoxyosones occurred to form, respectively, HMF [5-(hydroxymethyl)furfural] or furfural, as a 1,2-enolization indicator (Figure 2.12), and the

furanones HHMFone [4-hydroxy-2-(hydroxymethyl)-5-methylfuran-3(*2H*)-one] or norfuraneol [4-hydroxy-5-methylfuran-3(*2H*)-one], as a 2,3-enolization indicator (Figure 2.10). The formation of 2-osulones by transition-metal catalyzed oxidation from 1,2-enaminol is also proposed (Figure 2.12) (Davidek et al., 2002).

The degradation of Amadori compounds involving a retro-aldol reaction is depicted in Figure 2.13. Previous studies (Huyghues-Despointes and Yaylayan, 1996, Keyhani and Yaylayan, 1996) have indicated that DFG generates 1-glycine-1-deoxy-D-glyceraldehyde and glyceraldehyde through a retro-aldol cleavage at C-3 to C-4 (Figure 2.13). Glyceraldehyde can react with free glycine and produce more of 1-glycine-1-deoxy-D-glyceraldehyde that subsequently undergoes a β-elimination to form methylglyoxal and release glycine. Moreover, methylglyoxal can also be produced from glyceraldehyde through the catalytic action of the amino acid (Figure 2.13).

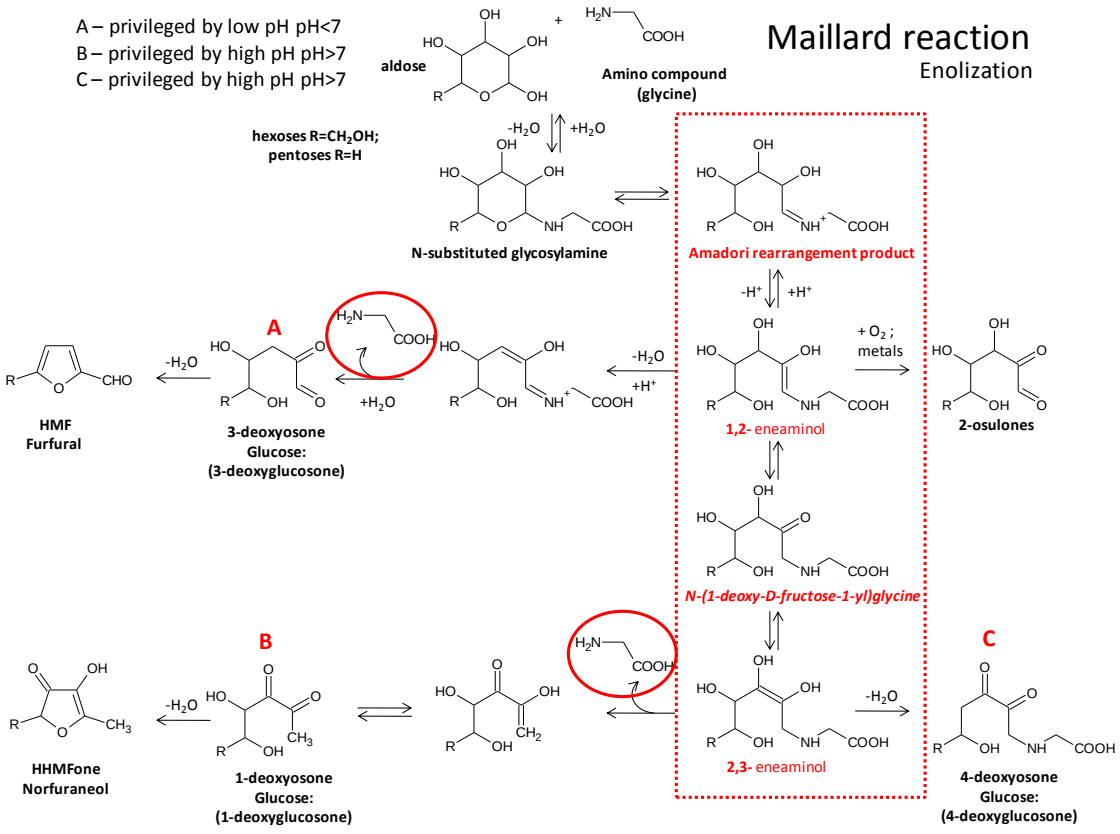

Figure 2.12. Degradation of the Amadori product through enolization pathway.

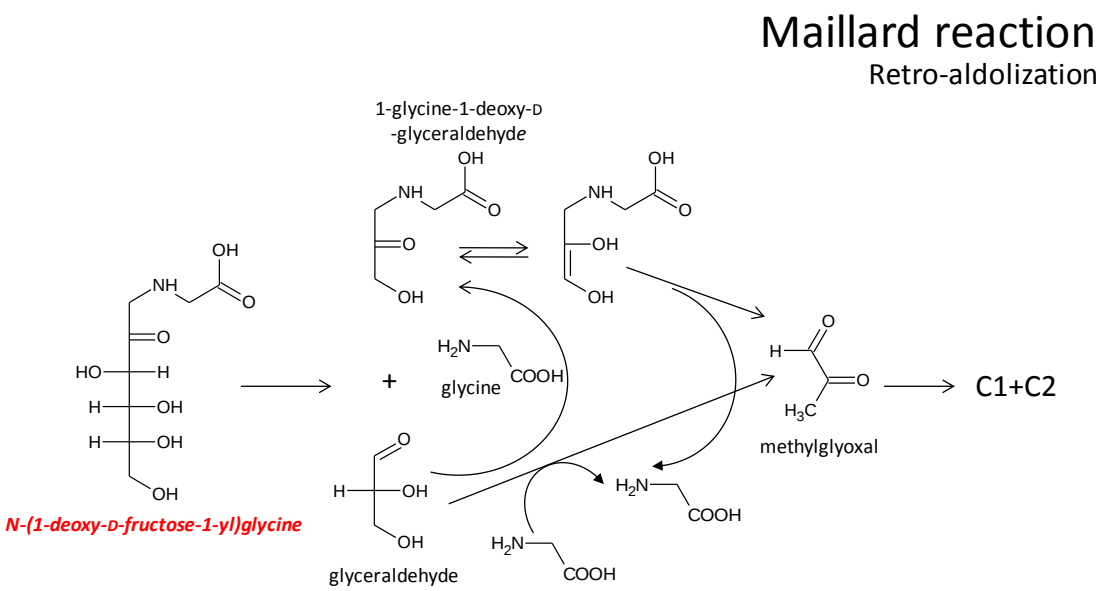

Figure 2.13. Degradation of the Amadori product through retro-aldol pathway. Adapted from Martins et al., 2003a.

The effect of the combination of pH and temperature on the decomposition of *N*-(1-deoxy-D-fructos-1-yl)glycine was studied at 100°C and 120°C, with initial pH values of 5.5 and 6.8 (Martins et al., 2003a, Martins et al., 2003b). Results have showed that an increase in pH seems to favor the formation of 1-deoxyosone (1DG), and independently of the taken pathway, enolization or retro-aldolization, DFG degradation is accompanied by amino acid release. Moreover, along with glycine, acetic acid was the main end product formed. Mannose was preferably formed at pH 5.5. On the contrary, at pH 6.8, glucose was formed in higher amounts than mannose. Also, independently of the temperature, at higher pH fructose was also detected. pH, more than temperature, had an influence on the reaction products formed.

2.3.2.2. Formation of organic acids and parent sugars

According to the Lobry-de-Bruyn-Alberda-van-Eckenstein-rearrangement all three sugars, glucose, mannose and fructose are in equilibrium with the same intermediate, the 1,2-enediol. However, fructose is also in equilibrium with the 2,3-enediol (Figure 2.14). In addition, thermal dehydration of these sugars to give 1-deoxyglucosone (1DG) and 3-deoxyglucosone (3DG) is well known (Weenen and Tjan, 1994, Ledl and Schleicher,

1990) (Figure 2.14). These four intermediate compounds can be regarded as acid precursors. The enediol compounds preferentially cleave at the C-C double bond, while scission of the deoxyglucosones is mainly at the α-dicarbonyl group. For example, 3-deoxyglucosone (3DG) can yield formic acid and 2-deoxyarabinose by cleavage of the C1-C2 bond (Figure 2.14). By this mechanism only one isotopic isomers of each of the four acids can be formed: C1-labelled formic acid, C2-labeled acetic and hydroxyacetic (glycolic) acids and C3-labelled lactic acid (Ginz et al., 2000). Formic acid and acetic acid are formed from DFG degradation pathways by 3-deoxyglucosone (3DG) dicarbonyl cleavage and by 1-deoxyglucosone (1DG) dicarbonyl cleavage, respectively (Figure 2.14) (Ginz et al. 2000, Martins et al., 2003a).

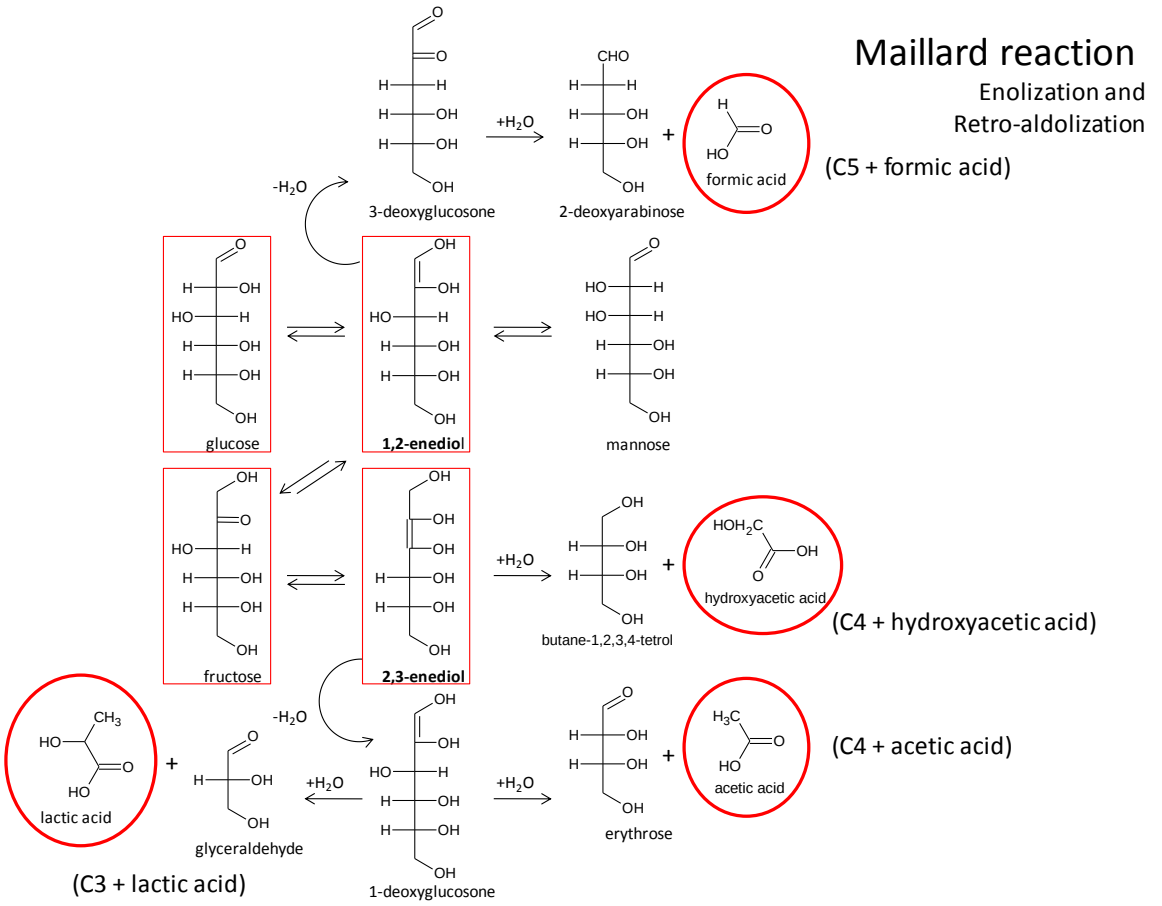

Figure 2.14. Organic acids formation and parent sugars from primary thermal degradation products. Adapted from Ginz et al., 2000.

2.3.2.3. Different formation pathways of "Strecker aldehydes"

"Strecker degradation" produces "Strecker aldehydes" and α-amino carbonyl compounds, both critical intermediates in the generation of aromas during Maillard reaction. Strecker aldehydes can be formed directly either from free amino acids or from Amadori products. Several pathways have been proposed in the literature for the mechanism of this transformation. On the other hand, Amadori rearrangements of ammonia with reducing sugars can also generate α-amino carbonyl compounds without the formation of Strecker aldehydes. In addition, isomerization of the imine bond of the Schiff base formed between a reducing sugar and an amino acid can initiate a transamination reaction and convert the amino acid into the corresponding α-keto acid and the sugar into its α-amino alcohol derivative. The reverse of this reaction, has been documented to produce Amadori products. The α-keto acids can either decarboxylate to produce "Strecker aldehydes" or undergo "Strecker degradation" (as α-dicarbonyl compound) with amino acids to also produce Strecker aldehydes.

It is particularly referred to as SD, when α-dicarbonyl compounds (Figure 2.15 and Figure 2.18) act as oxidizing agents to achieve decarboxylation of amino acids which is usually followed by hydrolysis of the resulting imine to produce free ammonia (if inorganic oxidizing agents are used) or a primary amine such as α-amino ketone and an aldehyde, referred to as Strecker aldehyde (Figure 2.15 and Figure 2.18). Conversely, the amino acid can undergo oxidative decarboxylation itself (Figure 2.16 and Figure 2.17). The α-dicarbonyl compound however, similar to the α-hydroxycarbonyl compound during Amadori rearrangement (AR), undergoes reductive amination and is converted into α-amino ketone, instead of its amino acid analog as in the case of Amadori rearrangement process (Figure 2.15). In addition, Amadori rearrangements of free ammonia with α-hydroxycarbonyl compounds also produce identical intermediates to that of the SD of amino acids with corresponding α-dicarbonyl compound, without the formation of Strecker aldehyde (Figure 2.15). Therefore, both processes (SD and AR) induce reductively the amination of different sugar fragments (α-dicarbonyl compounds vs α-hydroxycarbonyl compounds) by the action of the amino acid (Figure 2.15).

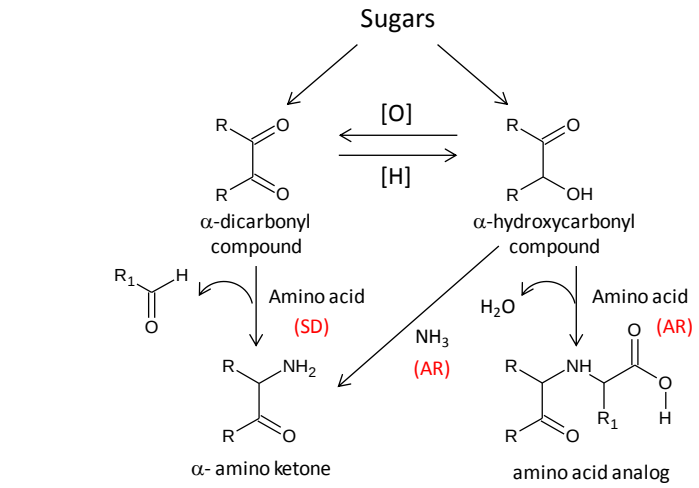

Figure 2.15. Comparison of "Strecker degradation" and Amadori rearrangement (Yaylayan, 2003).

i. From amino acids through oxidizing agents

Soft oxidizing agents such as sodium hypochlorite, *N*-bromosuccinimide, silver(II) picolinate, and lead tetraacetate (Barrett, 1985) can cause oxidative decarboxylation of amino acids at ambient temperatures, followed by hydrolysis of the resulting imine a to give Strecker aldehyde (Figure 2.16).

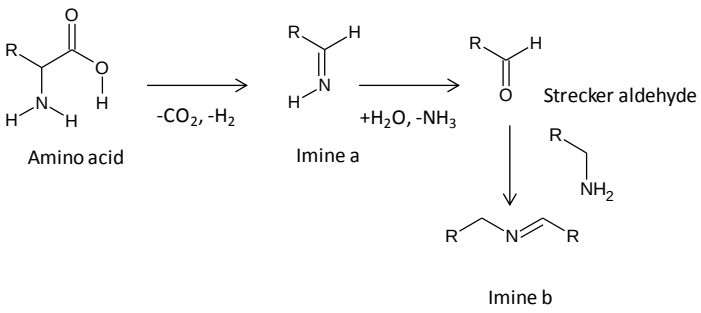

Figure 2.16. Formation of "Strecker aldehydes" from oxidative decarboxylation of amino acids.

ii. From amino acids through temperature

Moreover, in the absence of oxidizing agents, amino acids alone can also undergo thermal deamination and produce "Strecker aldehydes" at temperatures above 200°C (Yaylayan and Keyhani, 2001). These authors have detected the formation of the imine b (Figure 2.16) formed between the Strecker aldehyde and the resulting amine from decarboxylation of the amino acid when pyrolyzed alone at 250°C for 20 s. On the other hand, (Shu, 1998) detected the formation of "Strecker aldehydes" of amino acids heated at 200°C for 7 min in the presence of 3-hydroxybutan-2-one. The author also detected tetramethylpyrazine (TMP) coming from the reaction between the α-hydroxycarbonyl compound (3-hydroxybutan-2-one) and the ammonia released from the amino acid, and proposed a decarbonylation mechanism followed by deamination from the amino acid to justify the formation of Strecker aldehyde (Figure 2.17).

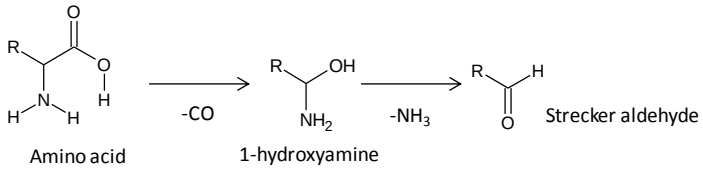

Figure 2.17. Formation of "Strecker aldehydes" from thermal decarbonylation of amino acids.

iii. From amino acids through α-dicarbonyl compounds

Alloxan is the original α-dicarbonyl compound used by Strecker (1862) to effect decarboxylation/deamination of amino acids and formation of the aldehyde named after him.

The mechanism of Strecker aldehyde formation through α-dicarbonyl-assisted oxidation is shown in Figure 2.18.

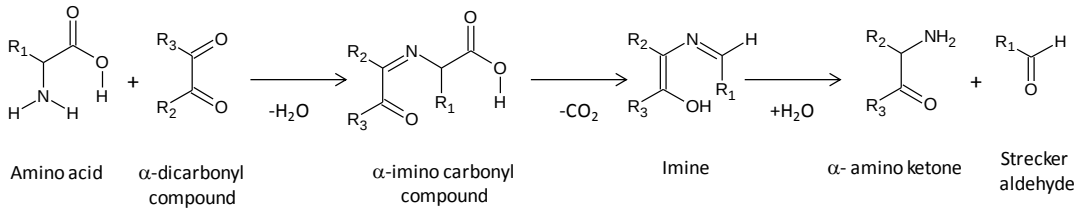

Figure 2.18. Formation of "Strecker aldehydes" from α-dicarbonyl assisted oxidative decarboxylation of amino acids.

iv. From direct formation through Amadori compounds

Formation of Strecker aldehyde directly from Amadori rearrangement product was first suggested by Cremer and others (2000) followed by Hofmann and Schieberle (2000). Both groups still proposed different pathways: A in Figure 2.19; and B in Figure 2.20.

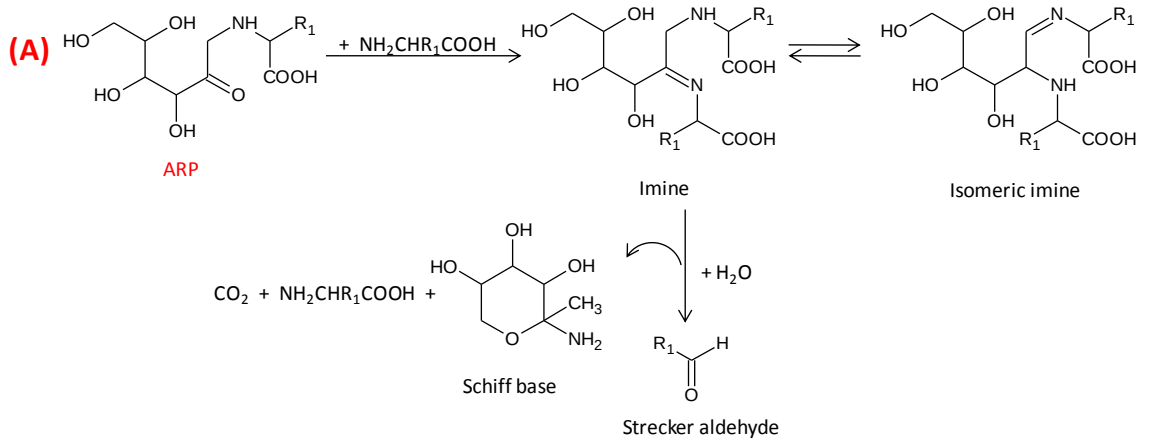

Figure 2.19. Formation of Strecker aldehyde directly from Amadori rearrangement product. Pathway A proposed by Cremer and others (2000).

Pathway A: the authors proposed the reaction of free amino acid (either added or released from ARP) with ARP to form an imine in equilibrium with its isomeric imine (Figure 2.19). Elimination of the free amino acid initiated by decarboxylation can produce the corresponding Strecker aldehyde in addition to a Schiff base of 1-deoxyfructose with ammonia (Figure 2.19).

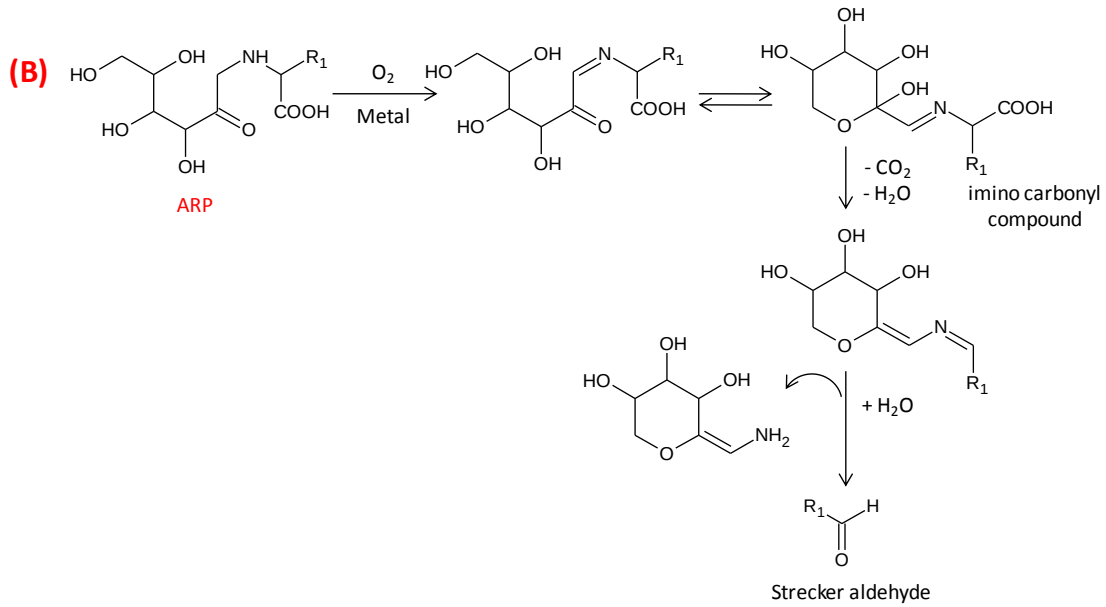

Figure 2.20. Formation of Strecker aldehyde directly from Amadori rearrangement product. Pathway B proposed by Hofmann and Schieberle (2000).

Pathway B: a mechanism based on a metal-catalyzed oxidation of the eneaminol moiety of the ARP into an imino carbonyl compound similar to oxidation of enediols into α-dicarbonyls (Figure 2.20). This intermediate can either get hydrolyzed into glucosone or undergo a decarboxylation reaction with the elimination of water. The produced intermediate can undergo hydrolysis to give the Strecker aldehyde (Figure 2.20).

In a related study, Hofmann et al. (2000) have demonstrated that during Strecker degradation, the α-imino carbonyl intermediate formed after decarboxylation and hydration steps can also undergo air oxidation and form an intermediate that, after an isomerization step and a further hydrolysis, can generate a Strecker acid (Figure 2.21).

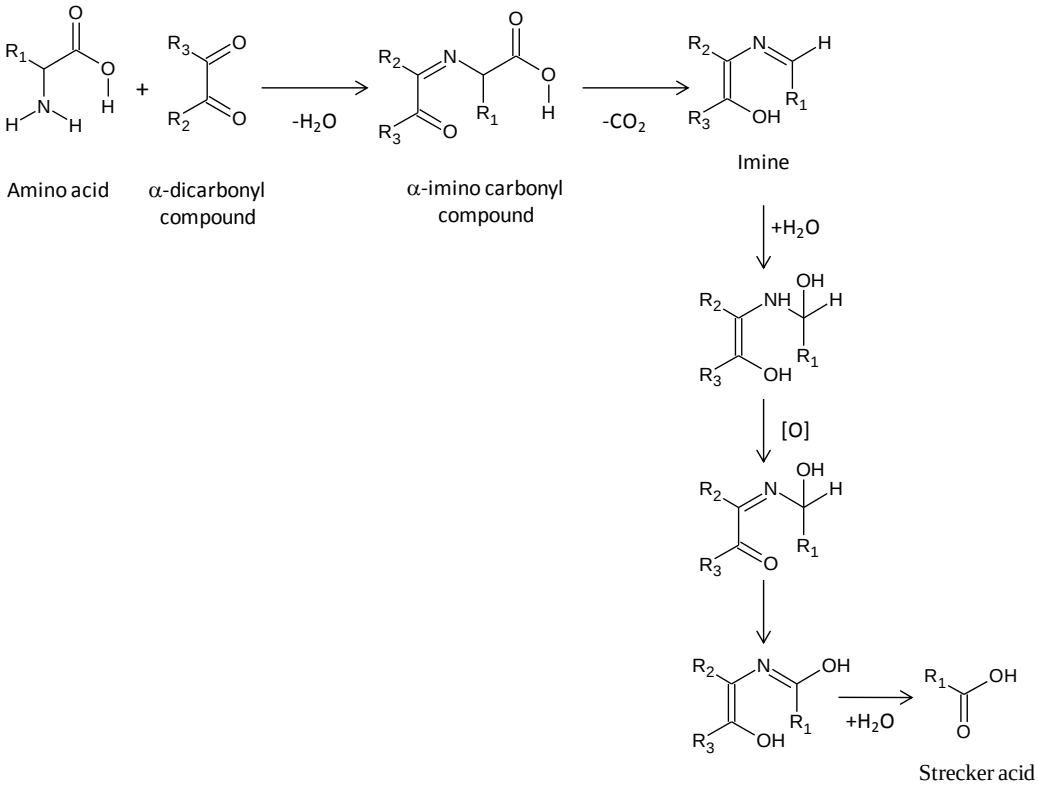

Figure 2.21. Formation of Strecker acids from Strecker degradation. Adapted from Hofmann et al. (2000).

v. From amino acids through α-keto acids

α-keto acids can act as α-dicarbonyl compounds, and also cause oxidative decarboxylation of amino acids, being themselves converted into the corresponding amino acids (Figure 2.22). The isomerization of the imine bond of the Schiff base formed between a reducing sugar and an amino acid can initiate a transamination reaction and convert the amino acid into the corresponding α-keto acid and the sugar into its α-amino alcohol derivative (Figure 2.22). The reverse of this reaction has been documented to produce Amadori products. The α-keto acids can either decarboxylate to produce "Strecker aldehydes" or undergo "Strecker degradation" (as α-dicarbonyl compound) with amino acids to also produce Strecker aldehydes.

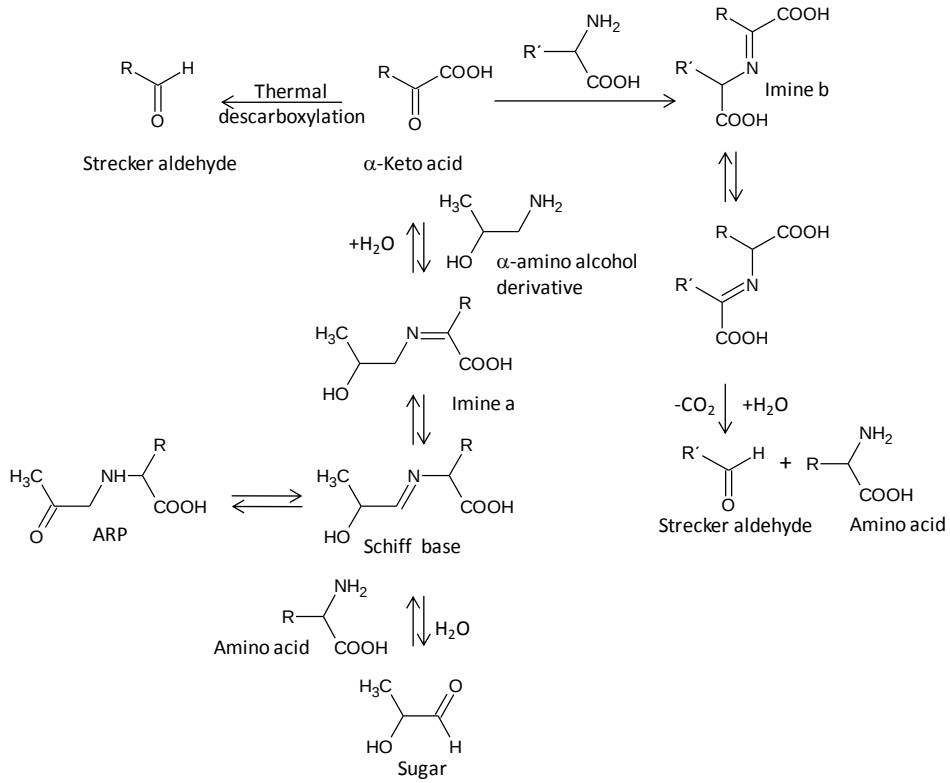

Figure 2.22. Formation of "Strecker aldehydes" through α-keto acids.

vi. From amino acids through quinones

Quinones are produced during enzymatic and non-enzymatic phenolics oxidation. These molecules are electronic equivalents of α-dicarbonyl compounds and are therefore potential SD reactants (Rizzi, 2006, Rizzi, 2008).

In 1979, Motoda investigated the SD of alanine, valine, leucine, and isoleucine with (+)-catechin using a purified PPO. The author also reported the formation of the Strecker aldehyde 3-methylbutanal from leucine for a variety of catechol derivatives in which dihydroxyphenols appeared to be more active than trihydroxyphenols. For this enzyme reaction of leucine with (+)-catechin, the formation of aldehyde followed Michaelis-Menten kinetics. A generalized reaction scheme describing the formation of "Strecker aldehydes" from catechins is given in Figure 2.23. The initial steps of this mechanism were first proposed in 1948, by James et al., to explain the stoichiometric quantity of oxygen consumed in model reactions of amino acids with catechol and a phenolase isolated from *Atropa belladonna L.* The amino acid degradation mechanism was explored more fully in terms of the oxidative deamination of amino acids by Trautner and Roberts (1950) and

later, the two step oxidation sequence was confirmed with kinetic data by Valero et al. (1988). The amino acid degradation mechanism was later employed by Bokuchava and Skobeleva (1969) to reduce the formation of "Strecker aldehydes" from catechins during tea fermentation.

It is proposed (Rizzi, 2006) that initial catechin oxidation is followed immediately by 1,4-conjugate addition (Michael addition) of one molecule of amino acid to the quinone to produce a 4-amino catechol intermediate (**1**; Figure 2.23). This intermediate also act as substrate for PPO while consuming a second mole of oxygen to form the Strecker reactant, a 4-amino-1,2-benzoquinone (**2**; Figure 2.23). This *ortho*-quinone can then react with a second molecule of amino acid, to form an amine/carbonyl condensation product (**3**; Figure 2.23). This condensation product will decarboxylate to form the intermediate **4** (Figure 2.23) and then hydrolyze to form a Strecker aldehyde and a presumed transamination product (**5**; Figure 2.23).

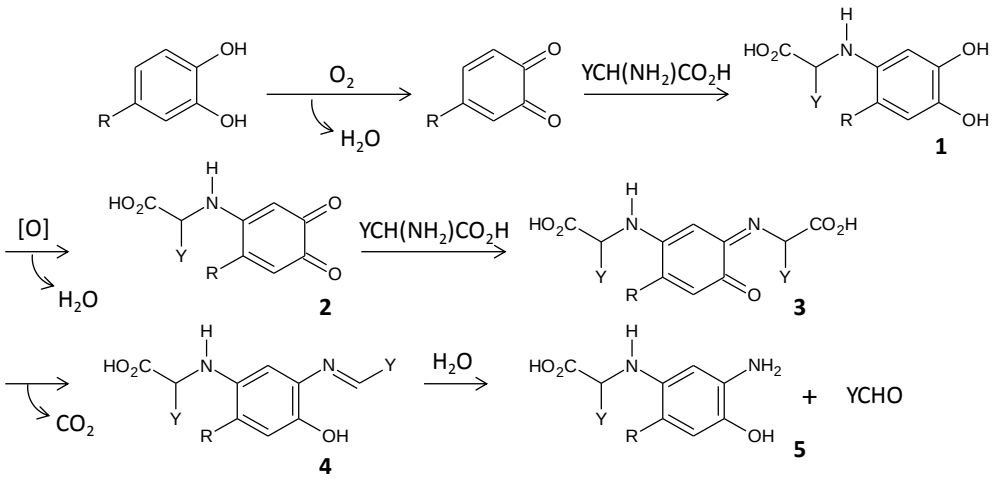

Figure 2.23. Proposed Michael addition reaction of *ortho*-quinones with α-amino acids to produce the "Strecker aldehydes". Adapted from Rizzi, 2006.

By using ferricyanide ion as oxidant, as an alternative of enzymes, caffeic acid, chlorogenic acid, (+)-catechin, and (−)-epicatechin react with methionine and phenylalanine to produce the "Strecker aldehydes" methional and phenylacetaldehyde, in pH 7.17 phosphate buffer at 20°C (Rizzi, 2006). On the other hand, reaction products between 4-methyl-1,2-benzoquinone (Q4MeC) and α-amino acids, investigate by Nikolantonaki and Waterhouse (2012), do not corroborate this mechanism. The proposed

reaction of products forming during the first steps of "Strecker degradation" of methionine and phenylalanine, using the *ortho*-quinone Q4MeC as reactant, were not observed (**1**; Figure 2.23). As a result, the authors stated that under low pH model wine conditions Rizzi's Strecker-type reaction could not be observed, and point towards to a Fenton-type oxidation of the related alcohols as the source of the aldehydes perceived to affect wine aroma so strongly (Wildenradt and Singleton, 1974, Escudero et al., 2000, Silva Ferreira et al., 2002, Silva Ferreira et al., 2003, Loscos et al., 2010). Nevertheless, under wine pH conditions, this route has to be confirmed, in order to determine if "Strecker aldehydes" can be formed with the participation of quinones, as "Strecker degradation" reagents.

2.4. Sugar reactions - Caramelization

2.4.1. Occurrence of sugars in wine

Sugar caramelization can occur with carbohydrates but requires higher temperatures. In fact, wine caramelization occurs during production of baked sherry and during excessive pasteurization of sweet wines. In the same way, browning overtones derived from caramelization may be present in red and white wines vinified from raisined berries (Kroh, 1994, Zoecklein et al., 1995).

2.4.2. Sugar reactions

Caramelization of sugars occurs at high temperatures (> 80ºC) and low water content. Sugar reactions are accelerated by isomerization, water elimination, and oxidation, leading to caramel flavors and pigments. The general types of products and consequences of this reaction include pleasant flavors and colors in many foods and beverages, like caramel aroma in coffe, and beverage color in beer, but can also lead to undesirable flavors and colors like "burnt-sugar" smell and darkness. In this reaction enediols and dicarbonyls are formed with the development of, respectively, caramel flavors and pigments. Brown-colored products with a typical caramel aroma are obtained by melting sugar or by heating sugar syrup in the presence of acidic and/or alkaline catalysts. The process can be headed towards aroma formation or more towards brown pigment accumulation. Heating of

saccharose syrup in an alkaline solution enhances molecular fragmentation and, thereby, formation of aroma substances. Primarily dihydrofuranones, cyclopentenolones, cyclohexenolones and pyrones are formed. On the other hand, heating glucose syrup with sulfuric acid in the presence of ammonia provides intensively colored polymers ("sucre couleur"). These brown pigments, known as melanoidins, contain variable amounts of nitrogen and have varying molecular weights and solubilities in water. Little is known about the structure of these compounds. Studies have been conducted on fragments obtained after Curie point pyrolysis or after oxidation with ozone or sodium periodate.

2.5. Oxygen and ROS in wine

2.5.1. Occurrence of oxygen and ROS in wine

Free radicals species are encountered in many reactions used in chemical industry, in many biological systems, and in the processes responsible for the spoiling of food and beverages. Reactive oxygen species (ROS) is a collective term used to describe oxygen radicals, such as superoxide anion ($O_2^{\bullet-}$) and its conjugate acid hydroperoxyl radical ($HO_2^{\bullet}$), hydroxyl ($HO^{\bullet}$), peroxyl ($ROO^{\bullet}$), and alkoxyl ($RO^{\bullet}$) radicals, and certain other non-radical species that are either potential oxidizing agents or are easily converted into radicals, such as hydrogen peroxide (H_2O_2), ozone (O_3), hypochlorous acid (HOCl), singlet oxygen ($^1O_2$), and lipid peroxide (LOOH) (Shchepinov, 2007, Pourova et al., 2010). Reactions of ROS with food and beverages produce undesirable volatile compounds, carcinogens, destroy essential nutrients, and change the functionalities of proteins, lipids and carbohydrates.

As it has been stated before, during the chemical oxidation of wine, the oxidative processes begin by the oxidation of polyphenols. These substrates are sequentially oxidized to semi-quinone radicals and benzoquinones while oxygen is reduced to hydrogen peroxide, and the whole process is mediated by the redox cycle of Fe^{3+}/Fe^{2+} and Cu^{2+}/Cu^{+} (Figure 2.24) (Danilewicz, et al., 2008).

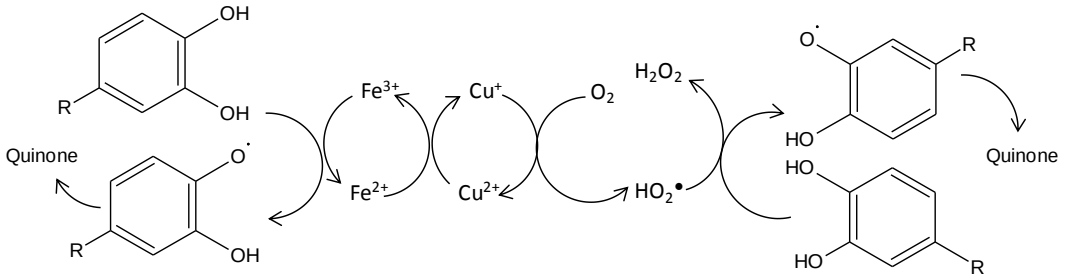

Figure 2.24. Proposed catalytic action of iron and copper ions in the oxidation of catechols to produce *ortho*-quinones and hydrogen peroxide (Danilewicz et al., 2008).

Hydrogen peroxide in association with ferrous ions generates hydroxyl radicals ($HO^{\bullet}$), which is known as the Fenton reaction (Figure 2.25). Hydroxyl radical is a reduced product of oxygen and it is recognized to oxidize almost any organic molecule found in wine (Waterhouse and Laurie 2006). Moreover, due to its non-selectivity it will react with the first species it encounters, depending on their concentration (Danilewicz, 2003, Danilewicz 2007, Li et al., 2008), such as ethanol, tartaric acid, glycerol, sugars and organic acids (Danilewicz, 2003, Waterhouse and Laurie 2006).

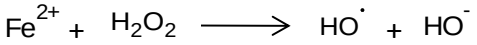

Figure 2.25. Fenton reaction.

2.5.2. Oxygen and ROS reactions in wine

Danilewicz (2003) and then Waterhouse and Laurie (2006) have examined the proposed mechanisms by which oxygen and its intermediate reducing products react with wine, as well as the participation of transition metal ions in these reactions. In these reviews, authors have concluded that oxygen thus not react directly with phenolic compounds without the presence of transition metal ions. Moreover, the influence of iron, copper, and manganese ions on wine oxidation has been studied measuring the evolution of different compounds (anthocyanins, tannins, total phenol content and acetaldehyde), and an intervention of these cations in the oxidative processes was found, since the evolution of the parameters sensitive to oxidation depends on the concentration of these cations in wine (Cacho et al., 1995).

The limitation on the reactivity of triplet oxygen is overcome by the stepwise addition of a single electron, which can be provided by reduced transition metals ions. The initial transfer of an electron leads to the formation of superoxide anion ($O_2^{\bullet-}$) which, at pH wine, exists in the protonated form hydroperoxyl radical ($HO_2^{\bullet}$) (Figure 2.26). The transfer of a second electron will produce peroxide anion (O_2^{2-}) which, at wine pH, exists in the protonated form hydrogen peroxide (H_2O_2) (Figure 2.26). The next reduction step creates an oxidative agent even more reactive than the previously, the hydroxyl radical ($HO^{\bullet}$), via the Fenton reaction (Figure 2.26) giving water as the final oxygen reducing product (Danilewicz 2003, Waterhouse and Laurie 2006). Both iron reactions require ferrous form of iron (Fe^{2+}). Phenolic compounds can readily reduce Fe^{3+} to Fe^{2+} in wine conditions to produce quinones. Quinones are electrophiles which condense directly with nucleophilic polyphenols (Danilewicz, 2003), sulfhydryl compounds and amino compounds, and in this process the produced dimers or polymers can rearrange their structure thought an enol-like conversion reaction to form new diphenols. Additionally, these dimers or polymers have lower redox potentials than the initial phenols and are much easier oxidazed.

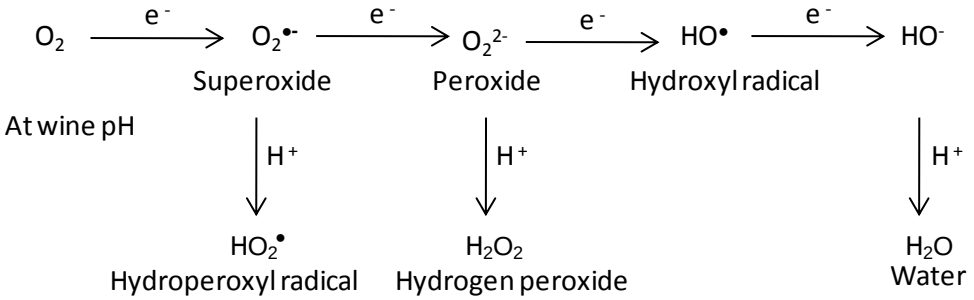

Figure 2.26. Oxygen reduction (Waterhouse and Laurie, 2006).

When phenolic compounds react with ROS, the reaction rate of each phenolic depends on its ability to form a stable product radical. Polyphenols containing a 1,2-dihydroxybenzene ring (a *ortho*-catechol moiety) or a 1,2,3-trihydroxybenzene (a galloyl group) are easier to oxidize because the resulting phenoxyl semi-quinone radical can be stabilized by a second oxygen atom. Briefly, nearly all wine phenolic compounds are very reactive toward the hydroperoxyl radical. Monophenols and their equivalent *meta*-dihydroxybenzene derivative and substituted phenols (especially methoxy derivatives) are not as readily oxidized because they do not produce stabilized semi-quinone radicals. Likewise,

malvidin-3-glucoside, the main anthocyanin present in red wine, is not readily oxidized. Oligomeric and polymeric phenolic compounds (procyanidins and condensed tannins) react similarly with ROS as compared to monomeric *ortho*-catechol derivatives (Waterhouse and Laurie, 2006).

The presence of phenolic radicals in wine has been supported by ESR (electron spin resonance) spectroscopy studies (Troup et al., 1994). Further, it was first detected stable free radicals in red and white wines. In addition they had showed that the radical concentrations and therefore the antioxidant action of white wines were increased by skin and oak exposure (Troup and Hunter, 2002). Recent studies with spin trapping have been used to detect and identify several free radical species in wine under oxidative conditions. In this report, the 1-hydroxylethyl radical was the unique radical species observed when α-(4-pyridyl-1-oxide)-*N*-*tert*-butylnitrone was used as a spin trap in a heated (55ºC), low-sulfite (15 mg/L) red wine. This radical appears to arise from ethanol oxidation via the hydroxyl radical, and this latter species was confirmed by using a high concentration (1.5 M) of the 5,5-dimethylpyrroline-*N*-oxide spin trap, thus providing the first direct evidence of the Fenton reaction in wine (Elias et al., 2009a). Moreover, the addition of either iron, copper, or iron and copper in combination to a red wine resulted in a marked increase in observed spin adducts, demonstrating that trace levels of metal ions are essential catalysts in the oxidation of wine. The addition of catechin to a white wine containing an excess of sulfur dioxide had no effect on the initial rate of radical formation, but was prooxidative in the latter stages of the experiment. Finally, sulfur dioxide was shown to inhibit radical formation in a concentration-dependent manner (Elias et al., 2009b).

Hydrogen peroxide in association with ferrous ions tends to generate ROS such as the hydroxyl radical ($HO^{\bullet}$), which is known as the Fenton reaction (Figure 2.25). Hydroxyl radical is a reduced product of oxygen with a short life-time in water (about 10^{-6} s) and it is recognized to oxidize almost any organic molecule found in wine (Waterhouse and Laurie 2006). Moreover, because of its non-selectivity it will react with the first species it encounters, depending on their concentration (Danilewicz, 2003, Danilewicz 2007, Li et al., 2008), such as ethanol, tartaric acid, glycerol, sugars and organic acids (Danilewicz, 2003, Waterhouse and Laurie 2006). Fenton oxidation of ethanol and tartaric acid (Figure 2.27) generates, respectively, acetaldehyde and glyoxylic acid (Es-Safi et al., 1999b, Singleton et al., 2000, Danilewicz, 2003, Li et al., 2008), however, the oxidation of tartaric

acid by hydroxyl radical was described to produce dihydroxyfumaric acid (Danilewicz, 2003). This oxidative degradation pathway was confirmed by Clark et al. (2008) (Figure 2.28), where dihydroxyfumaric acid was itself reacted with (+)-catechin in a wine-like solution and the yellow pigments formed were identified as xanthylium cations. Furthermore, the concentration of these pigments increased if the wine-like system also contained 0.6 mg/L of Cu^{2+}. These results clearly demonstrate a link between the production of yellow xanthylium cation pigments from (+)-catechin and the degradation of tartaric acid by the hydroxyl radical (Clark et al., 2008). In addition, butane-2,3-diol is oxidized to butan-2-one, 3-hydroxybutan-2-one, and butane-2,3-dione under Fenton conditions (Danilewicz, 2003). The α-hydroxy acids of wine are also subtracts, L(-)-lactic and L(-)-malic acids being oxidized to pyruvic and 2-oxobutanedioic acid, respectively.

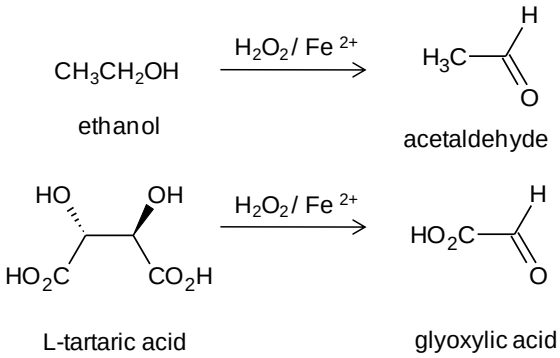

Figure 2.27. Reaction of ethanol and L-tartaric acid with hydrogen peroxide in association with ferrous ions (Danilewicz, 2003).

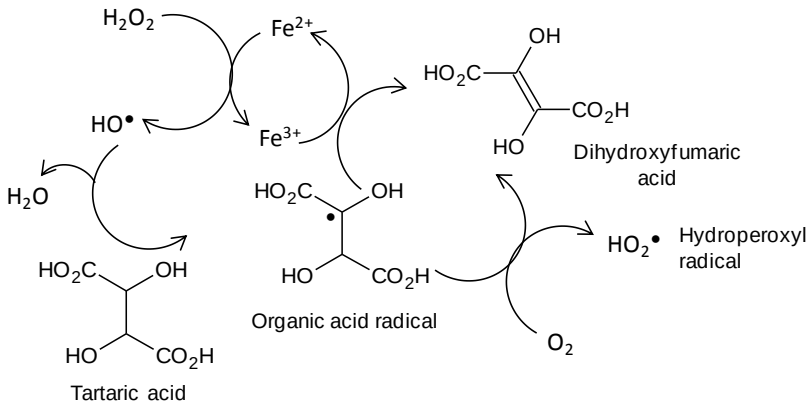

Figure 2.28. The proposed degradation of the tartaric acid via Fenton chemistry mechanisms (Clark et al., 2008).

2.6. Preventing of browning and aromatic degradation in wine: use of antioxidants

2.6.1. Sulfur dioxide in wine

In order to protect musts and wines sulfur dioxide (SO_2) is used in a wide range from pressing to bottling, especially in white wines. Antimicrobial and antioxidant activity are the two most important properties of sulfur dioxide. It regulates the growth of harmful yeast and bacterial growth in the wine and protects against browning. SO_2 have also the ability to add to carbonyl compounds to form non volatile bisulfite adducts and thus preventing unpleasant sensory properties and browning. Concentrations of added SO_2 to wine generally range from 50 to 200 mg/L. In wine, there is an equilibrium between molecular and ionic forms of sulfur dioxide. At wine pH, it can exist in the molecular form, SO_2, but is 94 to 99% in the ionic form as the bisulfite ion, HSO_3^-. Once in solution, in wine, sulfur dioxide can bind with several molecules such as acetaldehyde, anthocyanins, pyruvic acid, glutaric acid, glucose or many phenolic compounds. Thus, there are commonly two fractions of SO_2 in the wine, the "free SO_2", referred to HSO_3^- and SO_2, and the "bound SO_2", indicating sulfur dioxide that is bound mainly to unsaturated compounds. Solely the "free SO_2" is active against oxidation. Sulfur dioxide does not react directly with oxygen but with the oxygen reduced form, hydrogen peroxide (Figure 2.29). As such, SO_2 can inhibit aldehydes formation by competing for hydrogen peroxide. It is

generally believe that is necessary a concentration of approximately 10 mg/L of "free SO_2" to ensure acceptable protection against oxidation (Godden et al., 2005). Nevertheless, the acetaldehyde formation is still occurring as a consequence of the considerable amounts of ethanol in wine. SO_2 also play an important role in reducing quinones, formed during the oxidation process, back to their phenol form, where the presence of metals is crucial.

In a wine-model system [12% (v/v) aqueous ethanol containing tartaric acid at pH=3.6)], under aerial oxygen saturation conditions, no significant oxidation is observed in SO_2, unless iron and copper ions are present. When these metal ions are added a slow oxidation is observed and bound SO_2 also increase to a small but significant extent. These results are consistent with a radical chain mechanism initiated by metal catalysis, in which powerful oxidizing radicals, capable of oxidizing ethanol to acetaldehyde, are produced (Danilewicz, 2007). This increase in bound SO_2 can be prevented by polyphenols that scavenge these intermediate radicals and thus inhibit SO_2 autoxidation, which consequently should not occur in wine. In a wine-model system, when 4-methylcatechol (4-MeC) is present, at a concentration that simulate the reducing capacity of red wine, again no significant SO_2 oxidation is observed without addition of iron and copper ions. After the oxidation of the catechol, hydrogen peroxide is generated and will react with the SO_2 (Figure 2.29). In the presence of both metal ions the rate of SO_2 oxidation is markedly increased compared to SO_2 alone and then is dependent on the catechol concentration. These results demonstrate the crucial importance of metal ions in allowing polyphenol oxidation and that the rate of SO_2 consumption is dependent on the rate of catechol oxidation. When iron and copper ions are added separately, only a modest increase in rate of catechol oxidation is observed. However, when combined, marked synergism is observed and the rate then became very sensitive to copper concentration. It is proposed that copper, by interacting with oxygen, facilitates redox cycling of iron. Exposure of red wines to the above conditions produced similar results regarding SO_2 oxidation (Danilewicz, 2007).

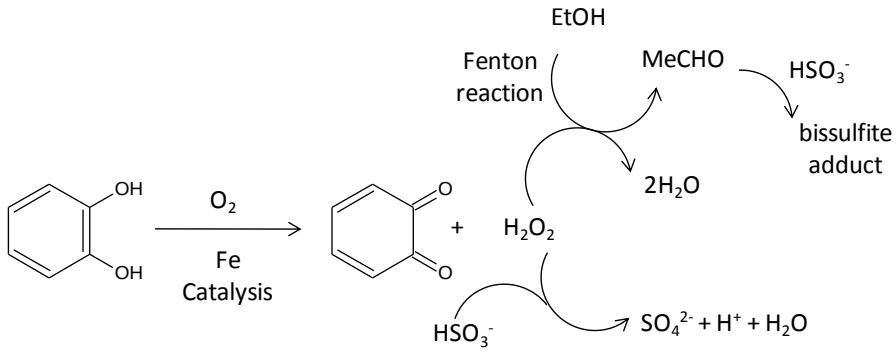

Figure 2.29. The scavenging of hydrogen peroxide formed by the oxidation of catechols by SO_2, so preventing oxidation of ethanol by the Fenton reaction (Danilewicz, 2007).

Bisulfite is known to react rapidly with hydrogen peroxide but it should also be capable of reacting with the quinone (Figure 2.30). Moreover, in the catechol oxidation, hydrogen peroxide and a quinone are formed, both of which reacting with SO_2. The aerial oxidation of catechol in the presence of benzenesulfinic acid (BA), for quinones trapping, slowly produced the BA-quinone adduct in high yield. Nevertheless, it is quickly prepared by adding ferric chloride, demonstrating that the quinone is produced and that the catechol is rapidly oxidized by Fe^{3+} ions. This reaction is important in the catalytic function of the metal (Danilewicz et al., 2008). The oxygen and SO_2 molar reaction ratio is 1:2, which is consistent with one mole equivalent of SO_2 reacting with hydrogen peroxide and a second with the quinone. It was observed that, when BA was incorporate to the oxidation system, to trap the quinone, the oxygen/SO_2 ratio was reduced to 1:1. Moreover, the rate of the reaction of oxygen with SO_2 increased with catechol concentration. However, the rate of reaction of oxygen is also markedly accelerated by SO_2 and by BA, and it is proposed that substances that react with quinones accelerate catechol autoxidation. Moreover, the oxygen/SO_2 molar reaction ratio in analysed red wines was found to be 1:~1.7, suggesting that some nucleophilic substances may be competing with bisulfite for quinones. The rate of reaction of oxygen is also accelerated by SO_2 in red wine (Danilewicz et al., 2008).

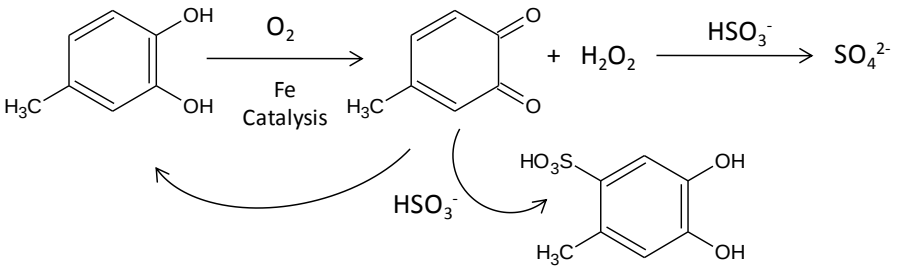

Figure 2.30. The interaction of bisulfite with hydrogen peroxide and quinones following catechol oxidation (Danilewicz et al., 2008).

2.6.2. Ascorbic acid in wine

Ascorbic acid is naturally present in grapes but is usually rapidly consumed after crushing, typically due to ascorbic acid either scavenging oxygen or reducing *ortho*-quinone derivatives formed from the enzymatic oxidation of phenolic compounds. The ascorbic acid present in white wine is mostly due to exogenous additions, often just before the bottling of white wine, although it may be used at various stages in the wine production process. The levels of ascorbic acid added may vary considerably, but it is typically added at rates ranging from 50 to 150 mg/L (Barril et al., 2009). Ascorbic acid is added to white wine due to its efficient ability to scavenge molecular oxygen, but in the process it is initially converted to dehydroascorbic acid and hydrogen peroxide. The dehydroascorbic acid then undergoes rapid degradation into a variety of species including numerous carboxylic acids, ketones, and aldehydes. In fact, the estimative of the formal potential by cyclic voltammetry, which quantifies the reducing power of antioxidants, have demonstrated that ascorbic acid is realizable for oxidation, considering it powerful reducing power (E = 210 mV) in a wine solution of 12% ethanol, 0.05 M tartaric acid, and pH 3.6 (Kilmartin et al., 2001).

After reducing sugars, ascorbic acid appears to be the most widely studied carbonyl component in the processes of non-enzymatic browning. Ascorbic acid undergoes a reaction with amino acids similar to that of sugars (except that amino acids are not necessary for browning). Ascorbic acid is very reactive and its degradation leads to the formation of dicarbonyl intermediates and subsequently browning compounds (Davies and Wedzicha, 1992, Davies and Wedzicha, 1994). Along with browning, ascorbic acid is also

a source of aroma/flavor compounds, namely, in the presence of amino acids via the Maillard reaction (Yu and Zhang, 2010a, Yu and Zhang, 2010b).

The influence of ascorbic acid in the composition, color and flavor properties of a Riesling and a wooded Chardonnay wine has been studied. Ascorbic acid additions to the Riesling wine were made four days (90 mg/L) and two days (10 mg/L) prior to bottling, totaling 100 mg/L. For the wooded Chardonnay, an addition (60 mg/L) was made eight days prior to bottling and another (15 mg/L) six days prior to bottling, totaling 75 mg/L of added ascorbic acid. Results have showed that addition of ascorbic acid at bottling resulted in wines with no difference in aroma or less oxidized and/or fresher fruity aromas. Moreover, concerning color, for the Chardonnay wines, the effect of ascorbic acid addition at bottling assessed between two weeks and two years after bottling suggested that wines without addition were browner and had more overall color intensity. For the Riesling wines, ascorbic acid addition had no significant effect in brownness and overall color intensity, although the Riesling wines with ascorbic acid were generally higher in yellow color (Skouroumounis et al., 2005).

On the contrary, recent studies have shown the increased production of phenolic pigments from model wine systems of ascorbic acid and (+)-catechin and demonstrated that a degradation product emanating from ascorbic acid was able to react with (+)-catechin and form colored xanthylium cations (Bradshaw et al., 2001, Bradshaw et al., 2003, Barril et al., 2008, Barril et al., 2009). In general, phenolic pigments formed during the storage of white wine are undesirable as they are perceived as indicative of wine spoilage. Furthermore, the stereochemical influence of ascorbic acid and erythorbic acid on oxidation processes in a model wine system was studied and xanthylium cation pigments were identified as the major contributor to color development. Also, the production of pigment precursors, previously identified as furanone-substituted flavan-3-ols, was confirmed and their corresponding xanthylium cation pigments were lower in the presence of erythorbic acid than ascorbic acid. These results demonstrate that erythorbic acid is more efficient at minimizing oxidative color development than ascorbic acid in the model wine system (Clark et al., 2010). In recent studies (Roussis et al., 2007, Lambropoulosa et al., 2007, Roussis et al., 2008, Lavigne et al., 2007), alternative options have been assessed for the prevention of oxidation during wine storage, including the addition of caffeic and gallic acids and glutathione. To find the most suitable compound that could replace or

supplement sulfur dioxide, it is very important to understand the chemical roles of SO_2 during wine aging. Concentrations of aromatic volatiles during storage of white wine with reduced (35 mg/L) or typical (55 mg/L) amount of free sulfur dioxide for up to 210 days (7 months) were measured to evaluate how decreased SO_2 affects wine volatiles. Additions of caffeic acid (60 mg/L), glutathione (20 mg/L), or their mixture (30 mg/L + 10 mg/L, respectively) to wine with reduced amount of SO_2 were also examined. In control and treated wines, concentrations of acetate esters, ethyl esters, terpenes, and fatty acids decreased during wine storage, while concentrations of higher alcohols remained constant. Wine samples with reduced or typical amount of SO_2 had statistically equal concentrations of volatiles, with the exception of ethyl acetate, which was higher in the latter. Caffeic acid, glutathione, or their mixture slowed the decrease of several volatile esters and terpenes such as ethyl acetate, isoamyl acetate, ethyl caproate, ethyl caprylate, ethyl caprate, and linalool. These results suggest that SO_2 gives only limited protection to wine volatiles but that caffeic acid, glutathione, or their mixture protects several aromatic volatiles of white wine with reduced amount of SO_2 (Roussis et al., 2007). Furthermore, the decrease of isoamyl acetate, ethyl hexanoate and linalool during storage is protected by SO_2 additions at, respectively, 20 (isoamyl acetate), 40 (ethyl hexanoate) and 60 mg/L (linalool). Mixtures of glutathione with caffeic acid or gallic acid were also protective, where additions of glutathione + caffeic acid were more effective than additions of glutathione + gallic acid. These results suggested that SO_2 protects some wine aroma volatiles, but only at high concentrations. On the other hand, mixtures of the wine constituents glutathione + caffeic acid or gallic acid are more effective at concentrations similar to those existing in wines (Lambropoulosa et al., 2007, Roussis et al., 2008).

2.7. References

Atanasova, V., Fulcrand, H., Le Guernevé, C., Cheynier, V., & Moutounet, M. (2002). Structure of a new dimeric acetaldehyde malvidin-3-glucoside condensation product. *Tetrahedron Letters, 43,* 6151-6153.

Barrett, G. C. (1985). Reactions of amino acids. In "Chemistry and Biochemistry of amino acids." ed. by G.C. Barrett, Chapman and Hall, London-New York, 355-375.

Bakker, J., & Timberlake, C. F. (1997). Isolation, identification, and characterization of new colour-stable anthocyanins occurring in some red wines. *Journal of Agricultural and Food Chemistry, 45,* 35-43.

Barril, C., Clark, A. C., & Scollary, G. R. (2008). Understanding the contribution of ascorbic acid to the pigment development in model white wine systems using liquid chromatography with diode array and mass spectrometry detection techniques. *Analytica Chimica Acta, 621,* 44-51.

Barril, C., Clark, A. C., Prenzler, P. D., Karuso, P., & Scollary, G. R. (2009). Formation of pigment precursor (+)-1´´-methylene-6´´-hydroxy-2*H*-furan-5´´-one-catechin isomers from (+)-catechin and a degradation product of ascorbic acid in a model wine system. *Journal of Agricultural and Food Chemistry, 57,* 9539-9546.

Betes-Saura, C., Andres-Lacueva, C., & Lamuela-Raventos, R. M. (1996). Phenolics in white free run juices and wines from Penedès by high-performance liquid chromatography: Changes during vinification. *Journal of Agricultural and Food Chemistry, 44,* 3040-3046.

Bokuchava, M. A., & Skobeleva, N. I. (1969). The chemistry and biochemistry of tea and tea manufacture. *Advances in Food Research, 17,* 215-241.

Boulton, R. B., Singleton, V. L., Bisson, L. F., & Kunkee, R. E. (2001). Principles and Practices of Winemaking (Chinese Trans.). Beijing: China Light Industry Press.

Bradshaw, M. P.; Prenzler, P. D., & Scollary, G. R. (2001). Ascorbic acid-induced browning of (+)-catechin in a model wine system. *Journal of Agricultural and Food Chemistry, 49,* 934-939.

Bradshaw, M. P., Prenzler, P. D., Scollary, G. R., & Cheynier, V. (2003). Defining the ascorbic acid crossover from anti-oxidant to pro-oxidant in a model wine matrix containing (+)-catechin. *Journal of Agricultural and Food Chemistry, 51,* 4126-4132.

Cacho, J., Castells, J. E., Esteban, A., Laguna, B., & Sagristá, N. (1995). Iron, copper, and manganese influence on wine oxidation. *American Journal of Enology and Viticulture, 46,* 380-384.

Câmara, J. S., Alves, M. A., & Marques, J. C. (2006). Changes in volatile composition of Madeira wines during their oxidative ageing. *Analytica Chimica Acta 563,* 188-197.

Castellari, M., Matricardi, L., Arfelli, G., Galassi, S., & Amati, A. (2000). Level of single bioactive phenolic compounds in red wine as a function of the oxygen supplied during storage. *Food Chemistry, 69,* 61-67.

Cheynier, V. F., Trousdale, E. K., Singleton, V. L., Salgues, M. J., & Wylde, R. (1986). Characterization of 2-S-glutathioylcaftaric acid and its hydrolysis in relation to grape wines. *Journal of Agricultural and Food Chemistry, 34,* 217-221.

Cheynier, V. F., & Van Hulst, M. W. J. (1988). Oxidation of trans-caftaric acid and 2-S-glutathionylcaftaric acid in model solutions. *Journal of Agricultural and Food Chemistry, 36,* 10-15.

Cheynier, V., Fulcrand, H., Guyot, S., Oszmianski, J., & Moutounet, M. (1995). Reactions of enzymically generated quinones in relation to browning in grape musts and Wines. In

Lee, C. Y. & Whitaker, J. R. (Eds.), Enzymatic browning and its prevention in foods, ACS Symposium Series, Vol. 600, American Chemical Society: Washington, DC, 130-143.

Cheynier, V., Fulcrand, H., & Moutounet, M. (2000). Ossidazione dei polifenoli nei mosti d'uva (Oxidation of polyphenols in wine musts). *Vignevini*, *27* (11) 52-56.

Cheynier, V. (2005). Polyphenols in foods are more complex than often thought. *American Journal of Clinical Nutrition, 81*, 223S-9S.

Clark, A. C. (2008). The production of yellow pigments from (+)-catechin and dihydroxyfumaric acid in a model wine system. *European Food Research and Technology, 226*, 925-931.

Clark, A. C., Vestner, J., Barril, C., Maury, C., Prenzler, P. D., & Scollary, G. R. (2010). The influence of stereochemistry of antioxidants and flavanols on oxidation processes in a model wine system: ascorbic acid, erythorbic acid, (+)-catechin and (-)-epicatechin. *Journal of Agricultural and Food Chemistr*y, 58, 1004-1011.

Cremer, D. R., Vollenbroeker, M., & Eichner, K. (2000). Investigation of the formation of "Strecker aldehydes"from the reaction of Amadori rearrangement products with a-amino acids in low moisture model systems. *European Food Research and Technology, 211,* 400-403.

Cruz, L., Teixeira, N., Silva, A. M. S., Mateus, N., Borges, J., & De Freitas, V. (2008). Role of vinylcatechin in the formation of pyranomalvidin-3-glucoside-(+)-catechin. *Journal of Agricultural and Food Chemistry, 56,* 10980-10987.

Cutzach, I., Chatonnet, P., & Dubourdieu, D. (1999). Study of the formation mechanisms of some volatile compounds during the aging of sweet fortified wines. *Journal of Agricultural and Food Chemistry, 47,* 2837-2846.

Danilewicz, J. C. (2003). Review of reaction mechanisms of oxygen and proposed intermediate reduction products in wine: Central role of iron and copper. *American Journal of Enology and Viticulture, 54,* 73-85.

Danilewicz, J. C. (2007). Interaction of sulfur dioxide, polyphenols, and oxygen in a wine-model system: Central role of iron and copper. *American Journal of Enology and Viticulture*, 58, 53-60.

Danilewicz, J. C., Seccombe, J. T., & Whelan, J. (2008). Mechanism of interaction of polyphenols, oxygen, and sulfur dioxide in model wine and wine. *American Journal of Enology and Viticulture, 59,* 128-136.

Davidek, T., Nathalie, C., Aubin, S., & Blank, I. (2002). Degradation of the Amadori compound *N*-(1-Deoxy-d-fructos-1-yl)glycine in aqueous model systems. *Journal of Agricultural and Food Chemistry, 50,* 5472-5479.

Davies, C. G. A., & Wedzicha, B. L. (1992). Kinetics of the inhibition of ascorbic acid browning by sulphite. *Food Additives and Contaminents, 9,* 471-477.

Davies, C. G. A., & Wedzicha, B. L. (1994). Ascorbic acid browning: The incorporation of C1 from ascorbic acid into melanoidins. *Food Chemistry, 49,* 165-167.

De Beer, D., Joubert, E., Gelderblom, W. C. A., & Manley, M. (2002). Phenolic compounds: A review of their possible role as in vivo antioxidants of wine. *South African Journal of Enology and Viticulture, 23,* 48-61.

De Beer, D., Joubert, E., Marais, J., & Manley, M. S. (2008). Effect of oxygenation during maturation on phenolic composition, total antioxidant capacity, colour and sensory quality of Pinotage wine. *South African Journal for Enology and Viticulture 29,* 13-25.

De Freitas, V. A. P., Glories, Y., & Monique, A. (2000). Developmental changes of procyanidins in grapes of red Vitis Vinifera varieties and their composition in respective wines. *American Journal of Enology and Viticulture*, *51*, 397-403.

De Revel, G., Marchand, S., & Bertrand, A. (2004). Identification of Maillard-Type Aroma Compounds in Wine-like Model Systems of Cysteine-Carbonyls: Occurrence in Wine. *ACS Symposium Series*, *871*, 353-364.

Du Toit, W. J., Marais, J., Pretorius, I. S., & Du Toit, M. (2006). Oxygen in Must and Wine: A review. *South African Journal of Enology and Viticulture*, *27*, 76-94.

Dubernet, M., & Ribéreau-Gayon, P. (1973). Presence et significance dans les moutes et les vins de la tyrosine du raisin. *Connaissance de la vigne et du vin*, *7*, 283-302.

Elias, R. J., Andersen, M. L., Skibsted, L. H., & Waterhouse, A. L. (2009a). Identification of free radical intermediates in oxidized wine using electron paramagnetic resonance spin trapping. *Journal of Agricultural and Food Chemistry*, *57*, 4359-4365.

Elias, R. J., Andersen, M. L., Skibsted, L. H., & Waterhouse, A. L. (2009b). Key factors affecting radical formation in wine studied by spin trapping and EPR spectroscopy. *American Journal of Enology and Viticulture*, *60*, 471-476.

Escribano-Bailón, M. T., Guerra, M. T., Rivas-Gonzalo, J. C., & Santos-Buelga, C. (1995). Proanthocyanidins in skins from different grape varieties. *Zeitschrift für Lebensmittel-Untersuchung und -Forschung*, *200*, 221-224.

Escudero, A., Cacho, J., & Ferreira, V. (2000a). Isolation and identification of odorants generated in wine during its oxidation: a gas chromatography-olfactometry study. *European Food Research and Technology*, *211*, 105-110.

Escudero, A., Hernandez-Orte, P., Cacho, J., & Ferreira, V. (2000b). Clues about the role of methional as a character impact odorant of some oxidized wines. *Journal of Agricultural and Food Chemistry, 48,* 4268-4272.

Escudero, A., Asensio, E., Cacho, J., & Ferreira, V. (2002). Sensory and chemical changes of young white wines stored under oxygen. An assessment of the role played by aldehydes and some other important odorants. *Food Chemistry, 77,* 325-331.

Es-Safi, N. E., Cheynier, V., & Moutounet, M. (2002). Role of aldehydic derivatives in the condensation of phenolic compounds with emphasis on the sensorial properties of fruit-derived foods. *Journal of Agricultural and Food Chemistry, 50,* 5571-5585.

Es-Safi, N. E., Le Guernevé, C., Labarbe, B., Fulcrand, H., Cheynier, V., & Moutounet, M. (1999a). Structure of a new xanthylium salt derivative. *Tetrahedron Letters, 40,* 5869-5872.

Es-Safi, N. E., Fulcrand, H., Cheynier, V., & Moutounet, M. (1999b). Competition between (+)-catechin and (-)-epicatechin in acetaldehyde-induced polymerization of flavanols. *Journal of Agricultural and Food Chemistry, 47,* 2088-2095.

Es-Safi, N. E., Le Guernevé, C., Cheynier, V., & Moutounet, M. (2000). New phenolic compounds formed by evolution of (+)-catechin and glyoxylic acid in hydroalcoholic solution and their implication in colour changes of grape-derived foods. *Journal of Agricultural and Food Chemistry, 48,* 4233-4240.

Fors, S. (1983). Sensory properties of volatile Maillard reaction products and related compounds. A literature review. In The Maillard reaction in foods and nutrition. *ACS Symposium Series, 215,* 185-286.

Francia-Aricha, E. M., Guerra, M. T., Rivasgonzalo, J. C., & Santosbuelga, C. (1997). New anthocyanin pigments formed after condensation with flavanols. *Journal of Agricultural and Food Chemistry, 45,* 2262-2266.

Francia-Aricha, E. M., Rivas-Gonzalo, J. C., & Santos-Buelga, C. (1998). Effect of malvidin-3-monoglucoside on the browning of monomeric and dimeric flavanols. *Zeitschrift Fur Lebensmittel-Untersuchung Und-Forschung a-Food Research and Technology*, *207,* 223-228.

Friedman, M. (1996). Food browning and its prevention: An overview. *Journal of Agricultural and Food Chemistry, 44,* 631-653.

Fulcrand, H., Cheynier, V., Oszmianski, J., & Moutounet, M. (1997). An oxidized tartaric acid residue as a new bridge potentially competing with acetaldehyde in flavan-3-ol condensation. *Phytochemistry, 46,* 223-227.

Fulcrand, H., Dueñas, M., Salas, E., & Cheynier, V. (2006). Phenolic reactions during winemaking and ageing. *American Journal of Enology and Viticulture, 57,* 289-297.

Gambuti, A., Rinaldi, A., Ugliano, M., & Moio, L. (2013). Evolution of phenolic compounds and astringency during aging of red wine: effect of oxygen exposure before and after bottling. *Journal of Agricultural and Food Chemistry, 61,* 1618-1627.

Ginz, M., Balzer, H. H., Bradbury, A. G. W., & Maier, H. G. (2000). Formation of aliphatic acids by carbohydrate degradation during roasting of coffee. *European Food Research and Technology, 211,* 404-410.

Godden, P., Lattey, K., Francis, L., Gishen, M., Cowey, G., Holdstock, M., Robinson, E., Waters, E., Skouroumounis, G., Sefton, M. A., Capone, D., Kwiatkowski, M., Field, J., Coulter, A., D'Costa, N. & Bramley, B. (2005). Towards offering wine to the consumer in optimal condition-the wine, the closures and other packaging variables: A review of awri research examining the changes that occur in wine after bottling. *The Australian and New Zealand Wine Industry Journal. 20,* 20-30.

Granvogl, M., Beksan, E. & Schieberle, P. (2012). New insights into the formation of aroma-active Strecker aldehydes from 3-oxazolines as transient intermediates. *Journal of Agricultural and Food Chemistry, 60,* 6312-6322.

Hashiba, H. (1978). Isolation and identification of Amadori compounds from miso, white wine and sake. *Agricultural and Biological Chemistry, 42*, 1727-1731.

Hidalgo, F. J., & Zamora, R. (2004). Strecker-type degradation produced by the lipid oxidation products 4,5-epoxy-2-alkenals. *Journal of Agricultural and Food Chemistry, 52,* 7126-7131.

Hodge, J. E. (1953). Chemistry of browning reactions in model systems. *Journal of Agricultural and Food Chemistry, 1*, 928-943.

Hofmann, T., & Schieberle, P. (2000). Formation of aroma-active Strecker-aldehydes by a direct oxidative degradation of Amadori compounds. *Journal of Agricultural and Food Chemistry, 48,* 4301-4305.

Hofmann, T., Münch, P., & Schieberle, P. (2000). Quantitative model studies on the formation of aroma-active aldehydes and acids by Strecker-type reactions. *Journal of Agricultural and Food Chemistry, 48,* 434-440.

Huyghues-Despointes, A., & Yaylayan, V. A. (1996). Retro-aldol and redox reactions of Amadori compounds: Mechanistic studies with variously labelled D-[^{13}C] glucose. *Journal of Agricultural and Food Chemistry, 44,* 672-681.

James, W. O., Roberts, E. A. H., Beevers, H., & De Kock, P. C. (1948). The secondary oxidation of amino-acids by the catechol oxidase of Belladonna. *Biochemical Journal, 43,* 626-636.

Keim, H., De Revel, G., Marchand, S., & Bertrand, A. (2002). Method for determining nitrogenous heterocycle compounds in wine. *Journal of Agricultural and Food Chemistry, 50,* 5803-5807.

Keyhani, A., & Yaylayan, V. A. (1996). Elucidation of the mechanism of pyrazinone formation in glycine model systems using labeled sugars and amino acids. *Journal of Agricultural and Food Chemistry, 44,* 2511-2516.

Kilmartin, P. A., Zou, H., & Waterhouse, A. L. (2001). A cyclic voltammetry method suitable for characterizing antioxidant properties of wine and wine phenolics. *Journal of Agricultural and Food Chemistry, 49,* 1957-1965.

Kroh, L.W. (1994). Caramelisation in food and beverages. *Food Chemistry, 51,* 373-379.

Kutyrev, A. A., & Moskva, V. V. (1991). Nucleophilic reactions of quinones. *Russian Chemical Reviews, 60,* 72-78.

Lambropoulosa, I., & Roussis, I. G. (2007). Inhibition of the decrease of volatile esters and terpenes during storage of a white wine and a model wine medium by caffeic acid and gallic acid. *Food Research International, 40,* 176-181.

Lavigne, V., Pons, A., & Dubourdieu, D. (2007). Assay of glutathione in must and wines using capillary electrophoresis and laser-induced fluorescence detection. Changes in concentration in dry white wines during alcoholic fermentation and ageing. *Journal of Chromatography A, 1139,* 130-135.

Ledl, F., & Schleicher, E. (1990). New aspects of the Maillard reaction in foods and in the human body. *Angewandte Chemie International Edition (English), 29,* 565-706.

Lee, D. F., Swinny, E. E., & Jones, G. P. (2004). NMR identification of ethyl-linked anthocyanin-flavanol pigments formed in model wine ferments. *Tetrahedron Letters, 45,* 1671-1674.

Li, H., Guo, A., & Wang, H. (2008). Mechanisms of oxidative browning of wine. *Food Chemistry, 108,* 1-13.

Ling, A. R., & Malting J. (1908). *Journal of the Institute of Brewing, 14,* 494-521.

Loscos, N., Hernandez-Orte, P., Cacho, J, & Ferreira V. (2010). Evolution of the aroma composition of wines supplemented with grape flavour precursors from different varietals during accelerated wine ageing. *Food Chemistry, 120,* 205-216.

Maillard, L. C. (1912). Action des acides aminés sur les sucres. Formation des Mélanoidins par voie méthodique. *Compte-rendu de l'Académie des sciences, 154,* 66-68.

Main, G. L. Juice fining treatments to reduce browning and use of sulfur dioxide in white wine production (1992). Ph.D. Thesis, University of Arkansas, AR, United States.

Marchand, S, De Revel, G., & Bertrand, A. (2000). Approaches to wine aroma: Release of aroma compounds from reactions between cysteine and carbonyl compounds in wine. *Journal of Agricultural and Food Chemistry, 48,* 4890-4895.

Marchand, S.; De Revel, G., & Bertrand, A. (2002). Possible mechanism for involvement of cysteine in aroma production in wine. *Journal of Agricultural and Food Chemistry, 50,* 6160-6164.

Marchand, S., Almy, J., & De Revel, G. (2011). The cysteine reaction with diacetyl under wine-like conditions: proposed mechanisms for mixed origins of 2-methylthiazole, 2-methyl-3-thiazoline, 2-methylthiazolidine, and 2,4,5-trimethyloxazole. *Journal of Food Science, 76(6),* C861-8.

Martins, S. I. F. S., Marcelis, A. T. M. & Van Boekel, M. A. J. S. (2003a). Kinetic modeling of the Amadori *N*-(1-deoxy-D-fructos-1-yl)glycine degradation pathways. Part I - Reaction mechanism. *Carbohydrate Research, 338,* 1651-1663.

Martins, S. I. F. S., & Van Boekel, M. A. J. S. (2003b). Kinetic modelling of the Amadori *N*-(1-deoxy-D-fructos-1-yl)glycine degradation pathways. Part II - Kinetic analysis. *Carbohydrate Research, 338,* 1665-1678.

Mateus N, Silva A. M. S., Santos-Buelga, C., Rivas-Gonzalo, J. C., & De Freitas, V. (2002). Identification of anthocyanin-flavanol pigments in red wines by NMR and mass spectrometry. *Journal of Agricultural and Food Chemistry, 50,* 2110-2116.

Mateus, N., Silva, A. M. S., Rivas-Gonzalo, J. C., Santos-Buelga, C., & De Freitas, V. (2003). A new class of blue anthocyanin-derived pigments isolated from red wines. *Journal of Agricultural and Food Chemistry, 51,* 1919-1923.

Motoda, S. (1979). Formation of aldehydes from amino acids by polyphenol oxidase. *Journal of Fermentation Technology, 57,* 395-399.

Nikolantonaki, M., & Waterhouse, A. L. (2012). A Method to quantify quinone reaction rates with wine relevant nucleophiles: A key to the understanding of oxidative loss of varietal thiols. *Journal of Agricultural and Food Chemistry, 60,* 8484-8491.

Oliveira e Silva, H., Guedes de Pinho, P., Machado, B., Hogg, T., Marques, J. C., Câmara, J. S., Albuquerque, F., & Silva Ferreira, A. C. (2008). Impact of forced-aging process on Madeira wine flavour. *Journal of Agricultural and Food Chemistry, 56,* 11989-11996.

Peleg, H., Gacon K., Schlich, P., & Noble, A. C. (1999). Bitterness and astringency of flavan-3-ol monomers, dimers and trimers. *Journal of the Science of Food and Agriculture, 79,* 1123-1128.

Pourova, J., Kottova, M., Voprsalova, M., & Pour, M. (2010). Reactive oxygen and nitrogen species in normal physiological process. *Acta Physiologica, 198,* 15-35.

Prieur, C., Rigaud, J., Cheynier, V., & Moutounet, M. (1994). Oligomeric and polymeric procyanidins from grape seeds. *Phytochemistry, 36*, 781-784.

Pripis-Nicolau, L., Revel, G., Bertrand, A., & Maujean, A. (2000). Formation of flavor components by the reaction of amino acid and carbonyl compounds in mild conditions. *Journal of Agricultural and Food Chemistry, 48,* 3761-3766.

Quinn, K. M., & Singleton, V. L. (1985). Isolation and identification of ellagitannins from white oak and an estimation of their roles in wine. *American Journal of Enology and Viticulture, 36*, 148-155.

Ribéreau-Gayon, P., Glories, Y., Maugean, A., & Dubourdieu, D. (Ed.) (2000) Handbook of Enology (Volume 2): The chemistry of wine stabilization and treatments, England: John Wiley & Sons, New York.

Rigaud, J., Cheynier, V., Souquet, J. M., & Moutounet, M. (1991). Influence of must composition on phenolic oxidation kinetics. *Journal of the Science of Food and Agriculture, 57*, 55-63.

Rivas-Gonzalo, J. C., Bravo-Haro, S., & Santos-Buelga, C. (1995). Detection of compounds formed through the reaction of malvidin 3-monoglucoside and catechin in the presence of acetaldehyde. *Journal of Agricultural and Food Chemistry, 43,* 1444-1449.

Rizzi, G. P. (2006). Formation of strecker aldehydes from polyphenol-derived quinones and α-amino acids in a nonenzymic model system. *Journal of Agricultural and Food Chemistry, 54*, 1893-1897.

Rizzi, G. P. (2008). The strecker degradation of amino acids: Newer avenues for flavor formation. *Food Reviews International, 24*, 416-435.

Robards, K., Prenzler, P. D., Tucker, G., Swatsitang, P., & Glover, W. (1999). Phenolic compounds and their role in oxidative processes in fruits. *Food Chemistry, 66,* 401-436.

Roussis, I. G., Lambropoulos, I., & Tzimas, P. (2007). Protection of volatiles in a wine with low sulfur dioxide by caffeic acid or glutathione. *American Journal of Enology and Viticulture, 58,* 274-278.

Roussis, I. G. & Sergianitis, S. (2008). Protection of some aroma volatiles in a model wine medium by sulfur dioxide and mixtures of glutathione with caffeic acid or gallic acid. *Flavour and Fragrance Journal, 23,* 35-39.

Salas, E., Duenas, M., Schwarz, M., Winterhalter, P., Cheynier, W., & Fulcrand, H. (2005). Characterization of pigments from different high speed countercurrent chromatography wine fractions. *Journal of Agricultural and Food Chemistry, 53,* 4536-4546.

Salgues, M., Cheynier, V., Gunata, Z., & Wylde, R. (1986). Oxidation of grape juice 2-S-glutathionylcaffeoyltartaric acid by Botrytis cinerea laccase and characterization of a new substance: 2,5-di-S-glutathionylcaffeoyltartaric acid. *Journal of Food Science, 51,* 1191-1194.

Sánchez-Ferrer, A., Rodríguez-López, J. N., García-Cánovas, F., & García-Carmona, F. (1995). Tyrosinase: a comprehensive review of its mechanism. *Biochimica et Biophysica Acta, 1247,* 1-11.

Shchepinov, M. S. (2007). Reactive Oxygen Species, Isotope Effect, Essential Nutrients, and Enhanced Longevity. *Rejuvenation Research, 10 (1),* 47-60.

Shonberg, A., & Moubacher, R. (1952). The Strecker degradation of α-amino acids. *Chemical Reviews, 50,* 261-277.

Shu, C-K. (1998). Pyrazine formation from amino acids and reducing sugars - a pathway other than Strecker degradation. *Journal of Agricultural and Food Chemistry, 46*, 1515-1517.

Silva Ferreira, A. C., Guedes de Pinho, P., Rodrigues, P., & Hogg, T. (2002). Kinetics of oxidative degradation of white wines and how they are affected by selected technological parameters. *Journal of Agricultural and Food Chemistry, 50,* 5919-5924.

Silva Ferreira, A. C., Hogg, T., & Guedes de Pinho, P. (2003). Identification of key odorants related to the typical aroma of oxidation-spoiled white wines. *Journal of Agricultural and Food Chemistry, 51,* 1377-1381.

Silva Ferreira, A. C., Reis, S., Rodrigues, C., Oliveira, C., & Guedes de Pinho, P. (2007). Simultaneous determination of ketoacids and dicarbonyl compounds, key Maillard intermediates on the generation of aged wine aroma. *Journal of Food Science, 72 (5),* S314-S318.

Simpson, R. F. (1982). Factors affecting oxidative browning of white wine. *Vitis, 21,* 233-239.

Singleton, V. L., Trousdale, E., & Zaya, J. (1979). Oxidation of wines I. Young white wines periodically exposed to air. *American Journal of Enology and Viticultur*e, *30,* 49-54.

Singleton, V. L. (1987). Oxygen with phenols and related reactions in musts, wines, and model systems: Observations and practical implications. *American Journal of Enology and Viticulture, 38,* 69-77.

Singleton, V. L., & Cilliers, J. J. L. (1995). Phenolic Browning: A Perspective from Grape and Wine. Research Enzymatic Browning and Its Prevention *ACS Symposium Series*, Vol. 600 Chapter 3, 23-48.

Singleton, V. L. (2000). A survey of wine ageing reactions, especially with oxygen. In Proceedings of the ASEV 50th Anniversary Annual Meeting. American Society for Enology and Viticulture, Davis, California, 323-336.

Skouroumounis, G. K., Kwiatkowski, M. J., Francis, I. L., Oakey, H., Capone, D. L., Peng, Z., Duncan, B., Sefton, M. A., & Waters, E. J. (2005). The influence of ascorbic acid on the composition, colour and flavour properties of a Riesling and a wooded Chardonnay wine during five years' storage. *Australian Journal of Grape and Wine Research, 11,* 355-368.

Souquet, J. M., Cheynier, V., Brossaud, F., & Moutounet, M. (1996). Polymeric proanthocyanidins from grape skins. *Phytochemistry, 43,* 509-512.

Sousa, A., Mateus, N., Silva, A. M. S., Vivas, N., Nonier, M. F., Pianet, I., & De Freitas, V. (2010). Isolation and Structural Characterization of Anthocyanin-furfuryl Pigments. *Journal of the Science of Food and Agriculture, 58,* 5664-5669.

Strecker, A. (1862). Notiz über eine eigenthümliche oxydation durch alloxan. *Justus Liebigs Annalen der Chemie, 123,* 363-365.

Sun, B. S., Pinto, T., Leandro, M. C., Ricardo da Silva, J. M., & Spranger, M. I. (1999). Transfer of catechins and proanthocyanidins from solid parts of the grape cluster into wine. *American Journal of Enology and Viticulture, 50,* 179-184.

Tao, J., Dykes, S. I., & Kilmartin, P. A. (2007). Effect of SO_2 concentration on polyphenol development during red wine micro-oxygenation *Journal of the Science of Food and Agriculture, 55,* 6104-6109.

Timberlake, C. F., & Bridle, P. (1976). Interactions between anthocyanins, phenolic compounds, and acetaldehyde and their significance in red wines. *American Journal of Enology and Viticulture, 27,* 97-105.

Tominaga, T., Guimbertau, G., & Dubourdieu, D. (2003). Role of certain volatile thiols in the bouquet of aged champagne wines. *Journal of Agricultural and Food Chemistry, 51,* 1016-1020.

Trautner, E. M., & Roberts, E. A. H. (1950). The chemical mechanism of the oxidative deamination of amino acids by catechol and polyphenolase. *The Australian journal of science, B3,* 356-380.

Tressl, R., Nittka, C., & Kersten, E. (1995). Formation of isoleucine-specific Maillard products from [1-^{13}C]-D-glucose and [1-^{13}C]-D-fructose. *Journal of Agricultural and Food Chemistry, 43,* 1163-1169.

Troup, G. J., Hutton, D. R., Hewitt, D. G., & Hunter, C. R. (1994). Free radicals in red wine, but not in white? *Free Radical Research, 20,* 63-68.

Troup, G. J., & Hunter, C. R. (2002). EPR, free radicals, wine, and the industry: some achievements. *Annals of the New York Academy of Sciences, 957,* 345-347.

Valero, E., Escribano, J., & Garcia-Carmona, F. (1988). Reactions of 4-methyl-*o*-benzoquinone, generated chemically or enzymatically, in the presence of L-proline. *Phytochemistry, 27,* 2055-2061.

Waterhouse, A. L. (2002). Wine Phenolics. *Annals of the New York Academy of Sciences, 957,* 21-36.

Waterhouse, A. L., & Laurie V. F. (2006). Oxidation of Wine Phenolics: A Critical Evaluation and Hypotheses. *American Journal of Enology and Viticulture, 57,* 306-313.

Weenen H., & Tjan, S. B. (1994). 3-Deoxyglucosone as flavour precursor. In: Maarse H, van der Heij DG (eds) *Trends in flavour research*, Elsevier, London, 327-333.

Whitaker & Lee (1995). In Chemistry of Enzymatic Browning 2-6. Enzymatic Browning and Its Prevention Editor(s): Chang Y. Lee and John R. Whitaker Volume 600, American Chemical Society, Washington, DC, Cap 1 - Recent Advances in Chemistry of Enzymatic Browning.

Wildenradt, H. L., & Singleton, V. L. (1974). The production of aldehydes as a result of oxidation of polyphenolic compounds and its relation to wine aging. *American Journal of Enology and Viticulture, 25*, 119-126.

Wilfred Vermerris & Ralph Nicholson (2006). In Phenolic Compound Biochemistry USA, Springer, New York, Cap 2 - Chemical Properties of Phenolic Compounds.

Yanagimoto, K., Ouchi, H., Lee, K.-G., & Shibamoto, T. (2004). Antioxidative activity of fractions obtained from brewed coffee. *Journal of Agricultural and Food Chemistry, 52*, 592-596.

Yaylayan, V. A., & Keyhani, A. (2001). Carbohydrate and amino acid degradation pathways in L-methionine/D-[^{13}-C]glucose model systems. *Journal of Agricultural and Food Chemistry, 49*, 800-803.

Yaylayan, V. A. (2003). Recent advances in the chemistry of Strecker degradation and Amadori rearrangement: implications to aroma and colour formation. (Review). *Food Science Technology Research, 9*, 1-6.

Yu, A. N., & Zhang, A. D. (2010a). The effect of pH on the formation of aroma a compounds produced by heating a model system containing L-ascorbic acid with L-threoine/L-serine. *Food Chemistry, 119*, 214-219.

Yu, A. N., & Zhang, A. D. (2010b). Aroma compounds generated from thermal reaction of L-ascorbic acid. *Food Chemistry, 121*, 1060-1065.

Zhai, H., Du, J., Guan, X., Qiao, X., & Pan, Z. (2001). Cultivating and processing technologies for wine grapes. Beijing: China Agricultural Press.

Zoecklein, B. C., Fugelsang, K. C., Gump, B. H., & Nury, F. S. (1995). Wine analysis and production. New York: Kluwer Academic/Plenum Publisher.

3. Chapter 3 - Material and Methods

3.1. Wine characterization

Two different wines, a dry white wine and a sweet red Port wine were used for the proposed study of oxidative browning and aromatic degradation of wine. These two wines have different concentrations on the main substrates for the degradation reactions. Port wine is a fortified wine, which involves the addition of natural grape spirit to the fermenting juice. Fermentations are relatively short, about two days, and are intentionally interrupted at a point when approximately half of the grapes natural sugar has been converted into alcohol, resulting in a wine containing about 18-20% of alcohol, and higher levels of sugars (40 to 130 g/L). Thus, this wine is a sweet wine where sugars are readily available for Maillard and caramelization reactions. However, dry wine has residual reducing sugars (1 to 3 g/L) that also may participate in these reactions, and therefore can be employing for the study. Port wine has also different contents in compounds coming from the fermentative process (amino acids, alcohols, organic acids, etc). Hence, using different grape varietals, white grapes for the dry white wine and red grapes for the sweet Port wine, originates dissimilar concentrations in phenolic compounds.

The used wines (white and red Port wines) are from Douro Portuguese wine region (winemaking procedures depend on the producers) and are young wines having both 1 year-old. The vintage years were 2011 and 2012 for, respectively, white and red Port wine.

The analyzed white and red Port wines have an ethanol content of respectively 12% and 20%, and a sugar content of respectively 3.0 (± 0.1) and 105.3 (± 0.4), both analyses conducted by liquid chromatography with RI detection (Chapter 3; 3.7. HPLC with refractive index (RI) detection).

The quantification of phenolic compounds present in both white and red Port wines is shown in Table 3.1, and was conducted by LC-MS (Chapter 3; 3.9. LC-Mass spectrometry: non-volatiles analysis). From the observation of this table we can see that, the red Port wine contain polyphenols at a higher concentration than the white wine, among which, anthocyanins, flavan-3-ols and quercetin which are in particularly high levels. Likewise, hydroxybenzoic acids and hydroxycinnamic esters are in higher levels. White wine

contains lower levels of polyphenols, mainly hydroxycinnamic acids, such as caffeic and *para*-coumaric acids, and hydroxycinnamic esters (Table 3.1).

Table 3.1. Phenolic compounds present in both white and red Port wines (N=2).

Compound	White wine (mg/L)	Port wine (mg/L)
Hydroxybenzoic acids:		
gallic acid	2.7 ± 0.1	6.9 ± 0.1
protocatechuic acid	1.0 ± 0.1	1.0 ± 0.1
syringic acid	nd	0.2 ± 0.0
Hydroxycinnamic acids:		
caffeic acid	1.1 ± 0.1	0.5 ± 0.0
para-coumaric acid	1.0 ± 0.1	0.7 ± 0.1
ferulic acid	0.5 ± 0.1	0.4 ± 0.1
Hydroxycinnamic esters:		
monocaffeoyl tartaric acid [a]	5.5 ± 0.1	35.1 ± 0.2
monocumaroyl tartaric acid [b]	4.3 ± 0.1	23.5 ± 0.1
feruloyl tartaric acid [c]	3.1 ± 0.1	4.8 ± 0.1
Flavan-3-ols:		
(+)-catechin	3.4 ± 0.1	13.8 ± 0.1
(-)-epicatechin	0.9 ± 0.1	8.0 ± 0.2
Flavonols:		
quercetin	nd	31.2 ± 0.2
Anthocyanins:		
delphinidin-3-glucoside [d]	nd	11.7 ± 0.2
petunidin-3-glucoside [d]	nd	14.0 ± 0.3
peonidin-3-glucoside [d]	nd	12.0 ± 0.3
mv-3-glucoside	nd	94.2 ± 0.1
mv-3-*O*-acetylglucoside [d]	nd	17.1 ± 0.2
(trans)-mv-3-*O*-coumaroylglucoside [d]	nd	29.3 ± 0.3

[a] Concentration expressed in caffeic acid equiv;

[b] Concentration expressed in coumaric acid equiv;

[c] Concentration expressed in ferulic acid equiv;

[d] Concentration expressed in malvidin 3-glucoside equiv;

mv = malvidin; nd = not detected.

White and red Port wines have respectively, 0.34 mg/L (± 0.02) and 0.27 mg/L (± 0.02) of Cu; and 2.54 mg/L (± 0.08) and 1.81 mg/L (± 0.06) of Fe, determined on a flame atomic absorption spectrometer (Chapter 3; 3.12.Analyses of Cu and Fe).
pH values were 3.2 (± 0.1) for white wine and 3.4 (± 0.1) for red Port wine.

3.2. Experimental isothermal storage forced aging protocol

3.2.1. White wine

Ten liters of white wine (pH = 3.2) were divided into 8 portions and placed on sealed vessels (Figure 3.1). Each set of 4 vessels was kept for 42 days at 4 different storage temperatures, respectively, 20, 30, 40 and 50ºC. Next, for all temperature regimes, 2 oxygen saturation levels were adjusted, during the protocol, as follows: i) no oxygen addition (Treatment I); and ii) oxygen addition every sampling point (Treatment II). Oxygen addition was made by air bubbling (20/80; O_2/N_2) (Gasin, Portugal) until oxygen content close to 8.0 mg/L. Analyses were performed weekly.

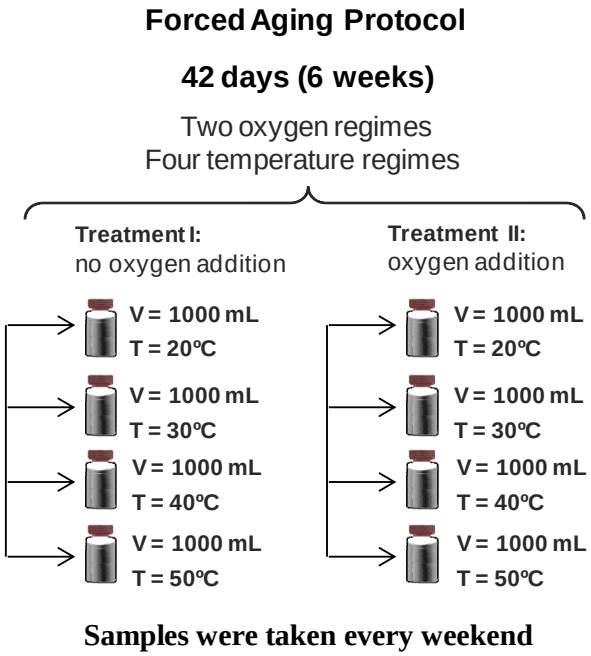

Figure 3.1. White wine forced aging protocol.

3.2.2. Red Port wine

Ten liters of red Port wine (pH = 3.4) were divided into 8 portions and placed on sealed vessels (Figure 3.2). Each set of 4 vessels was kept for 63 days at 4 different storage temperatures, respectively, 20, 30, 35 and 40ºC. Next, for all temperature regimes, 2 oxygen saturation levels were adjusted, during the protocol, as follows: i) no oxygen addition (Treatment I); and ii) oxygen addition every sampling point (Treatment II). Oxygen addition was made by air bubbling (20/80; O_2/N_2) (Gasin, Portugal) until oxygen content close to 8.0 mg/L. Analyses were performed weekly.

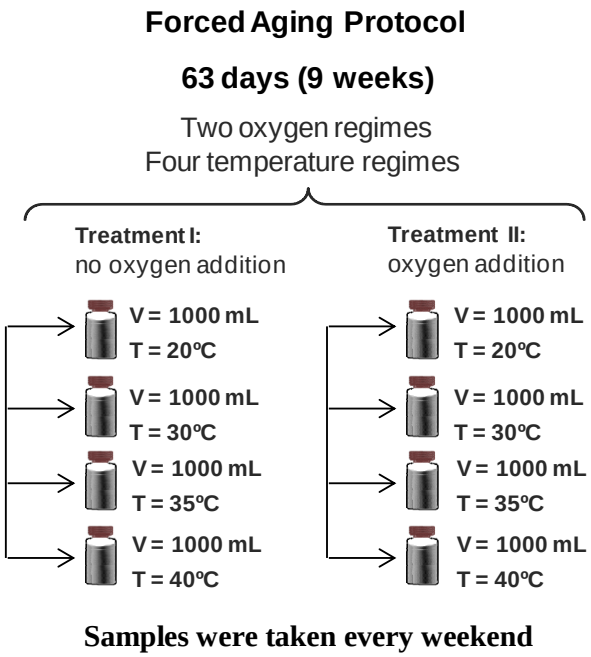

Figure 3.2. Red Port wine forced aging protocol.

3.3. Oxygen measurements

3.3.1. White wine

The concentration of dissolved oxygen was measured using a YSI Oxygen Probe 5010-W, coupled to a 5000 dissolved oxygen instrument. This model is designed to fit directly in the bottleneck for direct measurement of wine bottles with a dissolved oxygen accuracy of 0.1 mg/L or 2% of reading.

3.3.2. Red Port wine

The concentration of dissolved oxygen was measured in the above experimental design using a Fibox 3 LCD fiber optic oxygen transmitter, coupled to a polymer optical fiber of 2.5 meters and to planar oxygen sensitive spots (PSt3), from PreSens Precision Sensing GmbH (Germany), with a detection limit of 15 ppb (0 - 100 % oxygen). All measurements were made six times. Flasks were never open during the experimental protocol.

3.4. Generating of ROS (Reactive Oxygen Species)

A wine-model system was prepared with ethanol 12% (v/v) and 0.033 M tartaric acid, in saturated oxygen conditions (8.5 mg/L), and adjusted with NaOH solution to pH 3.6. Then, a reactive phenolic compound was added, in concentrations that simulate the reducing capacity of wines. The quinone was then formed by adding 0.4 ppm of Cu^{2+} in the form of copper sulfate pentahydrate, and 7.5 ppm of Fe^{2+} in the form of ferrous sulfate.

ROS were then produced by reduced transition metals ions [Fe(II) and Cu(I)] in the stepwise addition of a single electron on triplet oxygen (O_2). The initial transfer of an electron leads to the formation of superoxide radical anion ($O_2^{\bullet-}$) which, at pH 3.6, exists in the protonated form hydroperoxyl radical ($HO_2^{\bullet}$). The transfer of a second electron will produce peroxide anion (O_2^{2-}) which, at pH 3.6, exists in the protonated form hydrogen peroxide (H_2O_2). The next reduction step creates an oxidative agent even more reactive than the previously, the hydroxyl radical ($HO^{\bullet}$) giving water as the final oxygen reducing product.

3.5. Cyclic voltammetry

3.5.1. Introduction to electroanalytical methods - cyclic voltammetry

Electroanalytical methods are a class of techniques in analytical chemistry that study an analyte by measuring the potential (volts) and/or current (amperes) in an electrochemical cell containing the analyte. These methods can be broken down into several categories,

depending upon which aspects of the cell are controlled and which are measured. In principle, all electrochemical techniques can be divided in two classes, which are referring to as bulk electrochemical techniques (like conductometry) and interfacial electrochemical techniques. In general the interfacial electrochemical techniques can be divided into two categories: static techniques, not allowing current to pass through the analyte's solution (like potentiometry) or dynamic techniques, allowing current to flow through the analyte's solution. Finally, dynamic techniques can be divided in controlled-potential methods (potentiostatic methods), involved current measurements, and controlled-current methods (galvanostatic methods), involved potential measurements.

Cyclic voltammetry is a potentiostatic method used either to elucidate reaction mechanisms or to carry out quantitative and/or quantitative analysis. During the cyclic voltammetry experiment, a cyclic potential sweep is imposed on an electrode and the current response is observed. Various parameters can be defined from the voltammetric curves, including the potentials at which the current peaks on the anodic and cathodic scans (**Ep,a** and **Ep,c**) can occur. The potential midway between the two peak potentials (**Emid**) provides an estimate of the formal potential ($\mathbf{E^0}$) for the redox processes in the solution being employed. The easiness of reversibility for the redox process is indicated by the peak potential separation (**ΔEp**), which approaches a value around (57 - 60)/n mV for a fully reversible n-electron process at a slower scan rate. The degree of reversibility is also indicated by the ratio of the cathodic peak current (**Ip,c**) to the anodic peak current (**Ip,a**), with a value closer to one obtained for a more reversible system, or alternatively by the ratio of the cathodic peak area (**Sc**) to the anodic peak area (**Sa**). Analysis of the current response of a cyclic voltammogram can give information about the thermodynamics and kinetics of electron transfer at the electrode-solution interface, as well as the kinetics and mechanisms of solution chemical reactions initiated by the heterogeneous electron transfer.

3.5.2. Study of glass carbon electrode

Experiments were performed using a potentiostat (microAutolab Type III with an Autolab Faraday Cage) and voltammograms were obtained with a scan rate of 100 mV/s with an increment potential of 2.4 mV, between 0 V to 1.2 V. The working electrode was a 3 mm glassy carbon disk in combination with a Metrohm tipholder (Figure 3.3), cleaned by

polishing with 3 µm alumina powder during 30 s follow by fixing the potential to 1.5 V in a 0.1 mol/L NaOH solution during 5 s, between acquisitions a saturated calomel electrode was used as a reference electrode in conjunction with a platinum counter electrode (Figure 3.3). Each acquisition required 15 mL of sample. Oxygen was removed with a N_2 current flow during 5 min prior to analysis. Cyclic voltammetry experiments were controlled by the GPES 4.9 software provided by Ecochemie.

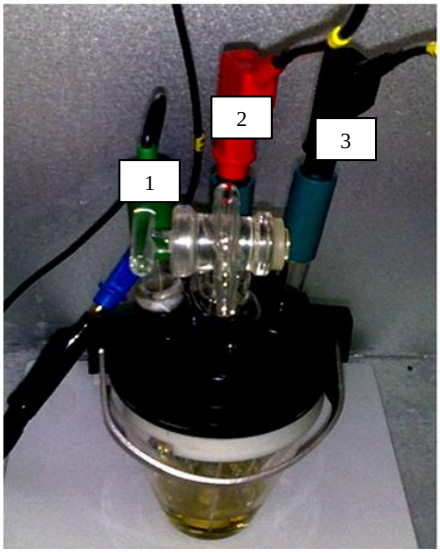

1. Reference calomel electrode;
2. Work electrode of glassy carbon disk;
3. Platinum counter electrode.

Figure 3.3. Voltammetric apparatus.

3.5.3. Effect of dilutions

In order to achieve the linear voltammetric range signals for the used detector, a study on the effect of wine dilutions in the cyclic voltammograms responses was performed. Experiments were undertaken in which wines were diluted 2, 5, 10, and 20-fold (for white wine) and 2, 5, 10, 20, 25, and 50-fold (for red Port wine). The cyclic voltammograms of wines were first measured in the undiluted wines, with pH adjusted to 3.6. Then, the wines were diluted until a linear dependence was reached between the voltammetric signals and the respective wine. A reference of the model wine solution was introduced as well. The study was made in triplicate. Data was normalized by mean normalization.

Wines were plotted addressing the number of the dilution and the corresponding voltammetric curves (Figure 3.4a and Figure 3.5a). Futhermore, a principal component analysis (PCA) was employed to the voltammetric oxidation signals. This procedure

illustrates the global electrochemical differences of the analysed wines, and the scores of the first component (PC1) can be used to assess the dependence between the oxidation electrochemical signals and the respective dilution (Figure 3.4b and Figure 3.5b). Results have showed that for the white wine a linear dependence was reached between the undiluted and the 5-fold diluted wine (Figure 3.4b; 98% of variance), indicating the linear region for the work electrode. Likewise, for the red Port wine a linear dependence was obtained in the range of 5-fold to 20-fold diluted wines (Fgure 3.5b; 97% of variance), indicating a linear region for the working electrode in this wine.

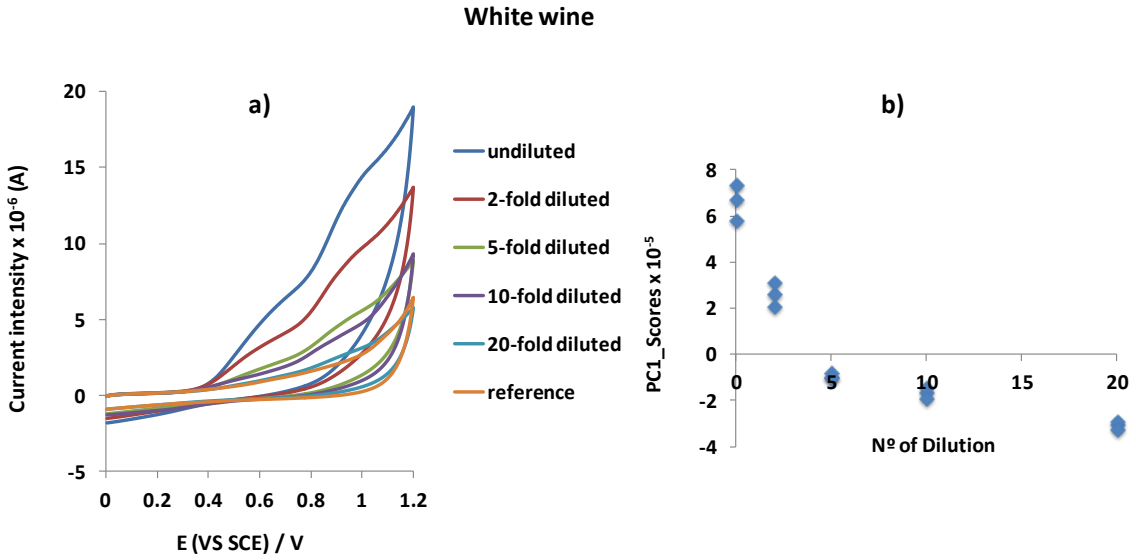

Figure 3.4a. Voltammetric curves addressing white wines dilutions. **3.4b**. PCA scores plot: First principal component as a function of dilution-fold for white wine.

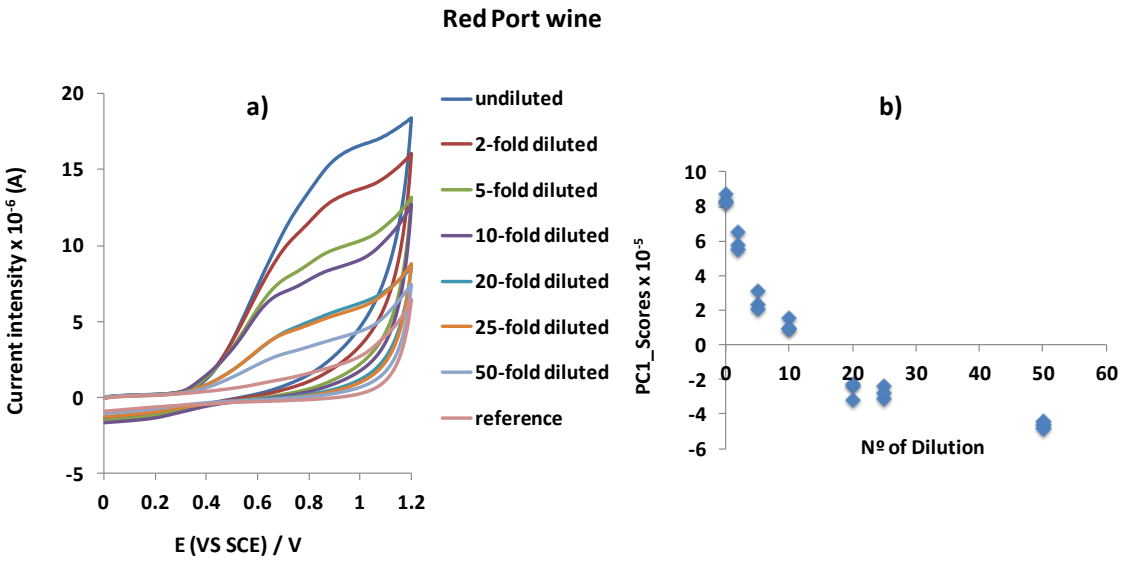

Figure 3.5a. Voltammetric curves addressing red Port wines dilutions. **3.5b**. PCA scores plot: First principal component as a function of dilution-fold for red Port wine.

Because of the obtained linear voltammetric range signals, in the present work, white wine was analysed without dilution (pH = 3.2), and red Port wine was diluted 20 times. All dilutions were made in a model wine solution consisting of 20% ethanol (v/v), 0.033 M tartaric acid, and pH 3.6 (adjusted with NaOH solution).

3.5.4. Repeatability of carbon electrode

The repeatability of the above voltammetric procedures was achieved by the analysis of the coefficient of variation of the first anodic peak current Ip,a at approximately 0.45 V. The repeatability study was obtained by repetitive analysis of ten samples of the same wine dilution. The coefficients of variation (% RSD) obtained were 11.3%, for the undiluted white wine, and 14.3% for the 20 times diluted red Port wine. The lower precision obtained for the red Port wine could be explained by a less reproducible surface relative to the polished glass carbon electrode.

3.6. HPLC with diode array detection (DAD)

3.6.1. Screening of low molecular weight phenolic compounds

A Beckman model 126 quaternary solvent system, equipped with a System 32 Karat 5.0 software and a 168 rapid scanning, UV-visible photodiode array detector, was used. The absorption spectra were recorded between 212 and 600 nm. Stationary Phase: XDB-C18 (150 x 4.6 mm x 5 μm) (Agilent, USA). Mobile Phase: Solvent A: acetonitrile (100%) (Merck pure grade) with 0.2% TFA; Solvente B: acetonitrile/water (5:95 v/v) (Merck pure grade and pure water) with 0.2% TFA (Sigma-Aldrich, Germany); flow rate = 1 mL/min.
For white wine, the following gradient was employed: 0-2 min (100% B); 2-6 min (90% B); 6-10 min (80% B); 10-12 min (100% B); 12-15 min (100% B). Each run took 15 min to complete. For red Port wine, the following gradient was employed: 0-2 min (100% B); 2-28 min (60% B); 28-30 min (100% B). Due to the red Port wine additional anthocyanins phenolic group, a longer chromatographic run was employed in these wines. Each run took 30 min to complete. As the linear concentration range of the used detector (0.5 to 85 mg/L), samples were analyzed undiluted in both wines. Hydroxybenzoic acids, flavan-3-ols, and furanic compounds (HMF and furfural) were detected at 280 nm. Hydroxycinnamic acids and its esters were detected at 320 nm. Anthocyanins were detected at 528 nm (red Port wine). Samples were analyzed in duplicate in both wines. Table 3.2 and Table 3.3 represent the analytical parameters of the working methods for, respectively, white and red Port wines. The methodology applied was adapted from Castro et al., 2012.

Table 3.2. Analytical parameters for the quantification of low molecular weight phenolic compounds for white wine. RSD (%) = 2.5 (N=8).

Compound	Retention time (min)	Slope	Intercept	R^2	LOD (mg/L)	LOQ (mg/L)	Linear range (mg/L)
Hydroxybenzoic acids:							
gallic acid	3.2	17778	-11395	0.999	0.7	2.2	0.5-60
protocatechuic acid	3.5	38329	24567	0.999	0.6	1.8	0.5-70
syringic acid	10.5	92144	-109346	0.999	0.9	2.9	0.5-75
Hydroxycinnamic acids:							
caffeic acid	10.3	108579	-16710	0.999	0.5	1.6	0.5-60
para-coumaric acid	12.3	130360	-42502	0.999	0.6	2.0	0.5-85
ferulic acid	12.6	106276	-17735	0.998	0.7	2.3	0.5-65
Flavan-3-ols:							
(+)-catechin	9.3	13371	-3530	0.998	0.6	2.0	0.5-60
(-)-epicatechin	10.8	15566	-1711	0.998	0.5	1.7	0.5-60
Furanic compounds:							
HMF	4.4	396088	-73272	0.999	0.4	1.3	0.2-40
Furfural	6.0	97385	78913	0.998	0.9	3.0	0.5-75

Table 3.3. Analytical parameters for the quantification of low molecular weight phenolic compounds for red Port wine. RSD (%) = 2.5 (N=8).

Compound	Retention time (min)	Slope	Intercept	R^2	LOD (mg/L)	LOQ (mg/L)	Linear range (mg/L)
Hydroxybenzoic acids:							
gallic acid	2.9	12832	6887	0.999	0.6	2.0	0.5-60
protocatechuic acid	3.0	27666	5130	0.999	0.5	1.8	0.5-70
syringic acid	12.0	83407	23498	0.998	0.9	2.9	0.5-75
Hydroxycinnamic acids:							
caffeic acid	11.9	145602	65192	0.999	0.7	2.2	0.5-60
para-coumaric acid	15.6	136566	49949	0.999	0.7	2.4	0.5-85
ferulic acid	16.6	110116	40050	0.999	0.6	2.1	0.5-65
Flavan-3-ols:							
(+)-catechin	10.6	13098	6863	0.998	0.6	1.9	0.5-60
(-)-epicatechin	13.4	15563	7907	0.999	0.6	1.9	0.5-60
Flavonols:					0.0	0.0	
quercetin	21.9	11480	12957	0.998	0.7	2.5	1.0-45
Furanic compounds:							
HMF	3.8	357508	85613	0.999	0.4	1.4	0.2-40
Furfural	7.8	187260	91259	0.999	0.7	2.5	0.5-75

3.6.2. Quantification of 3-deoxyglucosone (3DG)

The HPLC system consisted of a variable loop Accela autosampler (200 vial capacity set at 25°C), an Accela 600 LC pump and an Accela 80 Hz PDA detector (Thermo Fisher Scientific, San Jose, Ca, USA). The separation of the compounds was carried out at 30 °C with a flow rate of 0.5 mL/min by using a Kinetex® C18 (50 x 2.1 mm x 1.7 μm), equipped with a safety guard ULTRA cartridge, both supplied by Phenomenex (USA). The injection volume in the HPLC system was 10 μL and the mobile phase consisted of water/acetonitrile (99:1, v/v) (A) and acetonitrile (B), both with 0.1% of formic acid. The following gradient was employed: 0-1 min (97% A); 1-6 min (97-88.5% A); 6-8.5 min (88.5-80% A); 8.5-10 (80-60% A); 10-11 (60-0% A); 11-13.5 (0-97% A), followed by a re-equilibration of the column for 3 min before the next run. Each run took 13.5 min to complete. Single online detection was carried out in the diode array detector, at 317 nm,

and UV spectra in a range of 210-600 nm were also recorded. Before the injection, each sample was filtered through a 0.2 µm PTFE syringe filter.

A volume of 5.0 mL of wine or synthetic wine sample were mixed with 0.01 g of *ortho*-phenylenediamine to form the quinoxalines. Samples were stored overnight at room temperature, and were analyzed in duplicate. The peaks for quinoxalines are shown in Figure 3.6.

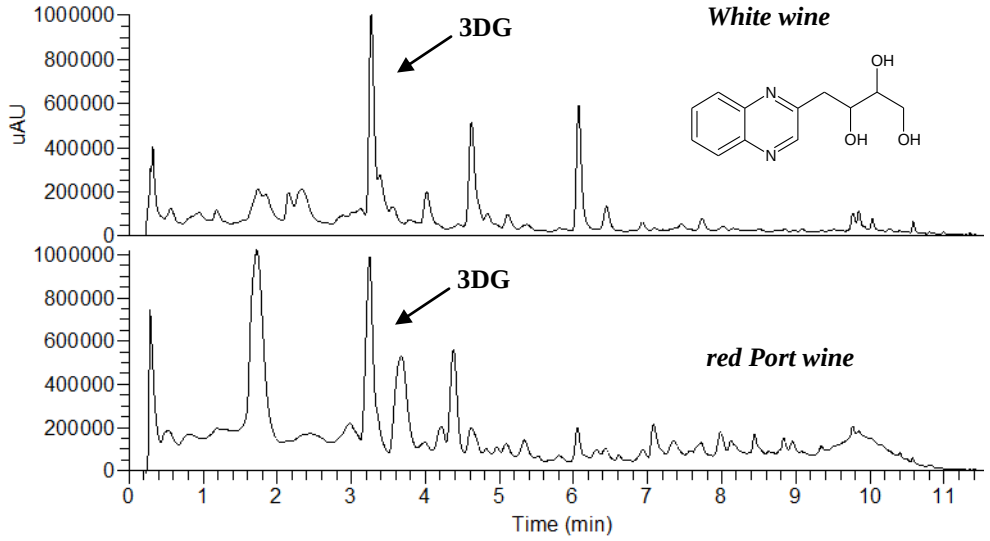

Figure 3.6. UV quinoxalines chromatograms of white wine (top) and red Port wine (bottom) recorded at 317 nm.

3DG was identified based on the retention time (Figure 3.6) and MS^n fragmentation pathway of the respective quinoxaline standard (Figure 3.7). Therefore, HPLC was coupled to a LCQ Fleet ion trap mass spectrometer (ThermoFinnigan, San Jose, CA, USA), equipped with an electrospray ionization source and operating in positive mode. The spray voltage was 5 kV and the capillary temperature was 300ºC. The capillary and tune lens voltages were set at 26 V and 115 V, respectively. CID-MS^n experiments were performed on mass-selected precursor ion at m/z 235. The isolation width of precursor ion was 1.0 mass units. The scan time was equal to 100 ms and the collision energy was 35 (arbitrary units), using helium as collision gas. The data acquisition was carried out by using Xcalibur® data system (ThermoFinnigan, San Jose, CA, USA); Retention time: 3.27 min; MS^2 [235]: 217, 199, 187, 157. Table 3.4 represents the analytical parameters and the repeatability and recovery of the working method.

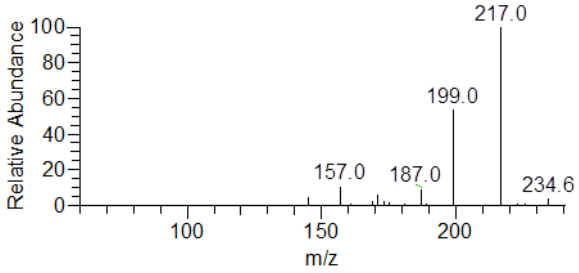

Figure 3.7. MS^n fragmentation pathway of the respective quinoxaline of 3DG standard.

Table 3.4. Analytical parameters of the working method for the quantification of 3DG.

Analytical parameters of the working method	
Linear concentration range (mg/L)	1-100
Linear regression (N=8)	y = 106050x-61185
R^2	0.999
LOD (mg/L)	2.6
LOQ (mg/L)	8.7
Repeatability and recovery of the working method	
RSD (%) (N=5)	2.5
Recovery (%) (N=5)	79.8

3.7. HPLC with refractive index (RI) detection

Residual sugars and ethanol and were quantified by HPLC with refractive index (RI) detection. A Beckman Model 126 quaternary solvent pump system equipped with an autosampler and a RI detector was employed. The acquisition was done using 32 Karat 5.0 software. Stationary-phase: Aminex hpx-87H (300 x 7.8 mm) from Bio-Rad. Mobile-phase: sulfuric acid (2.5 mM); flow rate = 0.6 mL/min. Table 3.5 represents the analytical parameters of the working method for the quantification of residual sugars (glucose and fructose) and ethanol. The methodology applied was adapted from Castellari et al., 2000.

Table 3.5. Analytical parameters for the quantification of glucose, fructose, and ethanol (N=8).

Compound	Retention time (min)	Slope	Intercept	R^2	LOD (g/L)	LOQ (g/L)	Linear range (g/L)
Glucose	9.0	235.1	14.4	0.995	0.6	2.0	0-20
Fructose	9.8	258.8	11.2	0.997	0.5	1.8	0-20
Ethanol	20.9	102.6	-1.90	0.998	1.3	4.5	0-20

3.8. HPLC with fluorescence detection

3.8.1. Amino acids

Amino acids were quantified by HPLC with fluorescence detection. A Beckman Model 126 quaternary solvent system equipped with a Spark Midas auto-sampler and a Waters 474 scanning fluorescence detector were employed. Detection was done at λext. 356 nm and λemis. 445 nm. The acquisition was done using a 32-Karat 5.0 software. Stationary-phase: Spherisorb ODS_2 (250 x 4.6 mm x 5 μm) (Merck, Germany). Mobile-phase: Solvent (A), consisting of 20g of $Na_2HPO_4.2H_2O$, 7.4 g of propionic acid (99% Sigma), 40 mL of dimethylsulfoxide (99% Aldrich) and 130 mL acetonitrile (Romil) in 2 L of ultrapure water titrated to pH 6.65 with 4 mol/L NaOH (Merck). Solvent (B), consisting of 33% methanol (Romil), 7% dimethylsulfoxide, 40% acetonitrile (Romil) and 20% ultrapure water (v/v). The flow rate was 0.7 mL/min and the following gradient was used: 0-2 min (5-10% B); 2-35 min (10% B); 35-45 min (10-35% B); 45-80 min (30-40% B); 80-110 min

(40-80% B); 110-115 min (80% B); 115-120 min (80-50% B); 120-123 min (50-5% B); 123-125 min (5% B). Sample preparation: Reagent A (internal standard solution): Natrium tetraphenylborat (99.5% Aldrich) 20 g/L, *ortho*-phthalaldehyde (OPA) (99% Merck) 0.5% (v/v), L-homoserine (98% Merck) 2.4 mg/L (IS1) and DL-norvaline (98% Merck) 2.4 mg/L (IS2). Reagent B: 35 g/L of IDA titrated to pH 9.5 with 4 mol/L NaOH. Reagent C: *ortho*-phthalaldehyde (OPA) (99% Merck) 4.5 g/L and methanol (99.9% Romil) 10% (v/v). These reagents were prepared with borate buffer consisting of boric acid (99.8% Merck) 6.2 g/L titrated to pH 9.5 with 4 mol/L NaOH.

The derivatisation reaction was performed by the Spark Midas auto-sampler: To 100 μL of sample, add 250 μL of reagent A, and 250 μL of reagent B, mix, and wait 3 min. Add 250 μL of reagent C mix and wait 3.5 min. Mix and inject. Separation and quantification were performed by injecting 20 μL of derivate using a HPLC system. The peaks for amino acids are shown in Figure 3.8. Table 3.6 represents the analytical parameters of the working method for the quantification of amino acids. The methodology applied was adapted from Pripis-Nicolau et al., 2001.

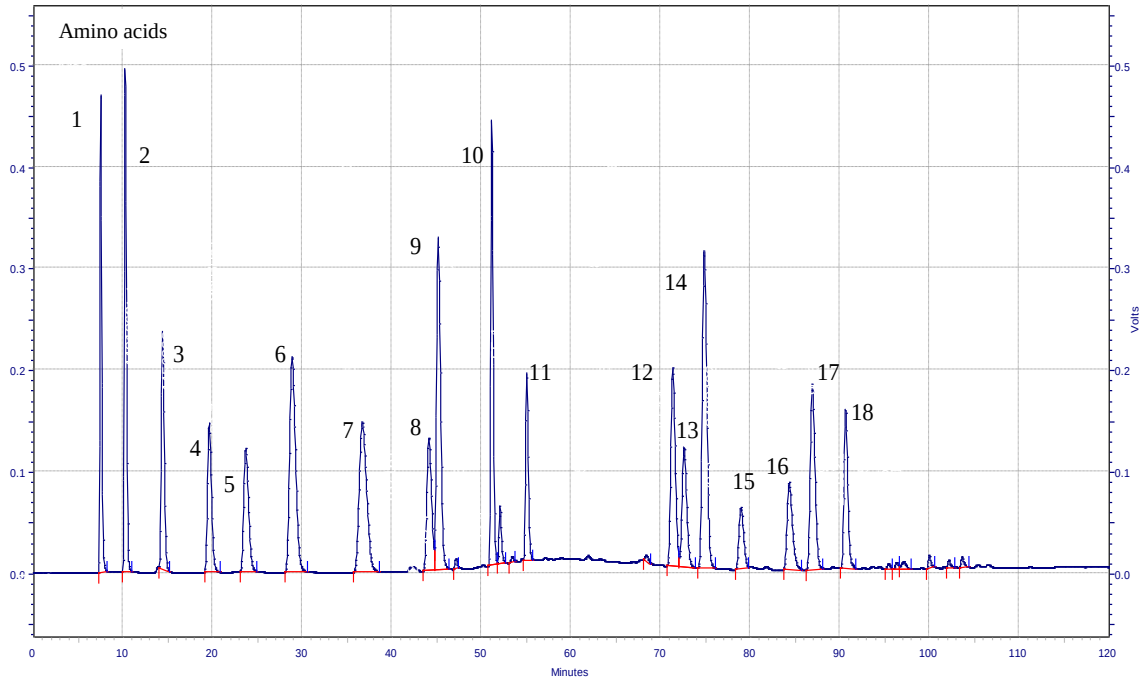

(1) (Asp); (2) (Glu); (3) (Cys); (4) (Asn); (5) (Ser); (6) (Gln); (7) (IS1); (8) (Thr); (9) (Arg); (10) (Ala); (11) (Tyr); (12) (Val); (13) (Met); (14) (IS2); (15) (Trp); (16) (Phe); (17) (Ile); (18) (Leu).

Figure 3.8. Fluorescence chromatograms of amino acids derivatives recorded at λext. 356 nm and λemis. 445 nm.

Table 3.6. Analytical parameters for the quantification of amino acids (N=8).

Compound	Retention time (min)	Slope	Intercept	R^2	LOD (mg/L)	LOQ (mg/L)	Linear range (mg/L)
Asp	7.0	0.1602	-0.0069	0.997	0.4	1.3	0.5-10
Glu	9.8	0.1073	-0.0116	0.998	0.6	2.0	0.5-10
Cys	12.6	0.1375	-0.0049	0.999	0.3	1.1	0.5-15
Asn	16.4	0.1900	0.0146	1.000	0.1	0.3	0.5-10
Ser	19.9	0.1827	0.0214	1.000	0.1	0.4	0.5-10
Gln	25.2	0.1287	0.1275	0.999	1.3	4.3	1.0-30
Thr	35.9	0.1630	-0.0196	0.997	0.7	2.2	0.5-10
Arg	43.4	0.1194	0.0635	0.996	2.2	7.2	1.0-30
Ala	48.6	0.1624	0.0317	0.998	0.8	2.6	0.5-15
Tyr	52.3	0.1630	-0.0196	0.997	0.7	2.2	0.5-10
Val	67.1	0.2677	0.0095	1.000	0.1	0.3	0.5-10
Met	68.1	0.1816	0.0010	1.000	0.1	0.3	0.5-10
Trp	75.1	0.0849	-0.0113	0.999	0.3	1.0	0.5-10
Phe	79.2	0.1282	-0.0001	1.000	0.1	0.3	0.5-10
Ile	81.8	0.2505	-0.0022	1.000	0.1	0.3	0.5-10
Leu	86.4	0.1569	0.0169	1.000	0.1	0.4	0.5-10

3.8.2. α-Ketoacids (β-phenylpyruvic acid)

β-Phenylpyruvic acid was quantified by HPLC-fluorescence after a reaction with *ortho*-phenylenediamine. A Beckman Model 126 quaternary solvent system equipped with a Spark Midas auto-sampler and a Waters 474 scanning fluorescence detector were employed. The stationary phase used was a XDB-C18 (150 x 4.6 mm x 5 μm) (Agilent, USA). The reaction product, a quinoxalinol derivative, was detected at λext. 350 nm and λemis. 410 nm. The methodology applied was adapted from Silva Ferreira et al., 2007.

3.9. LC-MS: non-volatiles analysis

Phenolics identification/quantification was conducted on a LC-MS Varian 1200 triple quadrupole mass spectrometer with electrospray ionization in positive and negative modes. The operating parameters of the ESI source was as follows: API drying gas 19 psi at 200ºC; API chamber temperature 50ºC; API nebulizing gas, Air 41 psi; Capillary voltage -85 to +25 V; Q2 collision cell pressure Argon 1.42 mTorr; Collision energy 15 to 25 V. Stationary Phase: XDB-C18 (150 x 4.6 mm x 5 μm) (Agilent, USA). Mobile Phase: Solvent A: acetonitrile (100%) (Merck pure grade) with 0.1% formic acid; Solvent B: acetonitrile / water (5:95 v/v) (Merck pure grade / ultra pure water, from a Millipore system) with 0.1% formic acid (Sigma-Aldrich, Germany); flow rate = 0.35 mL/min. The following gradient was employed: 0 min (95% B); 0-26 min (70% B); 26-28 min (95% B) 28-30 min (95% B). Each run took 30 min to complete.

Phenolics were identified by comparison with commercially available standards retention times and MS/MS data. LC-MS data is shown in Table 3.7.

For anthocyanins, neutral loss scanning mode were obtained for the identification of, respectively, anthocyanin-glycosides (neutral loss m/z 162), acetylglucosides (neutral loss m/z 204), and coumaroylglucosides (neutral loss m/z 308). For the identification of hydroxycinnamic esters, available published MS/MS data were used. Table 3.8 represents the analytical parameters of the working method for the quantification of phenolic compounds.

Table 3.7. LC-MS data of phenolic compounds.

Retention time (min)	Compound	[M - H]- [M]+	MS/MS fragments
		m/z*	m/z*
	Hydroxybenzoic acids:		
7.8	gallic acid	169	125
12.3	protocatechuic acid	153	109
14.5	syringic acid	197	182
	Hydroxycinnamic acids:		
14.3	caffeic acid	179	135
19.7	*para*-coumaric acid	163	119
19.9	ferulic acid	193	134
	Hydroxycinnamic esters:		
12.9	monocaffeoyl tartaric acid **	311	179
14.9	monocumaroyl tartaric acid **	295	163
16.4	feruloyl tartaric acid	325	193
	Flavan-3-ols:		
13.1	(+)-catechin	289	245
15.8	(-)-epicatechin	289	245
	Flavonols:		
27.6	quercetin	301	151
	Anthocyanins:		
15.5	delphinidin-3-glucoside	465	303
16.0	petunidin-3-glucoside	479	317
16.5	peonidin-3-glucoside	463	301
16.6	mv-3-glucoside	493	331
21.0	mv-3-*O*-acetylglucoside	535	331
22.4	*(trans)*-mv-3-*O*-coumaroylglucoside	639	331

* Positive ion mode: anthocyanins; negative ion mode: hydroxybenzoic acids, hydroxycinnamic acids and its esters, flavan-3-ols, and flavonols; mv = malvidin.** *cis/trans*.

Table 3.8. Analytical parameters for the quantification of phenolic compounds by LC-MS (N=8).

Compound	Retention time (min)	Slope	Intercept	R^2	LOD (mg/L)	LOQ (mg/L)	Linear range (mg/L)
Hydroxybenzoic acids:							
gallic acid	7.8	9497	-1311572	0.999	0.15	0.49	0.10-4.0
protocatechuic acid	12.3	20098	194648	1.000	0.10	0.32	0.10-4.0
syringic acid	14.5	16092	-1223392	0.998	0.28	0.94	0.15-6.0
Hydroxycinnamic acids:							
caffeic acid	14.3	62122	-947761	1.000	0.07	0.24	0.10-3.0
para-coumaric acid	19.7	30926	3754541	0.999	0.13	0.43	0.10-4.0
ferulic acid	19.9	5037	39298	0.999	0.12	0.41	0.10-4.0
Flavan-3-ols:							
(+)-catechin	13.1	7735	22557	0.999	0.11	0.35	0.10-4.0
(-)-epicatechin	15.8	9004	10933	0.999	0.09	0.30	0.10-4.0
Flavonols:							
quercetin	27.6	5389	-1385000	0.996	0.85	2.82	1.0-6.0
Anthocyanins:							
malvidin-3-glucoside	16.6	10854	24875	0.999	0.14	0.35	0.10-4.0

3.10. GC-MS: volatiles analysis

Samples were analysed using a Varian CP-450 gas chromatograph equipped with a Varian Saturn 240 MS. The mass range was 33 m/z to 350 m/z, in Full Scan mode, and the column was a FactorFour capillary VF-WAXms 15 m x 0.15 mm ID with DF 0.15 µm from Varian.

The injector port was heated to 220°C. The split vent was opened after 30 s. The oven temperature was 40°C (for 1 min), then increased at 5°C/min to 230°C (holding time of 2.5 min). The carrier gas was Helium C-60 (Gasin, Portugal), at 1 mL/min, constant flow. All mass spectra were acquired in the electron impact (EI) mode with the Ion Trap detector. The emission current was 30 µA and the maximum ionization time was 10000 µsec. The analysis was performed in Full Scan mode. For target analysis, compounds were identified by comparison with mass spectra, obtained from the samples, with those from pure commercially available standards injected using the same conditions, and by comparing the Kovat´s indices and the mass spectra present in the NIST 98 MS library. These selected

compounds were then normalized by the internal standard, octan-3-ol (99%, Sigma). Each run took 45 min to complete.

3.10.1. Liquid-liquid extraction

50 mL of sample was spiked with 50 µL of octan-3-ol in hydroalcoholic solution (1/1, v/v) at 500 mg/L (internal standard) and 5 g of anhydrous sodium sulfate. Extraction was carried out twice with 5 mL of CH_2Cl_2 (Merck, Spain). The two organic phases obtained were blended and dried over anhydrous sodium sulfate. This organic extract was injected (1 µL) on GC-MS. In the case of red Port wines, the resulted organic extract was concentrated to 1/10 under a nitrogen gas flow. The chromatograms of, respectively, white and red Port wines are shown in Figure 3.9. Table 3.9 represents the analytical parameters for the quantification of volatile compounds by GC-MS. The methodology applied was adapted from Silva Ferreira et al., 2003.

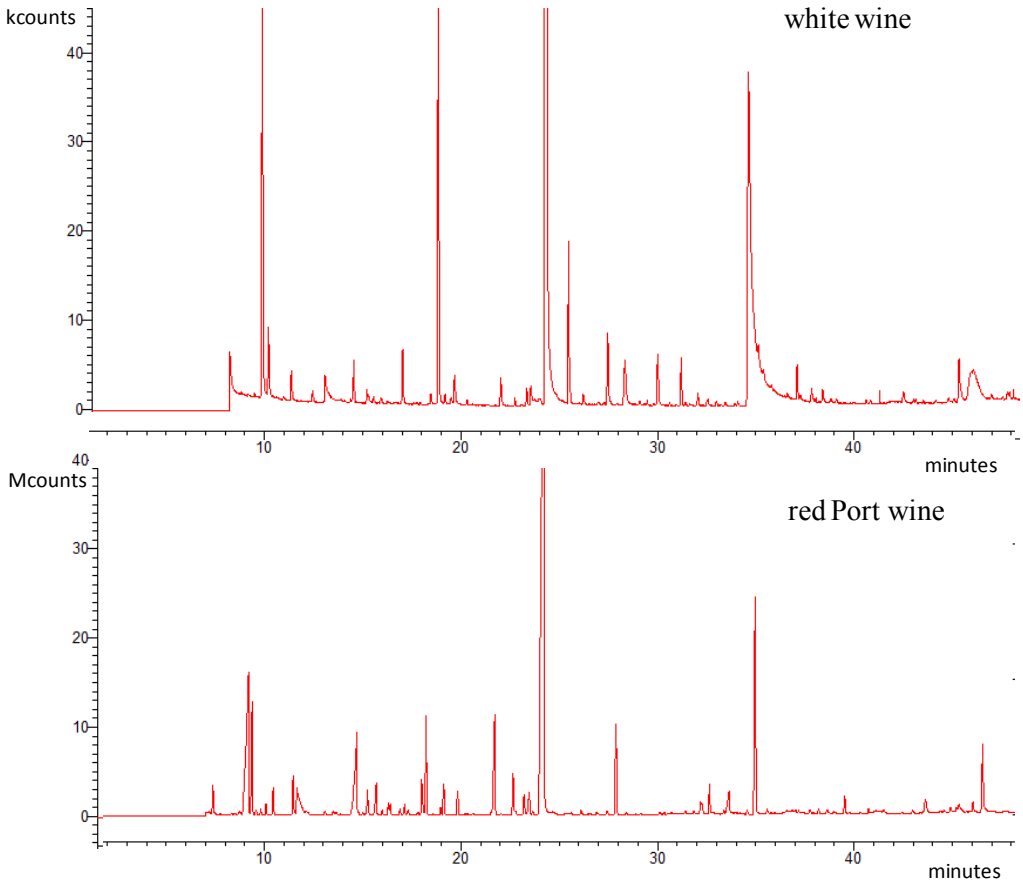

Figure 3.9. CG-MS chromatograms of white wine (top) and red Port wine (bottom).

Table 3.9. Analytical parameters for the quantification of volatile compounds by GC-MS (N=8).

Compound	Retention time (min)	m/z Quantifier ion	Slope	Intercept	R^2	LOD (µg/L)	LOQ (µg/L)
Aldehydes and heterocyclic acetals:							
Benzaldehyde	11.3	105	0.0125	0.4858	0.999	14.9	49.8
Vanillin	30.9	151	0.0019	-0.0136	1.000	9.8	22.8
Syringaldehyde	36.6	182	0.0017	-0.0032	0.999	10.1	33.6
cis-5-Hydroxy-2-methyl-1,3-dioxane	10.8	103	_	_	_	_	_
trans-5-Hydroxy-2-methyl-1,3-dioxane	18.1	103	_	_	_	_	_
cis-4-Hydroxymethyl-2-methyl-1,3-dioxolane	13.5	103	_	_	_	_	_
trans-4-Hydroxymethyl-2-methyl-1,3-dioxolane	14.9	103	_	_	_	_	_
Furan derivatives:							
2-Furfural	10.1	95	0.0138	0.6736	0.993	12.0	30.0
HMF	30.2	97	0.0066	0.2527	0.999	10.2	33.9
5-Methylfurfural	12.6	109	0.0132	0.5085	0.999	10.5	35.1
2-Acetyl-furan	11.3	95	_	_	_	_	_
2-(Hydroxyacetyl)furan	21.3	95	_	_	_	_	_
Ethyl 2-furoate	13.8	95	0.0023	0.0178	0.999	10.7	35.5
Furfuryl alcohol	14.8	97	0.0025	-0.0055	0.996	13.5	45.1
Enolic compounds:							
Sotolon	25.1	83	0.0004	0.0007	0.996	5.4	17.8
Maltol	20.7	126	0.0008	-0.0103	0.994	21.5	71.5
5-Hydroxymaltol	26.7	126	_	_	_	_	_
Pantolactone	22.1	71	0.0015	-0.0007	1.000	14.1	47.1
Streker aldehydes:							
Phenylacetaldehyde	14.0	91	0.0113	0.4934	0.997	10.6	35.3
Methional	9.8	48	0.0010	0.0494	0.996	12.6	32.0

HMF: 5-(Hydroxymethyl)furfural; Sotolon: 3-hydroxy-4,5-dimethylfuran-2(*5H*)-one; Maltol: 3-hydroxy-2-methyl-4*H*-pyran-4-one; 5-Hydroxymaltol: 3,5-dihydroxy-2-methylpyran-4-one (DMP); Pantolactone: 4,5-dihydro-3-hydroxy-4,4-dimethyl-2(*3H*)-furanone; Methional: 3-(methylthio)propionaldehyde.

cis- and *trans*-5-Hydroxy-2-methyl-1,3-dioxane and *cis*- and *trans*-4-hydroxymethyl-2-methyl-1,3-dioxolane concentration were expressed respectively in 1,3-dioxane and 1,3-dioxolane equiv.;

2-acetylfuran and 2-(hydroxyacetyl)furan were expressed in 5-methylfurfural equiv.;

5-hydroxymaltol concentration was expressed in maltol equiv.

Linear range: 10-500 µg/L (except for sotolon 5-100 µg/L).

3.10.2. Solid Phase Micro Extraction (SPME) extraction

5 mL of sample was spiked with 20 µL of octan-3-ol in hydroalcoholic solution (1/1, v/v) at 50 mg/L (internal standard) was placed on a vial of 20 mL capacity and 0.5 g of anhydrous sodium sulfate. SPME for volatile compound analysis was used to extract volatiles. The fiber used was a divinylbenzene/carboxen/polydimethylsiloxane (DVB/CAR/PDMS), 50/30 mm (Supelco, Bellefonte, Pa., USA) in a combipal automatic injector. The SPME needle was in contact with the headspace of the sample during 30 min under a temperature of 40ºC. Finally, it was removed from the vial and inserted into the injection port of the gas chromatograph for 10 min. The extracted chemicals were thermally desorbed, at 220°C, and transferred directly to the analytical column. The methodology applied was adapted from Oliveira et al., 2006.

3.11. GC-FID acetaldehyde analysis

3.11.1. Direct injection

Samples were analysed directly (5 mL) adding 50 µL of 4-methylpentan-2-ol (10 g/L), as internal standard, in a Varian 3900 GC gas chromatograph equipped with a CP-1177 Split/Splitless injector and a Flame Ionization Detector (FID) at 220ºC. The column was a CP-WAX 57 of 50 m (0.25 mm x 0.2 µm) from Varian. The injector port and the detector were heated to 220°C. The split vent was opened after 30 s. The oven temperature was 40°C (for 5 min), then increased at 3°C/min to 110°C, and then increased at 20°C/min to 180°C (holding time of 1.0 min). The carrier gas was Helium C-60 (Gasin, Portugal), at 1 mL/min, constant flow. Table 3.10 represents the analytical parameters for the quantification of acetaldehyde by GC-MS on direct injection and SPME extraction. The methodology applied was adapted from Pontes et al., 2009.

3.11.2. SPME extraction

5 mL of sample was spiked with 50 µL of 4-methylpentan-2-ol (1 g/L), as internal standard, and 0.5 g of anhydrous sodium sulfate. Sample was then immersed in a water-

bath at 40°C with a small stir magnet at 1300 r.p.m. SPME for volatile compound analysis was used to extract acetaldehyde. The fiber used was a divinylbenzene/carboxen/polydimethylsiloxane (DVB/CAR/PDMS), 50/30 mm (Supelco, Bellefonte, Pa., USA). The SPME needle was in contact with the headspace of the sample during 30 min. Finally, it was removed from the vial and inserted into the injection port of the gas chromatograph for 10 min. The extracted volatile coumponds were thermally desorbed, at 220°C, and transferred directly to the analytical column. The column was a CP-WAX 57 of 50 m (0.25 mm x 0.2 µm) from Varian. The injector port and the detector were heated to 220°C. The split vent was opened after 30 s. The oven temperature was 40°C (for 5 min), then increased at 3°C/min to 110°C, and then increased at 20°C/min to 180°C (holding time of 1.0 min). The carrier gas was Helium C-60 (Gasin, Portugal), at 1 mL/min, constant flow.

Table 3.10. Analytical parameters of the working method for the quantification of acetaldehyde.

Analytical parameters of direct injection	
Linear concentration range (mg/L)	1-200
Linear regression (N=8)	y = 0.0107x+0.0625
R^2	0.999
LOD (mg/L)	6.1
LOQ (mg/L)	20.4
Analytical parameters of SPME extraction	
Linear concentration range (mg/L)	1-200
Linear regression (N=8)	y = 0.0018x+0.0204
R^2	0.998
LOD (mg/L)	23.0
LOQ (mg/L)	46.7

3.12. Analyses of Cu and Fe

Analyses of Cu and Fe were performed on a flame atomic absorption spectrometer (Unicam Solaar 969) equipped with deuterium background corrector. Elements were measured using a hollow-cathode lamp specific for each element, and the combination of air-acetylene flame was used for the formation of free atoms. Selected elemental

wavelengths were respectively 324.8 nm and 259.9 nm, for Cu and Fe. All solutions were prepared using ultra pure water, from a Millipore system, and supra pure quality chemicals. The standard solutions developed for the calibration curves of each of the ions analyzed were prepared by rigorous dilution of 1000 mg/L certified chemicals standard solutions.

3.13. Folin-Ciocalteu (FC) Index

The total polyphenolics was evaluated by the Folin-Ciocalteu index (FC). The FC method described by Singleton and Rossi (1965) was used with some modifications. Briefly, 1 mL of each white wine (diluted 10 times) or 1 mL of red Port wine (diluted 50 times) were mixed with 5 mL of FC reagent, diluted 10 times in water, and 4 mL of sodium carbonate (75 g/L). The mixture was then incubated for 1 h at room temperature. After the reaction period, the absorbance at 750 nm was measured. All determinations were carried out in duplicate and gallic acid was used as standard in order to express the results as gallic acid equiv, by the follow expression: $mg\ equivalents\ of\ gallic\ per\ liter = (Abs - 0.0042)/0.0105$.

3.14. SO_2 determination

The free and combined sulfur dioxide was determined according to the Portuguese Norm, NP 2220:1987.

3.15. pH determination

pH measurements were performed using a pH-meter crison pH 2002, with a combined glass electrode with a precision of 0.1.

3.16. Multivariate analysis

Raw voltammetric and chromatographic signals were processed using respectively methodologies performed based on Unscrambler® and MATLAB 7.8.0 software's. For chromatographic signals, using appropriate algebric operations it is possible to calculate a

single array resulting from compression of *n* matrices (chromatographic run) held. The procedure goes through the initial fold matrix dimensions [retention time; wavelengths] on a vector [1; retention time x wavelengths]. The converted vectors can then be grouped by sets of samples with again an array of dimensions [number of samples; retention time x wavelengths]. For multivariate analysis, each matrix was unfolded to give a vector $s_{i(1,\,j)}$, where *i* corresponds to the number of samples and *j* corresponds to the number of variables of each analysis. Then all of them were row concatenated to give a matrix $\mathbf{Q}_{(i,\,j)}$. This **Q** matrix was then used to perform the PCA, which consisted in the decomposition of it into: $\mathbf{Q}_{(i,\,j)} = \mathbf{T}_{(i,\,k)}.\ \mathbf{P}^{\mathbf{T}}_{(k,\,j)}$, where **T** represents the scores matrix, **P** represents the loadings matrix and k corresponds to the number of principal components. The scores matrix (**T**) gives the relationships between the samples, whereas the loadings matrix (**P**) gives the importance of each variable (i.e. retention times and their correspondent absorption spectra). Finally, and in order to facilitate the interpretation of the loadings (**P**), each one of its columns k (principal components) were folded back to give a matrix, which was depicted as a 2D map: $\mathbf{P}_{k\,(j,\,1)} \rightarrow p_{k(l,\,m)}$, where $j = l\ .\ m$ such as *l* and *m* are, respectively, the number of scans (retention time) and the absorption values correspondent to each sample.

3.17. Chemicals

The following molecules were purchased to Sigma-Aldrich, (Portugal): hydroxybenzoic acids: gallic acid (G7384) (100%); protocatechuic acid (P5630) (100%); syringic acid (S6881) (95%); *para*-hydroxybenzoic acid (W398608) (99%); hydroxycinnamic acids: caffeic acid (C0625) (98%); *para*-coumaric acid (C9008) (98%); ferulic acid (128708) (99%); flavan-3-ols: (+)-catechin hydrate (C1251) (98%); (-)-epicatechin (E4018) (98%); flavonols: quercetin (Q4951) (95%); stilbenes: *trans*-resveratrol (R5010) (99%); phenanthroline (131377) (99%); malvidin 3-glucoside (72813) (90%); 3-deoxyglucosone (75762) (75%); β-phenylpyruvic acid (P8126); *ortho*-phenylenediamine (P-9029) (98%); octan-3-ol (218405) (99%); phenylacetaldehyde (107395) (90%); 3-(methylthio)propionaldehyde (methional) (W274711) (98%); 3-hydroxy-4,5-dimethylfuran-2(*5H*)-one (W363405) (97%); L-amino acids kit (LAA-21); homoserine (814359) (98%); 2-furfural (185914) (99%); 5-(hydroxymethyl)furfural (W501808) (99%); 5-methylfurfural (W270202) (98%); ethyl 2-furoate (W501301) (98%); furfuryl alcohol

(185930) (98%); 3-hydroxy-2-methyl-4*H*-pyran-4-one (maltol) (W265608) (99%); 4,5-dihydro-3-hydroxy-4,4-dimethyl-2(3*H*)-furanone (pantolactone) (237817) (99%). benzaldehyde (W212709) (98%); vanillin (V1104) (99%); syringaldehyde (W404926) (98%); acetaldehyde (A5076) (98%); 1,3-dioxane (283061) (97%); 1,3-dioxolane (239798) (99%).

The following molecules were purchased to Merck, (Germany): DL-norvaline (146716) (98%); EDTA (108421) (99%); AAS Standards Certipur: copper standard solution (119786) (100%) and iron standard solution (119781) (100%); Ethanol (24102) (99.8%); D(+)-Glucose (34635) (100%); D(-)-Fructose (104007) (100%).

3.18. References

Castellari, M., Versari, A., Spinabelli, U., Galassi, S., & Amati, A. (2000). An improved HPLC method for the analysis of organic acids, carbohydrates and alcohols in grape musts and wines, *Journal of Liquid Chromatography & Related Technologies*, *23*, 2047-2056.

Castro, C., Gunning, C., Oliveira, C., Couto, J. A., Teixeira, J., Martins, R., & Silva Ferreira, A. C. (2012). Saccharomyces cerevisiae oxidative response evaluation by cyclic voltammetry and gas chromatography – mass spectrometry *Journal of Agricultural and Food Chemistry*, *60*, 7252-7261.

Oliveira, C., Barbosa, A., Silva Ferreira, A. C., Guerra, J., & Guedes de Pinho, P. (2006). Carotenoid Profile in Grapes Related to Aromatic Compounds in Wines from Douro region. *Journal of Food Science*, 71, S001-007.

Pontes, H., Guedes de Pinho, P., Casal, S., Carmo, H., Santos, A., Magalhães, T., Remião, F., Carvalho, F., & Bastos, M. L. (200). GC Determination of Acetone, Acetaldehyde, Ethanol, and Methanol in Biological Matrices and Cell Culture. Journal of *Chromatographic Science, 47*, 272-278.

Pripis-Nicolau, L., De Revel, G., Marchand, S., Beloqui, A. A., & Bertrand, A. (2001). Automated HPLC method for the measurement of free amino acids including cysteine in

musts and wines; first applications. *Journal of the Science of Food and Agriculture, 81*, 731-738.

Silva Ferreira, A. C., Oliveira, C., Hogg, T., & Guedes de Pinho, P. (2003). Relationship between potentiometric measurements, sensorial analysis, and some substances responsible for aroma degradation of white wines. *Journal of the Science of Food and Agriculture*, *51*, 4668-4672.

Silva Ferreira, A. C., Reis, S., Rodrigues, C., Oliveira, C., & Guedes de Pinho, P. (2007). Simultaneous determination of ketoacids and dicarbonyl compounds, key Maillard intermediates on the generation of aged wine aroma. *Journal of Food Science, 72*, S314-S318.

4. Chapter 4 - Role of oxygen in wine

4.1. Oxygen uptake of white and red Port wines under four different temperatures and two oxygen regimes

The overall oxidation mechanism occurring in wines is illustrated in Figure 4.1. In this process, oxygen do not reacts directly with phenolic compounds without the presence of transition metal ions. It is also established that the rate of wine oxidation depends on temperature, concentration of dissolved oxygen, phenolic composition of wines, and pH.

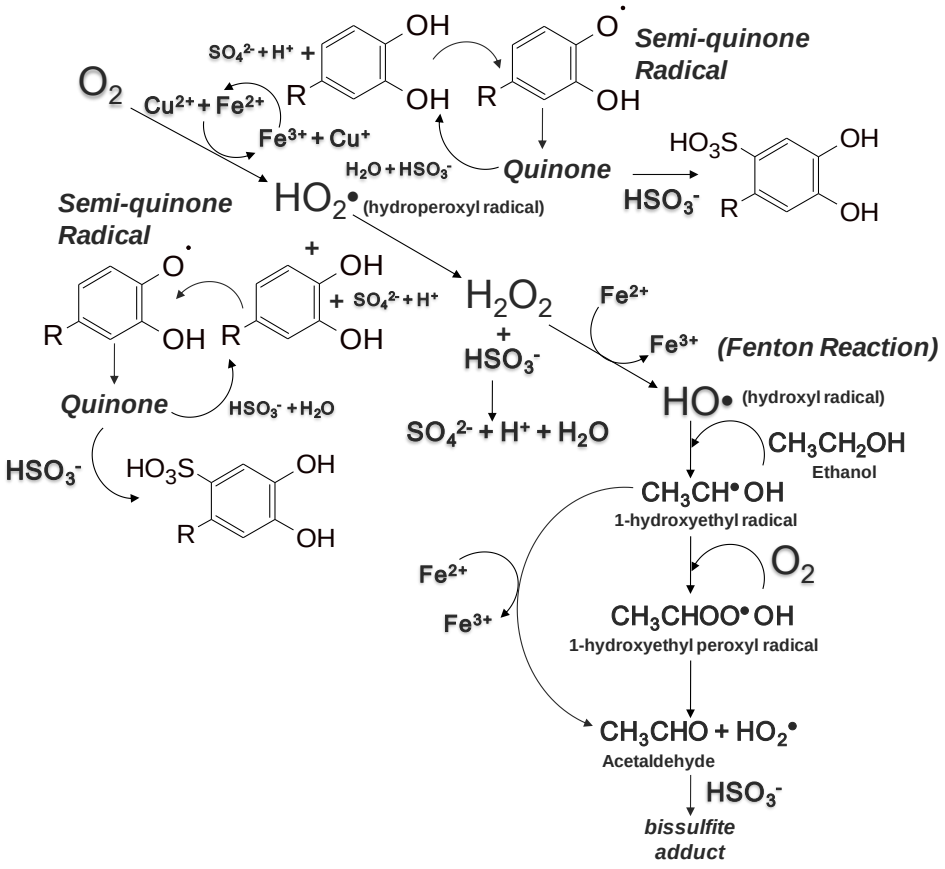

Figure 4.1. Oxidation mechanism occurring in wines.

Oxygen depletion was measure (Chapter 3; 3.3.) in the forced aging protocols of white and red Port wines (Chapter 3; 3.2.). Results have showed that, for treatment I (no supplemented oxygen addition) oxygen consumption is dependent to the applied temperature and that follows an Arrhenius-type relation (Macías et al., 2001) (Figure 4.2

and Figure 4.3). Figure 4.2 illustrates the dissolved oxygen depletion of white and red Port wines under the respectively four different applied temperatures.

The oxidation phenomena can be considered as oxidation reactions, where the two general reactants are dissolved oxygen (DO) and the oxidizable matter (A) (mainly polyphenols), and the general products are the oxidized matter (B) (mainly condensed polyphenols). This reaction can be described as: A + DO $\rightarrow$ B. The general oxidation rate depends on the concentration of the reactants, and the oxygen consumption rate (r) is expressed by the following ordinary differential equation: r = -d[DO]/dt = k[A][DO]. At low concentrations, as the concentration of the oxidizable matter (A) is much higher than the concentration of dissolved oxygen and constant, it can be assumed that oxygen is the limiting reactant. Thus, if it is considered, k[A] = K_{ox}, the oxidation rate depends only on the oxygen concentration, and by integrating the rate expression (r) the following equation is obtained $[DO]t = [DO]_0 e^{(-Kox\ t)}$. The dependence of the oxidation rate constant K_{ox} upon the temperature T is expressed by the Arrhenius equation: $K_{ox} = k_0\, e^{-Ea/RT}$, where k_0 is the pre-exponential factor, E_a is the activation energy, and R is the gas constant equal to 8.314 J/mol.K. According to the Arrhenius equation, the activation energy for oxygen depletion in wine can be calculated by plotting the natural logarithm of the rate constants, at the four applied temperatures, against the reciprocal of the absolute temperature: $ln(K_{ox}) = ln(k_0) - E_a/RT$.

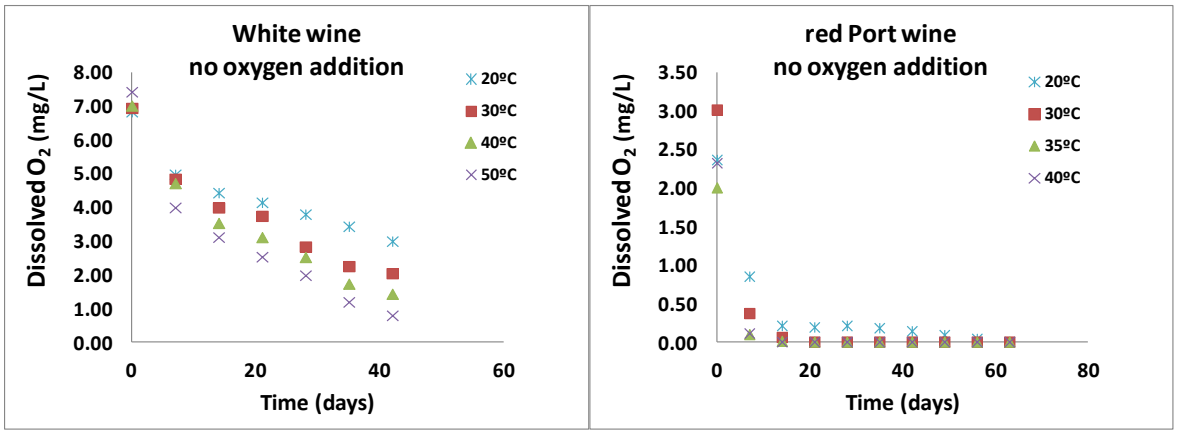

Figure 4.2. Oxygen depletion of the white wine samples kept at 20, 30, 40 and 50ºC, and for the red Port wine samples kept at 20, 30, 35 and 40ºC, with treatment I.

From a detailed observation of Figure 4.2, it can be concluded that oxygen is rapidly consumed in the first week of storage for all temperature regimes, and this depletion is faster at higher temperatures. Figure 4.3 represents the Arrhenius plot for the reaction of oxygen depletion for both white and red Port wines in treatment I. The activation energies (*Ea*), the pre-exponential factor (k_0), and the rate constants estimated at the reference temperature (k_{Tref}) of 35°C are reported in Table 4.1. Knowing the kinetic parameters of the reaction of oxygen depletion in wine, and the initial dissolved oxygen concentration, the dissolved oxygen concentration of the wine can be predicted at any time (t) and temperature (T) using the equations: $[DO]_t = [DO]_0 e(-K_{ox}\ t)$, and $K_{ox} = k_0\ e^{-Ea/RT}$.

From a detailed observation of Table 4.1, it can be concluded that although the activation energies (*Ea*) for oxygen depletion are similar for both white and red Port wines, the oxygen consumption rates are very different, much higher for the red Port wine. This means that the concentration of the oxidizable matter (A), mostly polyphenols, is in different concentrations being higher in the red Port wine.

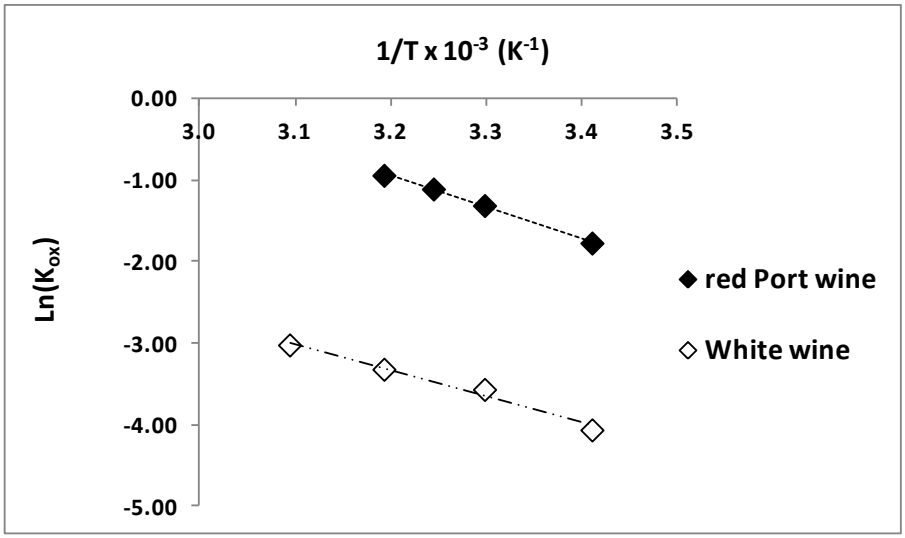

Figure 4.3. Arrhenius plot for both white and red Port wines in treatment I.

Table 4.1. Kinetic parameters of oxygen depletion in wine, given by Arrhenius equation.

Treatment I (no supplemented oxygen addition)				
	Ea (kJ/mol)	R	k_0 (s^{-1})	k_{TRef} x 10^{-10} (mol/L·s)
White wine	26.6 ± 10.9	-0.991	0.70 ± 0.05	6.69
Red Port wine	31.9 ± 4.7	-0.999	58.70 ± 0.01	70.5

Treference of 35°C, confidence intervals of 95%, and four storage temperatures.

For treatment II (oxygen addition every sampling point), although a kinetic approach was not feasible, because of the system perturbation, the oxygen consumption dependence, to the applied temperature, is also observed. In fact, in this treatment, the oxygen consumption was more effective achieving total values of consumed oxygen of 8.4, 11.7, 15.7, and 24.5 mg/L for, respectively, temperatures storage of 20, 30, 40 and 50ºC, for the white wine. The red Port wine had consumed higher values of 22.2, 27.7, 31.1, and 39.8 mg/L for, respectively, temperatures storage of 20, 30, 35 and 40ºC. Table 4.2 illustrates the overall consumed oxygen, induced by the different temperatures, in moles per liter.

Table 4.2. Overall consumed oxygen in moles per liter at the different storage temperatures.

White wine		**Red Port wine**	
Temperature	mol/L x 10^{-4}	**Temperature**	mol/L x 10^{-4}
20ºC	2.62	20ºC	6.94
30ºC	3.65	30ºC	8.67
40ºC	4.89	35ºC	9.72
50ºC	7.66	40ºC	12.40

4.2. Oxygen uptake of white and red Port wines in the presence of a chelating agent cocktail (EDTA + phenanthroline)

In the presence of Fe(II), molecular oxygen is reduced by a sequential one electron reduction to yield a superoxide radical anion ($O_2^{\bullet -}$) which, under acidic wine conditions, is quickly converted to a hydroperoxyl radical ($HO_2^{\bullet}$) (Figure 4.1). The transfer of a second electron will produce peroxide anion (O_2^{2-}), which, at wine pH, exists in the protonated hydrogen peroxide (H_2O_2) form (Figure 4.1). The next transition metal-catalyzed reduction stop yields the hydroxyl radical ($HO^{\bullet}$), via the Fenton reaction (Figure 4.1). The hydroxyl radical will oxidize almost any organic molecule found in wine and will react with the first species it encounters, depending on their concentration. In the same way, is already recognised that Cu(II) can interact with oxygen, facilitates the redox cycling of iron (Figure 4.1), while Fe(III) will oxidize the catechol couple (Figure 4.1). Fe(II) and Fe(III) ions represent the dominant two oxidation states of iron in wine. Iron speciation in wine has been measured in various studies, and it has been reported that the majority of free iron

is present as Fe(II) (Tašev et al., 2006, Elias and Waterhouse, 2010). In the presence of tartaric acid, the reduction potential of Fe(III)/Fe(II) is close to 350 mV at pH 3.6 (Green and Parkins 1961), being below that of the O_2/H_2O_2 couple (565 mV), thus making the oxidation of Fe(II) thermodynamically favourable. In this way, Fe(II) is a stronger reductant and Fe(III) is a weaker oxidant (Danilewicz, 2012). As, because the reduction potential of Fe(III)/Fe(II) couple is below that of the catechol couple, its oxidation by Fe(III) is thermodynamically disfavored, which presumably contributes to the slowness of the reaction, unless sulfite or other nucleophile such as glutathione is present to displace the unfavorable equilibrium and draw the reaction forward (Danilewicz 2011). For all the above reasons, the transition metals ions (iron and copper) are responsible for catalyzing a number of reactions in wine, and to prevent these metal-catalyzed oxidation processes, the most probable effective way is to completely remove all trace iron and copper from the juice, must, or wine. Previous works, have already suggested that the progressive removal of transition metals from wine slow and eventually minimize wine oxidation reactions (Danilewicz and Wallbridge, 2010). In the same way, the role of transition metal ions was previously studied using different chelating agents in wine-model solutions (Cantú et al., 2009). Results have showed that, in model solutions with 4-methylcatechol, the presence of 2,2'-bipyridine decreased the oxidation rate of the catechol when metal ions were added, namely, iron (5.0 mg/L), and iron+copper (5.0 mg/L + 0.15 mg/L). Moreover, in this study, EDTA was very effective in slowing the oxidation rate of the catechol with addition of copper alone (0.15 mg/L). Though, these studies were only conducted in wine-model systems. Additionally, the ability of some chelators to affect the formation of 1-hydroxyethyl radicals (Figure 4.1) and acetaldehyde (Figure 4.1) was made in wine using a spin trapping methodology (Kreitman et al., 2013). In this study, the Fe(II)-specific chelators were more effective than the Fe(III) chelators with respect to 1-hydroxyethyl radicals inhibition during the early stages of oxidation, and significantly reduced oxidation markers compared to a control during the study. However, while the addition of Fe(III) chelators was less effective or even showed an initial prooxidant activity, these Fe(III) chelators proved to be more effective antioxidants compared to Fe(II) chelators (Kreitman et al., 2013).

In this work, the impact of a single dose of a chelating agent cocktail in the oxygen uptake of both white and red Port wines was evaluated at two temperatures. For this purpose, the

white wine and the red Port wine described in Chapter 3 (3.1. Wine characterization) were adjusted to oxygen content close to 8.0 mg/L by air bubbling (20/80; O_2/N_2) (Gasin, Portugal). The parameters studied were adjusted as follows: *(i)* a first portion corresponds to the untreated wine (control) stored at 20ºC; *(ii)* a second portion corresponds to the untreated wine (control) stored at 40ºC; *(iii)* a third portion corresponds to adjusted EDTA and phenanthroline content of 500 μM each, and stored at 20ºC; *(iv)* and finally, a fourth portion corresponds to adjusted EDTA and phenanthroline content of 500 μM each, and stored at 40ºC. Each set was kept in sealed flasks with a capacity of 110 mL, up to the observation of oxygen depletion. EDTA is a polyaminocarboxylic acid and is widely used to "sequester" transition metal ions such as copper(II) and iron(III). Phenanthroline is a heterocyclic compound widely used to chelate iron(II). The concentrations used, 500 μM, (around 145 mg/L of EDTA and 90 mg/L of phenanthroline) are higher than the concentrations normally occurring in wines for the investigated transition metal ions (0.11 to 3.6 mg/L for copper and 2.8 to 16 mg/L for iron) (Ough and Amerine, 1988). Experimental was conducted in duplicate. The used chelating agents were chosen taking into account the recognized metal ions involved in wine oxidation (iron and copper), (Figure 4.1) (Waterhouse and Laurie, 2006, Kilmartin, 2009, Cantú et al., 2009, Oliveira et al., 2011). EDTA was used to "sequester" copper(II) and iron(III), and phenanthroline was used to chelate iron(II). In wine, reducing iron concentrations to less than 4 mg/L minimizes the risk of Fe-associated cloudiness, discoloration, metallic taste, and metal toxicity (Ough et al., 1982). In the same way, it is generally recommended that the copper concentration, in finished wines, should remain below 0.3 to 0.5 mg/L (Rankine, 1989). However, these recommendations do not take into account the relevant potential of metal ions in the wine oxidation process, even at low concentrations. Chelating agents are already used to avoid the precipitation of metal ions in foods and beverages. Chelators like EDTA, citric acid, calcium phytate, phytic acid, potassium ferrocyanide, and polyphosphates are used in low concentrations. Food manufacturers take advantage of EDTA's chelating properties by adding it to foods as a preservative. The U.S. Food and Drug Administration (FDA) regulate EDTA as a food additive and sets limits on concentrations and functions in specific foods and beverages. In beverages it is present at concentrations up to 25 mg/L as an "antigushing agent" in fermented malt beverages.

Figure 4.4 and 4.5 illustrates the dissolved oxygen depletion of respectively, white and red Port wines by the addition of a chelating agent cocktail (EDTA + phenanthroline), under two different temperatures (20 and 40ºC). Table 4.3 shows the overall uptake of dissolved oxygen in molar quantity of O_2 per liter per second, for all the applied treatments.

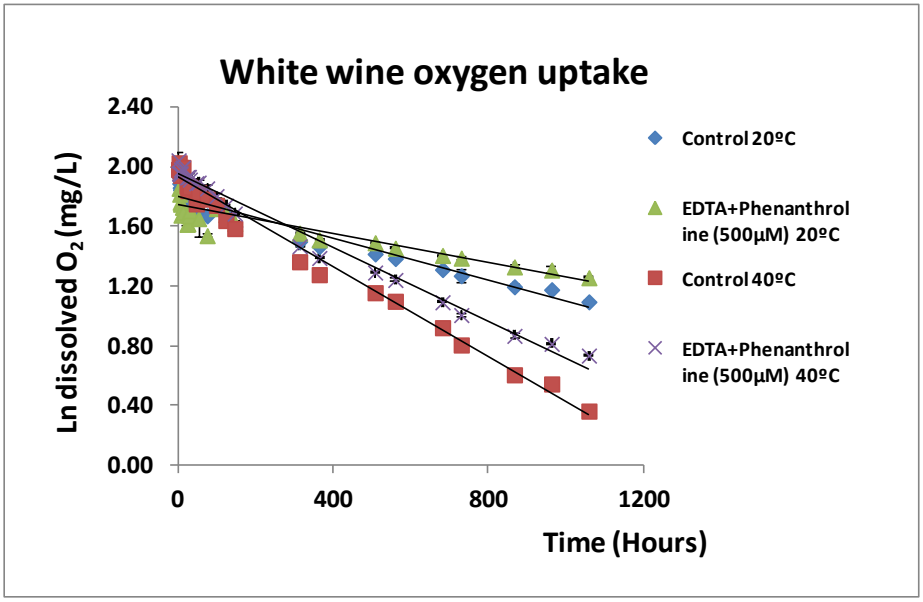

Figure 4.4. Oxygen depletion of white wine under the addition of a chelating agent cocktail (EDTA + phenanthroline) at two different temperatures (20 and 40ºC).

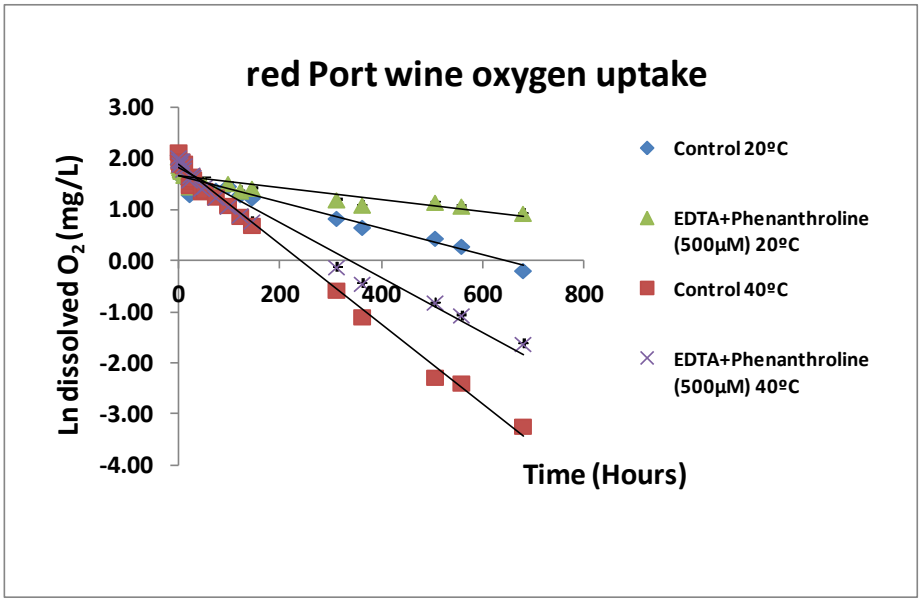

Figure 4.5. Oxygen depletion of red Port wine under the addition of a chelating agent cocktail (EDTA + phenanthroline) at two different temperatures (20 and 40ºC).

Table 4.3. Uptake of dissolved oxygen in moles of O_2 per liter per second (mol/L·s), under saturated oxygen conditions.

Uptake of dissolved oxygen (mol/L.s x 10^{-10})	White wine	Red Port wine
Control 20ºC	3.6	13.5
EDTA + Phenanthroline (500 µM) 20ºC	2.5	6.2
Control 40ºC	7.8	40.7
EDTA + Phenanthroline (500 µM) 40ºC	6.5	28.0

Results have shown that the use of the specific chelating agents (EDTA + phenanthroline) decrease the oxygen consumption by 32% and 54% at 20ºC for, respectively, white and red Port wines (Figure 4.4 and 4.5, and Table 4.3). On the other hand, this decrease was less prominent for 40ºC, by 18% and 32% for, respectively, white and red Port wines (Figure 4.4 and 4.5, and Table 4.3). This fact could be related with chelators degradation with temperature. Moreover, the observation of higher uptake of dissolved oxygen in the red Port wine was not consistent with the presence of higher metal ions concentration in this wine. In fact, these values, in Chapter 3 (3.1. Wine characterization), were lower in the red Port wine (Cu, 0.34 mg/L in white and 0.27 mg/L in Port; and Fe, 2.54 mg/L in white and 1.81 mg/L in Port). Nevertheless, the values were similar for the two analyzed wines.

4.3. Relation between oxygen uptake and phenolic composition of wines

4.3.1. Phenolic composition of wines versus oxygen uptake

When phenolic compounds react with ROS, the reaction rate of each phenolic depends on its ability to form a stable product radical. As previously seen (Chapter 1; Oxidation/ROS in Wine), polyphenols containing a 1,2-dihydroxybenzene ring (catechol moiety) or a 1,2,3-trihydroxybenzene (a galloyl group) are easier to oxidize because the resulting phenoxyl semi-quinone radical can be stabilized by a second oxygen atom. Briefly, nearly all wine phenolic compounds are very reactive toward the hydroperoxyl radical. Monophenols and their equivalent *meta*-dihydroxybenzene rings and substituted phenols (especially methoxy derivatives) are not as readily oxidized because they do not produce

stabilized semi-quinone radicals. In the same way, malvidin-3-glucoside, the main anthocyanin present in red wine, is not readily oxidized. Oligomeric and polymeric phenolic compounds (procyanidins and condensed tannins) react similarly with ROS as compared to monomeric catechol phenolics (Waterhouse and Laurie, 2006).

Results have shown that red Port wine had about 4 times higher uptake of dissolved oxygen compared to white wine (Table 4.3). Concerning the polyphenols content of the analyzed wines described in Chapter 3 (3.1. Wine characterization), the higher uptake of dissolved oxygen in the red Port wine is consistent with the fact that red wines contain polyphenols at a higher concentration than white wines, and with the knowledge that the oxidative processes begin by the oxidation of polyphenols, much more as they are readily oxidized. In fact, from the observation of Table 3.1 (Chapter 3, 3.1. Wine characterization) we can see that red Port wine has more hydroxybenzoic acids, in particular gallic acid (2.66 mg/L in white and 6.85 mg/L in Port). This phenolic compound belong to a group of polyphenols containing a 1,2,3-trihydroxybenzene and easy to oxidize because the resulting phenoxyl semi-quinone radical can be stabilized by a second oxygen atom (Kilmartin et al., 2001, Makhotkina and Kilmartin, 2009). Likewise, flavan-3-ols are in much higher concentration in red Port wine (catechin, 3.4 mg/L in white and 13.8 mg/L in Port; and epicatechin, 0.9 mg/L in white and 8.0 mg/L in Port). These phenolics are compounds containing a 1,2-dihydroxybenzene ring resulting, as well, in stable phenoxyl semi-quinone radicals and therefore readily to oxidize (Kilmartin et al., 2001, Makhotkina and Kilmartin, 2009, Oliveira et al., 2011). Quercetin, that is only present in the red Port wine, oxidizes at lower potentials, close to +0.4 V (Ag/AgCl reference electrode), (Kilmartin et al., 2001) and can therefore contribute to the acceleration of the wine oxidative process. Considering hydroxycinnamic acids, the amount of caftaric acid is higher in red Port wine than in white wine. This phenolic is oxidized at potentials around +0.4 V (Ag/AgCl reference electrode) (Makhotkina and Kilmartin, 2012), and is well known to be quickly oxidized during enzymatic browning (Singleton et al., 1985, Cheynier and Van Hulst, 1988, Cheynier et al., 1989). Anthocyanins belong to the wine flavonoid family and exist as glycosides through conjugation of anthocyanidins with primarily glucose. In *Vitis vinifera* varieties pigments are mainly in the 3-*O*-glucoside form. Five anthocyanidin bases are present in red grapes, namely, malvidin, delphinidin, peonidin, cyanidin and petunidin. Malvidin-3-*O*-glucoside (the predominant pigment in *Vitis vinifera*

varieties) is oxidized at higher potentials close to +0.65 V (Ag/AgCl reference electrode) (Kilmartin et al., 2001). However, this phenolic, as well the entire family, may react with flavanols either directly or mediated by other compounds such as acetaldehyde resulting from ethanol oxidation (Timberlake and Bridle, 1976, Rivas-Gonzalo et al., 1995, Lee et al., 2004). As such, this family of polyphenols can contribute to oxygen depletion.

In the proposed study, the pH of red Port wine is higher than that of white wine (Chapter 3 (3.1. Wine characterization). This fact could be a contribution factor for the higher uptake of dissolved oxygen in Port wine. Under normal wine conditions (pH 3.0 to 3.5) there is a slow rate of phenolic oxidation reactions. On the other hand, electrons are rapidly transfer from phenols to semi-quinones at pH 7 (Danilewicz, 2003) and in alkaline conditions there is a quicker estimate of oxygen consumption in wine (Singleton et al., 1979). Moreover, phenolic compounds under high pH conditions can react directly with oxygen.

4.3.2. Oxygen uptake of phenolic compounds in wine-model solutions

An attempt to evaluate the oxygen uptake of phenolic compounds has been done. For this purpose a wine-model system was prepared with ethanol 12% (v/v) and 0.033 M tartaric acid, in saturated oxygen conditions (8.5 mg/L), and the pH was adjusted to 3.6 with an aqueous NaOH solution. After that, the following reactive low molecular weight phenolic compounds were added individually, namely, catechin (0.2 mM), *para*-coumaric acid (0.3 mM), gallic acid (0.3 mM), caffeic acid (0.3 mM), syringic acid (0.2 mM), and ferulic acid (0.2 mM), in concentrations near to their higher limit normally occurring in wines (close to 45 mg/L). Then, the addition of 0.4 mg/L of Cu^{2+} in the form of copper sulfate pentahydrate, and 7.5 mg/L of Fe^{2+} in the form of ferrous sulfate, was done to induce the respective phenolic oxidation. Copper(II) and iron(II) were added in concentrations close to their higher limit normally occurring in wines (Ough and Amerine, 1988). A control with water and water plus transition metal ions was also analysed. Each individual compound was kept in sealed flasks till the observation of oxygen depletion. All measurements were made six times. Flasks were never open during the experimental protocol.

Figure 4.6 represents the oxygen depletions in the presence of catechin, *para*-coumaric acid, gallic acid, caffeic acid, syringic acid, and ferulic acid, in a wine-model system with transition metal ions.

Results have showed that, at the protocol conditions, gallic acid, catechin, and syringic acid were the only tested phenolics that had promote the uptake for dissolved oxygen, being gallic acid the more effective. Moreover, the uptake of dissolved oxygen in molar quantity of O_2 per liter per second was $5.8x10^{-10}$ for gallic acid, and $1.2x10^{-10}$ for both catechin and syringic acid. Gallic acid, a benzoic acid derivative with 3 available hydroxyl groups is easily oxidized (Kilmartin, 2009). Moreover, previously studies (Tulyathan et al., 1989) have already observed a high reactivity of gallic acid with oxygen (3 mol equiv of oxygen per 1 mol of gallic acid) in alkaline solutions. In the same way, (+)-catechin have an easily oxidizable catechol group which makes it more easily oxidizable than a phenolic acid with an isolated phenol group like *para*-coumaric acid (Kilmartin, 2009). It seems that gallic acid is an important reactive low molecular weight phenolic compound in wine oxidation.

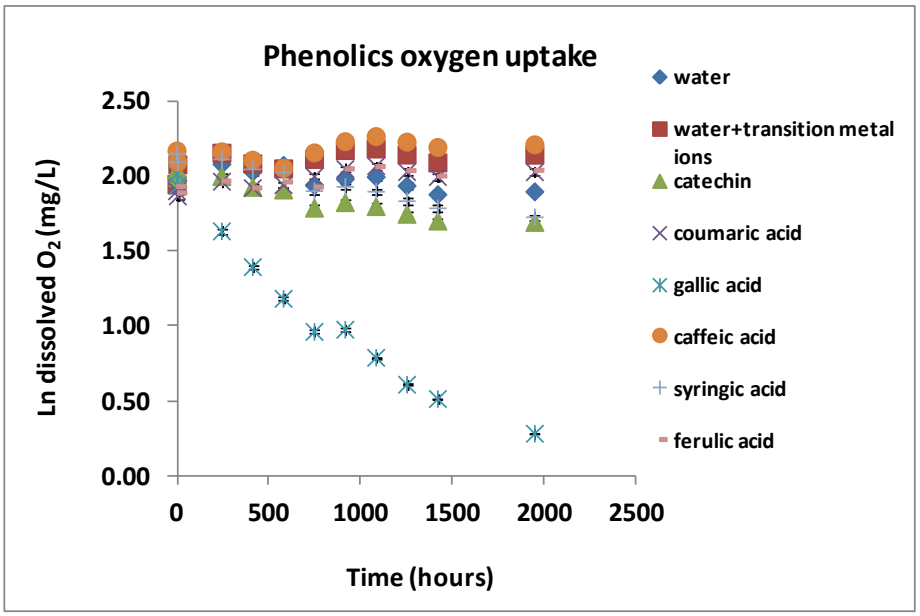

Figure 4.6. Oxygen depletion of the phenolic compounds: catechin, *para*-coumaric acid, gallic acid, caffeic acid, syringic acid, and ferulic acid.

Because gallic acid had a high reactivity with oxygen, a relationship between oxygen consumption of gallic acid (0.3 mM; 45 mg/L) and the studied wines have been made

(Table 4.4). From the observation of this table we can establish a relationship between wines and gallic acid oxygen uptake. We can express the oxygen uptake of the white wine, resulted from its overall intervenient on chemical oxidation, in 0.6 and 1.3 equiv of gallic acid (at concentration of 45 mg/L), for respectively the temperatures of 20 and 40ºC. In the same way, red Port wine oxygen uptake can be expressed in 2.3 and 7.0 equiv of gallic acid (at concentration of 45 mg/L), for respectively the temperatures of 20 and 40ºC.

Table 4.4. Relationship between gallic acid and wines oxygen consumption.

Relationship between oxygen consumption of both gallic acid* and wines		
Wine temperature	**white wine/gallic acid**	**red Port wine/gallic acid**
20ºC	0.6 ± 0.1	2.3 ± 0.4
40ºC	1.3 ± 0.1	7.0 ± 0.3

* in a wine-model system with transition metal ions (0.3 mM).

4.4. Quantification of key intermediaries' of oxygen reactions in wine

4.4.1. Quantification of sulfur dioxide in white wine

Sulfur dioxide analysis was performed (Chapter 3; 3.14.) in the forced aging protocol of white wines (Chapter 3; 3.2.). For the white wine aging protocol, samples were taken weekly (P0; and P1, 7th day sampling, to P6, 42th day sampling) (P0 + 6 weeks*2 oxygen regimes*4 temperatures*2 replica); total of ***98 samples***. The free and bound sulfur dioxide content is represented in, respectively, Figure 4.7 and Figure 4.8.

Sulfur dioxide does not react directly with molecular oxygen but with the oxygen reduced form, hydrogen peroxide (Oliveira et al., 2011). SO_2 can inhibit aldehydes formation by competing for hydrogen peroxide (Elias et al., 2010). SO_2 also play an important role in reducing quinones, formed during oxidation process, back to their phenol form (Danilewicz, 2007, Danilewicz et al., 2008).

Considering the forced aging protocol of white wine, results have showed that oxygen consumption and temperature exposure decreases the SO_2 content of the forced aged white wine samples (Figure 4.7 and Figure 4.8). Treatment II (oxygen addition) have promoted a

higher decrease in both free and bound SO_2. High relative consumption of SO_2 made clear that this wine was well protected from oxidation. Bound SO_2 does not decrease at 20ºC in both oxygen treatments (Figure 4.8). However, at 30, 40 and 50ºC a decrease is observed, much higher with oxygen treatment II. This fact could be related with the polyphenols scavenging of intermediate radicals that inhibit SO_2 autoxidation.

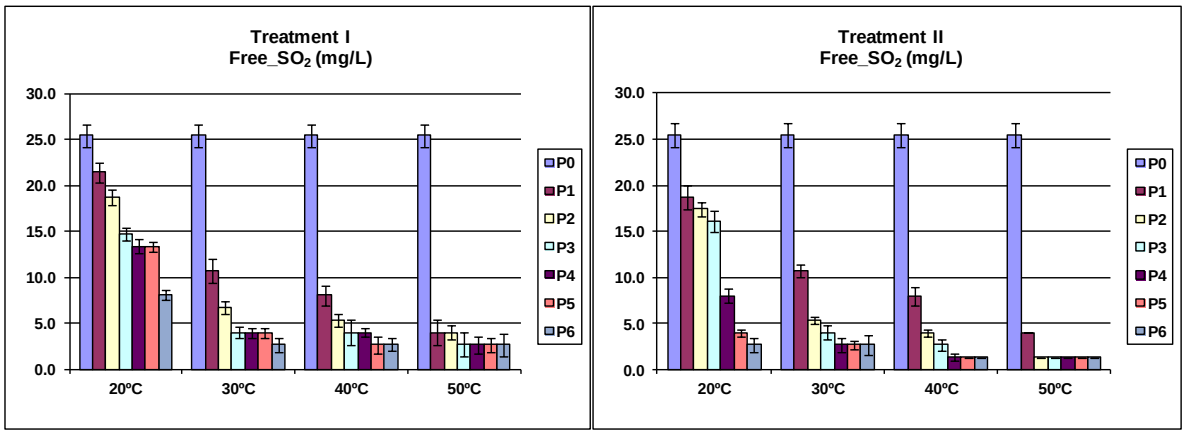

Figure 4.7. Free sulfur dioxide of the samples kept at 20, 30, 40 and 50ºC, with both oxygen treatments: treatment I and treatment II; (N=2).

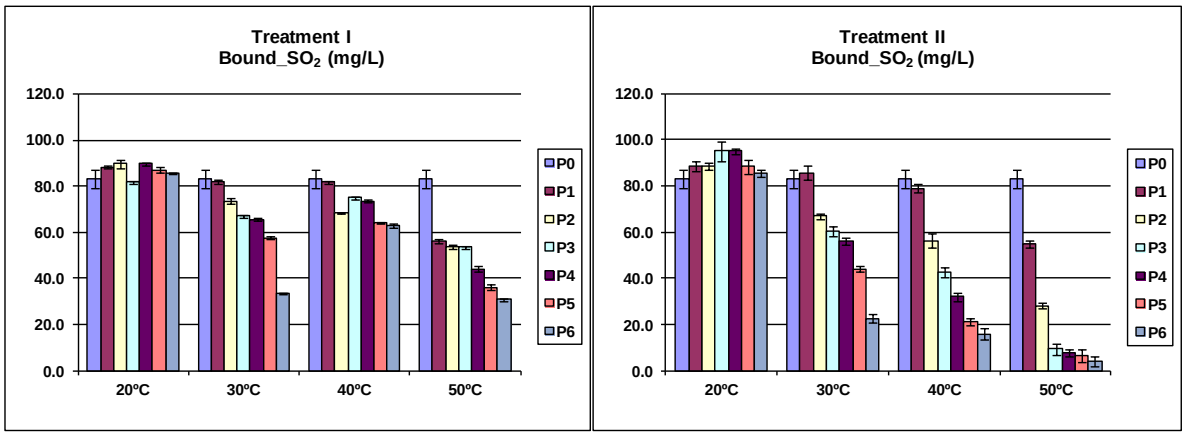

Figure 4.8. Bound sulfur dioxide of the samples kept at 20, 30, 40 and 50ºC, with both oxygen treatments: treatment I and treatment II; (N=2).

4.4.2. Quantification of aldehydes in white and red Port wines

During aging, aldehydes and mostly acetaldehyde (Figure 4.1), resulting essentially from ethanol oxidation, are important intermediates in chemical transformations occurring in

white and especially in red wines, leading to color and flavor changes. Acetaldehyde mechanism formation is shown in Figure 4.1. In the proposed mechanism, oxygen is converted to a hydroperoxyl radical which then directly oxidizes a catechol to its semi-quinone radical. Hydrogen peroxide is formed during this reaction, but it is incapable of directly oxidize ethanol (Laurie and Waterhouse, 2006). A more likely route for ethanol oxidation at wine pH is via the hydroxyl radical, which is formed by the Fenton reaction (Danilewicz, 2003, Waterhouse and Laurie, 2006) (Figure 4.1). Acetaldehyde can then undergo condensation reactions with anthocyanins and flavan-3-ols to form ethyl-linked oligomers. These may then react with additional acetaldehyde, anthocyanins, and flavan-3-ols to generate polymeric-type structures. Acetaldehyde can also be consumed in an acetalization reaction with glycerol, ethanol, and butane-2,3-diol with formation of the corresponding four heterocyclic acetals (in section 4.4.3. in this chapter), 1,1-diethoxyethane, and butane-2,3-diol acetal (Figure 4.13). Throughout these reactions, glycerol, ethanol, and butane-2,3-diol protects the wine against excessive acetaldehyde content and thus indirectly play an essential role in wine aroma. Beside these reactions, acetaldehyde can also be bound spontaneously with sulfur dioxide (HSO_3^-), Figure 4.1.

Quantification of acetaldehyde was performed by GC/FID (Chapter 3; 3.11) in the forced aging protocols (Chapter 3; 3.2.) of white (direct injection) and red Port wines (SPME extraction). For the white wine aging protocol, samples were taken on the first day, and weekly (P0; and P1, 7^{th} day sampling, to P6, 42^{th} day sampling) (P0 + 6 weeks*2 oxygen regimes*4 temperatures*2 replicates); total of ***98 samples***. For the red Port wine aging protocol, samples were taken on the first day, the 14^{th} day sampling (P2); the 28^{th} day sampling (P4); the 42^{th} day sampling (P6); the 56^{th} day sampling (P6); and the 63^{th} day sampling (P9) (P0 + 5 sampling points*2 oxygen regimes*4 temperatures*2 replicates); total of ***82 samples***.

Figure 4.9 and Figure 4.10 represents the evolution of acetaldehyde in oxygen treatments I and II for, respectively, white and red Port wines. Considering the above reactions, and by the observation of Figure 4.9, we can consider that acetaldehyde consumption is higher than ethanol oxidation, during the first 20 to 25 days of the white wine forced aging protocol. Then, acetaldehyde concentration begins to increase. Moreover, this rice is higher for a temperature of 20ºC and by oxygen exposure treatment II (Figure 4.9). By the observation of Figure 4.10, we can perceive that acetaldehyde consumption is higher than

ethanol oxidation, during all the protocol (63 days) of the red Port wine forced aging, and for the two applied oxygen treatments. This fact could be related to the already reported reaction of acetaldehyde with anthocyanins and flavan-3-ols of the red Port wines.

Quantification of benzaldehyde, vanillin and syringaldehyde was performed by GC-mass spectrometry (Chapter 3; 3.10.1) in the forced aging protocols of white and red Port wines (Chapter 3; 3.2.). For the white wine aging protocol, samples were taken on the first day, and weekly (P0; and P1, 7th day sampling, to P6, 42th day sampling) (P0 + 6 weeks*2 oxygen regimes*4 temperatures*2 replicates); total of ***98 samples***. For the red Port wine aging protocol, samples were taken on the first day, and weekly (P0; and P1, 7th day sampling, to P9, 63th day sampling) (P0 + 9 weeks*2 oxygen regimes*4 temperatures*2 replicates); total of ***146 samples***.

Figure 4.11 and Figure 4.12 represents the evolution of benzaldehyde in oxygen treatments I and II for, respectively, white and red Port wines. Benzaldehyde can be formed from benzyl alcohol oxidation or through phenylacetaldehyde in the presence of phenylalanine under thermal and/or oxidative conditions (Chu and Yaylayan, 2008). It was reported that although phenylalanine can generate different precursors that are able to form benzaldehyde, phenylacetaldehyde, the "Strecker aldehyde", is the most efficient and established precursor (Chu and Yaylayan, 2008).

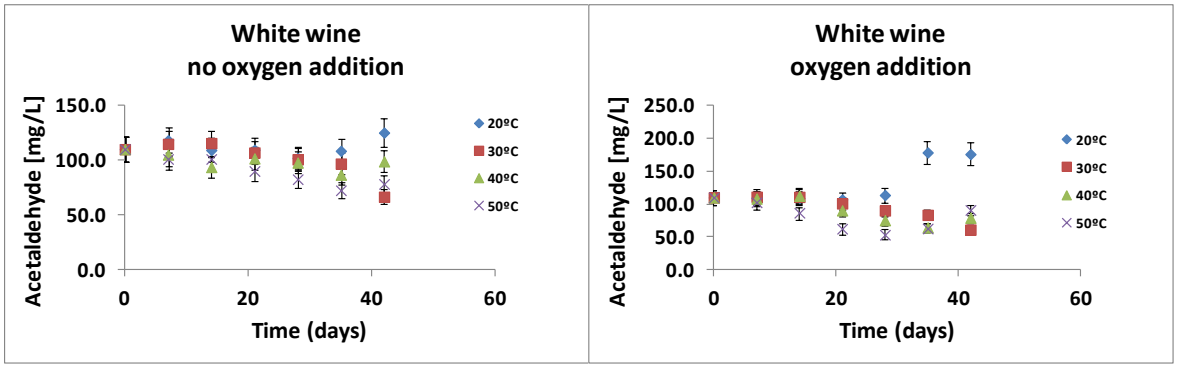

Figure 4.9. Evolution of acetaldehyde, during the white wine forced aging protocol, under respectively no oxygen addition (treatment I) and oxygen addition (treatment II).

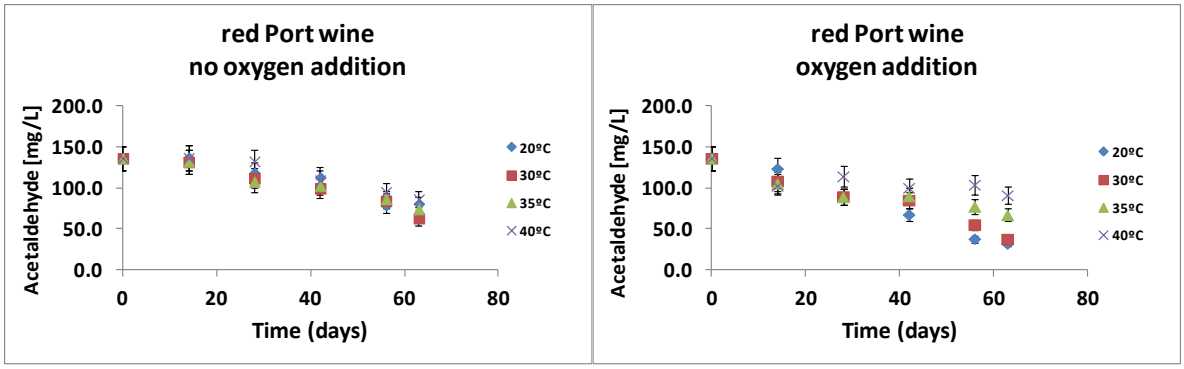

Figure 4.10. Evolution of acetaldehyde, during the red Port wine forced aging protocol, under respectively no oxygen addition (treatment I) and oxygen addition (treatment II).

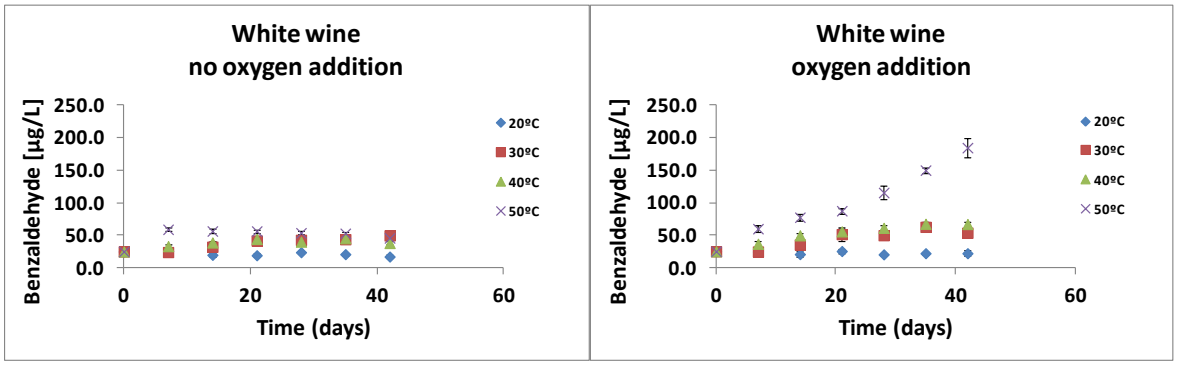

Figure 4.11. Evolution of benzaldehyde, during the white wine forced aging protocol, under respectively no oxygen addition (treatment I) and oxygen addition (treatment II).

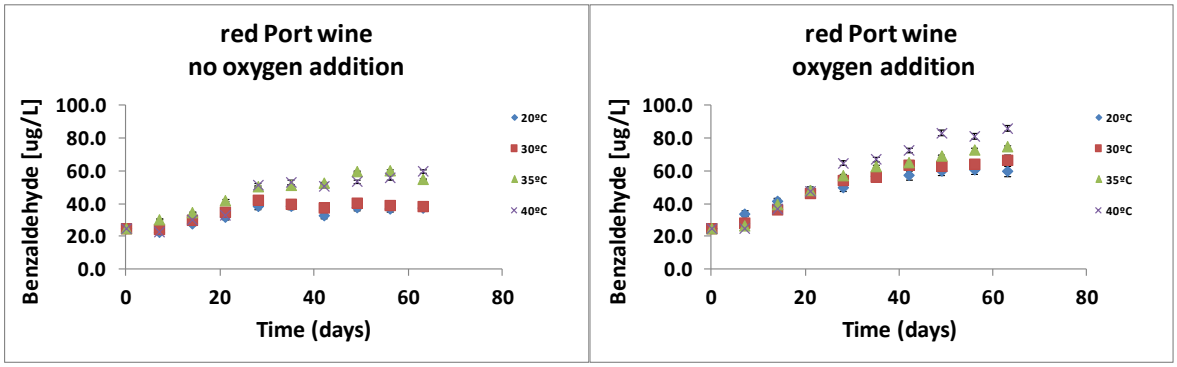

Figure 4.12. Evolution of benzaldehyde, during the red Port wine forced aging protocol, under respectively no oxygen addition (treatment I) and oxygen addition (treatment II).

As acetaldehyde, vanillin and syringaldehyde can react with wines anthocyanins and/or flavan-3-ols. Recently, pigments resulted from the condensation of malvidin-3-glucoside with catechin mediated by vanillin aldehyde have been characterized (Sousa et al. 2007,

Nonier et al., 2011). In the same way, the reaction of flavan-3-ols with vanillin and syringaldehyde was already evaluated (Vivas et al., 2008). Although these aldehydes are reported to occur in oak aged wines as released from wood (Escalona et al. 2002), in this work, no wine wood contact was used.

Table 4.5 represents the formation rates of the phenolic aldehydes vanillin and syringaldehyde during the accelerated spoilage of both white and red Port wines. By the observation of Table 4.5 we can see that the level of these compounds depends on the temperature regimes, as well as the oxygen treatments. Levels of these aldehydes are higher in the red Port wine. In fact, at 40ºC and after 42 days of forced aging, there is a significant increase in the amount of vanillin in both white and red Port wines, to 19.4 and 26.1 µg/L (for white wine), along with 100.2 and 126.8 µg/L (for red Port wine), for respectively treatment I and II. For syringaldehyde, at 40ºC and after 42 days of forced aging, levels of this compound have increased to 70.0 and 113.9 µg/L (for white wine), along with 126.0 and 431.7 mg/L (for red Port wine), for respectively treatment I and II. By the observation of Table 4.5 we can see that syringaldehyde as suffered a faster formation than vanillin during the forced aging protocols. This fact could indicate that vanillin is more reactive in the proposed condensation reaction with anthocyanins or flavan-3-ols, and therefore less available in the wines.

Table 4.5. Vanillin and syringaldehyde formation rates during the forced aging protocols in both white and red Port wines.

White wine (µg/L/day)	**Treatment I**				**Treatment II**			
	20ºC	**30ºC**	**40ºC**	**50ºC**	**20ºC**	**30ºC**	**40ºC**	**50ºC**
Vanillin	0.230	0.302	0.357	0.402	0.212	0.375	0.528	3.169
Syringaldehyde	0.670	1.580	1.906	2.560	0.543	1.526	2.442	11.732
Red Port wine (µg/L/day)	**Treatment I**				**Treatment II**			
	20ºC	**30ºC**	**35ºC**	**40ºC**	**20ºC**	**30ºC**	**35ºC**	**40ºC**
Vanillin	1.190	1.758	2.108	2.411	1.602	2.347	3.176	3.462
Syringaldehyde	2.994	3.143	3.537	4.050	6.831	10.004	13.085	18.738

Treatment I - no oxygen addition; Treatment II - oxygen addition.

4.4.3. Quantification of heterocyclic acetals in white and red Port wines

Acetaldehyde can be consumed in an acetalization reaction with glycerol, at wine pH, with formation of the corresponding four heterocyclic acetals (Figure 4.13). By this reaction, glycerol protects the wine against excessive amount of acetaldehyde. In the same way, because acetaldehyde can be bound spontaneously with sulfur dioxide, higher values of this antioxidant can block the acetalization reaction.

Quantification of heterocyclic acetals, *cis*- and *trans*-5-hydroxy-2-methyl-1,3-dioxane, and *cis*- and *trans*-4-hydroxymethyl-2-methyl-1,3-dioxolane was performed by GC-mass spectrometry (Chapter 3; 3.10.1) in the forced aging protocols of white and red Port wines (Chapter 3; 3.2.). For the white wine aging protocol, samples were taken on the first day, and weekly (P0; and P1, 7^{th} day sampling, to P6, 42^{th} day sampling) (P0 + 6 weeks*2 oxygen regimes*4 temperatures*2 replicates); total of ***98 samples***. For the red Port wine aging protocol, samples were taken on the first day, and weekly (P0; and P1, 7^{th} day sampling, to P9, 63^{th} day sampling) (P0 + 9 weeks*2 oxygen regimes*4 temperatures*2 replicates); total of ***146 samples***.

Figure 4.14 and Figure 4.15 represents the formation of the heterocyclic acetals *cis*- and *trans*-5-hydroxy-2-methyl-1,3-dioxane and *cis*- and *trans*-4-hydroxymethyl-2-methyl-1,3-dioxolane, for respectively white and red Port wines forced aging protocols, at a temperature of 20ºC and 40ºC. By the observation of these figures we can see that the concentrations of the acetals *cis*- and *trans*-5-hydroxy-2-methyl-1,3-dioxane and *cis*- and *trans*-4-hydroxymethyl-2-methyl-1,3-dioxolane increase regularly with both white and red Port wines forced aging protocols. Furthermore, levels of these acetals are dependent on the temperature regimes, as well as the oxygen treatments. Futhermore, we can see that the 4-hydroxymethyl-2-methyl-1,3-dioxolane content was higher than that of 5-hydroxy-2-methyl-1,3-dioxane at 20ºC. However, at 40ºC, the 5-hydroxy-2-methyl-1,3-dioxane content was greater than that of 4-hydroxymethyl-2-methyl-1,3-dioxolane. This observation is mainly due to *cis*-5-hydroxy-2-methyl-1,3-dioxane that had a superior increase in both white and red Port forced aging protocols, at higher temperatures (Figures 4.14 and 4.15). This fact was already reported by other authors where, dioxolane levels were higher than dioxane levels in young Port wines up to 2 years old, but gradually an inversion was observed as a function of time between these two isomers (Silva Ferreira et

al., 2002). The *cis*- form was always present at higher levels than the *trans*- form for each isomer. The ratio between *cis*- and *trans*- forms remained constant independently of the forced aging sample points. The calculated values were 3.5 ± 0.4 for the *cis/trans*-dioxane and 1.5 ± 0.3 for the *cis/trans*-dioxolanes, in white wines, and 2.6 ± 0.4 for the *cis/trans*-dioxane and 1.4 ± 0.2 for the *cis/trans*-dioxolanes, in red Port wines, the last values are in agreement with previsions authors (Silva Ferreira et al., 2002).

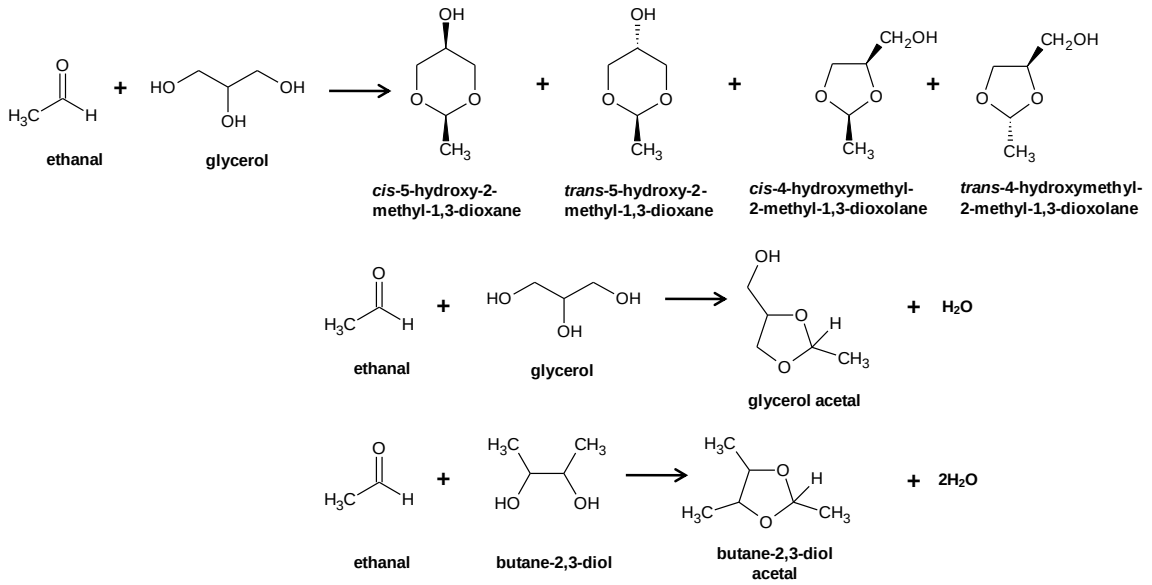

Figure 4.13. Acetalization of acetaldehyde (ethanal) in wine.

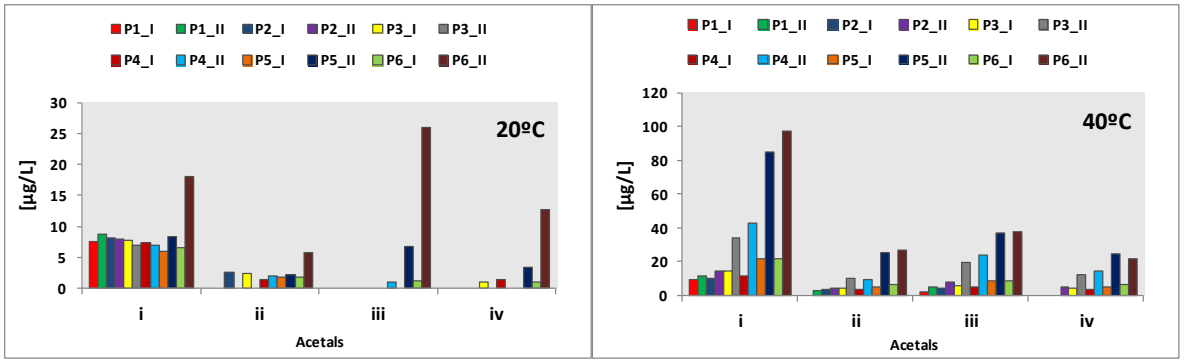

Figure 4.14. Formation of the heterocyclic acetals for the white wine forced aging protocols, at respectively 20ºC and 40ºC. (i) *cis*-5-hydroxy-2-methyl-1,3-dioxane; (ii) *trans*-5-hydroxy-2-methyl-1,3-dioxane; (iii) *cis*-4-hydroxymethyl-2-methyl-1,3-dioxolane; (iv) *trans*-4-hydroxymethyl-2-methyl-1,3-dioxolane; I - no oxygen addition; II - oxygen addition.

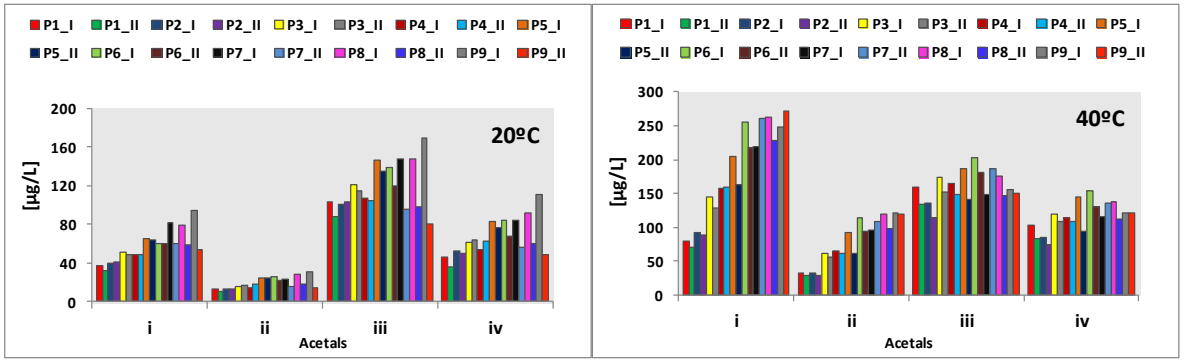

Figure 4.15. Formation of the heterocyclic acetals for the red Port wine forced aging protocol, at respectively 20ºC and 40ºC. (i) *cis*-5-hydroxy-2-methyl-1,3-dioxane; (ii) *trans*-5-hydroxy-2-methyl-1,3-dioxane; (iii) *cis*-4-hydroxymethyl-2-methyl-1,3-dioxolane; (iv) *trans*-4-hydroxymethyl-2-methyl-1,3-dioxolane; I - no oxygen addition; II - oxygen addition.

4.5. Influence of iron and copper on sulfur dioxide oxidation and acetaldehyde formation in the presence of gallic acid

A possible synergism between iron and copper on sulfur dioxide oxidation and acetaldehyde formation in the presence of gallic acid was investigated. For this purpose a wine-model solution was used. This wine-model was prepared with ethanol 12% (v/v) and

0.033 M tartaric acid, in saturated oxygen conditions (8.5 mg/L), with pH adjusted to 3.6 with NaOH. The solution was then adjusted as follows: a reactive phenolic compound (gallic acid) and sulfur dioxide (SO_2) were added in concentrations that simulate the reducing capacity of a red wine (1.5 g/L for gallic acid and close to 90 mg/L for SO_2). This portion was then adjusted with reduced transition metal ions (a control without addition of transition metals; addition of 0.4 ppm Cu^{2+}; addition of 7.5 ppm Fe^{2+}; and addition of 0.4 ppm Cu^{2+} + 7.5 ppm Fe^{2+}). This protocol was made in duplicate during 168 hours. Acetaldehyde and SO_2 were quantified as described in Chapter 3 (sections 3.11. and 3.14., respectively).

Figure 4.16 represents the SO_2 consumption along the 168 hours of the wine-model protocol. No significant SO_2 oxidation is observed without addition of iron and copper ions (Figure 4.16; control). Adding iron(II) [Fe (7.5 ppm)] and copper(II) [Cu (0.4 ppm)] ions separately, increase the rate of phenolic oxidation, and therefore, the rate of SO_2 oxidation. However, when combined a faster SO_2 oxidation is observed (Figure 4.16). It is proposed that copper(II), by interacting with oxygen, facilitates redox cycling of iron(II) (Danilewicz, 2007, Danilewicz et al., 2008, Cantú and Waterhouse 2009). An intervention of iron, copper, and manganese ions, in wine oxidation, was already been observed (Cacho et al., 1995, Benitez et al., 2002a, and Benitez et al., 2002b). These results demonstrate the key importance of metal ions in allowing phenolic oxidation and that the rate of SO_2 consumption is dependent on the rate of phenolic oxidation.

The oxygen and SO_2 molar reaction ratio is 1:2, which is consistent with one mole equiv of SO_2 reacting with hydrogen peroxide and a second with the quinone (Danilewicz et al., 2008). Moreover, the oxygen/SO_2 molar reaction ratio found in red wines was 1:~1.7, suggesting that some nucleophilic substances may be competing with SO_2 for quinones (Danilewicz et al., 2008). Figure 4.17 represents the acetaldehyde formation during the wine-model protocol.

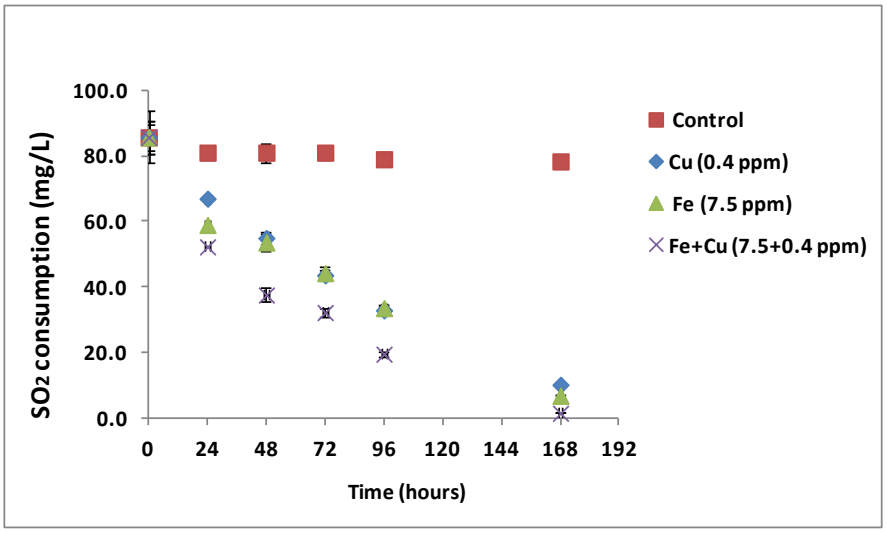

Figure 4.16. Sulfur dioxide oxidation in a wine-model system with gallic acid, sulfur dioxide and transition metal ions (N=2).

Having gallic acid been oxidized, hydrogen peroxide would have been generated and rather produce acetaldehyde, by reacting with ethanol, or reacts with the SO_2, which can inhibit aldehydes formation by competing for hydrogen peroxide (Elias et al., 2010). No significant acetaldehyde is formed without the addition of iron(II) and copper(II) ions (Figure 4.17; control). Adding iron(II) [Fe (7.5 ppm)] and copper(II) [Cu (0.4 ppm)] ions, separately, increase the rate of acetaldehyde formation, and when combined a noticeable increase in acetaldehyde formation is observed (Figure 4.17). These results suggested that SO_2 compete for reducing quinones, formed during oxidation process, back to their phenol, and for reacting with hydrogen peroxide to produce acetaldehyde.

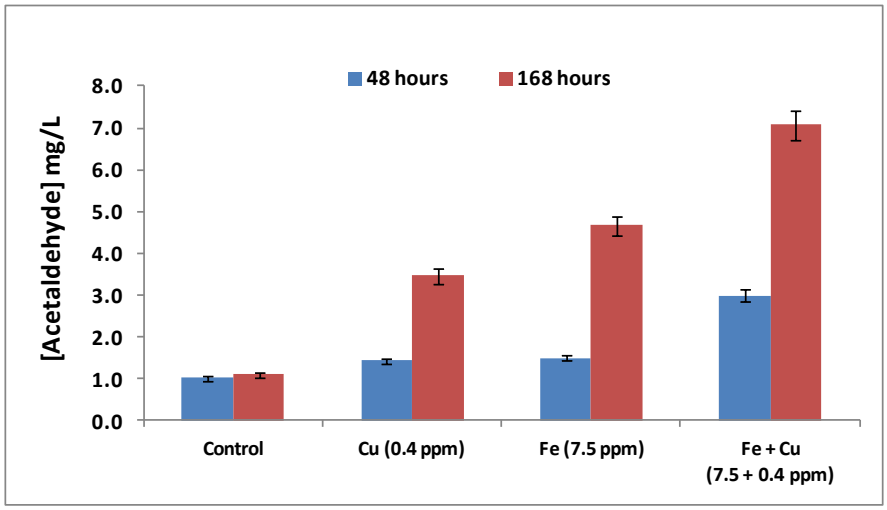

Figure 4.17. Acetaldehyde formation in a wine-model system with gallic acid, sulfur dioxide and transition metal ions (N=2).

4.6. Study of quinones reactions with wine nucleophiles in wine-model solutions by cyclic voltammetry

Quinones are electrophilic species which can add various nucleophiles, like wine antioxidants, such as sulfur dioxide or ascorbic acid, thiols, amino acids, and numerous polyphenols (such as epicatechin and other flavan-3-ols). These reactions are very important in wine aging because they mediate oxygen consumption during both production and bottle aging phases. Oxidation of wine polyphenols is thought to play a major role in wine thiols degradation. Volatile thiols such as 4-methyl-4-sulfanylpentan-2-one (4MSP, Figure 4.18) and 3-sulfanylhexan-1-ol (3SH, Figure 4.18) are aromatic molecules having an important organoleptic impact on white wines with respectively boxwood/broom or grapefruit/passionfruit notes. These molecules decrease dramatically with wine oxidation (Blanchard et al., 2004, Brajkovich et al., 2005, Lopes et al., 2009, Makhotkina, O., 2011). On the another hand, other thiols with undesirable aromas, like 3-(methylsulfanyl)propan-1-ol (methionol) or 2-sulfanylethanol (2-mercaptoethanol) (Figure 4.18) also decrease with wine oxidation. Port wine studies have conclude that old Port wine (barrel aged) never develops "off-flavors" associated with the presence of methionol (cauliflower) or 2-mercaptoethanol (rubber/burnt). In fact, temperature and oxygen are the major factors in the consumption of these molecules (Silva Ferreira et al., 2003a).

Sulfur dioxide (HSO_3^-, Figure 4.1), can convert *ortho*-quinones back to *ortho*-dihydroxyphenols and react directly with *ortho*-quinones to form sulfonic acids (Figure 4.1). Interestingly, the potential of ascorbic acid to recycle *ortho*-quinones back to *ortho*-dihydroxyphenols (catechols) has also been suggested by various authors (Isaacs and van Eldik, 1997, Danilewicz, 2003).

ortho-Quinones formed during the oxidation process of wine phenolic compounds can react with amino acids (Rizzi, 2006, Rizzi, 2008). This mechanism still is not fully understood as the Michael addition reaction of *ortho*-quinones with α-amino acids, proposed by Rizzi (2006), was not corroborated by Nikolantonaki and Waterhouse studies (2012). This mechanism will be later explored in Chapter 6.

In this section, an attempt was made in order to determine the interaction between *ortho*-quinones and wine nucleophiles, like the amino acids phenylalanine and methionine, the thiols 3-sulfanylhexan-1-ol (3SH), 4-methyl-4-sulfanylpentan-2-one (4MSP), and furan-2-ylmethanethiol (2FMT, Figure 4.18), and the antioxidants sulfur dioxide and ascorbic acid, by cyclic voltammetry. The use of phenylalanine and methionine is due to their important wine formation of potent "Strecker aldehydes". It was observed that wines stored at high temperatures and supplemented with high levels of dissolved oxygen suffered a rapid and pronounced oxidative spoilage aroma, which were related with the presence of 3-(methylthio)propionaldehyde (methional), responsible for "boiled-potato" odour notes, and phenylacetaldehyde, with "honey-like" odour notes (Silva Ferreira et al., 2002; Silva Ferreira et al., 2003b). The use of 3-sulfanylhexan-1-ol (3SH) and 4-methyl-4-sulfanylpentan-2-one (4MSP) was due to their important contribution to wine varietal aroma. Conversely, the use of furan-2-ylmethanethiol (2FMT) is due to its negative wine aroma impact with an odoriferous smelling of cooked meat. Sulfur dioxide and ascorbic acid were used due to their recognized wine antioxidant activity.

For this purpose, wine-model systems [ethanol 12% (v/v) and 0.033 M tartaric acid, pH = 3.6] with gallic acid, caffeic acid, or (+)-catechin at a concentration of 0.6 mM were used. The nucleofilic compounds were add in a concentration of 2.4 mM. Cyclic voltammograms were taken at a 3 mm glassy carbon electrode at 100 mV/s, with an increment potential of 2.4 mV, between -0.5 V to 1.2 V, in the absence and in the presence of nucleophiles. The study was made in triplicate. During the cyclic voltammetry experiment, the anodic and cathodic peak potentials at pH 3.6, of the studied polyphenols [Ep,a - anodic peak potential

(V); Ep,c - cathodic peak potential (V)], as well the anodic and cathodic peak currents at pH 3.6 [Ip,a - anodic peak current (A); Ip,c - cathodic peak current (A)] were evaluated (Table 4.6). Cyclic voltammetry is a method to produce polyphenol quinones in a controlled manner (oxidation curves). If a rapid interaction of nucleophiles with polyphenol quinones occurs, there will be less available for its reduction at the carbon electrode on the reverse potential sweep (reduction curves). Conversely, if no interaction of nucleophiles with polyphenol quinones occurs, the cathodic peaks will be retained on the reverse potential sweep.

Figure 4.18 represents some thiols structures. Figures 4.19 to 4.21 represents the cyclic voltammograms of respectively the amino acids phenylalanine and methionine, the thiols 3SH, 4MSP, and 2FMT, and the antioxidants sulfur dioxide and ascorbic acid, in the absence and in the presence of three representative phenolic compounds (gallic acid, caffeic acid, and (+)-catechin).

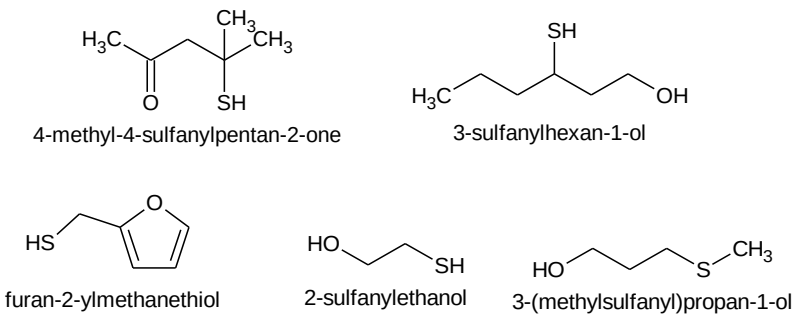

Figure 4.18. Structures of thiol derivatives present in wines.

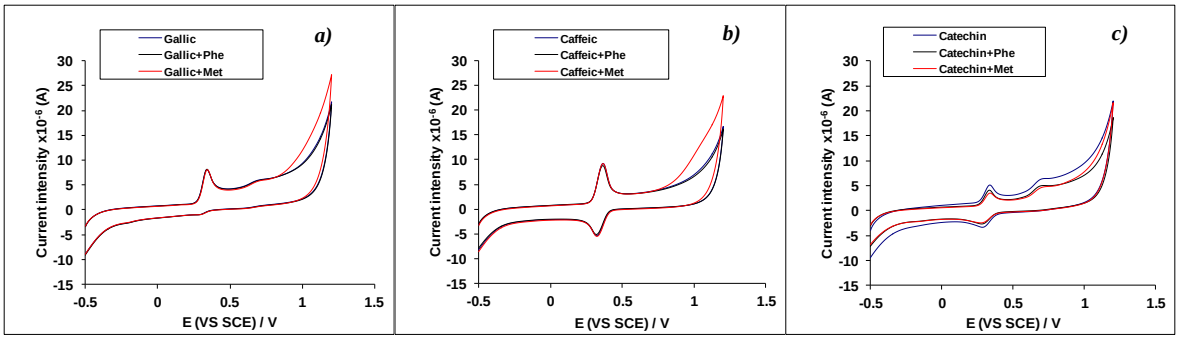

Figure 4.19. Cyclic voltammograms taken at a 3 mm glassy carbon electrode at 100 mV/s of a): 0.6 mM gallic acid in the absence (blue curve) and in the presence of (black curve) of 2.4 mM Phe, and in the presence of (red curve) of 2.4 mM Met; b): 0.6 mM caffeic acid in the absence (blue curve) and in the presence of (black curve) of 2.4 mM Phe, and in the presence of (red curve) of 2.4 mM Met; and c): 0.6 mM (+)-catechin in the absence (blue curve) and in the presence of (black curve) of 2.4 mM Phe, and in the presence of (red curve) of 2.4 mM Met.

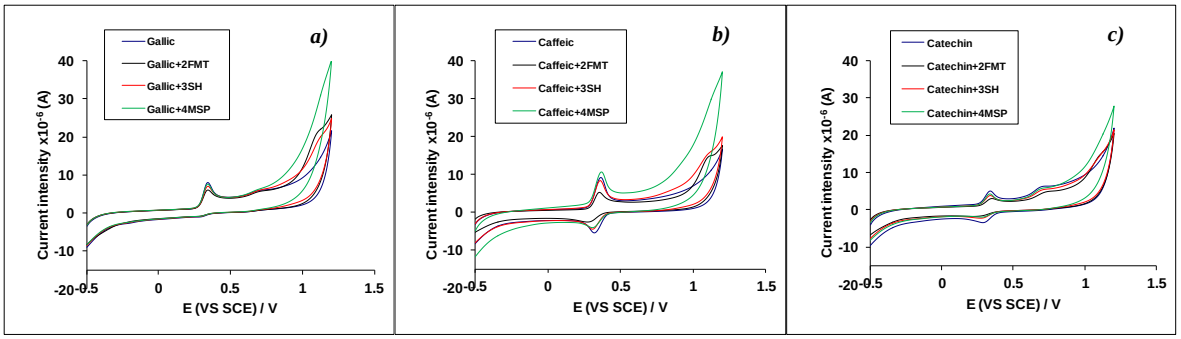

Figure 4.20. Cyclic voltammograms taken at a 3 mm glassy carbon electrode at 100 mV/s of a): 0.6 mM gallic acid in the absence (blue curve) and in the presence of (black curve) of 2.4 mM 2FMT, in the presence of (red curve) of 2.4 mM 3SH, and in the presence of (green curve) of 2.4 mM 4MSP; b): 0.6 mM caffeic acid in the absence (blue curve) and in the presence of (black curve) of 2.4 mM 2FMT, in the presence of (red curve) of 2.4 mM 3SH, and in the presence of (green curve) of 2.4 mM 4MSP; and c): 0.6 mM (+)-catechin in the absence (blue curve) and in the presence of (black curve) of 2.4 mM 2FMT, in the presence of (red curve) of 2.4 mM 3SH, and in the presence of (green curve) of 2.4 mM 4MSP.

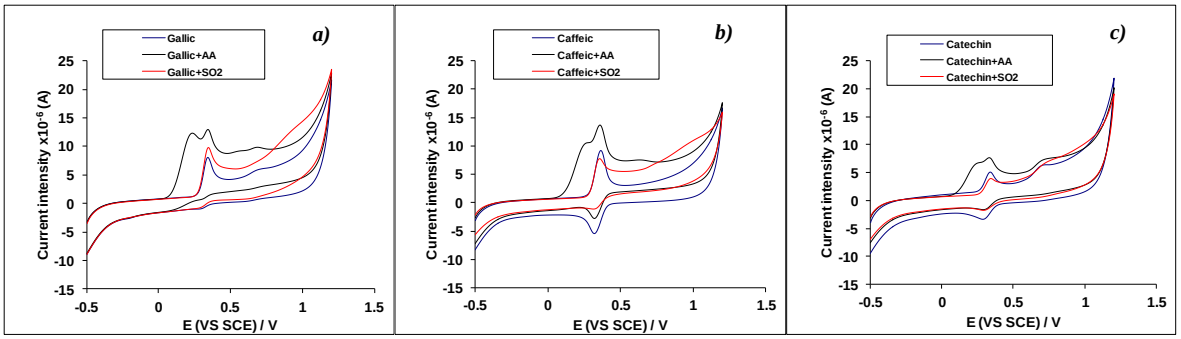

Figure 4.21. Cyclic voltammograms taken at a 3 mm glassy carbon electrode at 100 mV/s of a): 0.6 mM gallic acid in the absence (blue curve) and in the presence of (black curve) of 2.4 mM AA, and in the presence of (red curve) of 2.4 mM SO_2; b): 0.6 mM caffeic acid in the absence (blue curve) and in the presence of (black curve) of 2.4 mM AA, and in the presence of (red curve) of 2.4 mM SO_2; and c): 0.6 mM (+)-catechin in the absence (blue curve) and in the presence of (black curve) of 2.4 mM AA, and in the presence of (red curve) of 2.4 mM SO_2.

Table 4.6. Evaluation of the anodic and cathodic peak potentials at pH 3.6, of the studied polyphenols [Ep,a - anodic peak potential (V); Ep,c - cathodic peak potential (V)], as well the anodic and cathodic peak currents at pH 3.6 [Ip,a - anodic peak current (A); Ip,c - cathodic peak current (A)] during the cyclic voltammetry experiment.

Phenolic compound	**pH = 3.6**		
	Ep_1,a	**Ep_2,a**	**Ep_1,c**
gallic acid	0.354	0.735	0.273
caffeic acid	0.374		0.327
catechin	0.354	0.747	0.283
	Ip_1,a x10^{-6}	**Ip_2,a x10^{-6}**	**Ip_1,cx 10^{-6}**
gallic acid	8.08	6.14	-1.00
gallic+Phe	8.17	6.10	-1.00
gallic+Met	8.12	6.02	-0.95
gallic+3SH	7.01	6.25	-0.95
gallic+4MSP	7.59	6.65	-0.93
gallic+2FMT	6.03	5.85	-0.86
gallic+SO_2	9.70	8.02	-0.82
gallic+AA	12.95	9.66	-0.58
caffeic acid	9.20		-5.38
caffeic+Phe	8.79		-5.23
caffeic+Met	9.26		-5.44
caffeic+3SH	8.38		-4.40
caffeic+4MSP	10.61		-4.02
caffeic+2FMT	5.24		-2.57
caffeic+SO_2	7.73		-1.15
caffeic+AA	13.64		-2.82
catechin	5.08	6.39	-3.36
catechin+Phe	4.03	4.97	-2.72
catechin+Met	3.55	4.84	-2.39
catechin+3SH	3.80	5.51	-2.26
catechin+4MSP	4.29	5.98	-1.89
catechin+2FMT	2.98	4.82	-1.74
catechin+SO_2	3.97	6.83	-1.71
catechin+AA	7.64	7.44	-1.59

Amino acids

Results have show that phenylalanine and methionine have no influence on the anodic and cathodic peak current intensities of gallic and caffeic acids (Figure 4.17, a and b; and Table 4.6). On another hand, phenylalanine and methionine decreased the current intensities of the two anodic peaks of (+)-catechin, in 21 to 30%, as well the cathodic current intensity, in 19 to 29% (Figure 4.17c and Table 4.6). These results points to an interaction of the above amino acids with the (+)-catechin quinone.

Thiols

Results have show that 3-sulfanylhexan-1-ol (3SH) and 4-methyl-4-sulfanylpentan-2-one (4MSP) have decreased the cathodic current intensities of all the analysed polyphenols. Furthermore, the decrease rate follows, respectively for 3SH and 4SMP, the order: (+)-catechin (in 33 to 44%) > caffeic acid (in 18 to 25) > gallic acid (in 5 to 7 %) (Figure 4.18 and Table 4.6). These results indicate that 4MSP is more reactive with quinones than 3SH. Considering furan-2-ylmethanethiol (2FMT), the decrease of the cathodic current intensities of all the analysed polyphenols were higher than the former thiols. Moreover, 2FMT decreased the current intensities of the two anodic peaks of gallic acid, in 5 to 25%, as well the cathodic current intensity, in 14% (Figure 4.18a and Table 4.6). For caffeic acid, 2FMT decreased the current intensity of the anodic peak in 43%, as well the cathodic current intensity in 52% (Figure 4.18b and Table 4.6). In the same way, this thiol has decreased the current intensities of the two anodic peaks of (+)-catechin, in 25 to 41%, as well the cathodic current intensity, in 48% (Figure 4.18c and Table 4.6). These results points to a rapid interaction of 2FMT with the caffeic acid and (+)-catechin quinones.

Antioxidants

Results have show that ascorbic acid increased the anodic current and decreased the cathodic current for all analysed polyphenols, pointing to a rapid interaction of this antioxidant with the oxidized polyphenol quinones. The increases of the anodic peaks intensity were respectively for gallic acid, caffeic acid and (+)-catechin of 57 to 60%, 48%, and 16 to 51% (Figure 4.19 and Table 4.6). In the same way, this antioxidant has decreased the current intensities of the cathodic peaks of gallic acid, caffeic acid, and (+)-catechin, in respectively, 42, 48, and 53% (Figure 4.19 and Table 4.6), pointing to a rapid interaction of

ascorbic acid with the oxidized polyphenol quinones. These results do not corroborate the latest findings by Makhotina and Kilmartin (2009) where ascorbic acid had no indication to rapidly interact with *ortho*-quinones by cyclic voltammetry.

Results have shown that sulfur dioxide increased the anodic current peaks intensities of gallic acid in 20 to 31%, and have decreased its cathodic current peak intensity in 18% (Figure 4.19a and Table 4.6). For caffeic acid, sulfur dioxide decreased the current intensity of the anodic peak in 16%, as well the cathodic current intensity in 79% (Figure 4.19b and Table 4.6). Likewise, this antioxidant has decreased the current intensities of the two anodic peaks of (+)-catechin, in 0 to 22%, as well the cathodic current intensity, in 49% (Figure 4.19c and Table 4.6). These results points to a rapid interaction of sulfur dioxide with the gallic acid, caffeic acid and (+)-catechin quinones, and corroborate the latest findings by Makhotina and Kilmartin (2009) where sulfur dioxide had a rapid interaction with *ortho*-quinones by cyclic voltammetry.

Recent studies (Nikolantonaki and Waterhouse, 2012) have compared the first-order rate constants, measured by UV-vis absorbance at 400 nm, of a quinone of a non-wine like phenol 4-methylcatechol (4MeC) with several nucleophiles. In this study the authors point to a nucleophilicity scale toward the 4-methyl-1,2-benzoquinone (Q4MeC) in the wine like solution of: methionine ≈ phenylalanine < phloroglucinol < 4-methyl-4-sulfanylpentan-2-one << 3-sulfanylhexan-1-ol < furan-2-ylmethanethiol << sulfur dioxide ≈ ascorbic acid ≈ glutathione ≈ hydrogen sulfide (H_2S).

In the current study a nucleophilicity scale related to the cathodic current intensity decrease was attempted:

i) Considering the gallic acid quinone: phenylalanine < methionine ≈ 3-sulfanylhexan-1-ol < 4-methyl-4-sulfanylpentan-2-one < furan-2-ylmethanethiol < sulfur dioxide < ascorbic acid;

ii) Considering the caffeic acid quinone: methionine < phenylalanine < 3-sulfanylhexan-1-ol < 4-methyl-4-sulfanylpentan-2-one < ascorbic acid ≈ furan-2-ylmethanethiol < sulfur dioxide;

iii) Considering the catechin quinone: phenylalanine < methionine < 3-sulfanylhexan-1-ol < 4-methyl-4-sulfanylpentan-2-one < furan-2-ylmethanethiol ≈ sulfur dioxide < ascorbic acid.

These results corroborate Nikolantonaki and Waterhouse (2012) work where the lowest reactivity toward quinones is attributed to amino acids. Concerning thiols, 4MSP is more reactive with quinones than 3SH, but the highest reactivity is attributed to 2FMT. Sulfur dioxide and ascorbic acid have similar reactvities with quinones.

4.7. Conclusions

Although the activation energies (*Ea*) for oxygen depletion were similar for both white and red Port wines, the oxygen consumption rates were very different, much higher for the red Port wine. This means that the concentration of the oxidizable matter, mostly polyphenols, was at a higher concentration in the red Port wine.

To prevent the metal-catalyzed oxidation processes, the removal of transition metals from wine will minimize wine oxidation reactions, and consequently the wine oxygen consumption. In fact, a single specific chelating agent cocktail (EDTA + phenanthroline; 500 μM each) decreased the oxygen consumption by 32% and 54% at 20ºC for, respectively, white and red Port wines. On the other hand, this decrease was less prominent for the temperature of 40ºC, by 18% and 32% for, respectively, white and red Port wines.

Under wine conditions, gallic acid, catechin, and syringic acid were the only phenolics that have promoted the uptake for dissolved oxygen, over the tested phenolics (catechin, *para*-coumaric acid, gallic acid, caffeic acid, syringic acid, and ferulic acid). Moreover, the uptake of dissolved oxygen in molar quantity of O_2 per liter per second was 5.8×10^{-10} for gallic acid, and 1.2×10^{-10} for both catechin and syringic acid, being gallic acid the more effective. A relationship between oxygen consumption of gallic acid (0.3 mM; 45 mg/L) and the studied wines was made. We can express the oxygen uptake of the white wine, resulted from its overall intervenient on chemical oxidation, in 0.6 ± 0.1 and 1.3 ± 0.1 equiv of gallic acid (at concentration of 45 mg/L), for respectively the temperatures of 20 and 40ºC. In the same way, red Port wine oxygen uptake can be expressed in 2.3 ± 0.4 and

7.0 ± 0.3 equiv of gallic acid (at concentration of 45 mg/L), for respectively the temperatures of 20 and 40ºC.

White wine oxygen addition has promoted a higher decrease in both free and bound SO_2. High relative consumption of SO_2 made clear that the white wine was well protected from oxidation. Bound SO_2 does not decrease at 20ºC in both oxygen treatments. In contrast, a decrease is observed, at higher temperatures, related with the polyphenols scavenging of intermediate radicals that inhibit SO_2 autoxidation.

Considering white wine, during the first 20 to 25 days of forced aging protocol, acetaldehyde consumption was higher than ethanol oxidation. Then, acetaldehyde concentration begins to increase up to the end of protocol (42 days). Considering red Port wine, acetaldehyde consumption was always higher than ethanol oxidation, along the 63 days of the experiment, and for the two applied oxygen treatments. This fact could be related to the reaction of acetaldehyde with anthocyanins and flavan-3-ols of the red Port wines.

Phenolic aldehydes (vanillin and syringaldehyde) formation depends on the temperature regimes, as well as oxygen treatments. Levels of these aldehydes were higher in the red Port wine. Moreover, syringaldehyde has suffered a faster formation than vanillin during the forced aging protocols. This fact could indicate that vanillin is more reactive in the proposed condensation reaction with anthocyanins or flavan-3-ols, and therefore less available in wines.

Heterocyclic acetals formed during the acetalization reaction of acetaldehyde with glycerol are good oxidation markers. In fact, the acetals *cis*- and *trans*-5-hydroxy-2-methyl-1,3-dioxane and *cis*- and *trans*-4-hydroxymethyl-2-methyl-1,3-dioxolane increase regularly with both white and red Port wines forced aging protocols. Furthermore, levels of these acetals are dependent on the temperature regimes, as well as the oxygen treatments. 4-Hydroxymethyl-2-methyl-1,3-dioxolane content was higher than that of 5-hydroxy-2-methyl-1,3-dioxane at 20ºC, but at 40ºC, the 5-hydroxy-2-methyl-1,3-dioxane content was greater than that of 4-hydroxymethyl-2-methyl-1,3-dioxolane. The ratio between *cis*- and *trans*- forms is constant. The calculated values were 3.5 ± 0.4 for the *cis/trans*-dioxane and 1.5 ± 0.3 for the *cis/trans*-dioxolanes, in white wines, and 2.6 ± 0.4 for the *cis/trans*-dioxane and 1.4 ± 0.2 for the *cis/trans*-dioxolanes, in red Port wines.

As quinones are electrophilic species which can react with various nucleophiles, a nucleophilicity scale related to the cathodic current intensity decrease of gallic acid, caffeic acid, and (+)-catechin quinones with, phenylalanine, methionine, 3-sulfanylhexan-1-ol, 4-methyl-4-sulfanylpentan-2-one, furan-2-ylmethanethiol ascorbic acid, and sulfur dioxide was attempted by cyclic voltammetry. Results have shown that the lowest reactivity with quinones was attributed to amino acids. Concerning thiols, 4-methyl-4-sulfanylpentan-2-one was more reactive with quinones than 3-sulfanylhexan-1-ol, but the highest reactivity was attributed to furan-2-ylmethanethiol. Sulfur dioxide and ascorbic acid had higher and similar reactions with quinones.

4.8. References

Benítez, P., Castro, R., Sanchez-Pazo, J. A., & Barroso, C. G. (2002a). Influence of metallic content of fino sherry wine on its susceptibility to browning. *Food Research International*, *35*,785-791.

Benítez, P., Castro, R. & Barroso, C. G. (2002b). Removal of iron, copper and manganese from white wines through ion exchange techniques: Effects on their organoleptic characteristics and susceptibility to browning. *Analytica Chimica Acta, 458*, 197-202.

Blanchard, L., Darriet, P., & Dubourdieu, D. (2004). Reactivity of 3-mercaptohexanol in red wine: Impact of oxigen, phenolic fraction, and sulfur dioxide. *American Journal of Enology and Viticulture*, *55,* 115-120.

Brajkovich, M., Tibbits, N., Peron, G., Lund, C. M., Dykes, S. I., Kilmartin, P. A., & Nicolau, L. (2005). Effect of screwcap and cork closures on SO_2 levels and aromas in a Sauvignon Blanc wine. *Journal of Agricultural and Food* Chemistry, *53*, 10006-10011.

Cacho, J., Castells, J. E., Esteban, A., Laguna, B., & Sagristá, N. (1995). Iron, copper, and manganese influence on wine oxidation. *American Journal of Enology and Viticulture, 46,* 380-384.

Cantú, A., Gozza, A., Elias, R. J., & Waterhouse, A. L. (2009). Chelating agents - A new tool in preventing wine Oxidation? Personal communication In *Proceedings of the ASEV 60th Anniversary Annual Meeting*. American Society for Enology and Viticulture, Davis, California, 89-90.

Cheynier, V. F., & Van Hulst, M. W. J. (1988). Oxidation of trans-caftaric acid and 2-S-glutathionylcaftaric acid in model solutions. *Journal of Agricultural and Food Chemistry, 36*, 10-15.

Cheynier, V. F., Basire, N., & Rigaud, J. (1989). Mechanism of transcaffeoyltartaric acid and catechin oxidation in model solutions containing grape polyphenoloxidase. *Journal of Agricultural and Food Chemistry*, *37*, 1069-1071.

Chu, F. L., & Yaylayan, V. A. (2008). Model studies on the oxygen-induced formation of benzaldehyde from phenylacetaldehyde using pyrolysis GC-MS and FTIR. *Journal of Agricultural and Food Chemistry,* 56, 10697-10704.

Danilewicz, J. C. (2003). Review of reaction mechanisms of oxygen and proposed intermediate reduction products in wine: Central role of iron and copper. *American Journal of Enology and Viticulture, 54,* 73-85.

Danilewicz, J. C. (2007). Interaction of sulfur dioxide, polyphenols, and oxygen in a wine-model system: Central role of iron and copper. *American Journal of Enology and Viticulture, 58,* 53-60.

Danilewicz, J. C., Seccombe, J. T., & Whelan, J. (2008). Mechanism of interaction of polyphenols, oxygen, and sulfur dioxide in model wine and wine. *American Journal of Enology and Viticulture, 59,* 128-136.

Danilewicz, J. C., & Wallbridge, P. J. (2010). Further studies on the mechanism of interaction of polyphenols, oxygen and sulfite in wine. *American Journal of Enology and Viticulture, 61,* 166-175.

Danilewicz, J. C. (2011). Mechanism of autoxidation of polyphenols and participation of sulfite in wine: Key role of iron. *American Journal of Enology and Viticulture, 62,* 319-328.

Elias, R. J., Andersen, & Waterhouse, A. L. (2010). Controlling the Fenton reaction in wine. *Journal of Agricultural and Food Chemistry, 58,* 1699-1707.

Escalona, H., Birkmyre, L., Piggott, J. R., & Paterson, A. (2002). Effect of maturation in small oak casks on the volatility of red wine aroma compounds. *Analytica Chimica Acta, 458,* 45-54.

F. Noniera, M., Vivas, N., De Freitas, V., Vivas de Gaulejaca, N., & Absalon, C. (2011). A kinetic study of the reaction of (+)-catechin and malvidin-3-glucoside with aldehydes derived from toasted oak. *The Natural Products Journal, 1,* 47-56.

Green, R. W., & Parkins, G. M. (1961). Complexes of iron with d-tartaric and meso-tartaric acids. *The Journal of Physical Chemistry,* 65, 1658-1659.

Isaacs, N. S., & van Eldik, R. (1997). A mechanistic study of the reduction of quinones by ascorbic acid. *Journal of the Chemical Society, Perkin Transactions 2,* 1465-1468.

Kilmartin, P. A., Zou, H., & Waterhouse, A. L. (2001). A cyclic voltammetry method suitable for characterizing antioxidant properties of wine and wine phenolics. *Journal of Agricultural and Food Chemistry, 49,* 1957-1965.

Kilmartin, P. A. (2009). The oxidation of red and white wines and its impact on wine aroma *Chemistry in New Zealand, 73,* 18-22.

Laurie, V. F., & Waterhouse, A. L. (2006). Oxidation of glycerol in the presence of hydrogen peroxide and iron in model solutions and wine. Potential effects on wine colour. *Journal of Agricultural and Food Chemistry, 54,* 4668-4673.

Lee, D. F., Swinny, E. E., & Jones, G. P. (2004). NMR identification of ethyl-linked anthocyanin-flavanol pigments formed in model wine ferments. *Tetrahedron Letters*, *45*, 1671-1674.

Lopes, P., Silva, M. A., Pons, A., Tominaga, T., Lavigne, V., Saucier, C., Darriet, P.;Teissedre, P.-L., & Dubourdieu, D. (2009). Impact of oxygen dissolved at bottling and transmitted through closures on the composition and sensory properties of a Sauvignon Blanc wine during bottle storage. *Journal of Agricultural and Food Chemistry*, *57*, 10261-10270.

Macías, V. M., Palacios, Pina, I. Caro & Rodríguez, L. Pérez. (2001). Factors influencing the oxidation phenomena of sherry wine. *American Journal of Enology and Viticulture*, 52,151-155.

Makhotkina, O., & Kilmartin, P. A. (2009). Uncovering the influence of antioxidants on polyphenol oxidation in wines using an electrochemical method: Cyclic voltammetry. *Journal of Electroanalytical Chemistry, 633*, 165-174.

Makhotkina, O. (2011). Stability of New Zealand Sauvignon Blanc aroma compounds: Oxidation versus hydrolysis. PhD *University of Auckland*.

Nikolantonaki, M., & Waterhouse, A. L. (2012). A Method to quantify quinone reaction rates with wine relevant nucleophiles: A key to the understanding of oxidative loss of varietal thiols. *Journal of Agricultural and Food Chemistry, 60*, 8484-8491.

Oliveira, C. M., Silva Ferreira, A. C., De Freitas, V., & Silva, A. M. S. (2011). Oxidation mechanisms occurring in wines. *Food Research International, 44*, 1115-1126.

Ough, C. S., Crowell, E. A., & Benz, J. (1982). Metal content of California wines. *Journal of. Food Science*, *47*, 825-828.

Ough, C. S., & Amerine, M. A. (1988). Methods for Analysis of Musts and Wines. John Wiley, New York.

Rankine, B. C. (1989). Making Good Wine. Pan Macmillan: Sydney.

Rivas-Gonzalo, J. C., Bravo-Haro, S., & Santos-Buelga, C. (1995). Detection of compounds formed through the reaction of malvidin 3-monoglucoside and catechin in the presence of acetaldehyde. *Journal of Agricultural and Food Chemistry, 43*, 1444-1449.

Rizzi, G. P. (2006). Formation of strecker aldehydes from polyphenol-derived quinones and α-amino acids in a nonenzymic model system. *Journal of Agricultural and Food Chemistry*, *54*, 1893-1897.

Rizzi, G. P. (2008). The strecker degradation of amino acids: Newer avenues for flavor formation. *Food Reviews International, 24*, 416-435.

Silva Ferreira, A. C., Guedes de Pinho, P., Rodrigues, P., & Hogg, T. (2002). Kinetics of oxidative degradation of white wines and how they are affected by selected technological parameters. *Journal of Agricultural and Food Chemistry, 50*, 5919-5924.

Silva Ferreira, A. C., Rodrigues, P., Hogg, T., & Guedes de Pinho, P. (2003a). Influence of some technological parameters on the formation of dimethyl sulfide, 2-mercaptoethanol, methionol, and dimethyl sulfone in Port wines. *Journal of Agricultural and Food Chemistry, 51*, 727-732.

Silva Ferreira, A. C., Hogg, T., & Guedes de Pinho, P. (2003b). Identification of key odorants related to the typical aroma of oxidation-spoiled white wines. *Journal of Agricultural and Food Chemistry, 51*, 1377-1381.

Singleton, V. L., Trousdale, E., & Zaya, J. (1979). Oxidation of wines I. Young white wines periodically exposed to air. *American Journal of Enology and Viticultur*e, *30*, 49-54.

Singleton, V. L., Salgues, M., Zaya, J., & Trousdale. E. (1985). Caftaric acid disappearance and conversion to products of enzymic oxidation in grape must and wine. *American Journal of Enology and Viticulture*, *36*, 50-56.

Sousa, C., Mateus, N., Silva, A. M. S., Gonzalez-Paramas, A. M., Santos-Buelga, C., & De Freitas, V. (2007). Structural and chromatic characterization of a new malvidin-3-glucoside-vanillylcatechin pigment. *Food Chemistry, 102,* 1344-1351.

Tašev, K., Karadjova, I., Arpadjan, S., Cvetković, J., & Stafilov, T. (2006). Liquid/liquid extraction and column solid phase extraction procedures for iron species determination in wines. *Food Control, 17,* 484-488.

Timberlake, C. F., & Bridle, P. (1976). Interactions between anthocyanins, phenolic compounds, and acetaldehyde and their significance in red wines. *American Journal of Enology and Viticulture, 27*, 97-105.

Tulyathan V., Boulton, R. B, & Singleton, V. L. (1989). Oxygen uptake by gallic acid as a model for similar reactions in wine. *Journal of Agricultural and Food Chemistry, 37,* 844-849.

Waterhouse, A. L., & Laurie V. F. (2006). Oxidation of Wine Phenolics: A Critical Evaluation and Hypotheses. *American Journal of Enology and Viticulture, 57*, 306-313.

5. Chapter 5 - Role of phenolics degradation in wine

5.1. Introduction to wine phenolics degradation monitoring

Recently, studies using cyclic voltammetric measurements enabled the grouping of both quantitative and qualitative information concerning wine electroactive polyphenols (Kilmartin et al., 2001, Roginsky et al., 2006, Rodrigues et al., 2007, Martins et al., 2008, Makhotkina and Kilmartin, 2009, Makhotkina and Kilmartin, 2012). Wines originated from a forced aging degradation along with wines of different ages were monitored by cyclic voltammetry and the consumption rates of oxidizable species were estimated (Rodrigues et al., 2007).

The influence of sulfur dioxide, glutathione and ascorbic acid, on the cyclic voltammograms of four representative wine polyphenols (catechin, caffeic acid, rutin and quercetin) was investigated, using a glassy carbon electrode, in a model wine solution and in four wines (Makhotkina and Kilmartin, 2009). Results have showed that sulfur dioxide increased the anodic current and decreased the cathodic current for all the four polyphenols and all the four wines, pointing to a rapid interaction of SO_2 with the formed polyphenol quinones. However ascorbic acid produced no additional effect on the cyclic voltammograms of wine polyphenols and wines (Makhotkina and Kilmartin, 2009).

Voltammogram fingerprinting was already used for monitoring wine oxidation management (Martins et al., 2008). In this study, a supervised multivariate control chart was developed using a control sample as reference, and when white wines are plotted onto the chart, it is possible to monitor the oxidation status and to diagnose the effects of oxygen regimes and antioxidant activity (Martins et al., 2008).

The largest phenolic and non-phenolic peaks in HPLC chromatograms of Sauvignon blanc juice were separated using semi-preparative HPLC and characterized using MS and cyclic voltammetry. Six fractions included, caftaric acid, 2-*S*-glutathionyl caftaric acid, *cis*- and *trans*-coutaric acids, and two non-phenolic compounds were identified (Makhotkina and Kilmartin, 2012). In this study, the three anodic peaks at 0.4, 0.5 and 0.9 V (Ag/AgCl) showed a good correlation between the concentration of caffeic acid derivatives plus catechin and the first anodic peak; the concentration of flavonols and the second derivative of the second anodic peak; and the total phenolic content measured by the Folin-Ciocalteu

reagent and the area under voltammograms for scans taken to 0.7 V. The third peak in the juice cyclic voltammograms at 0.9 V appeared to be mainly due to the oxidation of non-phenolic compounds (Makhotkina and Kilmartin, 2012).

5.2. Voltammetric analysis of phenolic compounds

Cyclic voltammetry was used to access the "degradation status" of wines based on their electroactive phenolic composition. This strategy will be able to monitor and characterize the degradation process, enabling the grouping of qualitative information concerning wine electroactive phenolic compounds. In fact, voltammetric current is a function of concentration and peak position, where the most easily oxidized compounds occur at lower potentials while the less reactive compounds will be detected at higher potentials. Therefore, the pattern of the voltammetric oxidation curve will allow us to better understand both the type and amount of substances possessing antioxidant activity, displayed respectively on the range of potentials and current intensities implicated in wine degradation.

5.2.1. Effect of phenolic compounds addition in model wine solutions

To study the effect of phenolic profile, in the cyclic voltammograms responses, experiments were introduced in which the additions of phenolic compounds to a wine model solution were employed in combinations normally existing in wines (Table 5.1). The study was made in triplicate. The following common wine flavonoid compounds were used: i) flavonols (quercetin), and ii) flavan-3-ols [(+)-catechin and (-)-epicatechin]; the following common wine non-flavonoid compounds were used: i) derivatives of benzoic acid (*para*-hydroxybenzoic acid, protocatechuic acid, vanillic acid, gallic acid, and syringic acid), and ii) derivatives of cinnamic acid (*para*-coumaric acid, caffeic acid, and ferulic acid). The wine synthetic solutions were diluted, with pH adjusted to 3.6, in an interval range of 11.1 to 110.7 mg/L (Table 5.1). Solutions were plotted addressing the concentration of the added phenolics and the corresponding oxidation curves (Figure 5.1). In the same way, aiming to achive a linear region for the work electrode, a principal component analysis (PCA) was employed concerning the voltammetric oxidation signals

and the scores of the first component (PC1) (Figure 5.2). Data was normalized by mean normalization. Results have showed dependence between the oxidation analytical signals and the respective phenolics combination (Figure 5.1). Moreover, for the used concentrations (10 - 100 mg/L), a linear dependence was reached between the studied interval range and the scores of the first component (PC1) (r=0.992), indicating a linear region for the work electrode (Figure 5.2).

Table 5.1. Combinations of phenolic compounds concentrations normally present in wines.

Code	***1***	***2***	***3***	***4***	***5***	***6***	***7***	***8***	***9***
Protocatechuic acid	0.5	1.0	1.6	2.1	3.1	3.6	4.2	4.7	5.2
Hydroxybenzoic acid	0.7	1.4	2.2	2.9	4.3	5.0	5.8	6.5	7.2
Vanillic acid	0.5	1.0	1.5	2.0	3.0	3.5	4.0	4.5	5.0
Syringic acid	0.7	1.3	2.0	2.7	4.0	4.7	5.4	6.0	6.7
Caffeic acid	0.2	0.4	0.6	0.8	1.2	1.4	1.6	1.8	2.0
***para*-Coumaric acid**	0.7	1.3	2.0	2.7	4.0	4.7	5.4	6.0	6.7
Ferulic acid	0.4	0.9	1.3	1.8	2.6	3.1	3.5	4.0	4.4
Gallic acid	1.4	2.8	4.2	5.6	8.4	9.8	11.2	12.6	14.0
Quercetin	1.8	3.7	5.5	7.3	11.0	12.8	14.7	16.5	18.3
Catechin	2.0	3.9	5.9	7.8	11.7	13.7	15.6	17.6	19.5
Epicatechin	2.2	4.3	6.5	8.6	13.0	15.1	17.3	19.4	21.6
Total (mg/L)	***11.1***	***22.1***	***33.2***	***44.3***	***66.4***	***77.5***	***88.5***	***99.6***	***110.7***

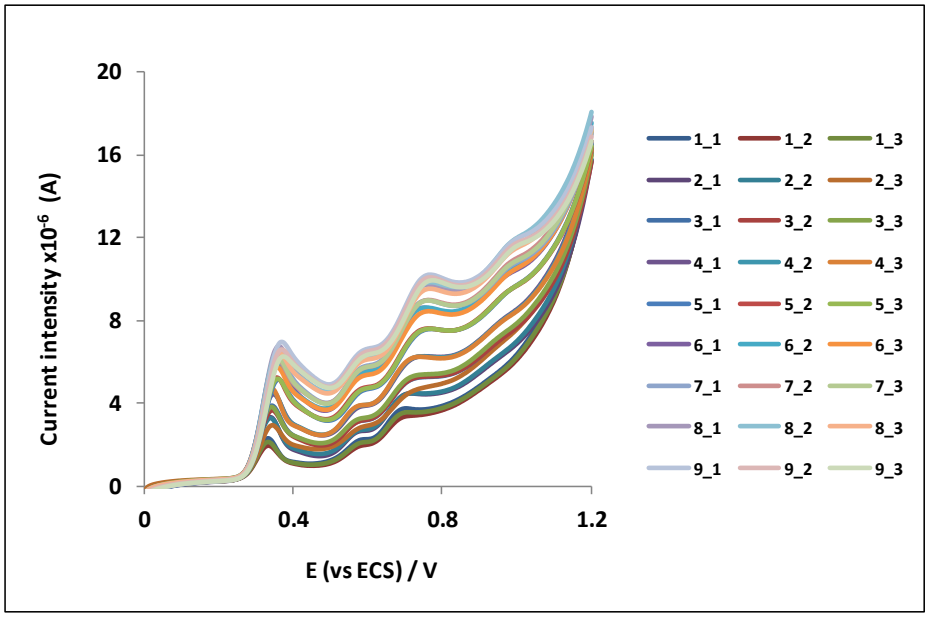

Figure 5.1. Oxidation curves of phenolics combinations (Table 5.1 codes) in a model wine solution.

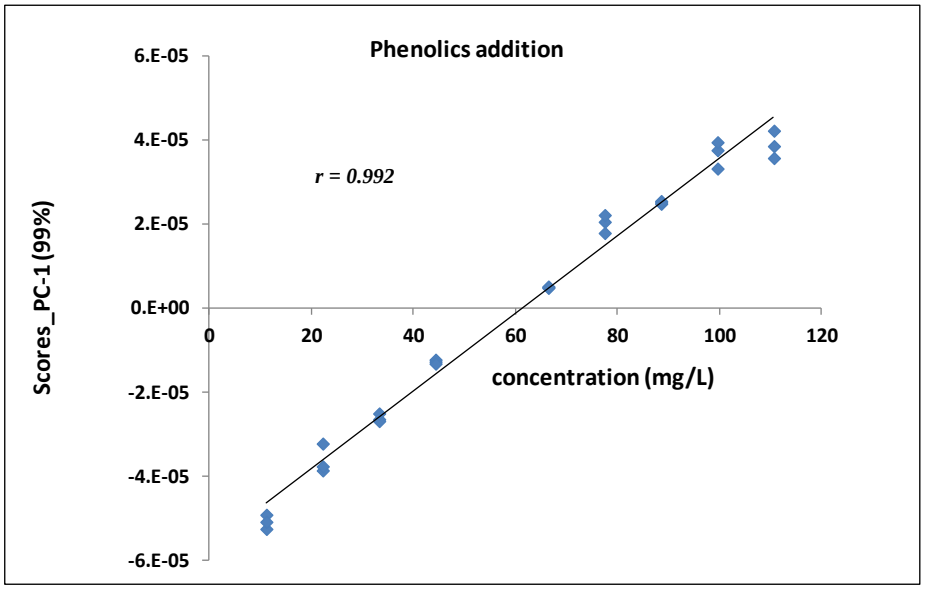

Figure 5.2. Relationship between PC1 scores and phenolics concentration.

5.2.2. Effect of pH on phenolic compounds voltammetric signals in model wine solutions

In this work, the white wine forced aging protocol was conducted undiluted at a pH of 3.2. Whereas, the red Port wines were diluted in a model wine solution at a pH of 3.6. Table 5.2 represents the anodic (Ep,a) and cathodic (Ep,c) peak potentials at pH 3.2 and pH 3.6, at a concentration of 2.5 mM, for the flavonol, quercetin; the flavan-3-ols, (+)-catechin and (-)-epicatechin; the derivatives of benzoic acid, *para*-hydroxybenzoic acid, protocatechuic acid, vanillic acid, gallic acid and syringic acid; and the derivatives of cinnamic acid, *para*-coumaric acid, caffeic acid and ferulic acid. In the same way, Table 5.3 represents the anodic (Ip,a) and cathodic (Ip,c) peak currents of the same analyzed phenolic compounds.

Table 5.2. Anodic and cathodic peak potentials at pH 3.2 and pH 3.6, of the studied polyphenols.

	pH = 3.2				pH = 3.6			
Phenolic compound	Ep_1,a	Ep_2,a	Ep_1,c	Ep_2,c	Ep_1,a	Ep_2,a	Ep_1,c	Ep_2,c
quercetin	0.371				0.349			
(+)-catechin	0.378	0.771	0.308		0.354	0.747	0.283	
(-)-epicatechin	0.354	0.735	0.303		0.332	0.710	0.276	
p -hydroxybenzoic acid	0.991		0.574	0.117	0.967		0.549	0.088
protocatechuic acid	0.457		0.374		0.432		0.347	
vanillic acid	0.752		0.657	0.378	0.730		0.632	0.356
gallic acid	0.374	0.759	0.295		0.354	0.735	0.273	
syringic acid	0.620		0.313		0.596		0.286	
p -coumaric acid	0.791				0.771			
caffeic acid	0.398		0.352		0.374		0.327	
ferulic acid	0.627-0.686		0.344		0.603-0.662		0.317	

Ep,a - anodic peak potential (V); Ep,c - cathodic peak potential (V); Phenolics concentration = 2.5 mM.

Table 5.3. Anodic and cathodic peak currents at pH 3.2 and pH 3.6, of the studied polyphenols.

	pH = 3.2				pH = 3.6			
Phenolic compound	Ip_1,a x10^{-6}	Ip_2,a x10^{-6}	Ip_1,c x10^{-6}	Ip_2,c x10^{-6}	Ip_1,a x10^{-6}	Ip_2,a x10^{-6}	Ip_1,c x10^{-6}	Ip_2,c x10^{-6}
quercetin	0.90				0.80			
(+)-catechin	2.53	4.26	-2.26		2.36	4.03	-2.20	
(-)-epicatechin	3.49	4.34	-2.52		3.29	3.99	-2.49	
p -hydroxybenzoic acid	11.61		-1.16	-2.27	11.39		-1.14	-2.18
protocatechuic acid	7.02		-3.80		6.71		-3.61	
vanillic acid	7.33		-0.44	-2.46	7.23		-0.43	-2.37
gallic acid	6.58	5.02	-0.99		6.18	4.83	-0.99	
syringic acid	5.27		-1.32		3.80		-1.19	
p -coumaric acid	8.45				8.25			
caffeic acid	7.42		-5.05		7.17		-4.77	
ferulic acid	4.50		-2.40		4.27		-2.20	

Ip,a - anodic peak current (A); Ip,c - cathodic peak current (A); Phenolics concentration = 2.5 mM.

By the observation of Table 5.2, it is possible to conclude that, with the increase of pH, the anodic and cathodic peak potentials are shifted toward less positive values. Along with this observation, higher pH values will induce phenolic oxidation, by the decrease on both anodic and cathodic peak current intensities (Table 5.3). This fact may be well explained by the fact that, under normal wine conditions, there is a slow rate of phenolic oxidation reactions, but electrons are rapidly transfer from phenols to semi-quinones at pH 7 (Danilewicz, 2003), and in alkaline conditions there is a quicker estimate of oxygen consumption in wine (Singleton et al., 1979), where the weakly acidic nature of phenolic compounds (pKa = 9-10) allows them to form phenolate anions (Waterhouse and Laurie, 2006).

Increasing the pH from 3.2 to 3.6 will induce phenolic oxidation in 1 to 10% of the initial concentration (Table 5.3). The only exception was for syringic acid that had a decrease of respectively 30% in the anodic peak current intensity.

5.2.3. Voltammetric curve pattern in white and red Port wines

Voltammetric fingerprinting was performed (Chapter 3; 3.5.) in the forced aging protocols of white and red Port wines (Chapter 3; 3.2.). For the white wine aging protocol, samples were taken weekly (6 weeks*2 oxygen regimes*4 temperatures*3 replicates); total of ***144 samples***.

For the red Port wine aging protocol, samples were taken biweekly (5 weeks*2 oxygen regimes*4 temperatures*3 replicates + 3 initial wine); total of ***123 samples***.

The accelerated spoilage, conducted with both temperature and oxygen supplements, promoted a modification of the wines phenolic composition that could be assessed by cyclic voltammetry. Figure 5.3 and Figure 5.4 illustrates the cyclic voltammetric signals of respectively white and red Port wines under 20ºC and the extreme applied temperatures, for both oxygen treatments I and II. The composition alteration was followed by a current decrease or maintenance on the applied range potentials (Figure 5.3 and Figure 5.4). By the observation of Figure 5.3, it can be proposed that the cyclic voltammograms of the white wine have two main anodic peaks. The first anodic peak at around 0.45 V is dominated by catechol-containing hydroxycinnamic acids (like caffeic acid), hydroxycinnamates (like monocaffeoyl tartaric acid) (Makhotkina and Kilmartin, 2012), catechin and gallic acid (Chapter 3; Table 3.1, and Table 5.2). The second anodic peak was seen at a potential around 0.85 V and can be attributed to polyphenols with a higher formal potential such as *para*-coumaric acid and its derivatives (Chapter 3; Table 3.1, and Table 5.2). The larger-sized phenolic compounds originated during the accelerated spoilage, and responsible for brown colors, could also be oxidized in the potential range of 0.85 to 1.2 V (Recamales et al., 2006, Salacha et al., 2008, Kallithraka et al., 2009) and contribute to the second anodic peak in the cyclic voltammograms of the white wines.

From Figure 5.4, it can be proposed that the cyclic voltammograms of the red Port wine have three main anodic peaks. The first anodic peak at around 0.35 V is dominated by catechin-type flavonoids, quercetin, hydroxycinnamates (like monocaffeoyl tartaric acid) and gallic acid (Chapter 3; Table 3.1, and Table 5.2). The second peak was seen at a potential around 0.55 V and can be attributed to malvidin-3-glucoside anthocyanins, present in the red Port wines (Kilmartin et al., 2001) and to other anthocyanins (Chapter 3; Table 3.1). The third anodic peak in the cyclic voltammograms of red Port wines at 0.75 V is dominated by the second oxidation of the catechin flavonoids and of the gallic acid that are present in red Port wines at a high concentration (Chapter 3; Table 3.1, and Table 5.2).

A decrease in the current intensities at the two anodic peak potentials Ep,a (0.45 and 0.85 V) was observed in both supplemented and non supplemented oxygen treatments during the time-course of white wine forced aging protocol (Figure 5.3). Likewise, a decrease in the current intensities at the two anodic peak potentials Ep,a (0.55 and 0.75 V) was

observed in both supplemented and non supplemented oxygen treatments during the time-course of red Pot wine forced aging protocol (Figure 5.4). The first anodic peak of red Port wines, at around 0.35 V, is maintained along the time-course forced aging protocol. Moreover, the observed current intensities decreases (in white and red Port wines) were higher with the oxygen treatment II (oxygen addition every sampling point) (Figure 5.3 and Figure 5.4). These current intensities will be correlated with phenolic composition in section 5.2.6 in this chapter.

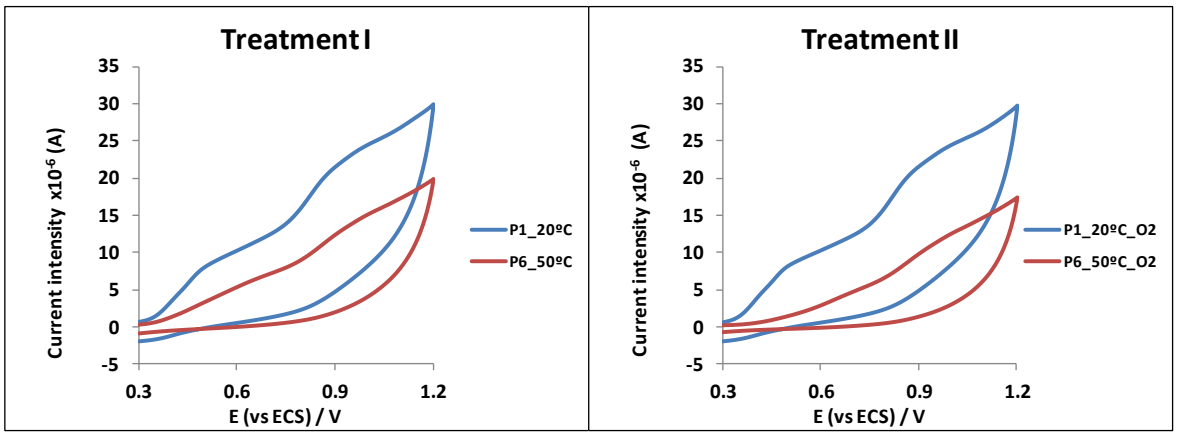

Figure 5.3. Cyclic voltammetric curves for white wine samples kept at 20 and 50ºC, for treatment I and II, during the 42 days of storage. Samples were used undiluted.

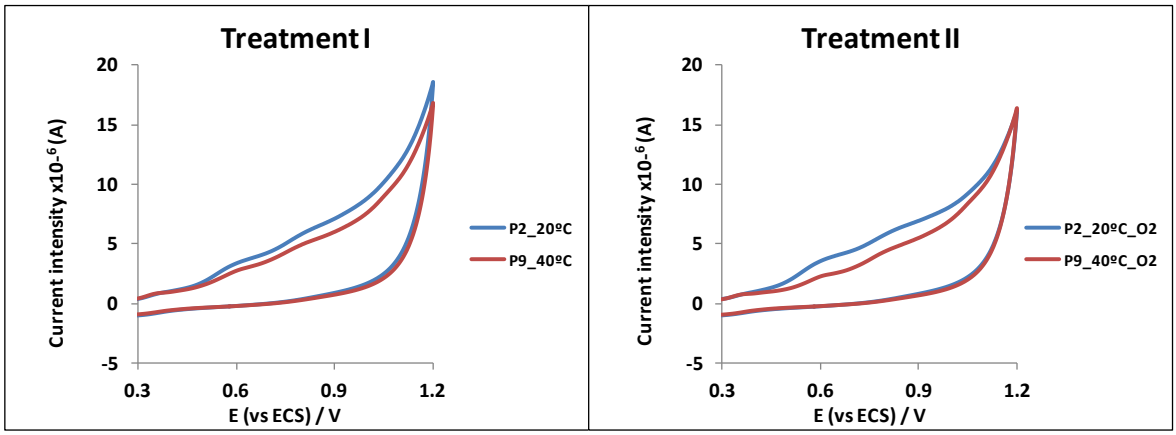

Figure 5.4. Cyclic voltammetric curves for red Port wine samples kept at 20 and 40ºC, for treatment I and II, during the 63 days of storage. Samples were used diluted 20x.

5.2.4. Effect of temperature on voltammetric signals in white and red Port wines

A principal component analysis (PCA) was applied to the voltammetric oxidation signals of both white and red Port wines forced aging protocols, in the two applied oxygen regimes (treatment I and II). This procedure illustrates the global electrochemical differences of the analysed wines, and the scores of the first component (PC1) can be used to assess the dependence between the electrochemical oxidation signals and temperature. In the same way, time-course degradation direction can be observed in relevant PC's scores. Data was normalized by mean normalization. Figure 5.5 and Figure 5.6 shows the temperature dependence of respectively treatment I and treatment II for the white wine aging protocol, while Figure 5.7 and Figure 5.8 shows the temperature dependence of respectively treatment I and treatment II for the red Port wine aging protocol.

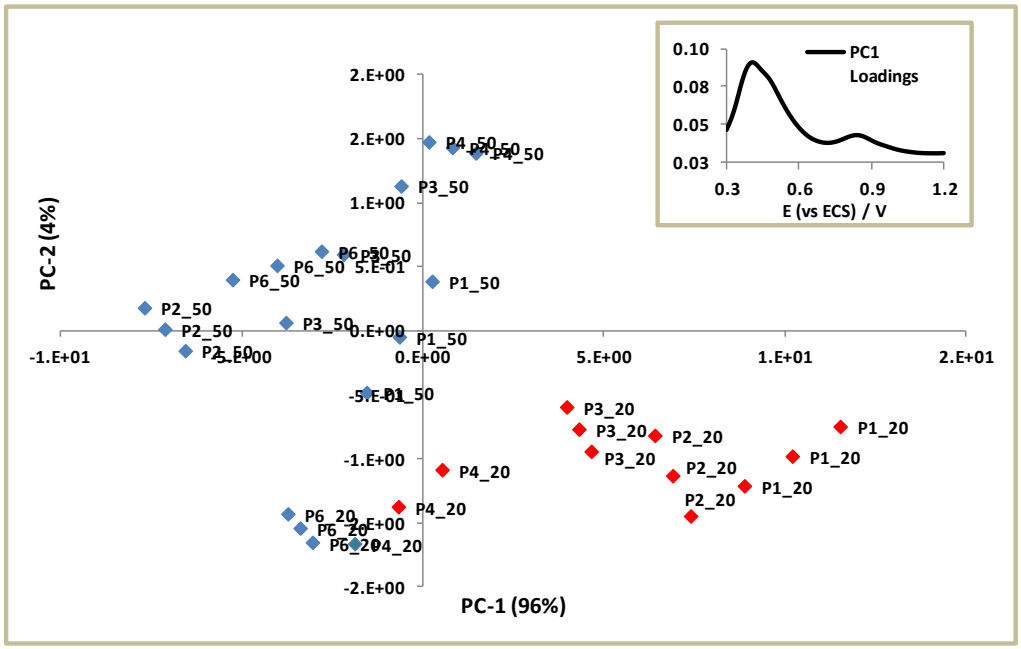

Figure 5.5. Scores scatter plot (PC1 vs PC2) of white wine voltammetric oxidation signals for oxygen treatment I (no supplemented oxygen addition) and corresponding PC1 loadings. Components 1 and 2 account for 100% of the total variance.

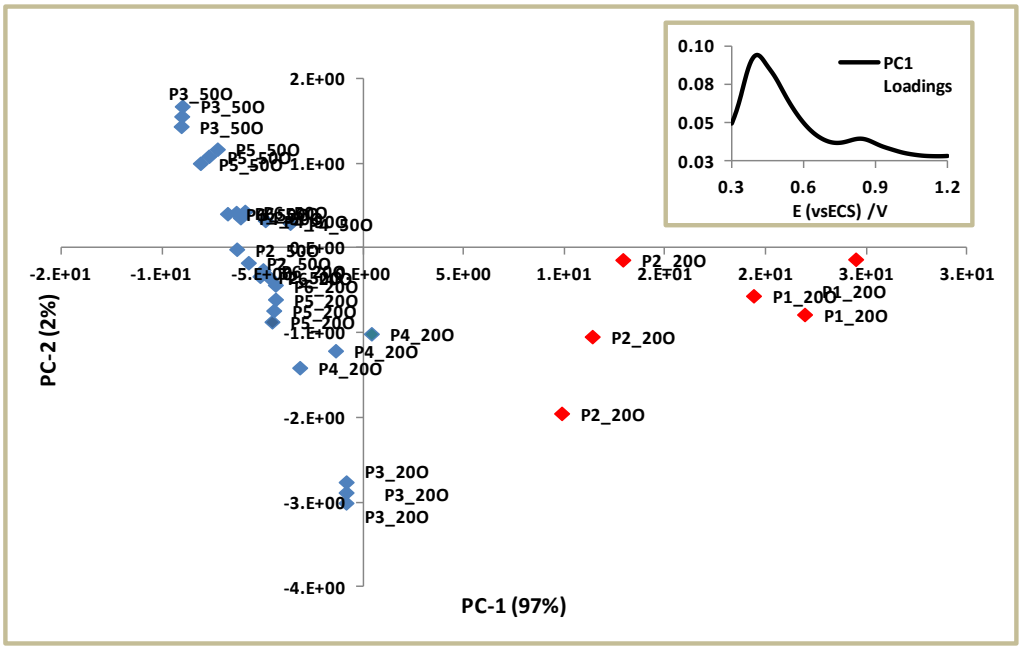

Figure 5.6. Scores scatter plot (PC1 vs PC2) of white wine voltammetric oxidation signals for oxygen treatment II (oxygen addition every sampling point) and corresponding PC1 loadings. Components 1 and 2 account for 99% of the total variance.

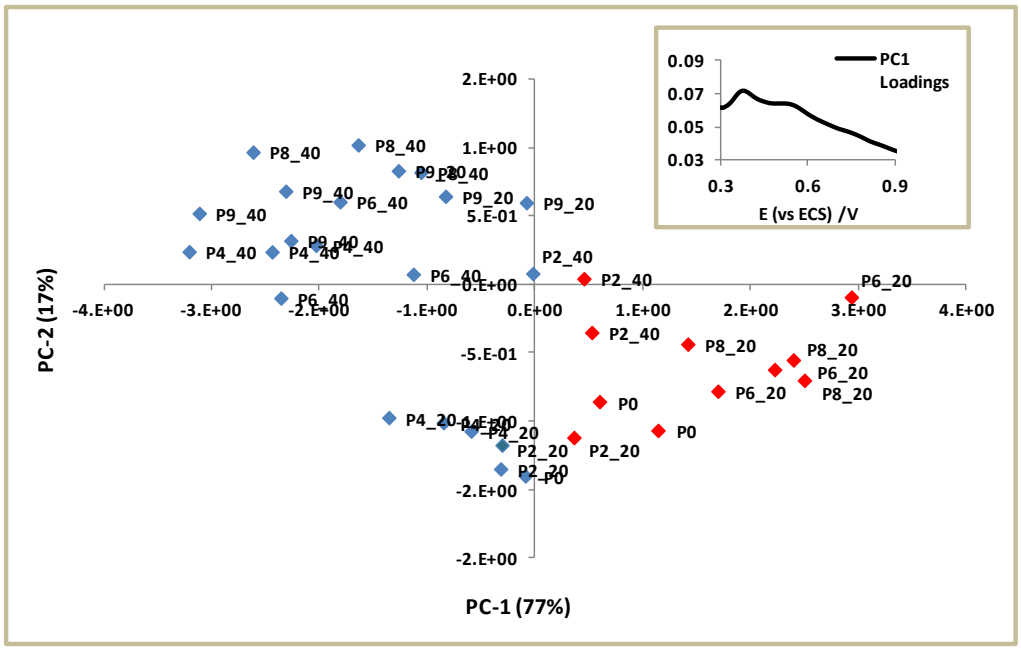

Figure 5.7. Scores scatter plot (PC1 vs PC2) of red Port wine voltammetric oxidation signals for oxygen treatment I (no supplemented oxygen addition) and corresponding PC1 loadings. Components 1 and 2 account for 94% of the total variance.

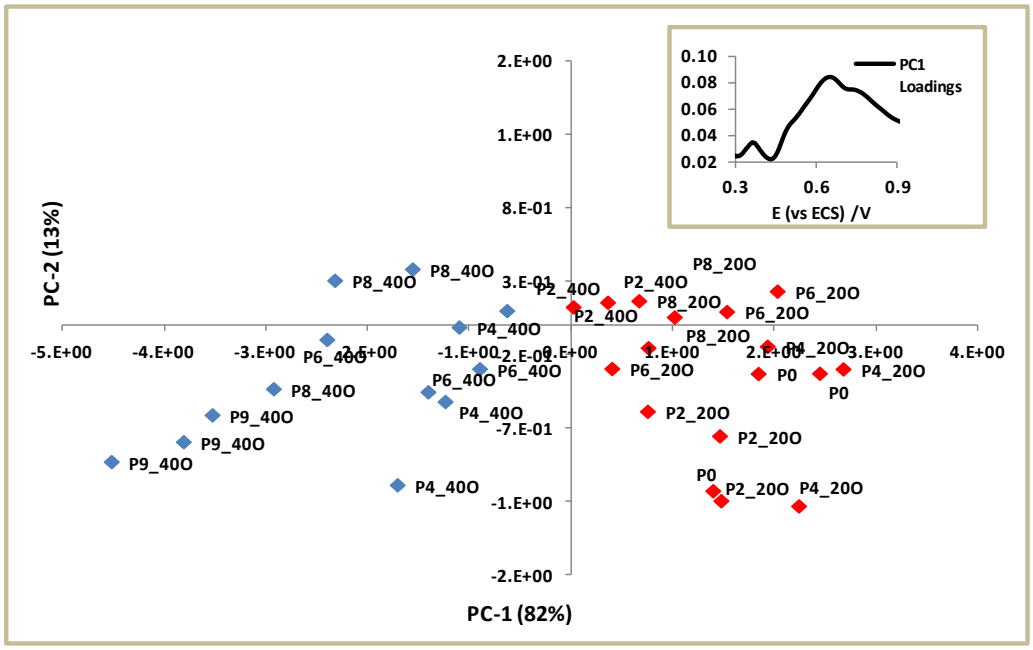

Figure 5.8. Scores scatter plot (PC1 vs PC2) of red Port wine voltammetric oxidation signals for oxygen treatment II (oxygen addition every sampling point) and corresponding PC1 loadings. Components 1 and 2 account for 95% of the total variance.

For the two applied oxygen regimes (treatment I and II), in both white and red Port wines, a clear trend was observed as a function of temperature and protocol extent, with a variability explained in principal component 1 (PC 1) of 100% and 99%, for white wine, and 94% and 95% for red Port wine. Plotting PC 1 scores results (Figures 5.5, 5.6, 5.7, and 5.8), we can see that the wines storage at lower temperatures, and in the first stages of degradation, are located in positive PC 1. In opposition, wines storage at higher temperatures, and in the last stages of degradation, are located in negative PC 1. Nevertheless, for red Port wines, this relation is not so clear. This fact could be related with the restoration of same phenolic compounds related with anthocyanins degradation explored after in this thesis.

5.2.5. Effect of oxygen on voltammetric signals in white and red Port wines

A partial least squares regression (PLSR) was applied to the wines voltammetric oxidation signals along the forced aging protocols. Data was normalized by mean normalization. Figure 5.9 and Figure 5.10 represents the relationship giving by PLSR between the

voltammetric oxidation signals and the consumed oxygen observed along the forced aging protocols of, respectively, white and red Port wines. The root-mean-square error (RMSE) was used to assess the model fitness.

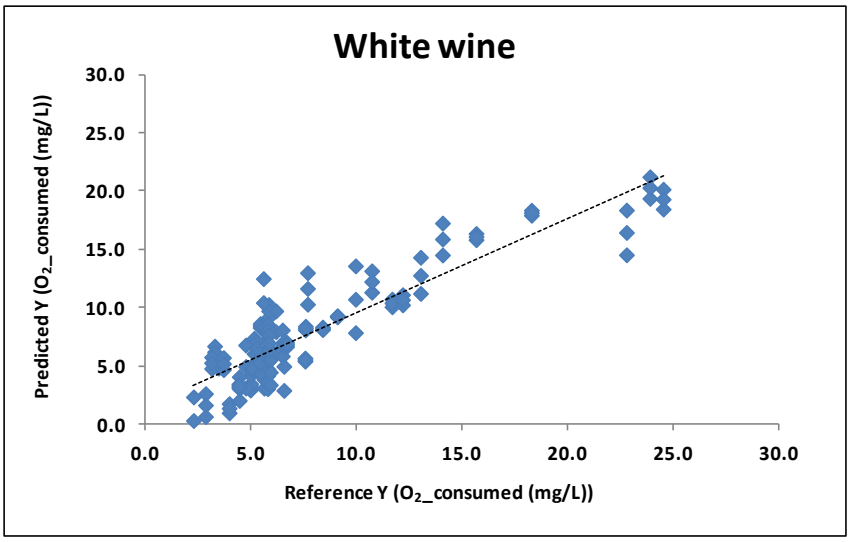

Figure 5.9. Relationship between white wine voltammetric oxidation signals and the consumed oxygen during the 42 days of storage. RMSE = 2.32 mg/L (LVs=5).

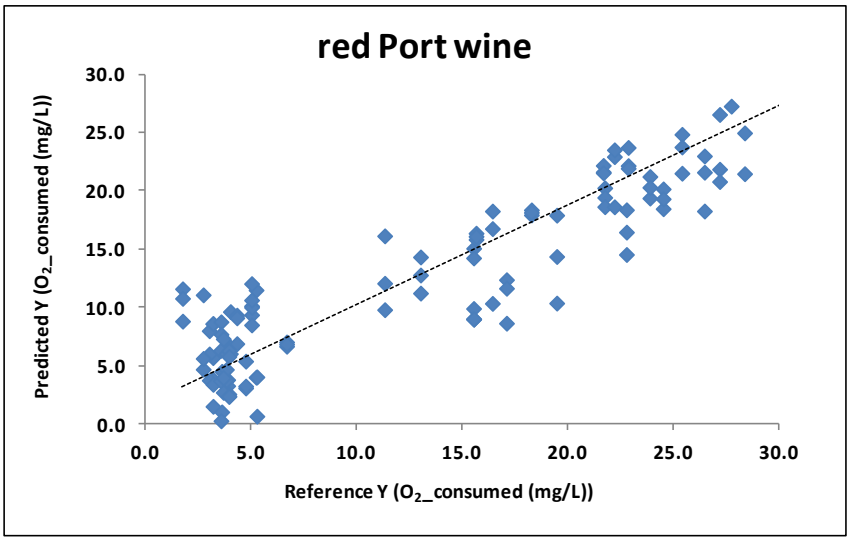

Figure 5.10. Relationship between red Port wine voltammetric oxidation signals and the consumed oxygen during the 63 days of storage. RMSE = 4.53 mg/L (LVs=5).

Results have shown that oxygen consumption along the forced aging protocols of both white and red Port wines can be predicted by voltammetric oxidation signals, with a

correlation coefficient (r) of 0.898 and 0.926 for, respectively, white and red Port wines. The LOD were 7.79 and 8.63 mg/L for, respectively, white and red Port wines.

5.2.6. Correlation between phenolic composition and voltammetric signals in white and red Port wines

The decreases in the current intensities at the two observed anodic peak potentials Ep,a (0.45 and 0.85 V) for the white wine forced aging protocol were correlated with the total phenolic content expressed by Folin-Ciocalteu index (FC) (Chapter 3; 3.13.). The FC index, also called the gallic acid equivalence method (GAE), is a mixture of phosphomolybdate and phosphotungstate used for the colourimetric assay of phenolic and polyphenolic antioxidants. In the same way, the decreases or maintenance in the current intensities at the three anodic peak potentials Ep,a (0.35, 0.55 and 0.75 V) for the red Port wine forced aging protocol were, as well, related with the FC index. Figure 5.11 and Figure 5.12 represent the relationship between the FC index and the observed anodic peak potentials for, respectively, white and red Port wines.

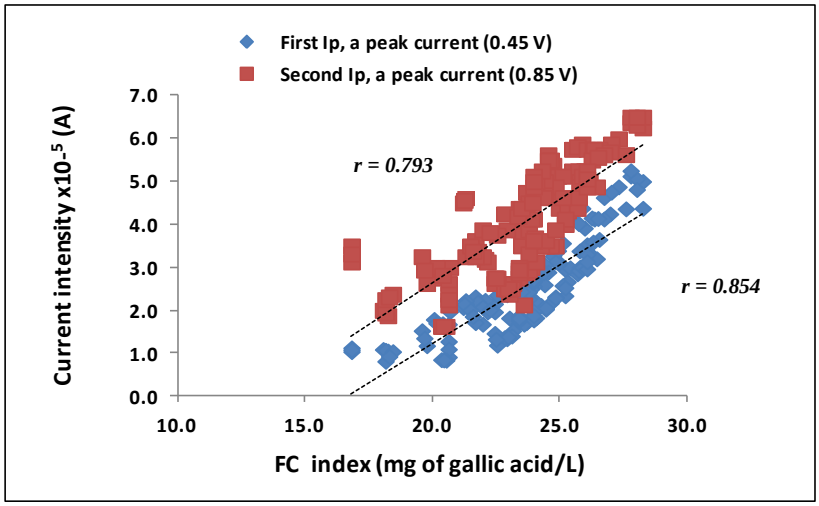

Figure 5.11. Representation of current intensities at the two anodic peak potentials Ep,a (0.45 and 0.85 V) versus the total phenolic content evaluated by the FC index.

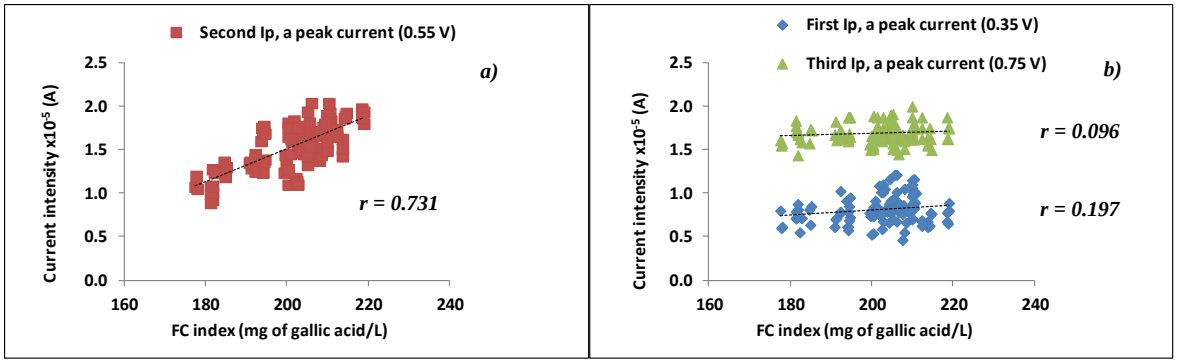

Figure 5.12. Representation of current intensities at the tree anodic peak potentials: a) Ep,a (0.55 V); and b) (0.35 and 0.75 V) versus the total phenolic content evaluated by the FC index.

In Figure 5.11 it is shown that the current intensity measured at the two anodic peak potentials Ep,a 0.45 and 0.85 V followed a linear relationship with the total phenolic content, evaluated by the FC index, with a correlation coefficient of 0.854 and 0.793, for respectively, the first and the second Ip,a peaks. Moreover, these relationship was greater with the first Ip,a peak indicating a more reactive oxidative phenolic zone, dominated by catechol-containing hydroxycinnamic acids, hydroxycinnamates, catechin and gallic acid (Chapter 3; Table 3.1, and Table 5.2).

In Figure 5.12 it is shown that only the current intensity measured at the anodic peak potential Ep,a 0.55 V followed a linear relationship with the total phenolic content, evaluated by the FC index, with a correlation coefficient of 0.731 (Figure 5.12a) attributed mainly to malvidin-3-glucoside and to other anthocyanins (Chapter 3; Table 3.1). The current intensities measured at the anodic peak potentials Ep,a 0.35 and 0.75 V are not correlated with the total phenolic content expressed by Folin-Ciocalteu index (FC) (Figure 5.12b). These peak potentials, in the cyclic voltammograms of red Port wines, may possibly be influenced by the increase of hydroxybenzoic acids during aging due to anthocyanins cleavage (Ribéreau-Gayon et al., 2006). Cyanidin 3-glucoside can release protocatechuic acid (Ep,a 0.43 V, pH 3.6); delphinidin 3-glucoside can release gallic acid (Ep,a 0.35 and 0.74 V, pH 3.6); peonidin 3-glucoside can release vanillic acid (Ep,a 0.73 V, pH 3.6); and malvidin 3-glucoside can release syringic acid (Ep,a 0.60 V, pH 3.6). This fact might contribute to maintenance or less decrease of the phenolic compounds responsible for these peak potentials.

5.3. Diode-Array Detector (DAD) analysis of phenolic compounds

A Diode-Array Detector (DAD) was used for the screening of the phenolic composition changes occurring in both white and red Port wines during the process of thermal and oxidative degradation. DAD belongs to a particular group of detectors called RIDs, "Rich Information Detector". Each chromatogram can be considered a set of points of compounds ("scans") obtained by a constant frequency over the time of elution. Each scan contains an absorbance spectrum in a range scan between 212 and 600 nm. Each sample can be then represented by a vector (i.e. chromatogram) obtained in a particular wavelength, or as an array surface, where the x-axis represents the retention time; the y-axis represents the wavelength range; and the z-axis represents the absorbance. Spectra duplicates were recorded for each wine. These data will provide high-throughput non-destructive information beyond traditional analytical chemistry methods.

5.3.1. Analysis of particular relevant wavelengths on phenolics composition changes

HPLC-DAD was performed (Chapter 3; 3.6.) in the forced aging protocols of white and red Port wines (Chapter 3; 3.2.). The relevant wavelengths, during the process of thermal and oxidative degradation of phenolics in wine, were achieved by the interpretation of samples array surfaces. Each analysis consisted in a matrix: $\boldsymbol{S_{(901x195)}}$, where 901 is the retention time **(x)** and 195 is the number of wavelengths **(y)**, for white wines; and $\boldsymbol{S_{(1801x195)}}$, where 1801 is the retention time **(x)** and 195 is the number of wavelengths **(y)**, for red Port wines. The relevant selected wavelengths will allow exploring an indispensable aid to the progress of knowledge of the “degradation status” of wines based on their phenolic composition. Figure 5.13 and Figure 5.14 illustrates the array surface (212 to 600 nm) of white wines under 20ºC and the extreme applied temperature, for both oxygen treatments I and II. In the same way, Figure 5.15 and Figure 5.16 illustrates the array surface (212 to 600 nm) of red Port wines under 20ºC and the extreme applied temperature, for both oxygen treatments I and II.

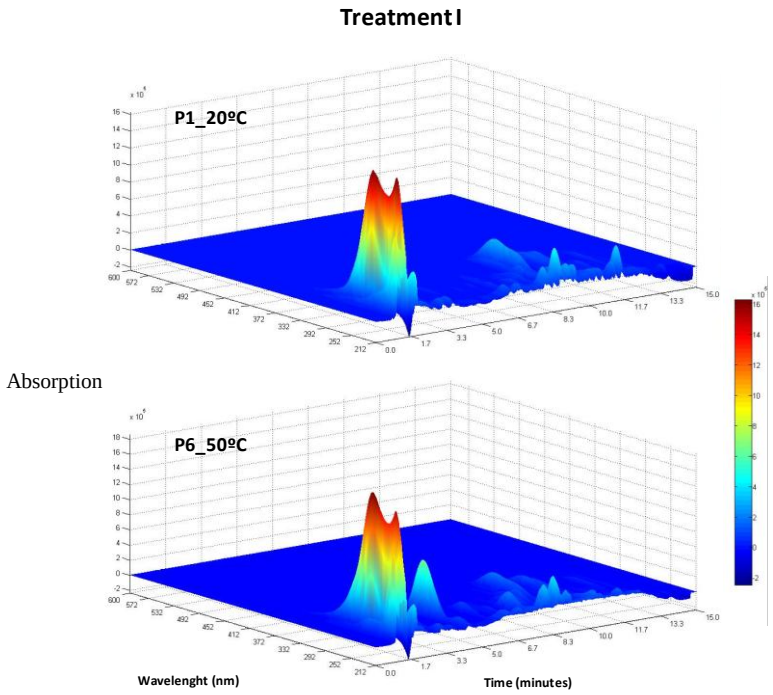

Figure 5.13. Array surface interpretation of white wine samples kept at 20 and 50ºC, for treatment I, during the 42 days of storage.

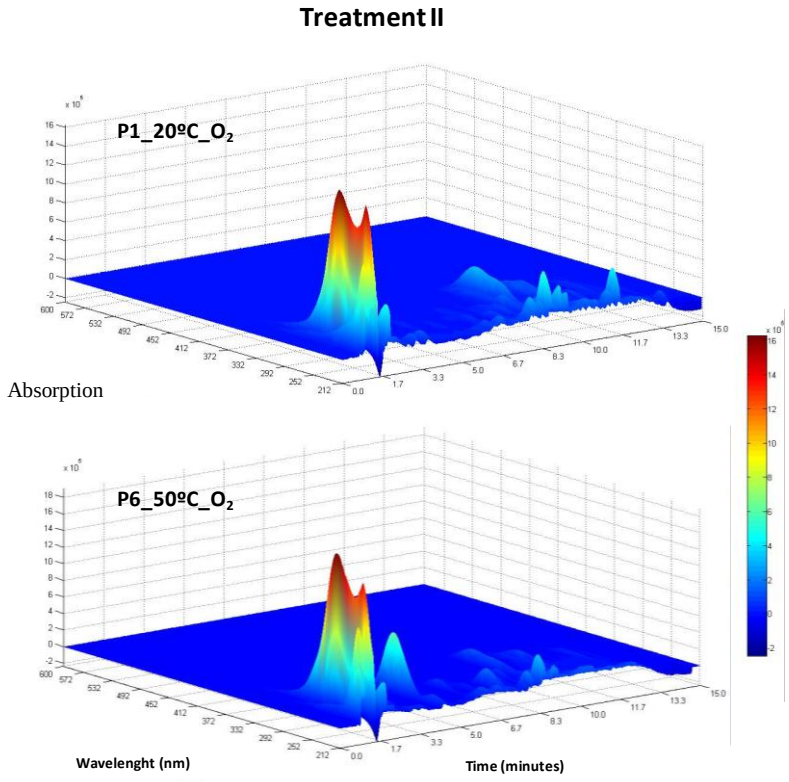

Figure 5.14. Array surface interpretation of white wine samples kept at 20 and 50ºC, for treatment II, during the 42 days of storage.

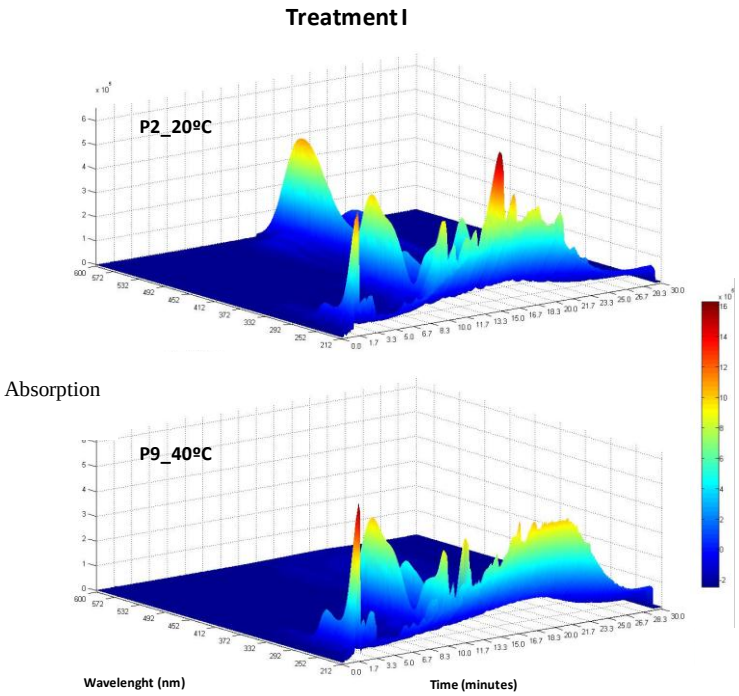

Figure 5.15. Array surface interpretation of red Port wine samples kept at 20 and 40ºC, for treatment I, during the 63 days of storage.

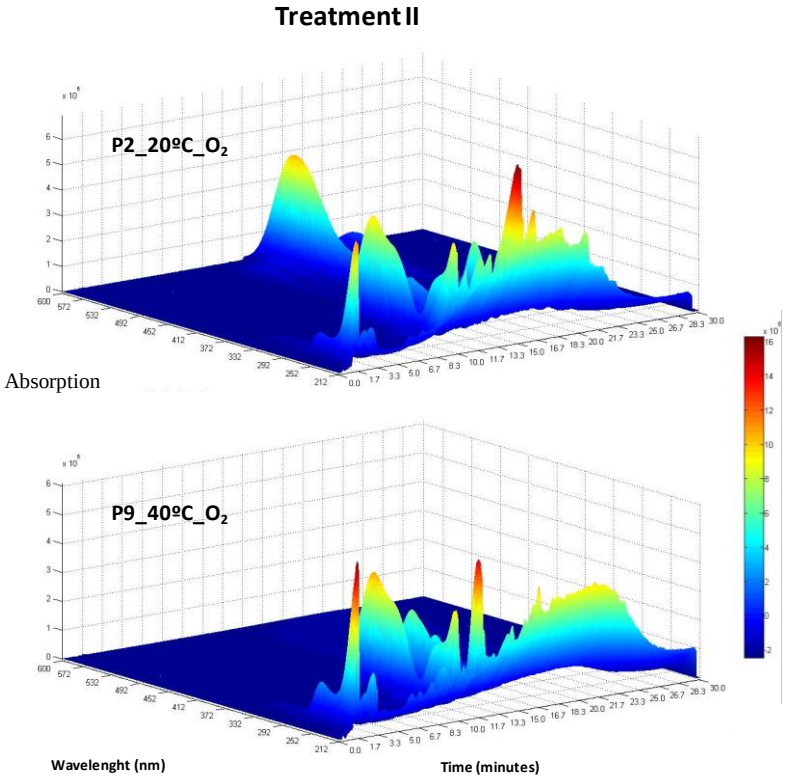

Figure 5.16. Array surface interpretation of red Port wine samples kept at 20 and 40ºC, for treatment II, during the 63 days of storage.

From the analysis of Figures 5.13 to 5.16, it is possible to verify that the electromagnetic surfaces (212 at 600 nm) do indeed contain distinguishing features for wines with different degradation levels. The main differences, for both white and red Port wines, typically rely on three absorption regions. The first wavelength region at 280 nm is closely connected with wine phenolic hydroxybenzoic acids, flavan-3-ols, flavonols and furanic compounds (Figure 5.13 to 5.16); the second wavelength region at 320 nm is related with hydroxycinnamic acids, hydroxycinnamic esters, GRP (2-*S*-glutathionyl-*trans*-caftaric acid) and GRP derivatives (Figure 5.13 to 5.16); and the third wavelength region, around 528 nm, is connected with wine anthocyanins and is responsible for the red wine color and astringency (Figure 5.13 and Figure 5.16).

The specific selected relevant wavelengths, 280, 320 and 528 (for red Port wines), on phenolics composition changes, were recorded along with the wavelength scanning between 212 and 600 nm. Figure 5.17 and Figure 5.18 illustrates the chromatograms of white wines, in the first sampling point, under 20ºC for oxygen treatment I (P1_20ºC), and in the last sampling point, under the extreme applied temperature for oxygen treatment II (P6_50ºC_O_2), intended for respectively 280 and 320 nm. Likewise, Figure 5.19, Figure 5.20 and Figure 5.21 illustrates the chromatograms of red Port wines, in the first sampling point, under 20ºC for oxygen treatment I (P1_20ºC), and in the last sampling point, under the extreme applied temperature for oxygen treatment II (P9_40ºC_O_2), projected for respectively 280, 320 and 528 nm.

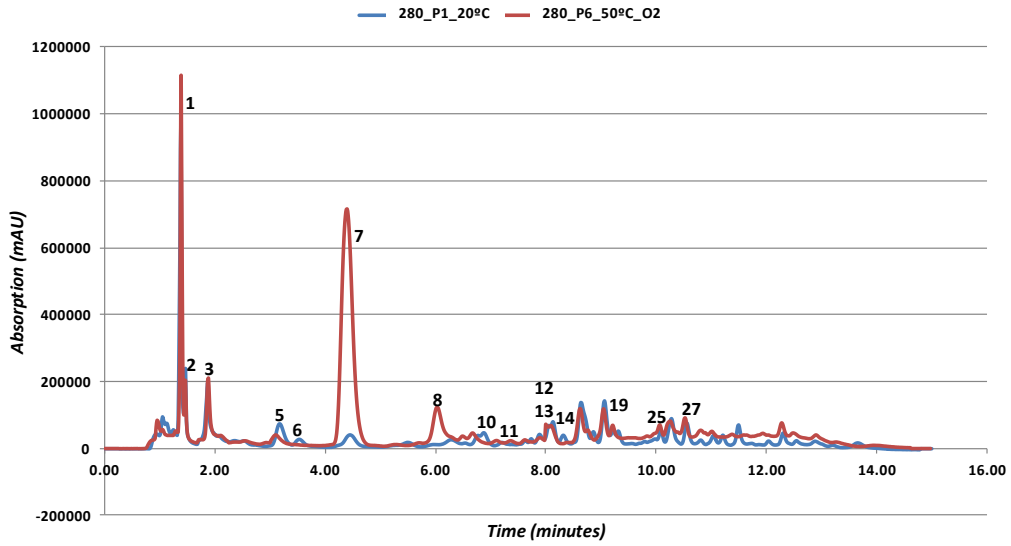

Figure 5.17. Chromatogram of white wines, P1_20ºC and P6_50ºC_O_2 at 280 nm.

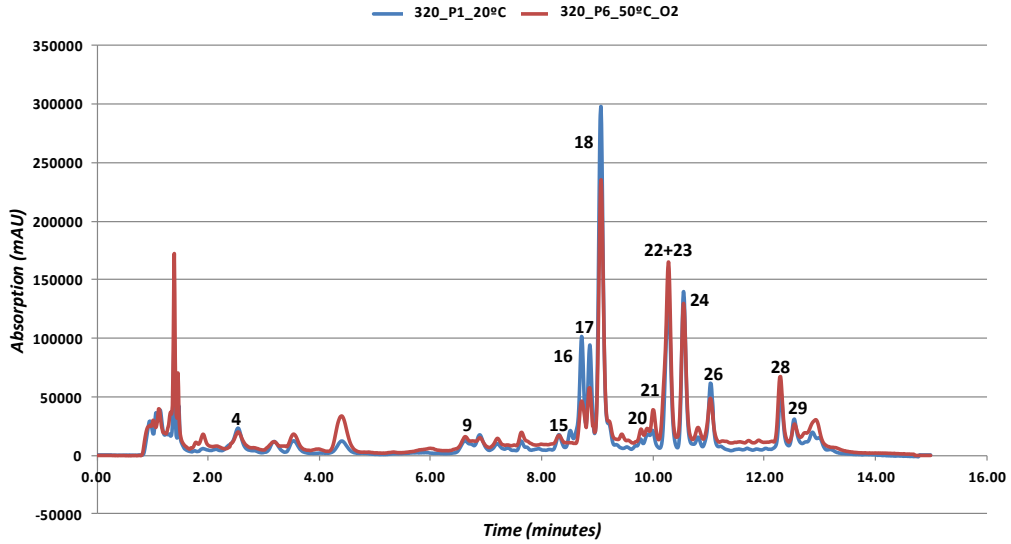

Figure 5.18. Chromatogram of white wines, P1_20ºC and P6_50ºC_O_2 at 320 nm.

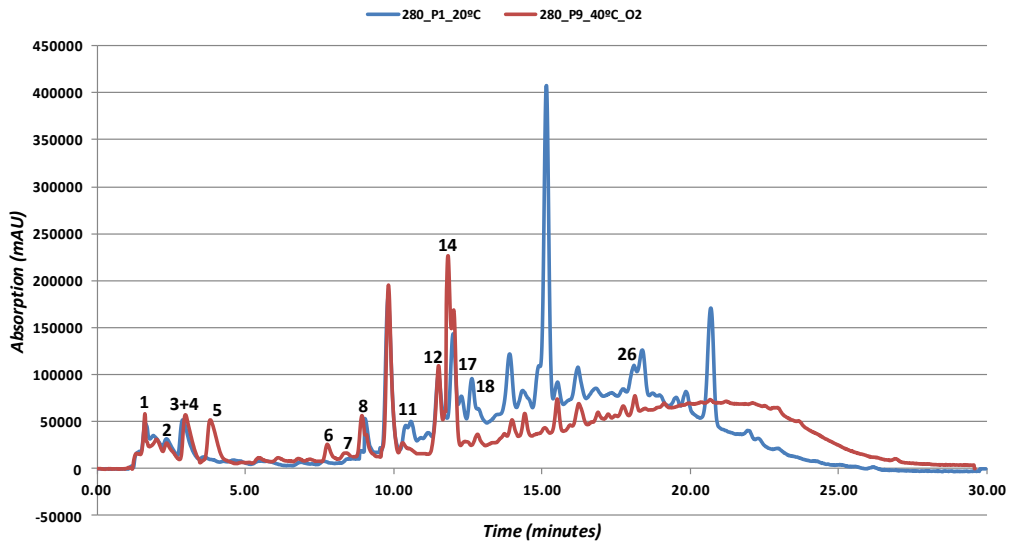

Figure 5.19. Chromatogram of red Port wines, P1_20ºC and P9_40ºC_O_2 at 280 nm.

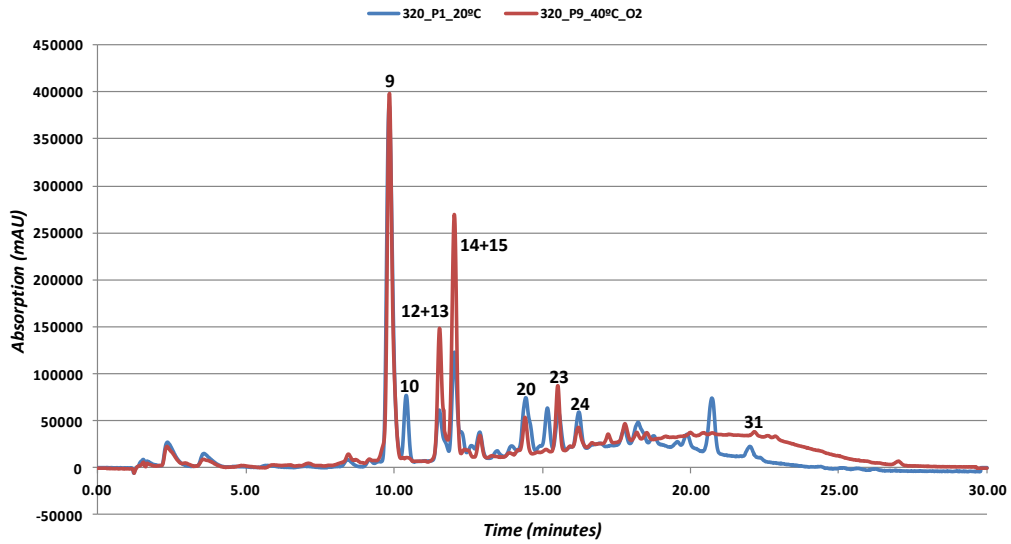

Figure 5.20. Chromatogram of red Port wines, P1_20ºC and P9_40ºC_O_2 at 320 nm.

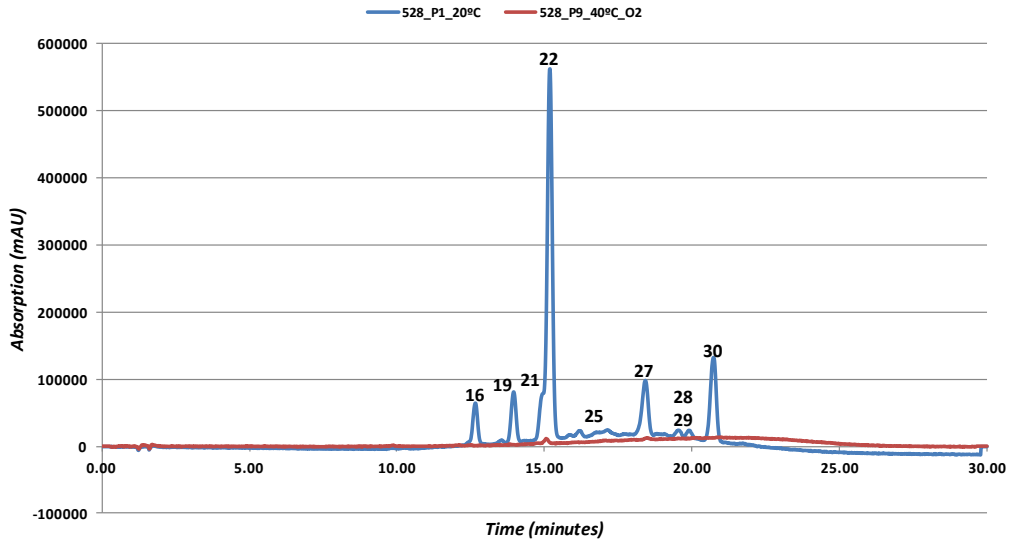

Figure 5.21. Chromatogram of red Port wines, P1_20ºC and P9_40ºC_O_2 at 528 nm.

From the analysis of Figures 5.17 to 5.21, it is possible to verify that the HPLC-DAD interpretation of the relevant wavelengths allowed the separation of 29 compounds for white wines, in less than 15 min, and 31 compounds for red Port wines, in less than 25 min. These faster chromatographic runs will be processed by a MVA strategy intended for identifying/measuring the composition changes occurring during the process of thermal and oxidative degradation of the wines.

5.3.2. Analysis of the overall array surface of phenolics composition changes

In this study, the overall procedure was not targeted to specific compounds, involving rather a set of metabolites, extracted from the wines collected at the different stages of oxidation. Data was obtained during the process of thermal and oxidative degradation of wines (Chapter 3; 3.2.) and focused on the widest possible phenolics metabolic profile. HPLC-DAD was pre-processed by performing baseline correction, peak alignment, peak identification, and chromatogram reconstruction. Afterwards peaks are sent for attempted identification.

For the white wine aging protocol, samples were taken weekly (P1, 7^{th} day sampling, to P6, 42^{th} day sampling) (6 weeks*2 oxygen regimes*4 temperatures*1 measurement); total of ***48 samples***.

For the red Port wine aging protocol, samples were taken on the 14^{th} day sampling (P2); the 28^{th} day sampling (P4); and the 63^{th} day sampling (P9) (3 sampling points*2 oxygen regimes*4 temperatures*1 measurement); total of ***24 samples***.

Using appropriate algebric operations it is possible to calculate a single array resulting from compression of *n* matrices (chromatographic run) held. The procedure goes through the initial fold matrix dimensions [retention time; wavelengths] on a vector [1; retention time x wavelengths]. The converted vectors can then be grouped by sets of samples with again an array of dimensions [number of samples; retention time x wavelengths]. For multivariate analysis, each matrix was unfolded to give a vector $s_{i(1,\,j)}$, where *i* corresponds to the number of samples and *j* corresponds to the number of variables of each analysis. Then all of them were row concatenated to give a matrix $\mathbf{Q}_{(i,\,j)}$. This **Q** matrix was then used to perform the PCA, which consisted in the decomposition of it into: $\mathbf{Q}_{(i,\,j)} = \mathbf{T}_{(i,\,k)}.\ \mathbf{P}^{\mathbf{T}}_{(k,\,j)}$, where **T** represents the scores matrix, **P** represents the loadings matrix and k corresponds to the number of principal components. The scores matrix (**T**) gives the relationships between the samples, whereas the loadings matrix (**P**) gives the importance of each variable (i.e. retention times and their correspondent absorption spectra). Finally, and in order to facilitate the interpretation of the loadings (**P**), each one of its columns k (principal components) were folded back to give a matrix, which was depicted as a 2D map: $\mathbf{P}_{k\,(j,\,1)} \rightarrow\ p_{k(l,\,m)}$, where $j = l\ .\ m$ such as *l* and *m* are, respectively, the number of scans (retention time) and the absorption values correspondent to each sample.

Figure 5.22 and Figure 5.24 represents the scores plots (PC1 and PC2) of the wine aging protocols, for respectively white and red Port wines. Figure 5.23 and Figure 5.25 represents the loadings interpretation of PC 1 in the overall array surfaces, for respectively white and red Port wines, will Table 5.4 and Table 5.5 accounts for the compounds identification based on loadings of PC 1.

For both white and red Port wines, a clear trend was observed as a function of oxidation extent, with a total variability explained in components 1 and 2 of 87%, 2%; and 95%, 1%, for respectively, white and red Port wines (Figure 5.22 and Figure 5.24). For white wines, from plotting PC 1 and 2 scores results (Figure 5.22), we can see that oxidized white wine samples are located in positive PC 1 (Figure 5.22). This fact indicates that, positive loadings contribution (Figure 5.23 and Table 5.4) corresponds to an increasing of compounds absorption. On another hand, negative loadings contribution (Figure 5.23 and Table 5.4) corresponds to a diminishing of compounds absorption.

For red Port wines, from plotting PC 1 and 2 scores results (Figure 5.24) we can see that oxidized red Port wine samples are located in negative PC 1 (Figure 5.24). This fact indicates that, negative loadings contribution (Figure 5.25 and Table 5.5) corresponds to a increasing of compounds absorption. On another hand, positive loadings contribution (Figure 5.25 and Table 5.5) corresponds to a diminishing of compounds absorption.

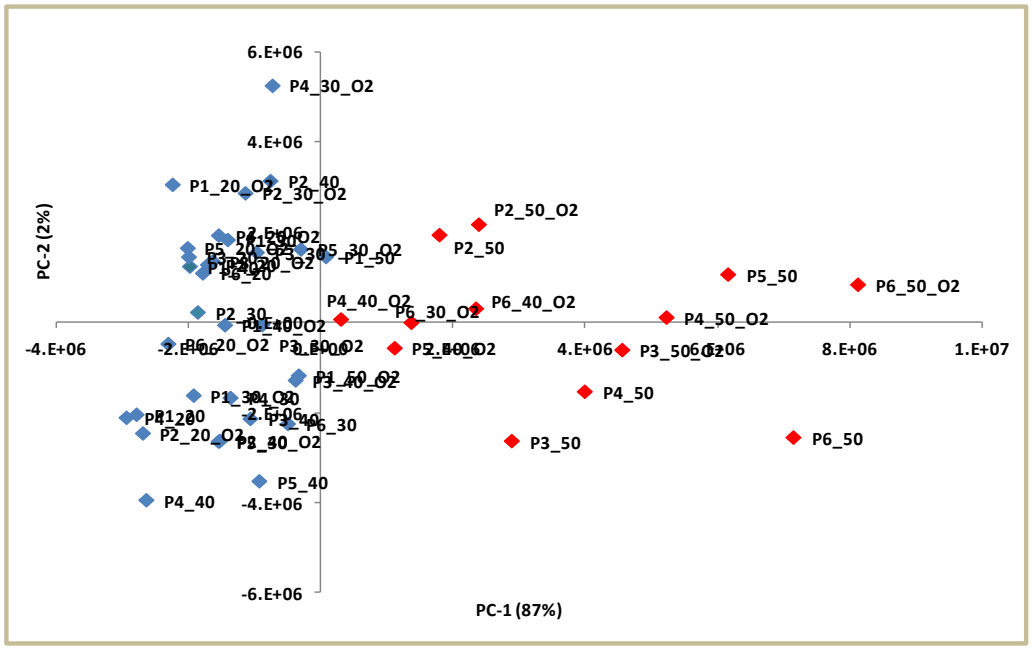

Figure 5.22. Scores scatter plot (PC1 vs PC2) of phenolics content of the overall array surface (212 at 600 nm) with different applied temperature regimes (20, 30, 40 and 50ºC) during the oxidation process (P1, P2, P3, P4, P5 and P6) of white wine. Components 1 and 2 account for 89% of the total variance.

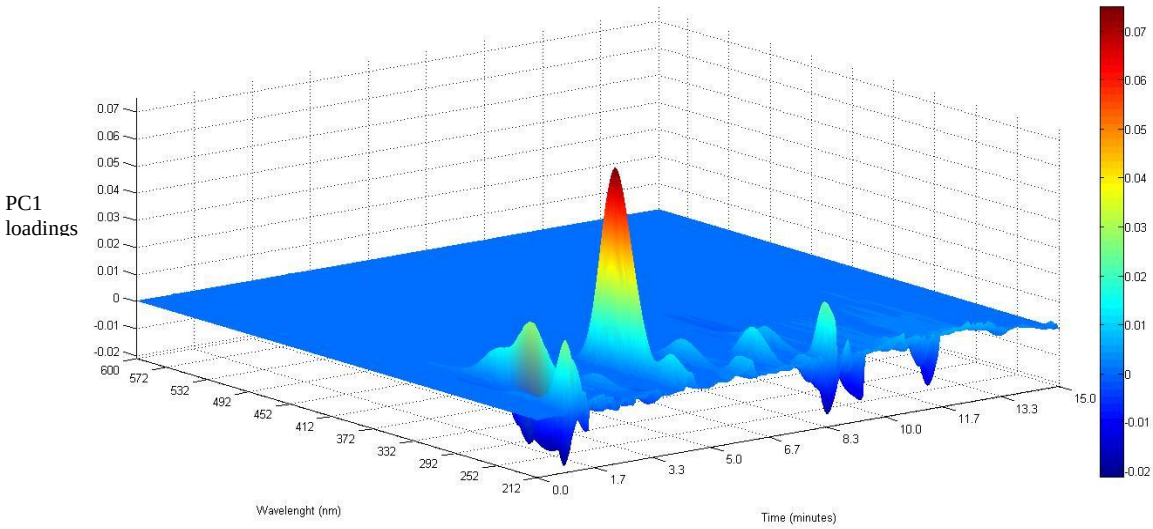

Figure 5.23. White wine surf loadings of plot 1 (PC 1) combining HPLC chromatographic data and the correspondent absorption (DAD) to each wavelength scan.

Table 5.4. White wine retention time's identification based on loadings values of PC 1.

Compound Nº	Retention time (min)	Loading contribution	Loading value
7	**4.40**	Positive	0.07495
1	**1.38**	Positive	0.02712
16	**8.72**	Negative	0.00853
18	**9.07**	Negative	0.00852
3	**1.88**	Positive	0.00742
8	**6.03**	Positive	0.00723
17	**8.87**	Negative	0.00615
23	**10.32**	Positive	0.00448
10	**6.88**	Negative	0.00233
19	**9.32**	Negative	0.00224
28	**12.30**	Positive	0.00221
12	**8.00**	Positive	0.00202
5	**3.18**	Negative	0.00197
27	**11.48**	Negative	0.00168
26	**11.03**	Negative	0.00166
14	**8.32**	Negative	0.00154
25	**10.82**	Negative	0.00145
21	**10.08**	Positive	0.00143
22	**10.28**	Negative	0.00131
15	**8.52**	Positive	0.00102
11	**7.63**	Positive	0.00074
20	**9.78**	Positive	0.00065
13	**8.10**	Positive	0.00056
4	**2.53**	Negative	0.00055
24	**10.55**	Negative	0.00036
2	**1.47**	Positive	0.00028
9	**6.62**	Positive	0.00021
6	**3.53**	Negative	0.00008
29	**12.55**	Negative	0.00002

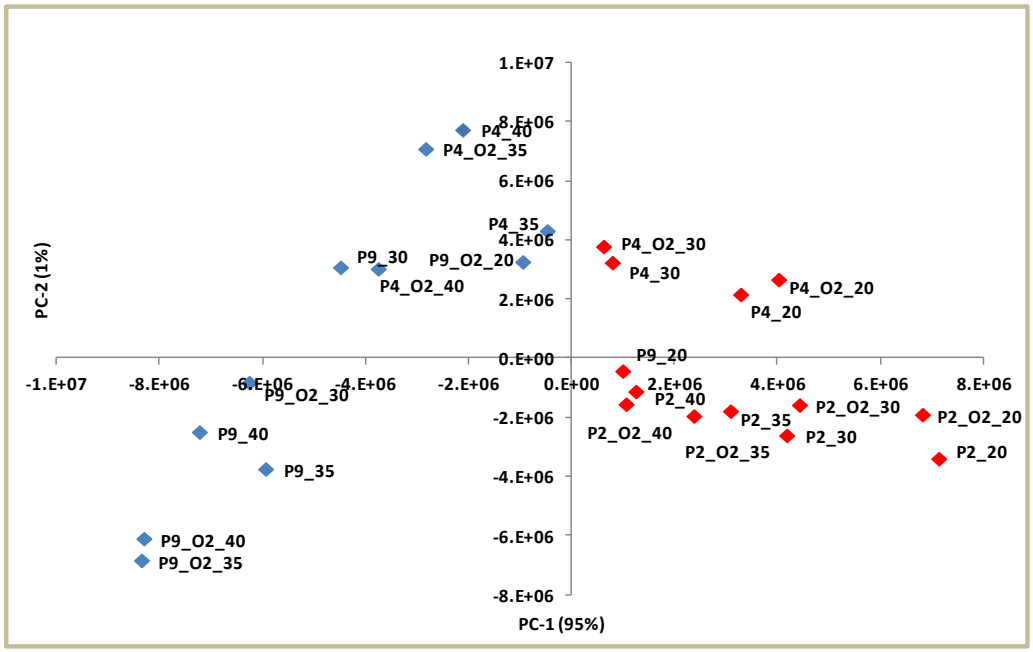

Figure 5.24. Scores scatter plot (PC1 vs PC2) of phenolics content of the overall array surface (212 at 600 nm) with different applied temperature regimes (20, 30, 35 and 40ºC) during the oxidation process (P2, P4 and P9) of red Port wine. Components 1 and 2 account for 96% of the total variance.

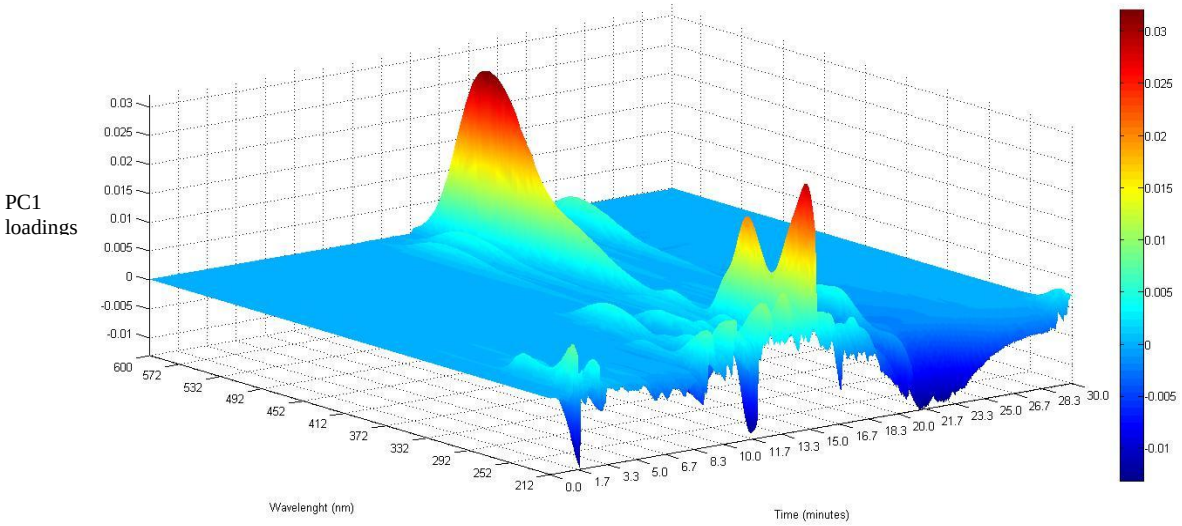

Figure 5.25. Red Port wine surf loadings of plot 1 (PC 1) combining HPLC chromatographic data and the correspondent absorption (DAD) to each wavelength scan.

Table 5.5. Red Port wine retention time's identification based on loadings values of PC 1.

Compound Nº	Retention time (min)	Loading contribution	Loading value
22	**15.18**	Positive	0.03099
14	**12.03**	Negative	0.01278
13	**11.85**	Negative	0.00678
30	**20.73**	Positive	0.00666
10	**10.42**	Positive	0.00461
19	**13.95**	Positive	0.00446
16	**12.65**	Positive	0.00314
21	**14.88**	Positive	0.00296
27	**18.42**	Positive	0.00287
18	**13.42**	Positive	0.00285
5	**3.78**	Negative	0.00229
15	**12.32**	Positive	0.00219
9	**9.83**	Positive	0.00189
24	**16.25**	Positive	0.00187
11	**10.62**	Positive	0.00169
20	**14.43**	Positive	0.00160
8	**9.38**	Positive	0.00133
17	**12.88**	Positive	0.00118
25	**16.83**	Positive	0.00084
6	**7.78**	Negative	0.00084
26	**18.13**	Positive	0.00079
1	**1.57**	Negative	0.00078
3	**2.88**	Negative	0.00076
28	**19.57**	Positive	0.00062
7	**8.92**	Negative	0.00059
29	**19.88**	Positive	0.00058
12	**11.53**	Positive	0.00051
31	**21.9**	Positive	0.00039
2	**2.32**	Positive	0.00017
4	**6.59**	Negative	0.00015
23	**15.55**	Negative	0.00013

By the analyses of Table 5.4 it is possible to conclude that the most relevant white wine oxidation marker is compound nº 7 (4.40 min), with a positive loading contribution (Figure 5.23) that corresponds to an increase of absorption during the thermal and oxidative wine

process. Likewise, compounds nº 1 (1.38 min), nº 3 (1.88 min), nº 8 (6.03 min), and nº 23 (10.32 min) have the same performance and enlarge during the oxidative process. Along with these, the three main compounds that are found to decrease, with the most negative loadings contribution (Figure 5.23), are compounds nº 16 (8.72 min), nº 18 (9.07 min), and nº 17 (8.87 min).

By the analyses of Table 5.5 it is possible to conclude that the most relevant red Port wine oxidation marker is compound nº 22 (15.18 min), with a positive loading contribution (Figure 5.25) that corresponds to a decrease of absorption during the thermal and oxidative wine process. Equally, compounds nº 30 (20.73 min), nº 10 (10.42 min), nº 19 (13.95 min), and nº 16 (12.65 min) have the same performance and decline during the oxidative process. Conversely, the 2 major compounds that are found to increase, with the most negative loadings contribution (Figure 5.25), are compounds nº 14 (12.03 min), and nº 13 (11.85 min). Compounds listed in Tables 5.4 and 5.5 will be tentatively identified by DAD and LC-MS analyses in the next section 5.3.3. on this chapter.

5.3.3. Identification of phenolic compounds in white and red Port wines

Table 5.6 and 5.7 represents the tentatively identification of the 29 and 31 compounds separated on the HPLC chromatographic runs for respectively, white and red Port wines, based on available standards, DAD and LC-MS (Chapter 3; 3.6. and 3.9.).

Concerning white wines, 15 of the 29 compounds were identified (Table 5.6). *Furanic compounds*: 5-(hydroxymethyl)furfural (HMF) and 2-furfural; *Hydroxycinnamic acids*: caffeic acid, *para*-coumaric acid, and ferulic acid; *Hydroxycinnamic esters*: *cis*-caftaric acid (*cis*-monocaffeoyl tartaric acid), *trans*-caftaric acid (*trans*-monocaffeoyl tartaric acid), *cis*-coutaric acid (*cis*-monocumaroyl tartaric acid), *trans*-coutaric acid (*trans*-monocumaroyl tartaric acid), and *trans*-fertaric acid (*trans*-feruloyl tartaric acid); *GRP* (2-*S*-glutathionyl-*trans*-caftaric acid); *Hydroxybenzoic acids*: gallic acid and protocatechuic acid; and *Flavan-3-ols*: (+)-catechin and (-)-epicatechin.

Concerning red Port wines, 21 of the 31 compounds were identified (Table 5.7). *Furanic compounds*: 5-(hydroxymethyl)furfural and 2-furfural; *Hydroxycinnamic acids*: caffeic acid, *para*-coumaric acid, and ferulic acid; *Hydroxycinnamic esters*: *trans*-caftaric acid, *cis*-coutaric acid, *trans*-coutaric acid, and *trans*-fertaric acid; *Hydroxybenzoic acids*: gallic acid, protocatechuic acid, and syringic acid; *Flavan-3-ols*: (+)-catechin and (-)-epicatechin; *Flavonols*: quercetin; *Anthocyanins*: delphinidin-3-glucoside (Dp-3G), petunidin-3-glucoside (Pt-3G), peonidin-3-glucoside (Pn-3G), malvidin-3-glucoside (Mv-3G), malvidin-3-*O*-acetylglucoside (Mv-3acG) and malvidin-3-*O*-coumaroylglucoside (Mv-3cmG).

Table 5.6. White wine compounds identification based on DAD and/or LC-MS.

Nº	Retention time (min)	λmax 1	λmax 2	Compound name	Identification
1	**1.38**	262			
2	**1.47**	276			
3	**1.88**	266			
4	**2.53**	292	328		
5	**3.18**	270		Gallic acid	available standard; HPLC-DAD; LC-MS
6	**3.53**	258	292	Protocatechuic acid	available standard; HPLC-DAD; LC-MS
7	**4.40**	286		HMF	available standard; HPLC-DAD
8	**6.03**	278		2-Furfural	available standard; HPLC-DAD
9	**6.62**	320			
10	**6.88**	288			
11	**7.63**	288			
12	**8.00**	278			
13	**8.10**	268			
14	**8.32**	280			
15	**8.52**	326			
16	**8.72**	(254)	330	*trans*-GRP	Cejudo-Bastante et al., 2010
17	**8.87**		326	*cis*-Caftaric acid	Fanzone et al., 2010
18	**9.07**	(296)	328	*trans*-Caftaric acid	Gutiérrez et al., 2005; Mozetič et al., 2006; Guerrero et al., 2009
19	**9.32**	280		Catechin	available standard; HPLC-DAD; LC-MS
20	**9.78**	320			
21	**10.08**	320			
22	**10.28**	(286)	312	*cis*-Coutaric acid	Gutiérrez et al., 2005; Mozetič et al., 2006
23	**10.32**	(296)	326	Caffeic acid	available standard; HPLC-DAD; LC-MS
24	**10.55**	(296)	314	*trans*-Coutaric acid	Gutiérrez et al., 2005; Mozetič et al., 2006
25	**10.82**	280		Epicatechin	available standard; HPLC-DAD; LC-MS
26	**11.03**	(300)	328	*trans*-Fertaric acid	Mozetič et al., 2006
27	**11.48**	280			
28	**12.30**	(296)	308	*para*-Coumaric acid	available standard; HPLC-DAD; LC-MS
29	**12.55**	(278)	320	Ferulic acid	available standard; HPLC-DAD; LC-MS

Table 5.7. Red Port wine compounds identification based on DAD and/or LC-MS.

Nº	Retention time (min)	λmax1	λmax2	λmax3	Compound name	Identification
1	**1.57**	262				
2	**2.32**	286	326			
3	**2.88**	270			Gallic acid	available standard; HPLC-DAD; LC-MS
4	**3.01**	258	292		Protocatechuic acid	available standard; HPLC-DAD; LC-MS
5	**3.78**	286	(328)		HMF	available standard; HPLC-DAD
6	**7.78**	278			2-Furfural	available standard; HPLC-DAD
7	**8.92**	278				
8	**9.38**	274				
9	**9.83**	(296)	328		*trans*-Caftaric acid	Gutiérrez et al., 2005; Mozetič et al., 2006; Guerrero et al., 2009
10	**10.42**	326				
11	**10.62**	280			Catechin	available standard; HPLC-DAD; LC-MS
12	**11.53**	(286)	312		*cis*-Coutaric acid	Gutiérrez et al., 2005; Mozetič et al., 2006
13	**11.85**	(296)	326		Caffeic acid	available standard; HPLC-DAD; LC-MS
14	**12.03**	276			Syringic acid	available standard; HPLC-DAD; LC-MS
15	**12.32**	(296)	314		*trans*-Coutaric acid	Gutiérrez et al., 2005; Mozetič et al., 2006
16	**12.65**	280	528		Delphinidin-3-Glucoside	HPLC-DAD; LC-MS
17	**12.88**	284				
18	**13.42**	280			Epicatechin	available standard; HPLC-DAD; LC-MS
19	**13.95**	278	528		Petunidin-3-Glucoside	HPLC-DAD; LC-MS
20	**14.43**	(300)	328		*trans*-Fertaric acid	Mozetič et al., 2006
21	**14.88**	278	517		Peonidin-3-Glucoside	HPLC-DAD; LC-MS
22	**15.18**	280	348	528	Malvidin-3-Glucoside	available standard; HPLC-DAD; LC-MS
23	**15.55**	(296)	308		*para*-Coumaric acid	available standard; HPLC-DAD; LC-MS
24	**16.25**	(278)	320		Ferulic acid	available standard; HPLC-DAD; LC-MS
25	**16.83**	280	528			
26	**18.13**	280				
27	**18.42**	280	528		Mv-3-*O*-acetylglucoside	HPLC-DAD; LC-MS
28	**19.57**	282	528			
29	**19.88**	282	528			
30	**20.73**	282	(388)	534	Mv-3-*O*-coumaroylglucoside	HPLC-DAD; LC-MS
31	**21.90**	280	372		Quercetin	available standard; HPLC-DAD; LC-MS

After white and Port wine compounds identification (Table 5.6 and Table 5.7) we could suggest that the most relevant white wine oxidation markers are 5-(hydroxymethyl)furfural and 2-furfural (Table 5.6), with positive loading contributions (Table 5.4) that corresponds to an increase of absorption, for these compounds, during the thermal and oxidative wine process. In the same way, two hydroxycinnamic acids, caffeic acid and *para*-coumaric acid (Table 5.6) have increased during the oxidative process, with positive loading contributions (Table 5.4). On the other hand the three phenolic compounds with the most negative loadings contribution (Table 5.4) are *trans*-GRP and *trans*- and *cis*-caftaric acid (Table 5.6), that corresponds to a decrease of absorption, for these molecules, during the thermal and oxidative wine process. Considering Port wine, the most relevant red Port wine oxidation marker is the anthocyanin malvidin-3-glucoside (Table 5.7) with a positive loading contribution (Table 5.5) that corresponds to a decrease of absorption during the thermal and oxidative wine process on this molecule. Equally, all the identified anthocyanins have decreased (Table 5.5 and Table 5.7). Kinetic modeling of anthocyanins oxidation in Port wines will be performed in section 5.4. Along with anthocyanins, the flavan-3-ols (+)-catechin and (-)-epicatechin (Table 5.7) have also had higher positive loadings contribution (Table 5.5), that corresponds to a high decrease of absorption, for these molecules, during the oxidative process. Conversely, the two major compounds that are found to increase, with the most negative loadings contribution (Table 5.5), are the hydroxybenzoic acid, syringic acid, and the hydroxycinnamic acid, caffeic acid (Table 5.7).

5.3.4. Quantification of relevant phenolic compounds in white and red Port wines

Quantification of relevant phenolic compounds, implicated in the thermal and oxidative processes in both white and red Port wines, was attempted by LC-MS (Chapter 3; 3.9. LC-Mass spectrometry: non-volatiles analysis). The hydroxycinnamic esters monocaffeoyl tartaric acid (caftaric acid), monocumaroyl tartaric acid (coutaric acid), and feruloyl tartaric acid (fertaric acid) were expressed in equiv. of, respectively, caffeic acid, *para*-coumaric acid and ferulic acid. 2-*S*-Glutathionyl-*trans*-caftaric acid (*trans*-GRP) was quantified by HPLC (Chapter 3; 3.6. HPLC with diode array detection (DAD)) and expressed in equiv. of caffeic acid.

Considering the white wine protocol, Figure 5.26 represents the evolution (mg/L/day) of *trans*-GRP, the hydroxycinnamic esters, *cis*-caftaric acid, *trans*-caftaric acid, *cis*-coutaric acid, *trans*-coutaric acid, and *trans*-fertaric acid, the hydroxycinnamic acids, caffeic acid, *para*-coumaric acid, and ferulic acid, the hydroxybenzoic acids, gallic acid and protocatechuic acid, and finally, the flavan-3-ols, (+)-catechin and (-)-epicatechin, for respectively, oxygen treatments I and II.

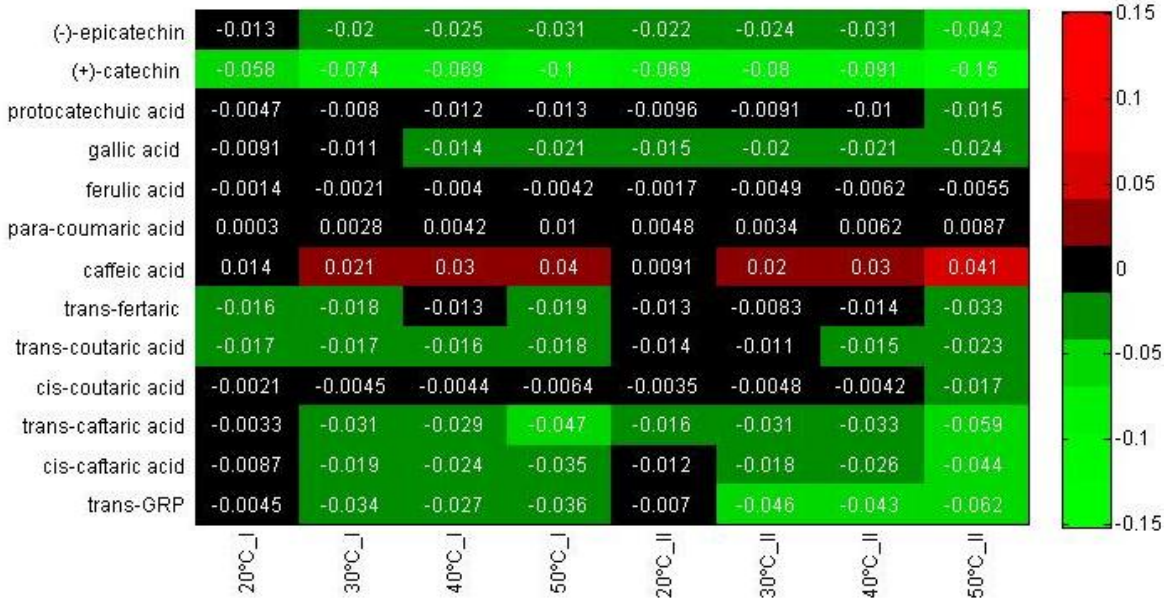

Figure 5.26. Phenolics formation or depletion during the forced aging protocols in white wines. I - no oxygen addition; II - oxygen addition. Data in appendix of this thesis.

Considering the red Port wine protocol, Figure 5.27 represents the evolution (mg/L/day) of the hydroxycinnamic esters, *trans*-caftaric acid, *trans*-coutaric, and *trans*-fertaric acid, the hydroxycinnamic acids, caffeic acid, *para*-coumaric acid, and ferulic acid, the hydroxybenzoic acids, gallic acid, protocatechuic acid, and syringic acid, and finally, the flavan-3-ols, (+)-catechin and (-)-epicatechin for, respectively, oxygen treatments I and II. Table 5.8 represents the anthocyanins depletion during the Port wine oxidation protocol.

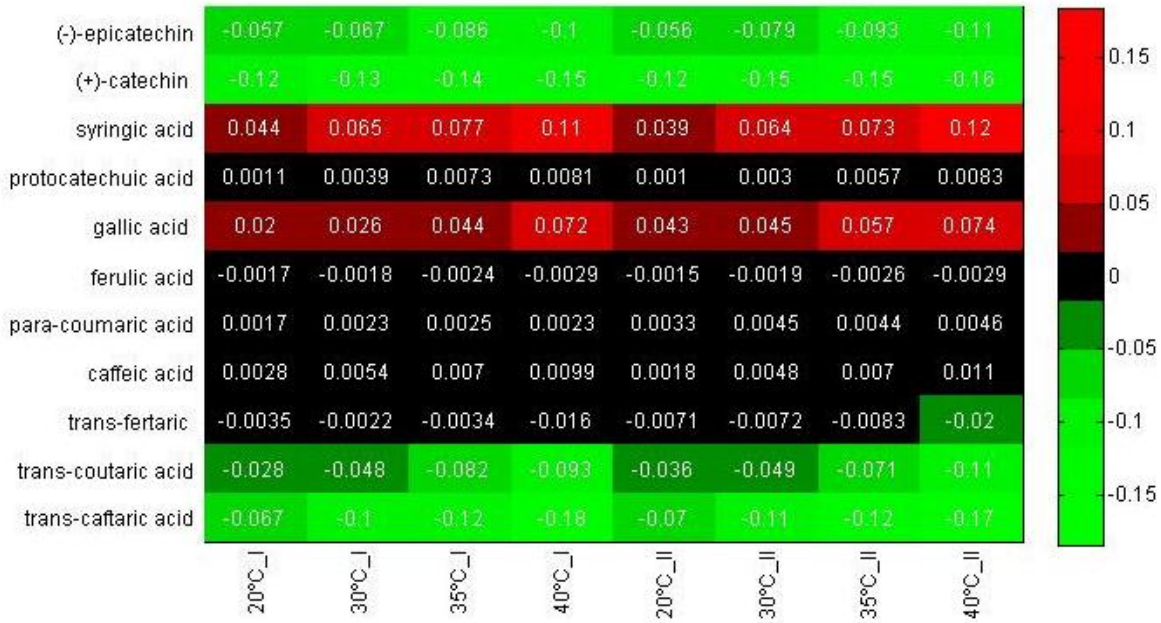

Figure 5.27. Phenolics formation or depletion during the forced aging protocols in red Port wines. I - no oxygen addition; II - oxygen addition. Data in appendix of this thesis.

Table 5.8a. Evolution of anthocyanins under treatment I (no oxygen addition).

Sample	Time	Temperature	(Dp-3G)	(Pt-3G)	(Pn-3G)	(Mv-3G)	(Mv-3acG)	(Mv-3cmG)
P0	0	20	11.7	14.0	12.0	94.2	17.1	29.3
P1_20	7	20	9.9	12.1	11.6	81.1	16.6	27.1
P1_30	7	30	9.3	11.8	11.6	76.8	14.1	26.7
P1_35	7	35	8.5	10.7	9.9	72.0	12.8	17.8
P1_40	7	40	5.5	7.2	7.8	48.2	9.5	12.9
P2_20	14	20	7.2	9.3	10.1	60.8	12.0	15.0
P2_30	14	30	4.9	6.5	5.3	45.4	9.2	11.0
P2_35	14	35	4.0	5.4	5.2	36.2	7.7	9.2
P2_40	14	40	2.9	4.1	3.7	27.0	6.4	7.1
P3_20	21	20	6.8	8.8	9.0	60.1	11.7	14.4
P3_30	21	30	4.0	5.3	5.2	36.2	8.2	9.1
P3_35	21	35	2.9	4.1	3.9	27.0	6.4	7.1
P3_40	21	40	2.7	3.9	3.2	16.9	5.1	4.5
P4_20	28	20	6.4	8.3	8.3	53.1	11.6	12.2
P4_30	28	30	2.9	4.2	4.9	31.4	8.1	7.6
P4_35	28	35	2.1	3.1	3.8	21.3	6.1	6.2
P4_40	28	40	1.5	2.4	2.9	13.9	5.1	4.4
P5_20	35	20	5.6	7.0	7.0	46.8	9.7	11.9
P5_30	35	30	2.8	4.1	4.8	31.4	7.6	6.5
P5_35	35	35	1.8	3.0	3.7	18.2	5.8	5.5
P5_40	35	40	0.6	1.1	1.5	7.3	3.9	3.0
P6_20	42	20	3.9	5.4	5.4	37.9	9.1	9.3
P6_30	42	30	1.8	2.7	3.3	18.8	7.0	5.7
P6_35	42	35	1.0	1.7	2.1	10.2	5.2	4.2
P6_40	42	40	0.6	1.0	1.5	6.8	3.7	3.0
P7_20	49	20	3.8	5.1	5.0	36.0	8.8	9.0
P7_30	49	30	1.5	2.5	3.2	17.7	5.8	4.9
P7_35	49	35	0.8	1.4	1.9	8.4	4.3	3.5
P7_40	49	40	0.4	0.8	1.1	5.0	3.6	2.7
P8_20	56	20	3.1	4.4	4.7	31.3	7.5	7.3
P8_30	56	30	1.4	2.2	2.7	13.8	5.3	4.8
P8_35	56	35	0.6	1.0	1.5	6.8	3.7	3.0
P8_40	56	40	0.4	0.7	1.0	3.1	2.6	2.5
P9_20	63	20	3.0	4.2	4.6	29.8	7.4	7.0
P9_30	63	30	1.3	2.0	2.6	13.1	5.7	4.4
P9_35	63	35	0.4	0.6	0.8	2.7	2.5	2.2
P9_40	63	40	0.3	0.5	0.9	2.8	2.6	2.4

Table 5.8b. Evolution of anthocyanins under treatment II (oxygen addition).

Sample	Time	Temperature	(Dp-3G)	(Pt-3G)	(Pn-3G)	(Mv-3G)	(Mv-3acG)	(Mv-3cmG)
P1_O_2_20	7	20	8.7	13.2	11.8	73.2	16.7	30.0
P1_O_2_30	7	30	9.3	11.1	10.5	77.8	15.7	27.6
P1_O_2_35	7	35	9.1	11.9	10.3	61.6	13.3	19.2
P1_O_2_40	7	40	6.3	8.3	8.1	48.2	9.6	17.5
P2_O_2_20	14	20	6.9	9.0	9.9	59.7	11.4	14.5
P2_O_2_30	14	30	4.8	6.9	6.6	45.4	11.3	11.1
P2_O_2_35	14	35	4.1	5.4	5.0	33.6	7.6	8.3
P2_O_2_40	14	40	2.5	3.7	4.0	25.1	5.7	6.5
P3_O_2_20	21	20	5.8	8.0	8.0	51.5	10.3	12.4
P3_O_2_30	21	30	4.1	6.5	5.8	43.7	9.0	9.1
P3_O_2_35	21	35	3.5	4.9	4.1	31.7	7.3	5.9
P3_O_2_40	21	40	1.9	2.8	3.6	17.0	5.1	4.6
P4_O_2_20	28	20	4.9	6.9	7.8	49.1	9.9	11.7
P4_O_2_30	28	30	2.9	4.4	4.9	32.7	7.3	7.2
P4_O_2_35	28	35	1.8	3.0	3.8	21.1	6.1	5.2
P4_O_2_40	28	40	0.9	1.7	2.4	10.4	4.0	4.3
P5_O_2_20	35	20	4.6	5.1	7.6	43.9	9.7	11.3
P5_O_2_30	35	30	1.9	3.6	4.9	26.8	6.8	6.4
P5_O_2_35	35	35	1.3	2.3	3.8	16.0	5.1	4.7
P5_O_2_40	35	40	0.5	0.9	1.3	5.1	3.0	2.5
P6_O_2_20	42	20	3.5	5.1	5.8	36.8	9.6	9.2
P6_O_2_30	42	30	1.0	1.9	2.7	14.6	5.3	5.0
P6_O_2_35	42	35	0.6	1.1	1.8	7.6	4.1	3.4
P6_O_2_40	42	40	0.3	0.5	0.9	3.0	2.7	2.3
P7_O_2_20	49	20	3.0	4.3	5.3	32.3	8.0	7.9
P7_O_2_30	49	30	0.9	1.6	2.4	12.1	4.6	4.0
P7_O_2_35	49	35	0.4	0.6	1.1	4.0	2.5	2.3
P7_O_2_40	49	40	0.2	0.3	0.6	1.6	1.6	1.7
P8_O_2_20	56	20	2.8	4.2	4.9	31.2	7.8	7.7
P8_O_2_30	56	30	0.8	1.3	2.1	10.0	4.3	3.7
P8_O_2_35	56	35	0.2	0.3	0.5	1.4	1.6	1.7
P8_O_2_40	56	40	0.2	0.3	0.5	1.4	1.4	1.7
P9_O_2_20	63	20	2.7	4.1	5.2	30.5	7.4	7.0
P9_O_2_30	63	30	0.6	1.2	1.9	8.3	3.9	3.2
P9_O_2_35	63	35	0.2	0.3	0.5	1.4	1.6	1.7
P9_O_2_40	63	40	0.2	0.3	0.5	1.4	1.4	1.7

Anthocyanins: delphinidin-3-glucoside (Dp-3G), petunidin-3-glucoside (Pt-3G), peonidin-3-glucoside (Pn-3G), malvidin-3-glucoside (Mv-3G), malvidin-3-*O*-acetylglucoside (Mv-3acG), and malvidin-3-*O*-coumaroylglucoside (Mv-3cmG); Time = days; Temperature = ºC; Concentration = mg/L.

By the observation of Tables 5.8a and 5.8b, we can see that *anthocyanins* decreased during the thermal and oxidative process of red Port wines, where oxygen supplements increase the consumption of this class of phenolics. Anthocyanins will be subject of a kinetic approach in the next section 5.4. of this chapter.

The evolution of phenolic and furanic compounds during the thermal and oxidative process of both white and red Port wines will be discussed in terms of compound families.

Furanic compounds: The formation of the Maillard compounds, 5-(hydroxymethyl)furfural and 2-furfural, will be discussed in Chapter 6.

Hydroxycinnamic esters and GRP: Esters of tartaric acid, namely caftaric acid, coutaric acid, and fertaric acid are highly hydrolyzed into their corresponding acids, caffeic, *para*-coumaric and ferulic acids, and this can explain its decreasing during the forced aging processes, in both white and Port wine samples (white wine; Figure 5.26, and Port wine; Figure 5.27). Along with this observation, this hydrolysis seems to depend on both the temperature and oxygen regimes (treatment I and II) although the oxygen regime seems to be a foremost factor in white wines (Figue 5.26 - treatment II). In the same way, GRP have decrease in the thermal and oxidative process, being more hydrolyzed with oxygen regimes (Figure 5.26 - treatment II). Moreover, for acyclic systems the *trans*- isomers are more stable than the *cis*- isomers, and this can explain the higher diminishing value of *cis*-caftaic and *cis*-coutaric acids in the white wines forced aging (Figure 5.26).

Hydroxycinnamic acids: caffeic and *para*-coumaric acids have increased during the forced aging protocols of both white and Port wines (white wine; Figure 5.26, and Port wine; Figure 5.27). These compounds are formed during the hydrolysis of the respective esters, caftaric and coutaric acids. On the contrary, ferulic acid has declined during the forced aging protocols of both white and Port wines (white wine; Figure 5.26, and Port wine; Figure 5.27). This fact could be related with the higher hydrolysis of caftaric and coutaric acids than fertaric acid. Because this ester (fertaric acid) is less hydrolyzed, the

corresponding hydroxycinnamic acid (ferulic acid) could suffer a higher degradation and therefore be more available to undergo oxidative degradation.

Hydroxybenzoic acids: Polyphenols containing a 1,2,3-trihydroxybenzene (gallic acid), or a 1,2-dihydroxybenzene ring (protocatechuic acid) are easiest to oxidize because the resulting phenoxyl semi-quinone radical can be stabilized by a second oxygen atom. Equivalent methoxy substituted phenols (syringic acid) are not as readily oxidized because they do not produce stabilized semi-quinone radicals. In fact, gallic and protocatechuic acids decrease during the white wine degradation process (Figure 5.26). Furthermore, oxygen supplements (Figure 5.26 - treatment II) increase the consumption of these easily oxidizable phenolic compounds in white wine. However, the hydroxybenzoic acids may increase during aging due to anthocyanins cleavage (Ribéreau-Gayon et al., 2006), and this can explain their enlargement during the forced aging process of red Port wine samples (Figure 5.27). The major increase was observed for syringic acid (Figure 5.27). This phenolic compound may be formed by malvidin-3-glucoside cleavage.

Flavan-3-ols: (+)-catechin and (-)-epicatechin decreased during the forced aging protocols of both white and Port wines (white wine; Figure 5.26, and Port wine; Figure 5.27). Furthermore, oxygen supplements increase the consumption of these easily oxidizable phenolic compounds in both white and Port wines (Figure 5.26 and 5.27 - treatment II).

5.4. Kinetic modeling of anthocyanins oxidation in Port wines

Red wines contain higher levels of polyphenols, among which, anthocyanins, procyanidins, and flavan-3-ols are in particularly highest levels (Waterhouse and Laurie, 2006, Kilmartin 2009). Some of the established effects of O_2 additions to red wine include a decrease in phenolic compounds such as (+)-catechin, (-)-epicatechin, quercetin, caffeic acid, and anthocyanins, and an increase in red polymeric pigments improving the wine color density (Castellari et al., 2000). More recently studies, on micro-oxygenation, have reported that monomeric anthocyanins decrease with the increase of oxygen consumption (Cano-López et al., 2006, Pérez-Magariño et al., 2007, Kontoudakis et al., 2011, Gambuti et al., 2013), along with the formation of new pigments derived from the combination of anthocyanins and flavan-3-ols with acetaldehyde, resulting from ethanol oxidation. Acetaldehyde, after capturing a proton, will react with flavan-3-ols to start the process of forming ethyl bridges

yielding methylmethine-linked flavanol adducts (Danilewicz, 2003, Cheynier, 2005, Fulcrand et al., 2006, Oliveira et al., 2011). In the same way, acetaldehyde will mediate the polymerization reaction between anthocyanins and flavan-3-ols yielding methylmethine-linked anthocyanin-flavanol adducts (Timberlake and Bridle, 1976, Rivas-Gonzalo et al., 1995; Lee et al., 2004, Oliveira et al., 2011). These reactions may begin again from the newly formed dimers leading to polymers. Acetaldehyde may also induce the self-condensation of anthocyanins leading to the formation of oligomeric methylmethine-linked anthocyanins (Atanasova et al., 2002, Salas et al., 2005), and also reacts directly with malvidin-3-*O*-glucoside to produce vitisin-B (Bakker and Timberlake, 1997).

The methylmethine-linked flavanol adducts generated with acetaldehyde are not stable and cleave into vinylflavanol oligomers (Francia-Aricha et al., 1997, Francia-Aricha et al., 1998, Es-Safi et al., 1999, Fulcrand et al., 1997, Fulcrand et al., 2006). These vinylflavanols can further react with malvidin-3-*O*-glucoside and carboxypyranomalvidin-3-*O*-glucoside (vitisin-A) to produce pyranoanthocyanins-flavanols (orange color) (Cruz et al., 2008) and vinylpyranoanthocyanin-catechins (portisins, blue color) pigments, respectively (Mateus et al., 2003). Some others aldehydes present is wines such as glyoxylic acid, resulting from the tartaric acid oxidation, and 2-furfural, 5-(hydroxymethyl)furfural (HMF), which are both sugar degradation products formed during the processing and storage of wine, can react with malvidin-3-glucoside leading to the formation of anthocyanin-furanic aldehyde adducts (Sousa et al., 2010). The acetaldehyde-mediated condensation was found to occur more generally than with glyoxylic acid, 2-furfural and 5-(hydroxymethyl)furfural (Es-Safi et al., 2002).

The effect of temperature on the stability of anthocyanins is well known. Simpson (1985) suggested that thermal degradation of anthocyanins could occur via two mechanisms: (i) from the hydrolysis of the 3-glycoside linkage to form the more labile aglycon; and (ii) from the hydrolytic opening of the pyrilium ring to form a substituted chalcone, which then degrades to brown insoluble phenolic compounds. Degradation of anthocyanins, under different temperatures, in model solutions has been reported (Romero and Bakker, 2000, Tseng et al., 2006). It was also found that the discolouration of anthocyanins in ethanolic solutions is faster than in aqueous solution (Tseng et al., 2006), and the increase of pH induce the rate of consumption of these phenolics (Romero and Bakker, 1999). Moreover, the disappearance of the anthocyanins, malvidin-3-glucoside, malvidin-3-*O*-

acetylglucoside, and malvidin-3-*O*-coumaroylglucoside were study in red wines with different contents of SO_2 (Dallas et al., 1995), and in red Port wines (Bakker et al., 1986, Mateus and De Freitas, 2001).

As high quality red Port wines require a period of aging in either bottle or barrels, where temperature and/or oxygen induce modifications on sensory properties of wines, such as the decrease of astringency or the stabilization of color (attributed to anthocyanins and derived pigments), a kinetic study was performed in a thermal and oxidative Port wine forced aging protocol. The knowledge and control of the kinetic parameters can greatly enhance the thermal and oxidative (consumed oxygen) conditions in terms of maximizing the rate of generation and/or formation of flavor and /or color.

The most usual kinetic model reported in literature to describe the kinetic of compound depletion are zero order [$c = c_0 + kt$], first order [$c = c_0 \exp(kt)$] or second order [$1/c = 1/c_0 + kt$] reaction models. Assuming a first order [$c = c_0 \exp(kt)$], the dependence of the rate constant k upon the temperature T is expressed by the Arrhenius equation: $k = k_0 e^{-Ea/RT}$, where k_0 is the pre-exponential factor, E_a is the activation energy and R is the gas constant equal to 8.314 J/mol.K. According to the Arrhenius equation the activation energy for anthocyanins depletion in wine can be calculated by plotting the logarithm of the rate constants at four temperatures against the reciprocal of the absolute temperature: $ln(k) = -Ea/RT + ln(k_0)$.

In order to gather more information concerning the relationship between anthocyanins, storage temperature and oxygen consumption, a kinetic study was performed. These models are very important to know the extent of a specific chemical reaction, the rate at which the changes occur and also to be able to optimize wine processing or storage conditions. In addition, the knowledge and control of the kinetic parameters can greatly enhance the thermal and oxidative processing conditions in terms of maximizing the rate of generation/formation of flavor/color.

Figure 5.28, 5.29 and 5.30 represents the Arrhenius plot for the reaction of anthocyanins depletion for both oxygen treatments, and respectively for delphinidin-3-glucoside (Dp-3G) and petunidin-3-glucoside (Pt-3G); peonidin-3-glucoside (Pn-3G) and malvidin-3-glucoside (Mv-3G); and malvidin-3-*O*-acetylglucoside (Mv-3acG) and malvidin-3-*O*-coumaroylglucoside (Mv-3cmG). The activation energies (*Ea*), the pre-exponential factor (k_0), and the rate constants estimated at a medium reference temperature (k_{Tref}) are reported

in Table 5.9. The temperature dependence of the reaction rate constant was well described by the Arrhenius equation for all the analyzed anthocyanins (Figure 5.28 to 5.30). In fact, a maximum degradation of the anthocyanins was obtained at higher temperatures, and it followed a first-order kinetics, already reported by other authors (Romero and Bakker, 2000, Tseng et al., 2006, Dallas et al., 1995, Mateus and De Freitas, 2001) both with and without oxygen addition. Knowing the kinetic parameters of reaction of anthocyanins degradation in wine, and initial anthocyanins concentration ([anthocyanin]$_0$), the anthocyanin composition of the wine can be predicted at any time (t) and temperature (T) using the equation: [anthocyanin]$_t$ = [anthocyanin]$_0$(1 - $k_0 e^{-Ea/RT} t$), in both the oxygen regimes applied.

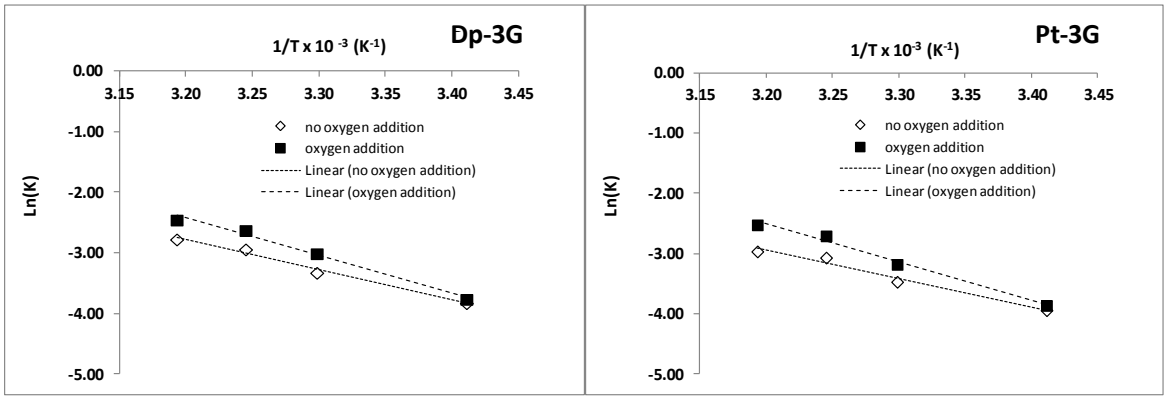

Figure 5.28. Arrhenius plot for delphinidin-3-glucoside (Dp-3G) and petunidin-3-glucoside (Pt-3G) depletion.

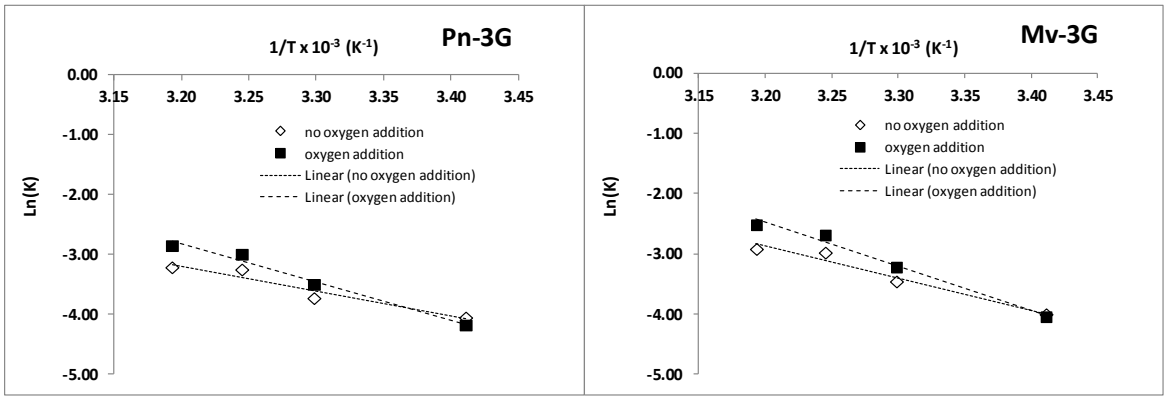

Figure 5.29. Arrhenius plot for peonidin-3-glucoside (Pn-3G) and malvidin-3-glucoside (Mv-3G) depletion.

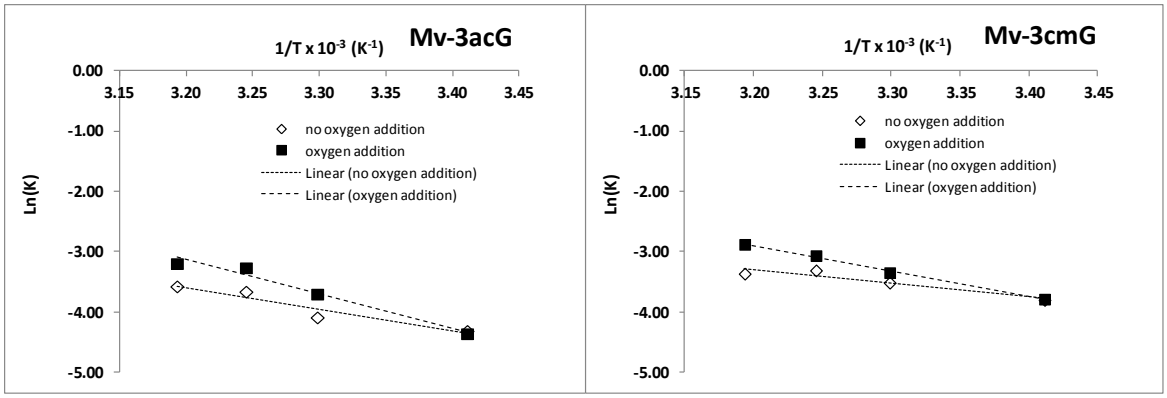

Figure 5.30. Arrhenius plot for malvidin-3-*O*-acetylglucoside (Mv-3acG) and malvidin-3-*O*-coumaroylglucoside (Mv-3cmG) depletion.

Table 5.9. Kinetic parameters of anthocyanins hydrolysis reaction in Port wine.

	no oxygen addition				***oxygen addition***			
Anthocyanin	**Ea (kJ/mol)**	**K_0 (day^{-1})**	**r**	**K_{TRef} (mg/L /day)**	**Ea (kJ/mol)**	**K_0 ($days^{-1}$)**	**r**	**K_{TRef} (mg/L /day)**
Mv-3-O-coumaroylglucoside	18.5±2.3	$4.6\mathbf{x10^{+1}}$	-0.95	*0.031*	35.2±0.8	$4.2\mathbf{x10^{+4}}$	-0.99	*0.039*
Mv-3-O-acetylglucoside	29.9±3.3	$2.8\mathbf{x10^{+3}}$	-0.96	*0.020*	46.9±3.0	$3.0\mathbf{x10^{+6}}$	-0.98	*0.027*
Peonidin 3-glucoside	34.6±3.5	$2.5\mathbf{x10^{+4}}$	-0.96	*0.029*	52.9±2.7	$4.1\mathbf{x10^{+7}}$	-0.99	*0.035*
Petunidin-3-glucoside	39.1±2.2	$1.8\mathbf{x10^{+5}}$	-0.99	*0.035*	52.9±2.2	$5.7\mathbf{x10^{+7}}$	-0.99	*0.047*
Delphinidin-3-glucoside	41.5±1.7	$1.8\mathbf{x10^{+5}}$	-0.99	*0.040*	51.6±2.1	$3.7\mathbf{x10^{+7}}$	-0.99	*0.052*
Malvidin-3-glucoside	44.1±3.2	$1.3\mathrm{x}\mathbf{10^{+6}}$	-0.98	*0.036*	60.7±2.9	$1.2\mathbf{x10^{+9}}$	-0.99	*0.045*

No oxygen addition - treatment I; oxygen addition - treatment II. $\mathbf{T_{Ref}}$ = medium temperature.

Values of activation energies (kJ/mol) for, respectively, Mv-3-*O*-coumaroylglucoside, Mv-3-*O*-acetylglucoside, peonidin-3-glucoside, petunidin-3-glucoside, delphinidin-3-glucoside, and malvidin-3-glucoside, for the two applied oxygen treatments (treatment I and treatment II), were as follows: 18.5 - 35.2; 29.9 - 46.9; 34.6 - 52.9; 39.1 - 52.9; 41.5 - 51.6; 44.1 - 60.7 (Table 5.10), and are within the range of most oxidation reactions (30 kJ/mol) (Formosinho, 1983).

The increasing content of oxygen consumption, from 3.7 to 22.2; 4.0 to 27.7; 5.0 to 31.1; and 5.3 to 39.8 mg/L, for respectively the temperatures storage of 20, 30, 35 and 40ºC, enlarge the consumption rates of the six analyzed anthocyanins in 1.3 folds (Table 5.9). Furthermore, the degradation rate constants follow the order: delphinidin-3-glucoside>petunidin-3-glucoside≃malvidin-3-glucoside>Mv-3-*O*-coumaroylglucoside>

peonidin-3-glucoside>Mv-3-*O*-acetylglucoside. Delphinidin-3-glucoside has the highest degradation rate follow by petunidin-3-glucoside, in both oxygen treatments. These anthocyanins have a 1,2,3-trihydroxybenzene ring (delphinidin-3-glucoside) and a 1,2-dihydroxybenzene ring (petunidin-3-glucoside) that are easiest to oxidize. Conversely, the anthocyanins with lower degradation rates were Mv-3-*O*-coumaroylglucoside, peonidin-3-glucoside, and Mv-3-*O*-acetylglucoside. Studies made on berries have concluded that, under high temperatures, only malvidin derivatives, which are highly methylated anthocyanins (3-*O*-glucoside, 3-*O*-coumaroylglucoside, and 3-*O*-acetylglucoside) have less degradation and can accumulate in berries (Mori et al., 2007). In general, methoxylation, and acylation lead to an increase in the thermal stability of anthocyanins (Jackman and Smith, 1996), and under oxidative conditions methoxy substituted phenols are not as readily oxidized because they do not produce stabilized semi-quinone radicals (Oliveira et al., 2011).

In this study the Mv-3-*O*-coumaroylglucoside disappearance was significantly faster than the corresponding degradation of Mv-3-*O*-acetylglucoside, which agrees with some works performed in model solutions (Romero and Bakker, 1999, Romero and Bakker, 1999) and in wine (McCloskey and Yengoyan, 1981), where the cinnamic acid acylated pigments disappear faster than the acetic acid acylated pigments. Considering the malvidin-3-glucoside, its degradation rate was higher than the corresponding malvidin derivatives, Mv-3-*O*-coumaroylglucoside and Mv-3-*O*-acetylglucoside, which is unlikewise with other works (Bakker et al., 1986, Mateus and De Freitas, 2001).

5.5. Conclusions

The accelerated spoilage, conducted with both temperature and oxygen supplements, promoted a modification of the wines phenolic composition that could be sensed by cyclic voltammetry and HPLC-DAD.

Cyclic voltammetry enabled the grouping of qualitative information concerning wine electroactive phenolic compounds. Cyclic voltammograms of the white wines had two main anodic peak potentials Ep,a (0.45 and 0.85 V), while cyclic voltammograms of the red Port wines had three main peak potentials Ep,a (0.35, 0.55 and 0.75 V).

The two identified white wine anodic peak potentials Ep,a (0.45 and 0.85 V) followed a linear relationship with the total phenolic content, evaluated by the FC index. Moreover, these relationship was greater with the first peak potential Ep,a (0.45 V) indicating a more reactive oxidative phenolic zone, dominated by catechol-containing hydroxycinnamic acids, hydroxycinnamates, catechin and gallic acid. For the red Port wines, the peak potential Ep,a (0.55 V) followed a linear relationship with the total phenolic content, evaluated by the FC index, attributed mainly to malvidin-3-glucoside and to other anthocyanins. Considering the other two identified red Port wine anodic peak potentials Ep,a (0.35 and 0.75 V) these were not correlated with the total phenolic content expressed by FC index. These peak potentials may possibly be influenced by the observed increase of hydroxybenzoic acids from red Port wine anthocyanins cleavage.

Oxygen consumption along the forced aging protocols of both white and red Port wines can be predicted by voltammetric oxidation signals.

Wine phenolics were quantified by HPLC-DAD and LC-MS. In general, temperature and oxygen treatments decrease the wine phenolics content. The only exceptions were for the hydroxycinnamic acids (caffeic and *para*-coumaric acids) which had increased from the hydrolysis of the respective esters (caftaric and coutaric acids) in both wines, and for the hydroxybenzoic acids (gallic and syringic acids) which had increased from anthocyanins cleavage, in the red Port wines.

The most relevant white wine phenolic oxidation markers were *trans*-GRP, *trans*- and *cis*-caftaric acid, and catechin-type flavonoids [(+)-catechin and (-)-epicatechin], which had the highest decreases during the thermal and oxidative white wine process. Considering red Port wine, the most relevant phenolic oxidation markers were anthocyanins and catechin-type flavonoids, which had the highest decreases during the thermal and oxidative red Port wine process. Both temperature and oxygen treatments affected the rate of phenolic degradation. In addition, temperature seems to influence mostly the phenolics kinetic degradation. In this way, the previous identified phenolics could be used as oxidation markers, and their modulation may well be used for the optimization of wine processing and/or storage conditions.

5.6. References

Atanasova, V., Fulcrand, H., Le Guernevé, C., Cheynier, V., & Moutounet, M. (2002). Structure of a new dimeric acetaldehyde malvidin-3-glucoside condensation product. *Tetrahedron Letters, 43,* 6151-6153.

Bakker, J., Preston, N. W., & Timberlake, C. F. (1986). The determination of anthocyanins in aging red wines: comparison of HPLC and spectral methods. *American Journal of Enology and Viticulture, 37,* 121-126.

Bakker, J., & Timberlake, C. F. (1997). Isolation, identification, and characterization of new colour-stable anthocyanins occurring in some red wines. *Journal of Agricultural and Food Chemistry, 45,* 4535-4543.

Cano-López, M., Pardo-Minguez, F., López-Roca, J. M., & Gómez-Plaza, E. (2006). Effect of microoxygenation on anthocyanin and derived pigment content and chromatic characteristics of red wines. *American Journal of Enology and Viticulture, 57,* 325-331.

Castellari, M., Matricardi, L., Arfelli, G., Galassi, S., & Amati, A. (2000). Level of single bioactive phenolic compounds in red wine as a function of the oxygen supplied during storage. *Food Chemistry, 69,* 61-67.

Cejudo Bastante, M. J., Perez Coello, M. S., & Gutiérrez, I. H. (2010). Identification of new derivatives of 2-*S*-glutathionylcaftaric acid in aged white wines by HPLC-DAD-ESI-MS^n. *Journal of Agricultural and Food Chemistry, 58,* 11483-11492.

Cheynier, V. (2005). Polyphenols in foods are more complex than often thought. *American Journal of Clinical Nutrition, 81,* 223-229.

Cruz, L., Teixeira, N., Silva, A. M. S., Mateus, N., Borges, J., & De Freitas, V. (2008). Role of vinylcatechin in the formation of pyranomalvidin-3-glucoside-(+)-catechin. *Journal of Agricultural and Food Chemistry, 56,* 10980-10987.

Dallas C., Ricardo-da-Silva, J. M., & Laureano, O. (1995). Degradation of oligomeric procyanidins and anthocyanins in a Tinta Roriz red wine during maturation. *Vitis, 34*, 51-56.

Danilewicz, J. C. (2003). Review of reaction mechanisms of oxygen and proposed intermediate reduction products in wine: Central role of iron and copper. *American Journal of Enology and Viticulture, 54*, 73-85.

Es-Safi, N. E., Fulcrand, H., Cheynier, V., & Moutounet, M. (1999). Competition between (+)-catechin and (-)-epicatechin in acetaldehyde-induced polymerization of flavanols. *Journal of Agricultural and Food Chemistry, 47*, 2088-2095.

Es-Safi, N. E., Cheynier, V., & Moutounet, M. (2002). Role of aldehydic derivatives in the condensation of phenolic compounds with emphasis on the sensorial properties of fruit-derived foods. *Journal of Agricultural and Food Chemistry, 50*, 5571-5585.

Formosinho, S. J. (1983). Fundamentos de Cinética Química. Fundação Calouste Gulbenkian, Lisboa, Portugal, 256.

Francia-Aricha, E. M., Guerra, M. T., Rivasgonzalo, J. C., & Santosbuelga, C. (1997). New anthocyanin pigments formed after condensation with flavanols. *Journal of Agricultural and Food Chemistry, 45*, 2262-2266.

Francia-Aricha, E. M., Rivas-Gonzalo, J. C., & Santos-Buelga, C. (1998). Effect of malvidin-3-monoglucoside on the browning of monomeric and dimeric flavanols. *Zeitschrift Fur Lebensmittel-Untersuchung Und-Forschung a-Food Research and Technology*, 207, 223-228.

Fulcrand, H., Cheynier, V., Oszmianski, J., & Moutounet, M. (1997). An oxidized tartaric acid residue as a new bridge potentially competing with acetaldehyde in flavan-3-ol condensation. *Phytochemistry, 46*, 223-227.

Fulcrand, H., Dueñas, M., Salas, E., & Cheynier, V. (2006). Phenolic reactions during winemaking and aging. *American Journal of Enology and Viticulture, 57,* 289-297.

Gambuti, A., Rinaldi, A., Ugliano, M., & Moio, L. (2013). Evolution of phenolic compounds and astringency during aging of red wine: effect of oxygen exposure before and after bottling. *Journal of Agricultural and Food Chemistry, 61,* 1618-1627.

Guerrero, R. F., Liazid, A., Palma, M., Puertas, B., González-Barrio, R., Gil-Izquierdo, A., García-Barroso, C., & Cantos-Villar, E. (2009). Phenolic characterisation of red grapes autochthonous to Andalusia. *Food Chemistry, 112,* 949-955.

Gutiérrez, I. H., Lorenzo, E. S-P., & Espinosa, A. V. (2005). Phenolic composition and magnitude of copigmentation in young and shortly aged red wines made from the cultivars, Cabernet Sauvignon, Cencibel, and Syrah. *Food Chemistry, 92,* 269-283.

Jackman, R. L., & Smith, J. L. (1996). Anthocyanins and betalains. In: Hendry GAF, Houghton JD, eds. Natural food colourants, 2nd edn. London: Chapman & Hall, 244-309.

Kallithraka, S., Salacha, M. I., & Tzourou, I. (2009). Changes in phenolic composition and antioxidant activity of white wine during bottle storage: Accelerated browning test versus bottle storage. *Food Chemistry, 113,* 500-505.

Kilmartin, P. A., Zou, H., & Waterhouse, A. L. (2001). A cyclic voltammetry method suitable for characterizing antioxidant properties of wine and wine phenolics. *Journal of Agricultural and Food Chemistry, 49,* 1957-1965.

Kilmartin, P. A. (2009). The oxidation of red and white wines and its impact on wine aroma. *Chemistry in New Zealand, 73,* 18-22.

Kontoudakis, N., González, E., Gil, M., Esteruelas, M., Fort, F., Canals, J. M., & Zamora, F. (2011). Influence of wine pH on changes in colour and polyphenol composition

induced by micro-oxygenation. *Journal of Agricultural and Food Chemistry, 59,* 1974-1984.

Lee, D. F., Swinny, E. E., & Jones, G. P. (2004). NMR identification of ethyl-linked anthocyanin-flavanol pigments formed in model wine ferments. *Tetrahedron Letters, 45,* 1671-1674.

Makhotkina, O., & Kilmartin, P. A. (2009). Uncovering the influence of antioxidants on polyphenol oxidation in wines using an electrochemical method: Cyclic voltammetry. *Journal of Electroanalytical Chemistry, 633,* 165-174.

Makhotkina, O., & Kilmartin, P. A. (2012). The phenolic composition of Sauvignon blanc juice profiled by cyclic voltammetry. *Electrochimica Acta 83,* 188-19.

Martins, R. C., Oliveira, R., Bento, F., Geraldo, D., Lopes, V. V., Guedes de Pinho, P., Oliveira, C. M., & Silva Ferreira, A. C. (2008). Oxidation management of white wines using cyclic voltammetry and multivariate process monitoring. *Journal of Agricultural and Food Chemistry, 56,* 12092-12098.

Mateus, N., & De Freitas, V. (2001). Evolution and stability of anthocyanin-derived pigments during Port wine aging. *Journal of Agricultural and Food Chemistry, 49,* 5217-5222.

Mateus, N., Silva, A. M. S., Rivas-Gonzalo, J. C., Santos-Buelga, C., & De Freitas, V. (2003). A new class of blue anthocyanin-derived pigments isolated from red wines. *Journal of Agricultural and Food Chemistry, 51,* 1919-1923.

McCloskey, L. P., & Yengoyan, L. S. (1981). Analysis of anthocyanins in Vitis vinifera wines and red colour versus aging by HPLC and spectrophotometry. *American Journal of Enology and Viticulture, 32,* 257-261.

Mori, K., Goto-Yamamoto, N., Kitayama, M., & Hashizume, K. (2007). Loss of anthocyanins in red-wine grape under high temperature. *Journal of Experimental Botany, 58*, 1935-1945.

Oliveira, C. M., Silva Ferreira, A. C., De Freitas, V., & Silva, A. M. S. (2011). Oxidation mechanisms occurring in wines. *Food Research International, 44*, 1115-1126.

Pérez-Magariño, S., Sánchez-Iglesias, M., Ortega-Heras, M., González-Huerta, C., & González-Sanjosé, M. L. (2007). Colour stabilization of red wines by microoxygenation treatment before malolactic fermentation. *Food Chemistry, 101*, 881-893.

Recamales, A. F., Sayago, A., González-Miret, M. L., & Hernanz, D. (2006). The effect of time and storage conditions on the phenolic composition and colour of white wine. *Food Research International, 39*, 220-229.

Ribéreau-Gayon, P., Glories, Y., Maujean, A., & Dubourdieu, D. (2006). Handbook of Enology. Volume 2: The Chemistry of Wine: Stabilization and Treatments. John Wiley & Sons Ltd.

Rivas-Gonzalo, J. C., Bravo-Haro, S., & Santos-Buelga, C. (1995). Detection of compounds formed through the reaction of malvidin 3-monoglucoside and catechin in the presence of acetaldehyde. *Journal of Agricultural and Food Chemistry, 43*, 1444-1449.

Rodrigues, A., Silva Ferreira, A. C., Guedes de Pinho, P., Bento, F., & Geraldo, D. (2007). Resistance to oxidation of white wines assessed by voltammetric means. *Journal of Agricultural and Food Chemistry, 55*, 10557-10562.

Roginsky, V., De Beer, D., Harbertson, J. F., Kilmartin, P. A., Barsukova, T., & Adams, D.O. (2006). The antioxidant activity of Californian red wines does not correlate with wine age. *Journal of the Science of Food and Agriculture, 86*, 834-840.

Romero, C., & Bakker, J. (1999). Interactions between grape anthocyanins and pyruvic acid with effect of pH and acid concentration on anthocyanin composition and colour in model solutions. *Journal of Agricultural and Food Chemistry, 47,* 3130-3139.

Romero, C., & Bakker, J. (2000). Effect of storage temperature and pyruvate on kinetics of anthocyanin degradation, vitisin A derivative formation, and colour characteristics of model solutions. *Journal of Agricultural and Food Chemistry, 48,* 2135-2141.

Salacha, M. I., Kallithraka, S., & Tzourou, I. (2008). Browning of white wines: Correlation with antioxidant characteristics, total polyphenolic composition and flavanol content. *International Journal of Food Science and Technology, 43,* 1073-1077.

Salas, E., Duenas, M., Schwarz, M., Winterhalter, P., Cheynier, W., & Fulcrand, H. (2005). Characterization of pigments from different high speed countercurrent chromatography wine fractions. *Journal of Agricultural and Food Chemistry, 53,* 4536-4546.

Simpson, K. L. (1985). Chemical changes in food during processing. In Chemical Changes in Natural Food Pigments (T. Richardson & J. W. Finley, eds.), 409-441, Van Nostrand Reinhold, New York, NY.

Singleton, V. L., Trousdale, E., & Zaya, J. (1979). Oxidation of wines I. Young white wines periodically exposed to air. *American Journal of Enology and Viticultur*e, *30,* 49-54.

Sousa, A., Mateus, N., Silva, A. M. S., Vivas, N., Nonier, M. F., Pianet, I., & De Freitas, V. (2010). Isolation and structural characterization of anthocyanin-furfuryl pigments. *Journal of the Science of Food and Agriculture, 58,* 5664-5669.

Timberlake, C. F., & Bridle, P. (1976). Interactions between anthocyanins, phenolic compounds, and acetaldehyde and their significance in red wines. *American Journal of Enology and Viticulture, 27,* 97-105.

Mozetič, B., Tomažič, I., Škvarč, A., & Trebše, P. (2006). Determination of polyphenols in white grape berries cv. Rebula. *Acta Chimica Slovenica, 53,* 58-64.

Tseng, Kuo-Chan, Chang, Hung-Min, & Wu, James Swi-Bea. (2006). Degradation kinetics of anthocyanin in ethanolic solutions. *Journal of Food Processing and Preservation, 30,* 503-514.

Waterhouse, A. L., & Laurie V. F. (2006). Oxidation of wine phenolics: A critical evaluation and hypotheses. *American Journal of Enology and Viticulture, 57,* 306-313.

6. Chapter 6 - Role of Maillard degradation in wine

6.1. Introduction to wine Maillard degradation

Although the Maillard reaction has been found in beer and other foods, there is little evidence for its occurrence in wine. However, because wine contains the necessary Maillard reaction substrates such as amino acids, proteins, and reducing sugars, the possibility of its occurrence should be more fully studied. Recent studies indicate a number of volatile compounds chemically linked with Maillard-like reactions between carbonyl compounds and amino acids in wine model systems (Kroh, 1994, Pripis-Nicolau et al., 2000, Marchand et al., 2002, De Revel et al., 2004, Marchand et al., 2011). Moreover, the production of Amadori compounds in wines has already been described by Hashiba in 1978, and more recently several Maillard-like compounds have been identified in a typical aroma or aging aromas of champagne wines (Keim et al., 2002, Tominaga et al., 2003) or sweet and fortified wines (Cutzach et al., 1999, Keim et al., 2002, Câmara et al., 2006, Silva Ferreira et al., 2007, Oliveira e Silva et al., 2008, Martins et al., 2013).

6.2. Quantification of key intermediaries' of Maillard reaction

Figure 6.1 represents a compressive scheme of degradation of the Amadori product from a sugar (aldose) and an amino acid, and Figure 6.2 illustrate representative structures of Maillard compounds from deoxyosones (i: from 1,2-enolization.; ii and iii: from 2,3-enolization), and iv: other pathways.

Two possible degradation pathways of the Amadori product (ARP) are the enolization pathway and the retro-aldolization pathway (Figure 6.1). Through enolization, the aminoenol intermediates (A; 1,2-eneaminol and B; 2,3-eneaminol) can lead to either 3-deoxyosone (3-deoxyglucosone; 3DG) from 1,2-eneaminol, and 1-deoxyosone (1-deoxyglucosone; 1DG) or 4-deoxyosone (4-deoxyglucosone; 4DG) from 2,3-eneaminol (Figure 6.1). At lower pH, 1,2-enolization is believed to be favored and therefore a higher yield of 3DG is expected. On the other hand as the pH increases to neutral/alkaline values, 2,3-enolization is believed to be favored and therefore 1DG and 4DG should be present in higher amounts (Figure 6.1). Then, cyclization/condensation of 3- and 1-deoxyosones

occurred to form, respectively, HMF [5-(hydroxymethyl)furfural] or 2-furfural, as a 1,2-enolization indicator (Figure 6.1; Figure 6.2 i), and the furanones HHMFone [4-hydroxy-2-(hydroxymethyl)-5-methylfuran-3(*2H*)-one] or norfuraneol [4-hydroxy-5-methylfuran-3(*2H*)-one], as a 2,3-enolization indicator (Figure 6.1; Figure 6.2 ii). The formation of 3- and 1-deoxyosones is accompanied by amino acid release, while 4-deoxyosone has the amino acid incorporated in its structure. The formation of 2-osulones by transition-metal catalyzed oxidation from 1,2-enaminol is also proposed (Figure 6.1) (Davidek et al., 2002). Other compounds are already recognized to be related with the degradation of the 3-deoxyosone such as 5-methylfurfural (Figure 6.2 i), and from 1-deoxyosone such as: 4-hydroxy-2,5-dimethylfuran-3*(2H)*-one (furaneol; DMHF), 2,4-dihydroxy-2,5-dimethylfuran-3*(2H)*-one (acetylformoin), 3-hydroxy-2-methyl-*4H*-pyran-4-one (maltol), 3,5-dihydroxy-2-methyl-*4H*-pyran-4-one (5-hydroxymaltol; DMP), 2,3-dihydro-3,5-dihydroxy-6-methyl-*4H*-pyran-4-one (DDMP), 1-(3-hydroxyfuran-2-yl)ethanone (isomaltol), 3-(2-hydroxypropanoyloxy)propanoic acid, and 2-acetylfuran (Figure 6.2 ii) (Food Chemistry, 2009). The degradation of 4-deoxyosone can forms 2-(2-hydroxyacetyl)furan (Figure 6.2 iii). Other structures, like ethyl 2-furoate, furfuryl alcohol, sotolon, pantalactone also related with Maillard reaction, are in addition represented (Figure 6.1 and Figure 6.2 iv). These compounds will be tentatively identified in section 6.3.

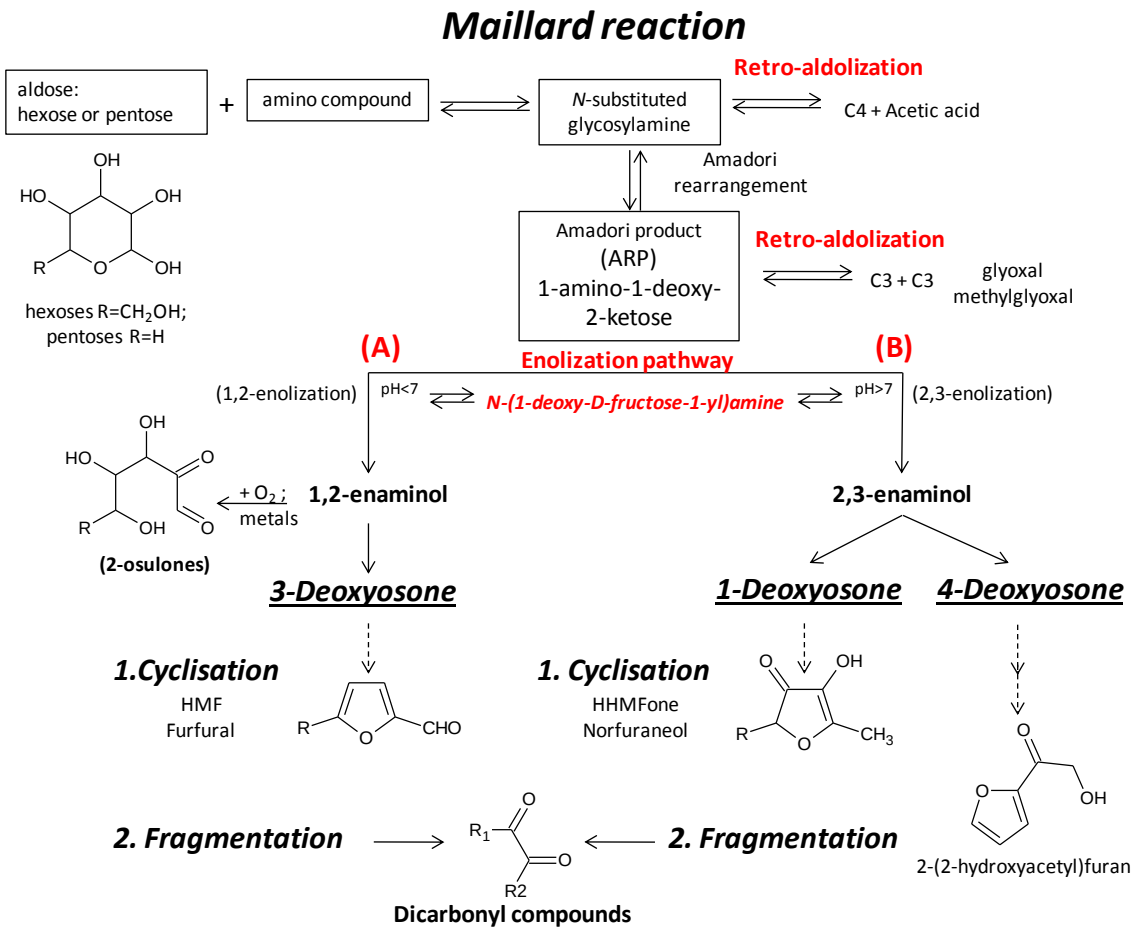

Figure 6.1. A compressive scheme of degradation of the Amadori product from a sugar (aldose) and an amino compound.

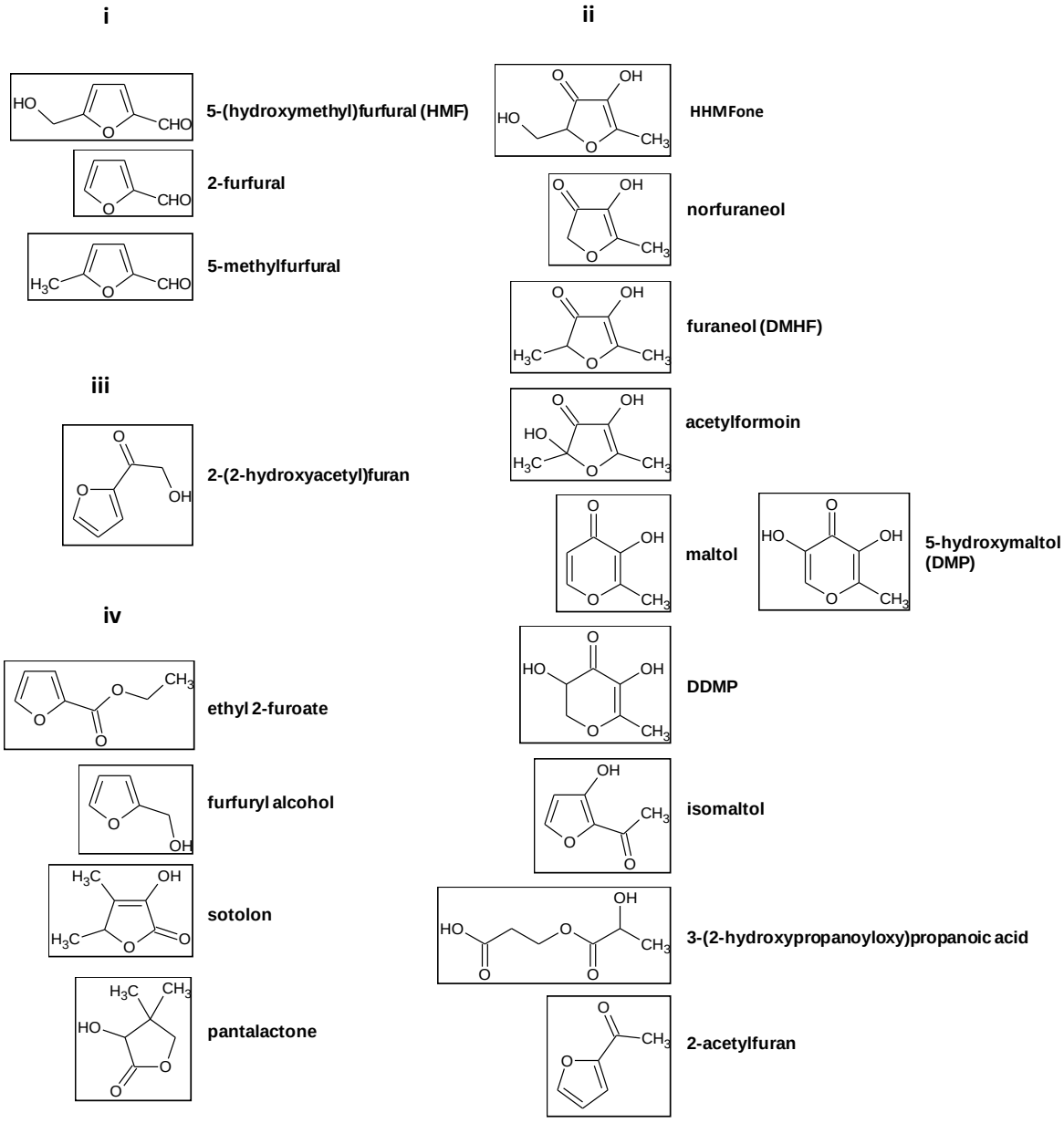

Figure 6.2. Representative structures of Maillard compounds from deoxyosones (i: from 1,2-enolization.; ii and iii: from 2,3-enolization), and iv: other pathways.

6.2.1. Quantification of sugars in white and red Port wines

Sugars are key intermediaries' of Maillard reaction. HPLC-RI was performed (Chapter 3; 3.7.) in the initial white and red Port wines (Chapter 3; 3.2.) in order to quantify reducing sugars. The sugar content of respectively white and red Port wines is represented in Table 6.1. As Port wine fermentations are relatively short, about two days, and are intentionally

interrupted by the addition of natural grape spirit to the fermenting juice, higher levels of sugars are found in the red Port wine (38.1 g/L and 67.2 g/L, respectively for glucose and fructose), in contrast to the white wine (1.6 g/L, for both glucose and fructose). In this way, the red Port wine is readily available for Maillard reactions. However, the white wine has residual reducing sugars that also may participate in these reactions.

Table 6.1. Sugar content of the analysed wines.

Sugar content (g/L)	Glucose	Fructose
White wine (N=2)	1.6 ± 0.1	1.4 ± 0.1
Red Port wine (N=2)	38.1 ± 0.2	67.2 ± 0.2

6.2.2. Quantification of amino acids in white and red Port wines

In musts and wines, the amino acids represent the most important form of total nitrogen. Furthermore, amino acids have higher reactivity with respect to carbonyl compounds (sugars and α-dicarbonyl compounds) according to the Maillard reaction. During Maillard reaction, α-dicarbonyl compounds can be formed through the rearrangement and retro-aldolization of the Amadori product (Figure 6.1), as well as the fragmentation of deoxyosones (Figure 6.1). In the same way, α-dicarbonyl compounds can be encountered in wines in redox equilibrium with the respective reduced forms, α-hydroxy ketones (α-hydroxycarbonyl compounds) and α-diols, after alcoholic and malolactic fermentations. Nucleophilic addition of amino acids to the carbonyl function of α-dicarbonyl and α-hydroxycarbonyl compounds may occur during wine bottling or wine storage.

The depletion of amino acids through the forced aging protocols of white and red Port wines depends on the consumption of amino acids attributed mainly to sugars (Figure 6.1), α-dicarbonyl and α-hydroxycarbonyl compounds (Chapter 2; Figure 2.13), and on their release during the process of cyclization/condensation of the deoxyosones (Chapter 2; Figure 2.10).

HPLC - fluorescence was performed (Chapter 3; 3.8.) in the forced aging protocols of white and red Port wines (Chapter 3; 3.2.). For the white wine aging protocol, samples were taken on the first day, and weekly (P0; and P1, 7^{th} day sampling, to P6, 42^{th} day sampling) (P0 + 6 weeks*2 oxygen regimes*4 temperatures*2 replicates); total of ***98***

samples. For the red Port wine aging protocol, samples were taken on the first day, the 14th day sampling (P2); the 28th day sampling (P4); and the 63th day sampling (P9) (P0 + 3 sampling points*2 oxygen regimes*4 temperatures*2 replicates); total of ***50 samples***. Figure 6.3 represents the initial concentrations of amino acids in the untreated wines (P0). Figures 6.4 and 6.5 represents the observed amino acids that have deplete during the forced aging protocols in both white and red Port wines. By the observation of Figure 6.3, it is possible to see that the initial white wine has about 4 times higher amino acids content than the red Port wine.

For white wine, amino acid levels founded in the untreated wine (P0, control) ranged from 2.4 mg/L (cysteine) to 165.0 mg/L (arginine), to a final concentration of 435.1 mg/L (Figure 6.3). Among the fifteen amino acids analysed, variations higher than the method error, were only observed for glutamic acid, cysteine, asparagine, arginine, alanine, methionine, and phenylalanine, in samples stored at 20, 30, 40 and 50ºC (Figure 6.4). For red Port wine, amino acid levels founded in the untreated wine (P0, control) ranged from 0.9 mg/L (methionine) to 24.1 mg/L (glutamic acid), to a final concentration of 99.6 mg/L (Figure 6.3). Among the fifteen amino acids analysed, variations higher than the method error, were only observed for glutamic acid, cysteine, asparagine, glutamine, methionine, and phenylalanine, in samples stored at 20, 30, 35 and 40ºC (Figure 6.5). These results indicate that amino acids do not have equal reactivity in the same matrix, and the reaction rates, involved on the different mechanism responsible for their degradation, namely Maillard degradation and others, seem to be dependent on the amino acid nature. Figure 6.6 and Figure 6.7 represents the evolution of glutamic acid (Glu) for oxygen treatments I and II, for respectively, white and red Port wines.

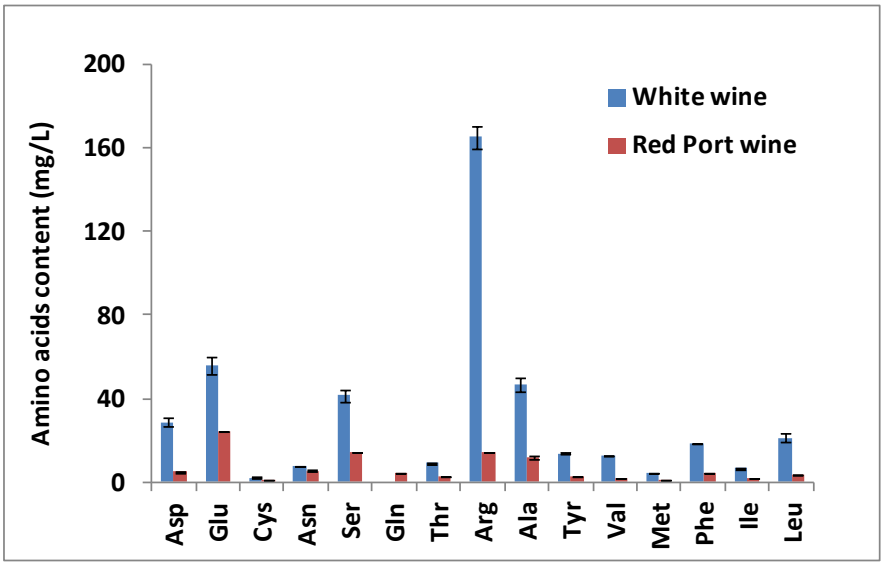

Figure 6.3. Amino acids content of both white and red Port untreated wines (P0).

Aspartic acid (Asp); glutamic acid (Glu); cystein (Cys); asparagine (Asn); serine (Ser); glutamine (Gln); threonine (Thr); arginine (Arg); alanine (Ala); tyrosine (Tyr); valine (Val); methionine (Met); phenylalanine (Phe); isoleucine (Ile); leucine (Leu); (N = 2). Data in appendix of this thesis.

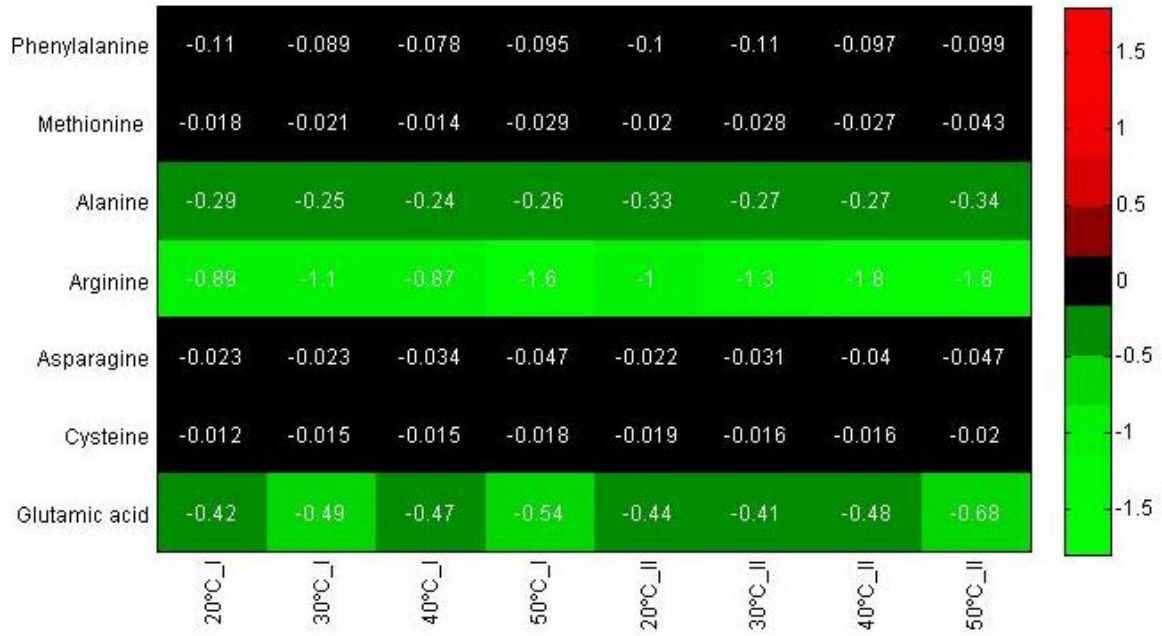

Figure 6.4. Amino acids depletion during the forced aging protocols in white wines (mg/L/day). I - no oxygen addition; II - oxygen addition. Data in appendix of this thesis.

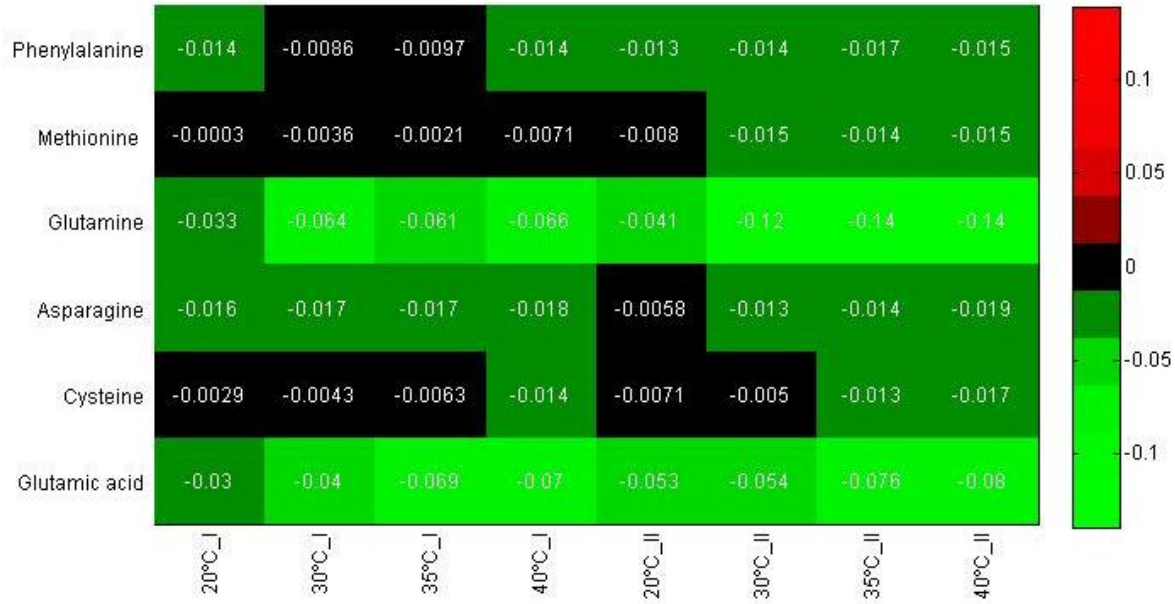

Figure 6.5. Amino acids depletion during the forced aging protocols in red Port wines (mg/L/day). I - no oxygen addition; II - oxygen addition. Data in appendix of this thesis.

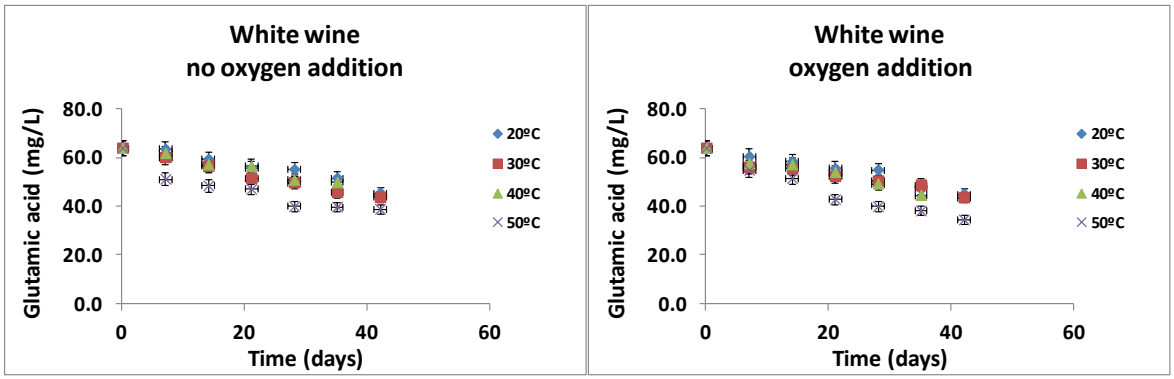

Figure 6.6. Evolution of glutamic acid, during the white wine forced aging protocol, under respectively no oxygen addition (treatment I) and oxygen addition (treatment II).

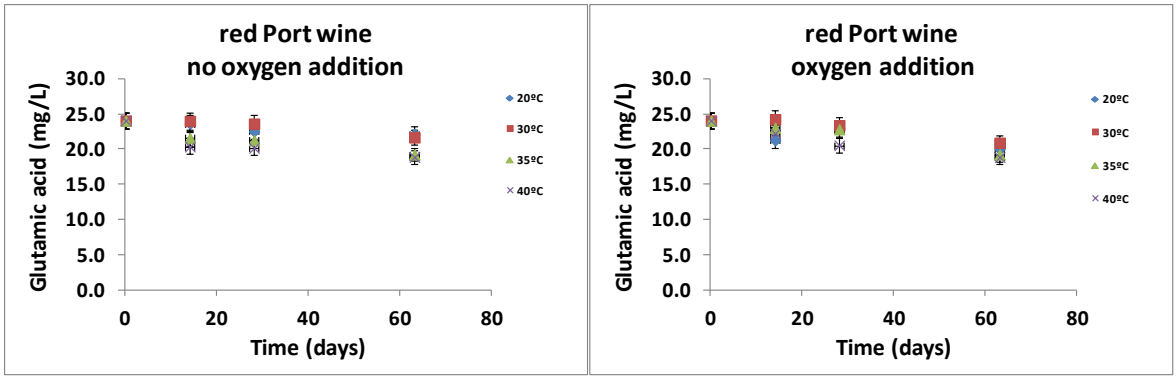

Figure 6.7. Evolution of glutamic acid, during the red Port wine forced aging protocol, under respectively no oxygen addition (treatment I) and oxygen addition (treatment II).

Figure 6.8 represents the proposed mechanism for glutamic acid degradation in wine. The direct cyclization into ethyl 5-oxopyrrolidine-2-carboxylate, or into ethyl 5-oxotetrahydrofuran-2-carboxylate (or diethyl 2-hydroxyglutarate) via 2-ketoglutaric acid is proposed. The 2-ketoglutaric acid can be formed from sugar catabolism or from the respective amino acid, by the Ehrlich pathway (Radler 1993). In fact, glutamic acid has suffered a faster degradation in both white and Port wines (Figure 6.4 and Figure 6.5). A good correlation coefficient was observed between glutamic acid and ethyl 5-oxopyrrolidine-2-carboxylate (Figure 6.8) (-0.743; white wine vs -0.748; red Port wine), and with ethyl 5-oxotetrahydrofuran-2-carboxylate (Figure 6.8) (-0.677; white wine vs -0.754; red Port wine). Also, glutamic acid depletion reactions seem to slightly increase by oxygen exposure (Figure 6.4 and Figure 6.5; II). This fact could be related with the possible formation of α-dicarbonyl compounds (Figure 6.8) from oxidation reactions along with the formation of these compounds from sugar catabolism. In addition, the higher concentration of this amino acid in white wine could justify its faster degradation in the white wines (Figure 6.4) in comparison to the red Port wines (Figure 6.5).

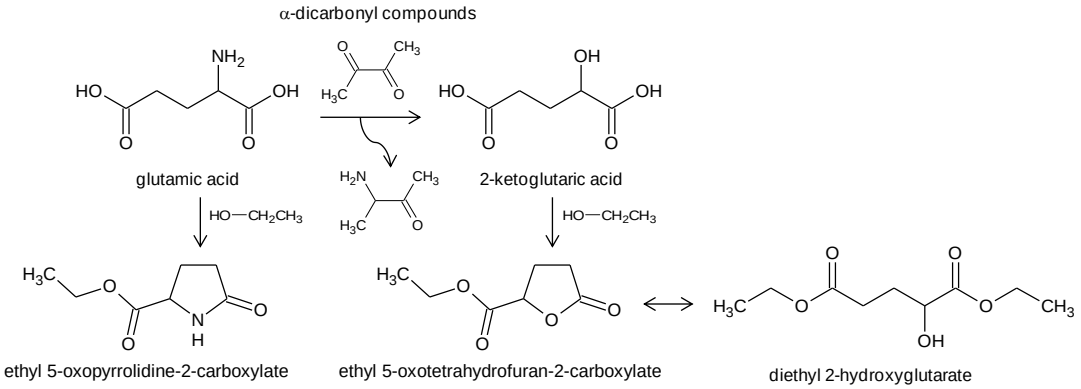

Figure 6.8. Proposed mechanism for degradation of glutamic acid in wines. Adapted from Ferreia, 1997.

Cysteine has suffered degradation in both white and red Port wines. In fact this amino acid can participate in Maillard reactions. In model wine systems, at pH 3.5 and temperature storage of 25ºC, the presence of cysteine with α-dicarbonyl compounds form many products with a heterocycle production such as pyrazines and methylpyrazines, methylthiazoles, acetylthiazoles, acetylthiazolines, acetylthiazolidines, trimethyloxazole, and dimethylethyloxazoles (Pripis-Nicolau et al., 2000, Marchand et al., 2002, Marchand et al., 2011). These various compounds present odors of sulfur, corn-like, pungent, nut, popcorn, roasted hazelnut, toasted, roasted, and ripe fruits. Cysteine depletion seems to slightly increase by oxygen exposure (Figure 6.4 and Figure 6.5; II). This could be related with the possible formation of α-dicarbonyl compounds from oxidation reactions, which will react with the amino acid.

Asparagine has suffered degradation in both white (Figure 6.4) and red Port (Figure 6.5) wines. This depletion could be related with the formation of acrylamide, a toxic volatile compound that is formed during the heating of food. Model experiments have shown that it is produced in reactions of asparagine with reductive carbohydrates or from the resulting cleavage products α-dicarbonyl compounds (butane-2,3-dione or methylglyoxal). However, the formation of acrylamide is promoted by temperatures >100ºC and/or longer reaction times. Cysteine and methionine also form acrylamide in the presence of glucose, but the yields are considerably lower than those from asparagine (Food Chemistry, 2008).

Arginine and alanine have suffered degradation only in the white wines (Figure 6.4). In fact, arginine and alanine are the two of the highest amino acid found in the white wines

(165.0 and 47.0 mg/L, Figure 6.3). Previous studies, indicates a number of volatile compounds chemically linked with Maillard-like reactions between sugars such as glucose and amino acids such as arginine and alanine (Kroh, 1994). These two amino acids have higher depletion reactions when were subject to treatment II, with oxygen addition (Figure 6.4). Once more, the possible formation of α-dicarbonyl compounds from oxidation reactions could be the explanation for these amino acids reduction. Methionine has suffered degradation in both wines (Figure 6.4 and Figure 6.5). Methionine is an essential amino acid and in many biochemical processes its main role is as a methyl-donor. It is very sensitive to oxygen and heat treatment. Thus, losses occur in many food processing operations such as heating or treatment with oxidizing agents. Methionine is readily oxidized to the sulfoxide and then to the sulfone (Figure 6.9). By the observation of Figures 6.4 and 6.5 we can establish a direct relation between oxygen addition and methionine reduction, which explain the much faster depletion of this amino acid in treatment II. In addition, the higher concentration of this amino acid in white wine (Figure 6.3) could justify its faster degradation in the white wines (Figure 6.4) in contrast to the red Port wines (Figure 6.5).

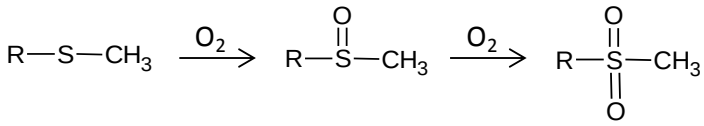

Figure 6.9. Methionine oxidation to the sulfoxide and then to the sulfone.

Phenylalanine has suffered degradation in both wines, although much higher in the white wines. This amino acid has higher depletion reactions when was subject to treatment II, with oxygen addition (Figure 6.4 and Figure 6.5). Furthermore, it was already observed that in white wines stored at high temperatures and supplemented with high levels of dissolved oxygen, wines suffered a rapid and pronounced oxidative spoilage aroma which was related with the presence of phenylacetaldehyde, with "honey-like" odour notes (Silva Ferreira et al., 2002). Phenylacetaldehyde can be formed via Strecker degradation of the respective amino acid.

Glutamine has suffered a degradation in Port wines, much faster when was subject to treatment II, with oxygen addition (Figure 6.5). Glutamine is one of the most abundant free amino acid found in unprocessed food. A study of the contribution of free glutamine to

nonenzymatic browning and fluorescence was investigated, using a heated aqueous model system with methylglyoxal, which shows a rapid and complete depletion of this amino acid (Niquet and Tessier, 2007).

6.2.3. Quantification of 3-deoxyosone (3DG)

6.2.3.1.Quantification of 3-deoxyosone (3DG) in white and red Port wines

In 1990, Huber and Ledl isolated and characterised 1-deoxyglucosone and 3-deoxyglucosone from heated Amadori products. More recently, in agreement with the previous reports, Tressl and others (1995) using ^{13}C-labeled sugars have given a new perspective to the reaction mechanism. It involves different reaction pathways, in which the key intermediates are the 1-, 3- and 4-deoxyosones (Chapter 2; Figure 2.9). The main difference was that 3-deoxyosone was reported to be the most important intermediate in color formation, formed through an intermediate prior to the ARP.

At lower pH, 1,2-enolization is believed to be privileged and, therefore, 3-deoxyosone (3DG) formation is expected in wine. Nevertheless, this intermediate has never been quantified in wines. Quantification of 3-deoxyosone (3DG) was performed (Chapter 3; 3.6.2) in the forced aging protocols of white and red Port wines (Chapter 3; 3.2.). For the white wine aging protocol, samples were taken on the first day, and weekly (P0; and P1, 7th day sampling, to P6, 42th day sampling) (P0 + 6 weeks*2 oxygen regimes*1 temperature = 40ºC*2 replicates); total of ***26 samples***. For the red Port wine aging protocol, samples were taken on the first day, the 14th day sampling (P2); the 28th day sampling (P4); the 42th day sampling (P6); the 56th day sampling (P8); and the 63th day sampling (P9) (P0 + 5 sampling points*2 oxygen regimes*1 temperature = 40ºC*2 replicates); total of ***22 samples***.

Figure 6.10 represents the evolution of 3-deoxyosone (3DG) for oxygen treatments I and II, at 40 ºC, for respectively, white and red Port wines forced aging protocols. By the observation of Figure 6.10, it is possible to see that both initial white and Port wines have similar 3DG concentration (20.0 mg/L for the white wine and 22.7 mg/L for the red Port wine). Nevertheless, the evolution of 3DG does not follow the same trend in the different wines. For the white wine, 3DG have decreased during the forced aging protocol, to a final

concentration of 16.3 and 15.8 mg/L, for respectively treatment I and II, while for the red Port wine this compound have increased to a final concentration of 33.1 and 29.9 mg/L, for respectively treatment I and II (Figure 6.10). Furthermore, these tendencies have not been significantly affected by oxygen consumption (Figure 6.10). These results indicates that, even in wines with lower concentration of sugar like the analysed dry white wine with residual reducing sugars (1.6 g/L, for both glucose and fructose), the Maillard reaction occurs, and the formation of 3DG, in both white and red Port wines, is not affected by oxygen consumption (Figure 6.10).

Figure 6.11 represents a hypothetic scheme of 3DG formation and depletion in wine. 3-Deoxyosone formation is dependent on the concentration of sugars and amino compounds. Conversely, its depletion is dependent on the rate of its cyclization/condensation or fragmentation to form either 2-furfural and HMF or cleaved fragments (Figure 6.1 and Figure 6.11), and on the possible combination with nucleophilic compounds due to its high electrophilic character, including amino compounds (Ghiron et al., 1988). Furthermore, 2-furfural and HMF can then react with other compounds like anthocyanidins or flavan-3-ols (Figure 6.11). For this reason, and to understand the different evolution of 3DG in the analysed white and red Port wines, we can hypothesize that the 3DG accumulation in red Port wine is due to its higher sugar concentration and also to a lower nucleophilic compounds available in this wine, which could be related with the lower amino acids content, 99.6 mg/L in contrast with the 435.1 mg/L in the white wine. In Strecker degradation, phenylalanine reacts with α-dicarbonyl compounds, preferentially leading to phenylacetic acids generation (Hofmann and Scheberle, 2000), while reacting with 3DG favors the formation of phenylacetaldehyde (Hofmann et al., 2000).

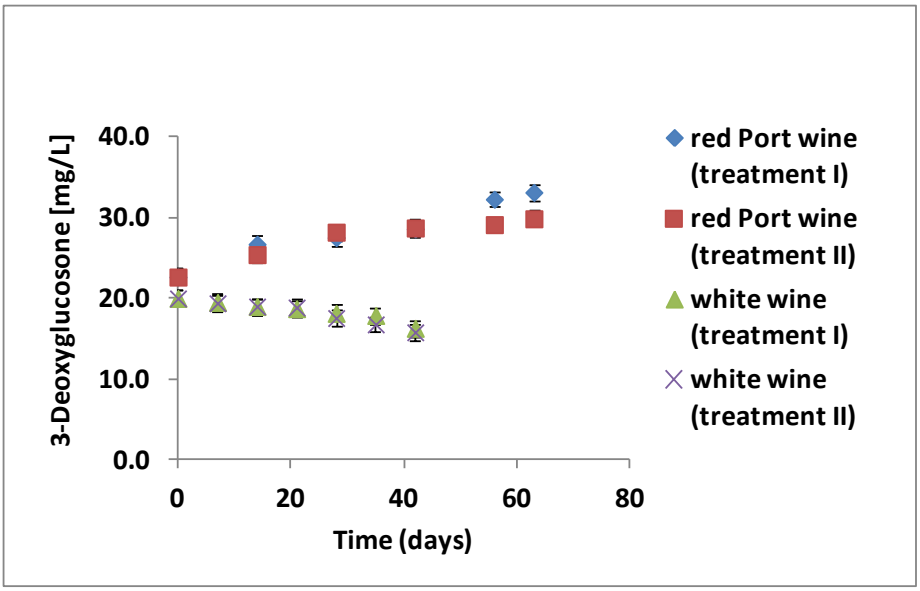

Figure 6.10. Evolution of 3-deoxyosone (3DG) for oxygen treatments I and II, at 40ºC, for respectively, white and red Port wines forced aging protocols; (N = 2).

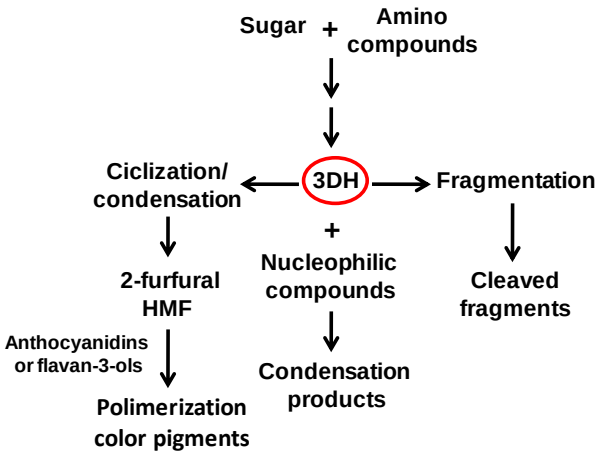

Figure 6.11. Compressive scheme of 3DG formation and depletion in wine.

White and red Port wines with different vintages (between 3 and 18 years old for white wines; and between 2 and 78 years old for red Port wines) have also been analysed to verify the evolution of 3DG in wines with natural aging. White wines were made according to the producers and came from several Portuguese wine regions; Port wines were made according to standard traditional Port winemaking procedures, aged in "pipas" (550 L spent-oak barrels) and came from Douro Portuguese wine region. Tables 6.2 and 6.3 represent the 3DG concentration of respectively white and red Port wines with different vintages.

In fact, by the observation of Tables 6.2 and 6.3, it is possible to verify that white and red Port wines with different vintages follow the same trend that of the forced aging wines. For the white wines, 3DG have a negative correlation coefficient with vintage (r = -0.939), and for red Port wines, 3DG have a positive correlation coefficient with vintage (r = 0.782).

Table 6.2. 3DG quantification in white wines from different vintages (between 3 and 18 years old); N= 2.

White wines	
Vintage	3DG (mg/L)
2010	29.9 ± 0.6
2008	12.1 ± 1.8
2002 (1)	3.9 ± 0.4
2002 (2)	nd
1997	nd
1996	nd
1995	nd

Table 6.3. 3DG quantification in red Port wines from different vintages (between 2 and 78 years old); N=2.

Red Port wines	
Vintage	3DG (mg/L)
1935	100.2 ± 0.6
1940	82.9 ± 0.8
1952	94.4 ± 1.2
1961	89.3 ± 1.4
1972	71.9 ± 2.2
1976	56.1 ± 0.1
1981	98.3 ± 1.1
1991	65.0 ± 0.6
1996	65.2 ± 2.5
2001	67.8 ± 0.7
2006	41.1 ± 1.2
2011	48.2 ± 0.7

6.2.3.2.Quantification of 3-deoxyosone (3DG) in model wine solutions. Comparison of 3DG formation between glucose and fructose

An attempt to evaluate the role of 3DG on wines with different content of sugars and amino acids was performed. For this purpose, a wine-model system, that simulated both the studied white and red Port wine sugars and amino acids content, was prepared. Glucose and fructose were analysed individually to understand the reactivity of these sugars.

Two liters of a wine-model system were prepared with ethanol 12% (v/v), 0.033 M of tartaric acid, and pH adjusted to 3.6 with NaOH solution. This wine-model was then adjusted into two sets of one liter as follows: (i) 100 mg/L of amino acids; and (ii) 400 mg/L of amino acids (Figure 6.12). Then, each set was divided into four parts of 250 mL as follows: (a) 50 g of glucose; (b) 50 g of frutose; (c) 2 g of glucose; and (d) 2 g of fructose. Samples were kept at 40ºC during 35 days. Experiment was conducted in duplicate.

Figure 6.13 represents the 3DG concentration in the eight analysed sets. By the observation of this Figure we can see that for the same level of amino acids content, higher concentration of sugars induced higher concentration of 3DG. Furthermore, the nature of the sugar is a main issue for the production of 3DG. 50 g/L of fructose produce 8 to 16 times higher levels of this dicarbonyl compound than 50 g/L of glucose, respectively for the same level of amino acids of 400 and 100 mg/L. 3DG was already found and quantified in carbonated soft drinks (CSD) (Wang Yu, 2009). In this study, it was realized that high fructose corn syrup in CSDs was the major source of this dicarbonyl compound with levels of 27.1 to 74.5 mg/L (Wang Yu, 2009). Finally, the increment of amino acids, from 100 to 400 mg/L, has no significant effect in 3DG production, with the exception of glucose at 50 g/L (ia and iia) (Figure 6.13).

In this experience, that simulate the white and red Port wine sugar and amino acids content, we can conclude that 3DG formation, during 35 days and at a temperature of 40ºC, is attributed to the fructose concentration (ib - red Port wine and iid - white wine). In fact, according to the Lobry-de-Bruyn-Alberda-van-Eckenstein-rearrangement, glucose and fructose are in equilibrium with the same intermediate, the 1,2-enediol, resulting in 3DG (Chapter 2; Figure 2.12). However, fructose is also in equilibrium with the 2,3-enediol ensuing in 1DG (Chapter 2; Figure 2.12).

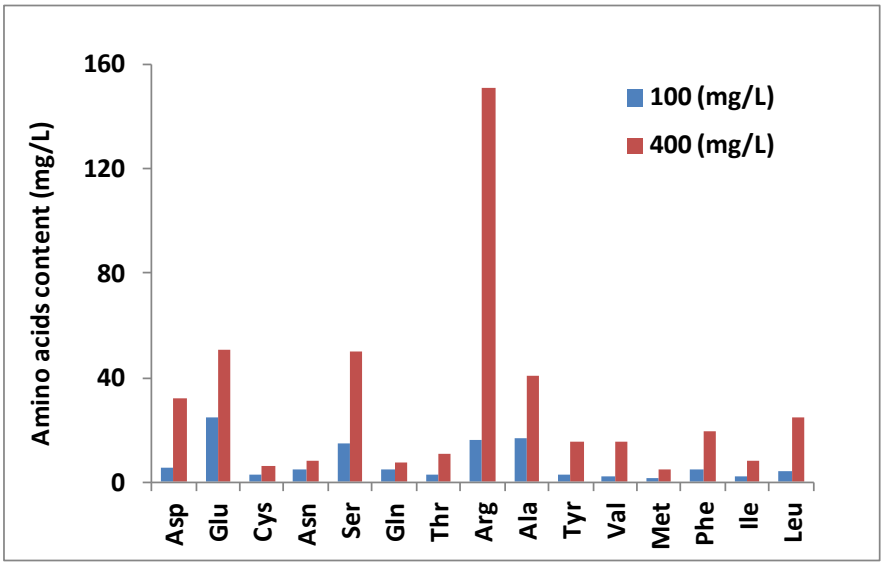

Figure 6.12. Amino acids content of the applied wine-model system.

Aspartic acid (Asp); glutamic acid (Glu); cystein (Cys); asparagine (Asn); serine (Ser); glutamine (Gln); threonine (Thr); arginine (Arg); alanine (Ala); tyrosine (Tyr); valine (Val); methionine (Met); phenylalanine (Phe); isoleucine (Ile); leucine (Leu). Data in appendix of this thesis.

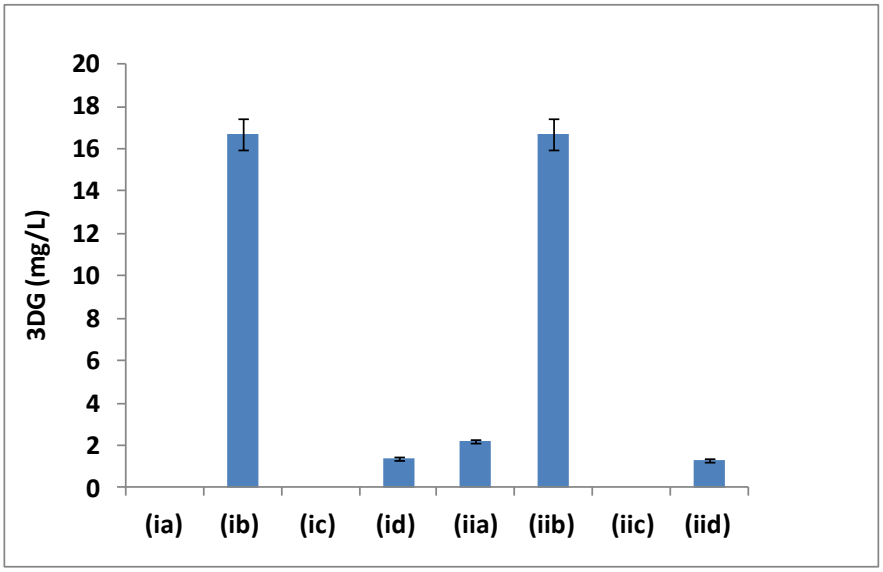

Figure 6.13. 3DG quantification in a wine-model system.

(ia) Glucose 50 g/L + 100 mg/L aa; (ib) Fructose 50 g/L + 100 mg/L aa; (ic) Glucose 2 g/L + 100 mg/L aa; (id) Fructose 2 g/L + 100 mg/L aa; (iia) Glucose 50 g/L + 400 mg/L aa; (iib) Fructose 50 g/L + 400 mg/L aa; (iic) Glucose 2 g/L + 400 mg/L aa; (iid) Fructose 2 g/L + 400 mg/L aa; N=2. Data in appendix of this thesis.

6.3. Quantification of compounds chemically linked with Maillard-like reactions

GC-mass spectrometry was used to evaluate the volatile compounds chemically linked with Maillard-like reactions. In this way, a liquid-liquid extraction was employed enabling the identification and quantification of this class of volatiles (Chapter 3; 3.10.1.) in the forced aging protocols of white and red Port wines (Chapter 3; 3.2.). For the white wine aging protocol, samples were taken on the first day, and weekly (P0; and P1, 7^{th} day sampling, to P6, 42^{th} day sampling) (P0 + 6 weeks*2 oxygen regimes*4 temperatures*2 replicates); total of ***98 samples***. For the red Port wine aging protocol, samples were taken on the first day, and weekly (P0; and P1, 7^{th} day sampling, to P9, 63^{th} day sampling) (P0 + 9 weeks*2 oxygen regimes*4 temperatures*2 replicates); total of ***146 samples***.

The accelerated spoilage, conducted with both temperature and oxygen supplements, promoted a modification of the volatile composition that could be sensed by GC-MS. Volatile compounds chemically linked with Maillard-like reactions will be quantified: furan derivatives, enolic compounds, and "Strecker aldehydes", respectively for white and red Port wines under the applied temperatures, for both oxygen treatments I and II.

6.3.1. Quantification of furan derivatives

Literature data indicate multiple sources of furanic compounds formation originating from: (i) thermal degradation/Maillard reaction reducing sugars, alone or in the presence of amino acids; (ii) thermal degradation of certain amino acids; (iii) thermal oxidation of ascorbic acid; (iv) poly-unsaturated fatty acids; and (v) carotenoids (Yaylayan 2006).

The main source of furan derivatives in food is the thermal degradation of carbohydrates such as glucose, lactose, and fructose (Maga, 1979). Also, amino acids such as serine or cysteine undergo thermal degradation producing furan derivatives without the need of any other source. Both of them are able to produce acetaldehyde (ethanal) and glycolaldehyde, by "Strecker reaction", which will both react participate in aldol condensations producing aldotetrose derivatives and, eventually, furan derivatives. On the other hand, alanine, threonine, and aspartic acid alone do not produce furan derivatives. These amino acids can

generate only acetaldehyde and they require the presence of reducing sugars, serine, or cysteine as a source of glycolaldehyde (Perez and Yaylayan, 2004).

6.3.1.1.Quantification of furan derivatives in white and red Port wines

Figure 6.14 and Figure 6.15 represents the respective furanic compounds formation: 2-furfural, 5-(hydroxymethyl)furfural, 5-methylfurfural, 2-acetylfuran, 2-(2-hydroxyacetyl)furan, ethyl 2-furoate, and furfuryl alcohol depletion for, respectively, white and red Port wines. The furanic aldehydes, 2-furfural, 5-(hydroxymethyl)furfural, and 5-methylfurfural (Figure 6.2) can be formed by cyclization/condensation of 3DG, via 1,2-enaminol, from respectively, fructose, glucose, and the 6-methylpentose rhamnose.

Figure 6.16 and Figure 6.17 represents the evolution of 2-furfural, under oxygen treatments I and II, for respectively, white and red Port wines. Figure 6.18 and Figure 6.19 represents the evolution of HMF, under oxygen treatments I and II, for respectively, white and red Port wines. Due to the linear concentration range of 2-furfural and HMF in GC-MS, these two furanic compounds were quantified by HPLC-DAD (Chapter 3; 3.6.).

By the observation of Figures 6.16 to 6.19 we can see that the level of these compounds depends on the temperature regimes, and are not modulate by oxygen treatments. In fact, at 40ºC and after 42 days of forced aging, there is a significant increase in the amount of 2-furfural in both white and red Port wines, to 2.5 mg/L (Figure 6.16; for white wine), along with 0.22 and 0.20 mg/L (Figure 6.17; for red Port wine), for respectively treatment I and II. For HMF, at 40ºC and after 42 days of forced aging, levels of this compound have increased to 18.8 and 20.5 mg/L (Figure 6.18; for white wine), along with 2.50 and 2.19 mg/L (Figure 6.19; for red Port wine), for respectively treatment I and II. 5-Methylfurfural followed the same trend. For the same time interval and applied temperature, values of this compound have increased to 61.0 and 60.5 µg/L (white wine), as well as 12.15 and 10.46 µg/L (red Port wine) for, respectively, treatment I and II. These results indicates that, the analysed white wine have produced about 10 times higher levels of the furanic aldehydes, 2-furfural or HMF, and about 6 times higher levels of 5-methylfurfural. In fact, the formation of these compounds is about 10 times higher in the white wine forced aging protocol (Figure 6.14) in contrast with the red Port wine forced aging protocol (Figure 6.15). This fact could be related with the reactivity of these aldehydes with anthocyanins or

flavan-3-ols (Figure 6.11) in the red Port wine forced aging protocol. In this study, the red Port wine linked to a rapid and at the same time complete depletion of anthocyanins or flavan-3-ols (Chapter 5). Some authors have already reported that, along with acetaldehyde, other aldehydes present is wines such as glyoxylic acid, resulting from the tartaric acid oxidation, and 2-furfural or HMF, which are both sugar degradation products formed during the processing and storage of wine, can react with anthocyanins leading to the formation of anthocyanin-furanic aldehyde adducts (Es-Safi et al., 2002, Sousa et al., 2010). In the same way, the formation of oligomeric bridged compounds having flavan-3-ols units linked by furfuryl or 5-(hydroxymethyl)furfuryl groups has been observed (Es-Safi et al., 2000, Vivas et al., 2008).

The previous presented furanic compounds, 2-acetylfuran, 2-(2-hydroxyacetyl)furan, ethyl 2-furoate, and furfuryl alcohol (Figure 6.2) have similar formation or depletion (furfuryl alcohol) rates in both white (Figure 6.14) and red Port wines forced aging protocols (Figure 6.15).

The formation of 2-acetylfuran through 1,4-dideoxyosone from glucose and amino acids, via 2,3-enaminol, was already reported (Cerny and Davidek, 2003, Wang and Ho, 2008). At 40ºC and after 42 days of forced aging, there is a significant increase in the amount of 2-acetylfuran in both white and red Port wines, to 17.3 and 21.4 µg/L (white wine), along with 16.5 and 15.3 mg/L (red Port wine) for, respectively, treatment I and II. Moreover, this compound is not modulating by oxygen treatments having similar formation rate constants in both treatments I and II (Figure 6.14 and Figure 6.15).

2-(2-Hydroxyacetyl)furan is one reaction product of 4-deoxyosone (4DG) (Figure 6.1) (Food Chemistry, 2008). However, this compound is preferentially formed in carbohydrate degradation, and favourite with fructose, in the absence of amine components, from the corresponding 2,3-enediol by water elimination (Food Chemistry, 2008). At 40ºC and after 42 days of forced aging, levels of this compound have increased to 54.9 and 42.3 µg/L (white wine), along with 66.0 and 55.0 µg/L (red Port wine) for, respectively, treatment I and II. 2-(2-Hydroxyacetyl)furan seems to be affected by oxygen exposure (Figure 6.14 and Figure 6.15). Higher values of this compound are found in treatment I. This could be related with the possible oxidation of the hydroxyl group (Figure 6.2) with treatment II.

Rapp and Guntert (1986) have shown that ethyl 2-furoate (Figure 6.2) can add from carbohydrates conversions in Riesling wines. Ethyl 2-furoate could be formed by the

esterification reaction between ethanol and 2-furancarboxylic acid, that is produced by Maillard reactions (Vernin and Parkanyi 1982). In fact, ethyl 2-furoate has increased in both white and red Port wines (Figure 6.14 and Figure 6.15). At 40ºC and after 42 days of forced aging, there is an increase in the amount of ethyl 2-furoate in both white and red Port wines, to 11.3 and 10.6 µg/L (white wine), along with 12.8 and 12.1 mg/L (red Port wine) for, respectively, treatment I and II. Moreover, this compound is not modulated by oxygen treatments, with similar formation rate constants (Figure 6.14 and Figure 6.15).

Furfuryl alcohol (Figure 6.2) comes from monosaccharides degradation (Yeo and Shibamoto, 1991) and Maillard reactions (Schirlekeller and Reineccius, 1992, Tressl et al., 1993, Chen and Ho, 1999, Ames et al, 2001). A mechanism for the formation of furfuryl alcohol from glucose in aqueous systems was given by Yaylayan, Keyhani and Wnorowski (Yaylayan, and Keyhani, 2000, Wnorowski and Yaylayan, 2000). The reaction involves the oxidation of glucose to gluconic acid, which is decarboxylated to a pentitol and followed by dehydration and cyclization to furfuryl alcohol. This compound has decreased in both white and red Port wines forced aging protocols (Figure 6.14 and Figure 6.15). These decreases were faster with treatment II (Figure 6.14 and Figure 6.15). This fact could be related with the oxidation of furfuryl alcohol into 2-furfural. Also, furfuryl alcohol after the elimination of water and addition of hydrogen sulfide can form 2-furfurylthiol (Food Chemistry, 2008).

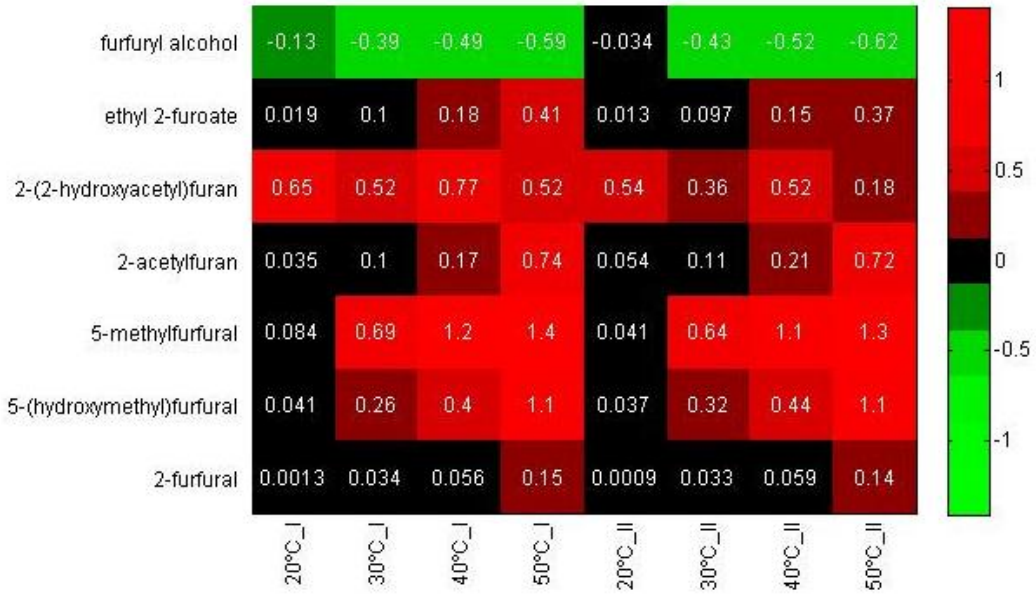

Figure 6.14. Furan derivatives formation or depletion (furfuryl alcohol) during the forced aging protocol of white wines. I - no oxygen addition; II - oxygen addition. Data in appendix of this thesis.

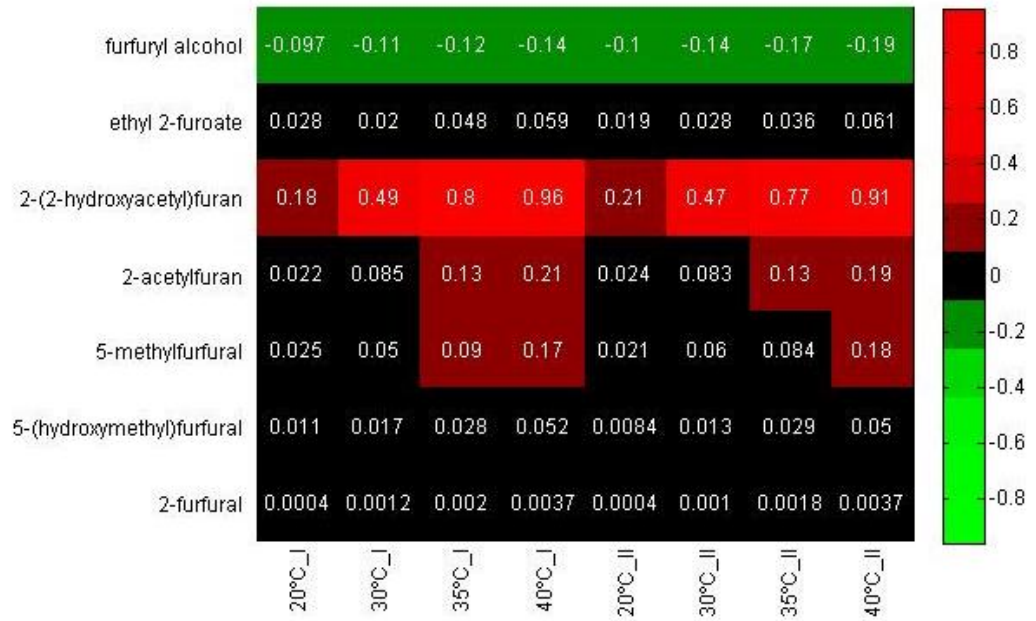

Figure 6.15. Furan derivatives formation or depletion (furfuryl alcohol) during the forced aging protocol of red Port wines. I - no oxygen addition; II - oxygen addition. Data in appendix of this thesis.

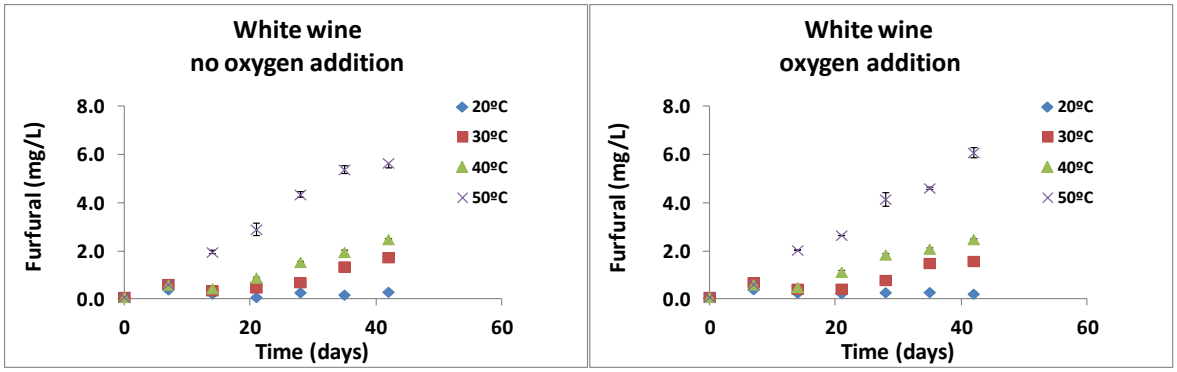

Figure 6.16. Evolution of 2-furfural, during the white wine forced aging protocol, under respectively no oxygen addition (treatment I) and oxygen addition (treatment II).

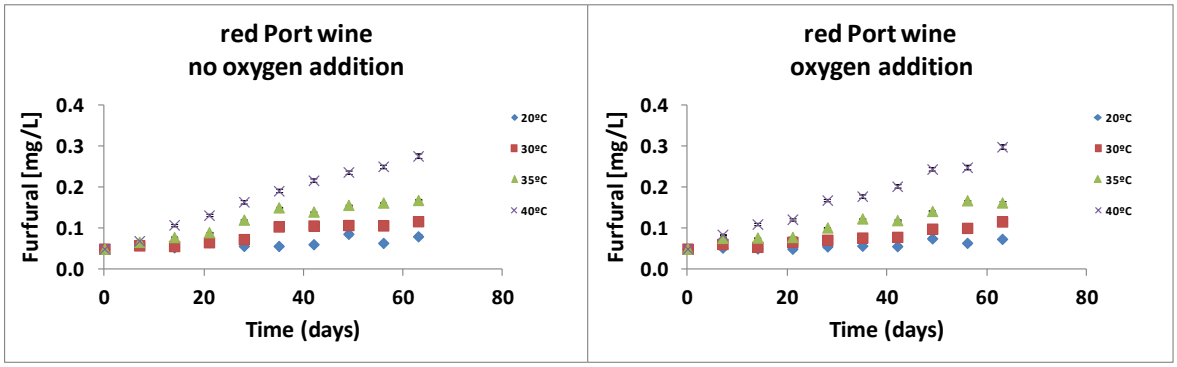

Figure 6.17. Evolution of 2-furfural, during the red Port wine forced aging protocol, under respectively no oxygen addition (treatment I) and oxygen addition (treatment II).

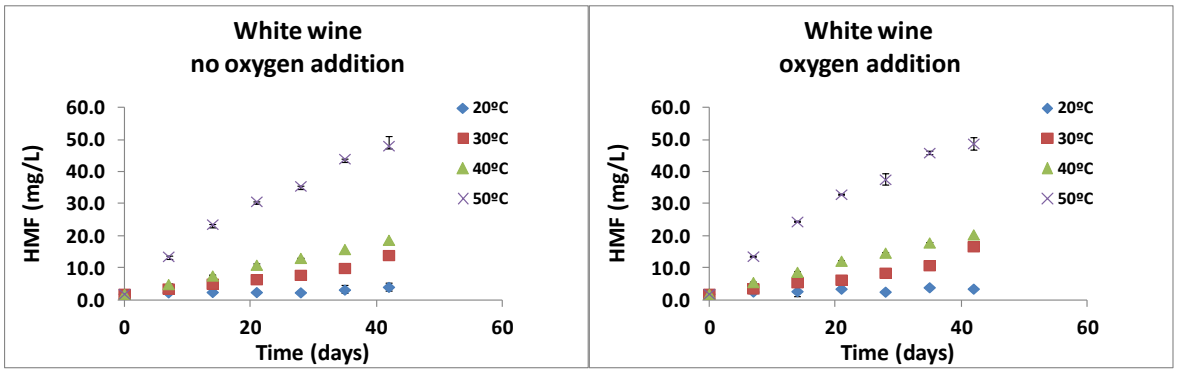

Figure 6.18. Evolution of 5-(hydroxymethyl)furfural, during the white wine forced aging protocol, under respectively no oxygen addition (treatment I) and oxygen addition (treatment II).

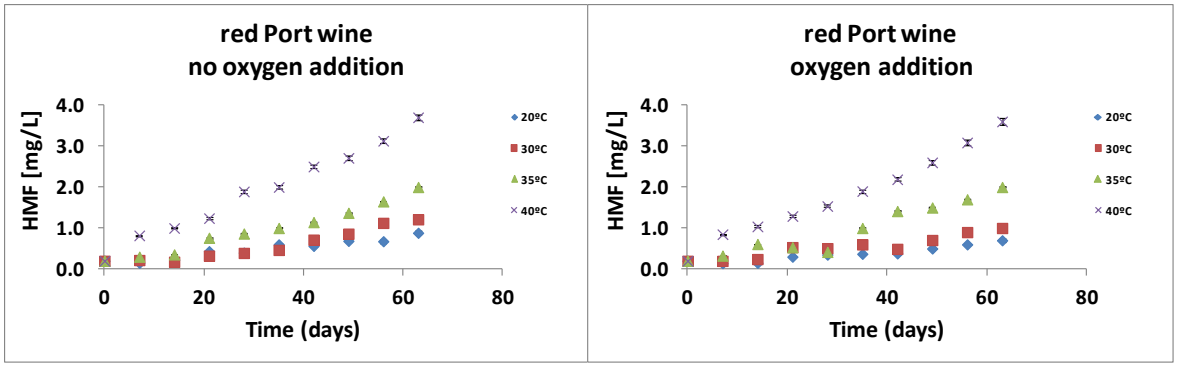

Figure 6.19. Evolution of 5-(hydroxymethyl)furfural, during the red Port wine forced aging protocol, under respectively no oxygen addition (treatment I) and oxygen addition (treatment II).

6.3.1.2.Quantification of furan derivatives in model wine solutions. Comparison of 2-furfural, 5-(hydroxymethyl)furfural, and 5-methylfurfural formation from glucose, fructose or 3DG

An attempt to evaluate the role of 2-furfural, 5-(hydroxymethyl)furfural (HMF), and 5-methylfurfural on model wines with different content of sugars and amino acids was performed. For this purpose, the same wine-model system given in section 6.2.3.2, that simulated both the studied white and red Port wines sugars and amino acids content, was used. Correlations between 3DG and these furanic aldehydes were also achieved. Figure 6.20 represent 2-furfural, HMF, and 5-methylfurfural concentrations in the eight analysed sets with different content in sugars and amino acids (Table 6.4). By the observation of this Figure we can see that for the same level of amino acids content (Table 6.4), higher concentration of sugars induced higher concentration of 2-furfural, HMF, and 5-methylfurfural (Figure 6.20). Furthermore, fructose is the major source of these furanic compounds. Reports have demonstrated that fructose shows a higher reactivity in HMF generation compared to glucose and sucrose (Antal et al., 1990, Lee and Nagy, 1990). Also, the increase of amino acids, from 100 to 400 mg/L, has no significant effect in 2-furfural, HMF, and 5-methylfurfural production, with the exception of glucose at 50 g/L (ia and iia) (Figure 6.20). Finally, 3DG is greatly correlated with the formation of 2-furfural and HMF, with a correlation coefficient (r) of, respectively, 0.992 and 0.996, proving their formation via 3DG.

Table 6.4. Analysed sets used for the 2-furfural, HMF, and 5-methylfurfural quantification in a wine-model system.

Wine-model system
35 days at 40ºC
(ia) Glucose 50 g/L + 100 mg/L aa
(ib) Fructose 50 g/L + 100 mg/L aa
(ic) Glucose 2 g/L + 100 mg/L aa
(id) Fructose 2 g/L + 100 mg/L aa
(iia) Glucose 50 g/L + 400 mg/L aa
(iib) Fructose 50 g/L + 400 mg/L aa
(iic) Glucose 2 g/L + 400 mg/L aa
(iid) Fructose 2 g/L + 400 mg/L aa

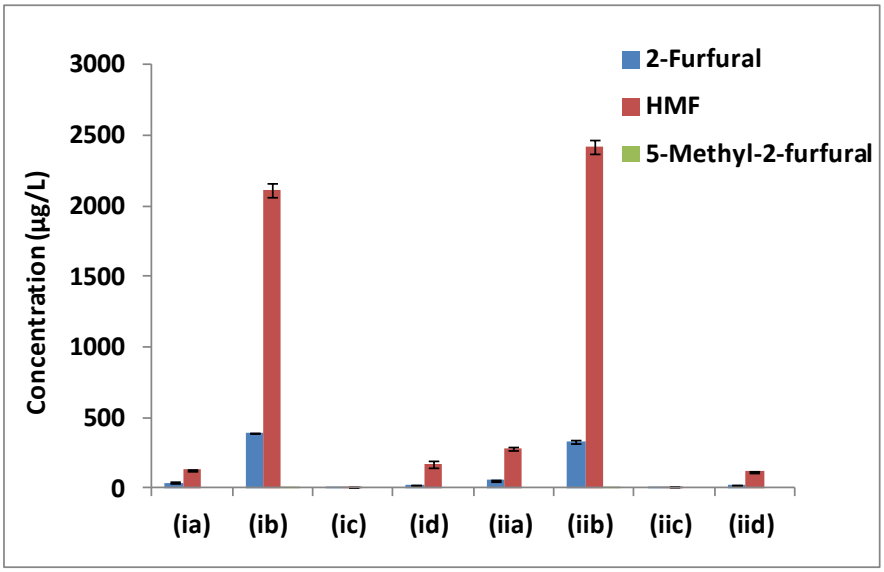

Figure 6.20. 2-Furfural, HMF, and 5-methylfurfural quantification in a wine-model system. N=2. Data in appendix of this thesis.

6.3.2. Quantification of enolic compounds in white and red Port wines

During the forced aging protocols of white and red Port wines the already known enolic compounds, arising from Maillard reactions, were tentatively identified, such as: sotolon [3-hydroxy-4,5-dimethylfuran-2(*5H*)-one], maltol (3-hydroxy-2-methyl-*4H*-pyran-4-one), 5-hydroxymaltol (3,5-dihydroxy-2-methylpyran-4-one; DMP), and pantolactone (4,5-

dihydro-3-hydroxy-4,4-dimethyl-2(*3H*)-furanone). Sotolon, maltol, and 5-hydroxymaltol were only found in the red Port wine forced aging protocol.

Sotolon [3-hydroxy-4,5-dimethyl-2(*5H*)-furanone] (Figure 6.2) presents a nutty, spicy or perceived 'aged' character and has been suggested as a key odourant in the aroma of aged port wines (Silva Ferreira et al., 2003, Silva Ferreira et al., 2005). Sotolon possesses a strong, typical odour reminiscent of nut and curry with a very low perception threshold (8-10 µg/L) (Pham et al. 1995). This compound was also found to contribute to the aroma of several other fortified wines, including Sherry wines (Dubois et al., 1976, Martin and Etievant 1991, Martin et al., 1992, Moreno et al., 2005), French fortified wines "vins doux naturels" (VDN) (Schneider et al., 1998), and Madeira wines (Câmara et al., 2004, Câmara et al., 2006). Other wines with oxidative character have also reported this odor active molecule, such as Jura wines "vin jaunes" (Pham et al., 1995), Tokay wines (Guichard et al., 1993), and Botrytised wines (Masuda et al., 1994). Several mechanisms for the presence of sotolon in foodstuff have been proposed. The first proposed explanation was that sotolon is formed as a result of aldol condensation between α-ketobutyric acid, via a degradation product of threonine, and pyruvic acid (Dubois et al., 1976), similar to the proposed mechanism for the formation of 5-ethyl-3-hydroxy-4-methyl-2(*5H*)-furanone (abexon) via protein hydroxylates (Sulser et al., 1967). An aldolization of α-ketobutyric acid with acetaldehyde is also proposed (Pham et al., 1995, Guichard et al., 1997, Cutzach et al., 1999). Other mechanisms, excluding α-ketobutyric acid have also been proposed. Particularly, sotolon formation from the chemical or enzymatic conversion of 4-hydroxisoleucine (Lerk and Ambuhl 1995, Blank et al., 1996); as a product of reaction from hexoses and pentoses in the presence of cysteine (Hofmann and Schieberle, 1997); from the aldol condensation of 2-hydroxyacetaldehyde (glycolaldehyde) with butane-2,3-dione (diacetyl) (Hofmann and Schieberle, 1996), and more recently from ascorbic acid degradation products (Konig et al., 1999, Pons et al., 2010). In addition, in Madeira wines (Câmara et al., 2006) it has been found that the highest concentrations of sotolon were found in the wines with highest residual sugar concentration.

Figure 6.21 represent the evolution of sotolon in the red Port wine forced aging protocol for, respectively, oxygen treatments I and II. By the observation of this Figure we can see that the formation of sotolon is clearly related to the temperature and the presence of oxygen. Also, it would seem that the temperature combined with the presence of O_2 could

have a synergistic effect on its formation (Martins et al., 2013). This statement could be explained by the fact that, during oxidative aging, ethanol is converted into acetaldehyde, thus allowing the formation of sotolon.

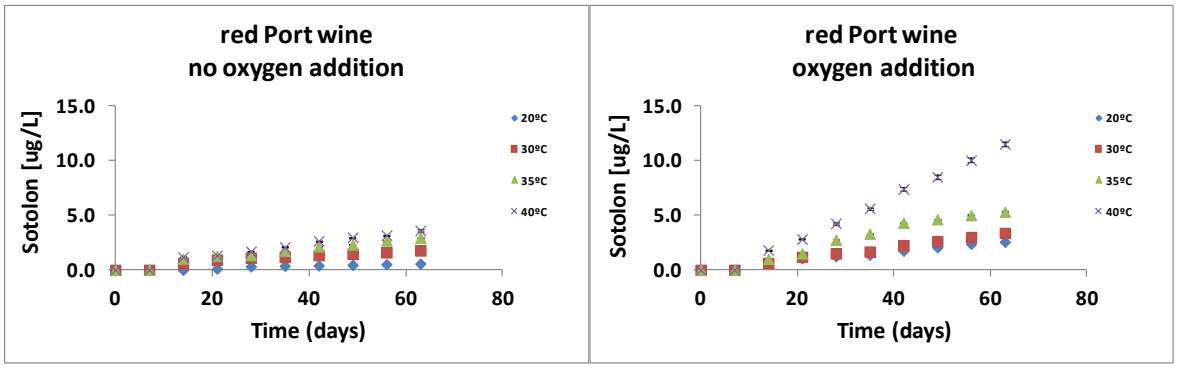

Figure 6.21. Evolution of sotolon [3-hydroxy-4,5-dimethylfuran-2(5*H*)-one], during the red Port wine forced aging protocol, under respectively no oxygen addition (treatment I) and oxygen addition (treatment II).

Maltol (Figure 6.2) is obtained from carbohydrates like maltose or lactose, and has a caramel-like odor. The direct formation of maltol from the Amadori product via 1-deoxyosone (1DG) (Figure 6.1) is also proposed. 5-Hydroxymaltol has been identified during the aging of sweet fortified wines (Cutzach et al., 1999). 2,3-Dihydro-3,5-dihydroxy-6-methyl-*4H*-pyran-4-one (DDMP, Figure 6.2) was found to be converted into maltol, 5-hydroxymaltol, and isomaltol (Shaw et al., 1971, Yaylayan and Mandeville, 1994). Nevertheless, DDMP have not been quantified, by the applied methodologies, in the analyzed wines.

Figure 6.22 and Figure 6.23 represents the evolution of maltol and 5-hydroxymaltol in the red Port wine forced aging protocol for, respectively, oxygen treatments I and II. Higher values of maltol and 5-hydroxymaltol are found in treatment I. This could be related with the possible oxidation, of the respectively one and two hydroxyl groups (Figure 6.2), with treatment II. Furthermore, 5-hydroxymaltol is highly dependent on temperature regimes (Figure 6.23).

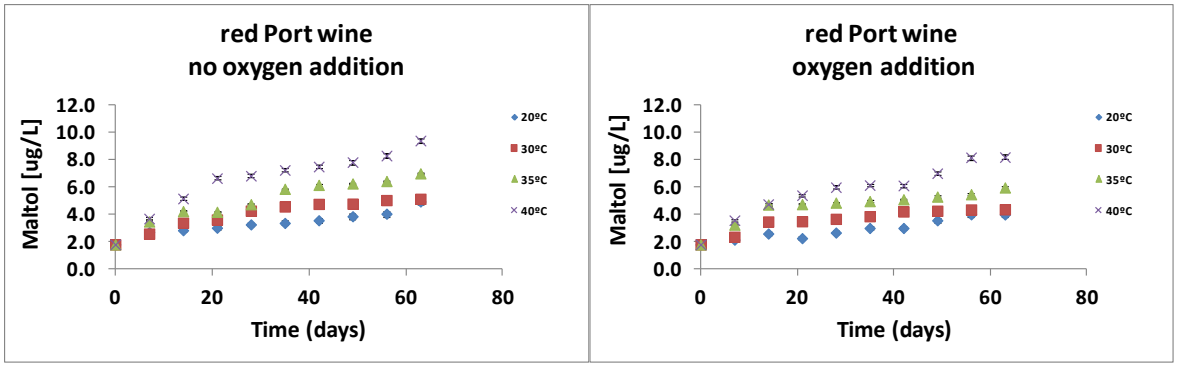

Figure 6.22. Evolution of maltol (3-hydroxy-2-methyl-4*H*-pyran-4-one), during the red Port wine forced aging protocol, under respectively no oxygen addition (treatment I) and oxygen addition (treatment II).

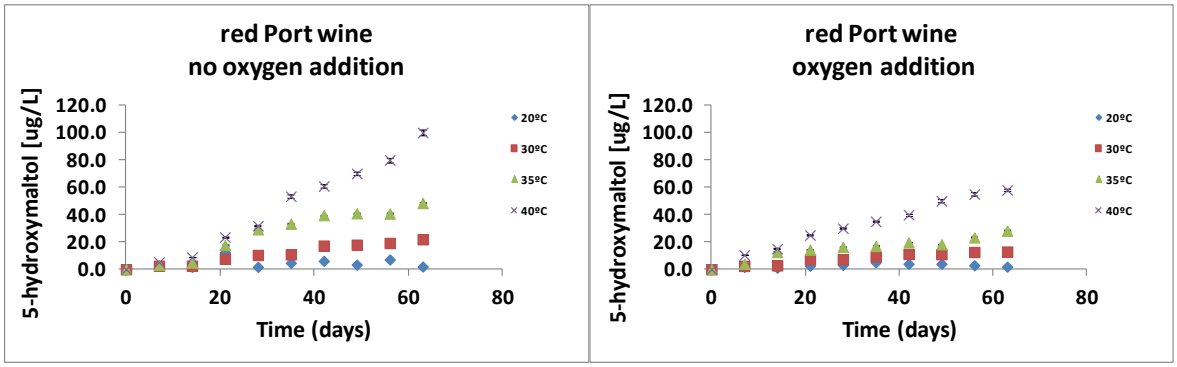

Figure 6.23. Evolution of 5-hydroxymaltol (3,5-dihydroxy-2-methylpyran-4-one; DMP), during the red Port wine forced aging protocol, under respectively no oxygen addition (treatment I) and oxygen addition (treatment II).

Pantolactone was identified and isolated from Californian and Spanish sherries (Webb et al., 1967), and sweet fortified wines (Cutzach et al., 1999). This lactone is formed during alcoholic fermentation due to the action of a reductase produced by yeast acting (King and Wilken, 1972). Figure 6.24 and Figure 6.25 represents the evolution of pantolactone in the oxygen treatments I and II for, respectively, white and red Port wines. This lactone increased slowly in the white wine forced aging (Figure 6.24) in contrast with the red Port wine forced aging (Figure 6.25). Also, its formation did not seem to be affected by oxidation and temperature exposure (Figure 6.24 and Figure 6.25).

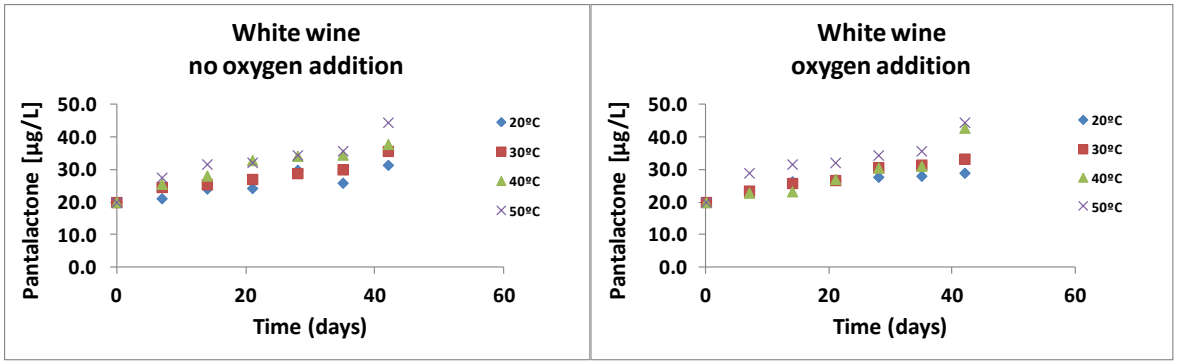

Figure 6.24. Evolution of pantolactone [4,5-dihydro-3-hydroxy-4,4-dimethyl-2(3*H*)-furanone], during the white wine forced aging protocol, under respectively no oxygen addition (treatment I) and oxygen addition (treatment II).

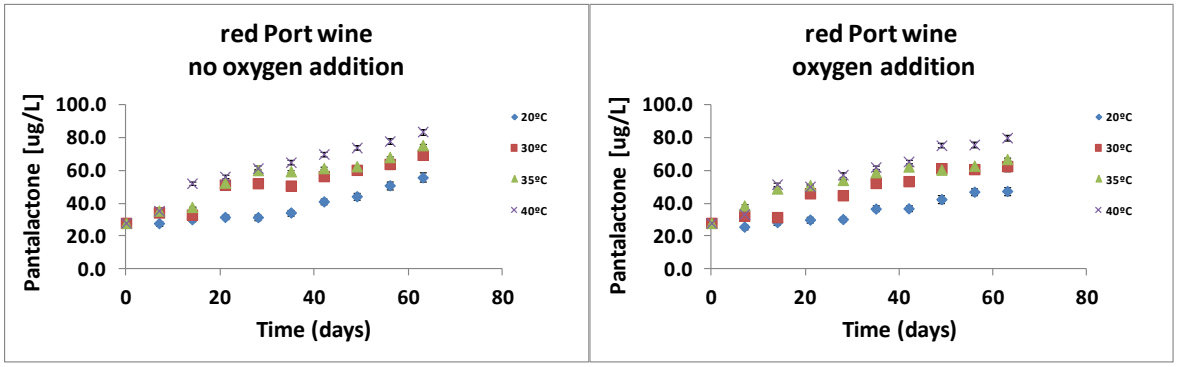

Figure 6.25. Evolution of pantolactone [4,5-dihydro-3-hydroxy-4,4-dimethyl-2(3*H*)-furanone], during the red Port wine forced aging protocol, under respectively no oxygen addition (treatment I) and oxygen addition (treatment II).

6.3.3. Quantification of "Strecker aldehydes" in white and red Port wines

The Strecker degradation of amino acids is described as a result of the Maillard reaction and involves the interaction of sugar-derived α-dicarbonyl compounds with free amino acids to form an aldehyde (Shonberg and Moubacher, 1952). This reaction has supported evidence that occurs in wine (Pripis-Nicolau et al., 2000, Escudero et al., 2000a, Escudero et al., 2000b Marchand et al., 2000, Keim, et al., 2002, Escudero et al., 2002, Silva Ferreira et al., 2002). Wines stored at high temperatures and supplemented with high levels of dissolved oxygen suffer a rapid and pronounced oxidative spoilage aroma, which are related with the presence of 3-(methylthio)propionaldehyde (methional), responsible for "cooked potato-like" odour notes, and phenylacetaldehyde, with "honey-like" odour notes

(Silva Ferreira et al., 2002). Phenylacetaldehyde and methional can be formed by the direct oxidation of the respective alcohol or via Strecker degradation of the respective amino acid (Silva Ferreira et al., 2002, Escudero et al., 2000b), but the main pathway for their formation is not clearly established. Some researchers suggest that the Strecker mechanism is the main pathway for the formation of methional (Silva Ferreira et al., 2002). Nevertheless, due to the temperature, pH, and dissolved oxygen regimes related to the storage conditions of wines, the question remains unanswered.

Phenylacetaldehyde and methional were tentatively quantified in the white and red Port wines protocols. As seen before, the respective amino acids phenylalanine (Phe) and methionine (Met) have suffered degradation in both white and red Port wines, much higher in the white wines (section 6.2.2 in this Chapter). In the same way, we must point that the initial white and red Port wines have different quantities of these amino acids, Phe: 18.6 and 4.4 mg/L; and Met: 4.3 and 0.9 mg/L, for respectively white and red Port wines (Figure 6.3). Phenylacetaldehyde was formed in both white and red Port wines. Figure 6.26 and Figure 6.27 represents the evolution of phenylacetaldehyde in the oxygen treatments I and II for, respectively, white and red Port wines. Methional was not formed in the red Port wines. Figure 6.28 represents the evolution of methional for, oxygen treatments I and II, for the white wines.

As shown in Figure 6.26 and Figure 6.27, the formation of phenylacetaldehyde showed that this compound depends on the temperature and oxygen concentration. The amounts found in this study, after 42 days at 40ºC and with oxygen addition (treatment II), were close to 40 µg/L in the white wine (Figure 6.26), and close to 60 µg/L in the red Port wine (Figure 6.27). These values are above the sensory threshold value in wines 25 µg/L (Silva Ferreira et al., 2002). Therefore, it can be concluded that the honey-like aroma can be explained by the formation of phenylacetaldehyde.

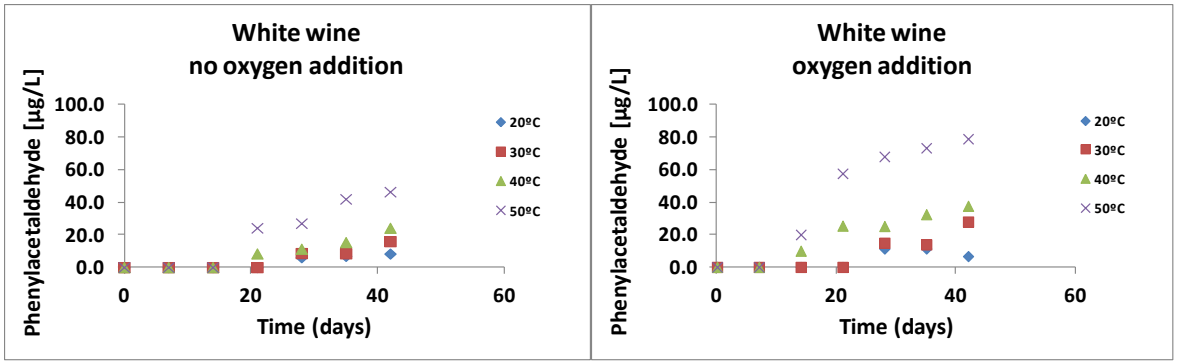

Figure 6.26. Evolution of phenylacetaldehyde, during the white wine forced aging protocol, under respectively no oxygen addition (treatment I) and oxygen addition (treatment II).

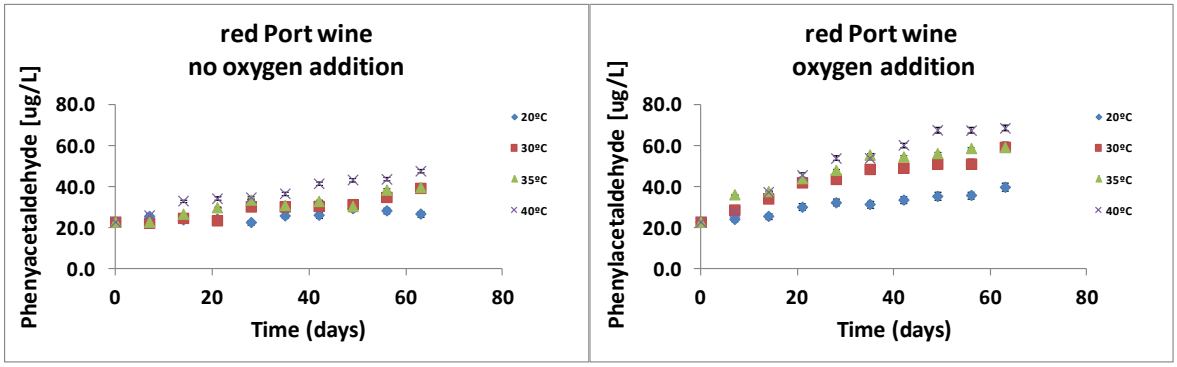

Figure 6.27. Evolution of phenylacetaldehyde, during the red Port wine forced aging protocol, under respectively no oxygen addition (treatment I) and oxygen addition (treatment II).

As shown in Figure 6.28, the formation of methional in the white wine forced aging is clearly related to the presence of oxygen in wine. The amounts of methional were mainly dependent upon, in decreasing order of importance, the temperature and the amount of dissolved oxygen. In fact, none of the treatments at 20°C led to the formation of this aldehyde. On the other hand, at 50°C, there was a considerable increase in the amount of methional over time. The large amounts of methional formed in the samples treated with oxygen (treatment II) are significant. After 42 days of storage at 50°C the concentration of methional was about 14 µg/L. This value was 2 times higher than the amount found with the oxygen treatment I, 7 µg/L, and above the sensory threshold value in wines of 0.5 µg/L (Escudero et al., 2000).

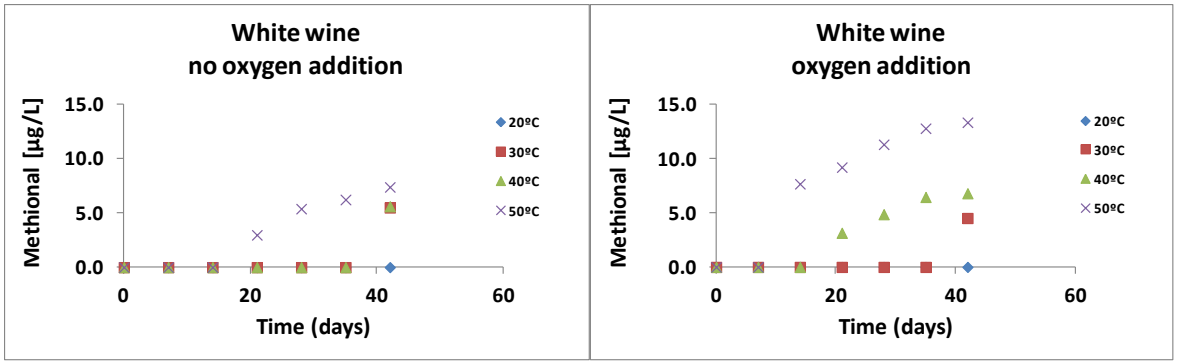

Figure 6.28. Evolution of methional, during the white wine forced aging protocol, under respectively no oxygen addition (treatment I) and oxygen addition (treatment II).

6.4. Approach to "Strecker mechanism" in wine: quinones - key intermediaries' on wine oxidation as "Strecker degradation reagents"

Typically, α-dicarbonyl compounds, such as glyoxal, pyruvaldehyde, butane-2,3-dione, and others, are reported as Strecker degradation (SD) reagents but, in principle, any dicarbonyl compound with extended conjugation can be used (Rizzi, 2006, Rizzi, 2008). The latter structural category can be extended to include *ortho*-quinones, formed during the oxidation process of wine phenolic compounds. Quinones are produced during enzymatic and non-enzymatic phenolics oxidation. These molecules are electronic equivalents of α-dicarbonyl compounds and are therefore potential SD reactants (Rizzi, 2006, Rizzi, 2008).

By using ferricyanide ion as oxidant, as an alternative to enzymes, caffeic acid, chlorogenic acid, (+)-catechin, and (-)-epicatechin react with methionine and phenylalanine to produce the "Strecker aldehydes" methional and phenylacetaldehyde, in pH 7.17 phosphate buffer at 20°C (Rizzi, 2006). In this transformation, a Michael addition of α-amino acids to *ortho*-quinones is proposed to produce the "Strecker aldehydes" (Chapter 2; Figure 2.23). On the other hand, reaction products between 4-methyl-1,2-benzoquinone (Q4MeC) and α-amino acids, investigate by Nikolantonaki and Waterhouse (2012), do not corroborate this mechanism. The 1,4-conjugate addition (Michael addition) of one molecule of amino acid to the quinone to produce a 4-amino catechol intermediate (Chapter 2; 1; Figure 2.23) was not observed. As a result, the authors stated that under low pH model wine conditions Rizzi's Strecker-type reaction could not be observed, and point

to a Fenton-type oxidation of the related alcohols as the source of the aldehydes perceived to affect wine aroma so strongly (Wildenradt and Singleton, 1974, Escudero et al., 2000a, Silva Ferreira et al., 2002, Silva Ferreira et al., 2003, Loscos et al., 2010). Nevertheless, under wine pH wine conditions, this route has to be confirmed, in order to determine if "Strecker aldehydes" can be formed with the participation of quinones, as "Strecker degradation reagents".

In this section, an attempt was made in order to determine if "Strecker aldehydes" can be formed with the participation of quinones, as "Strecker degradation reagents", at wine conditions. For this purpose, a wine-model system with phenylalanine or methionine with transition metal ions and three phenolic compounds (gallic acid, caffeic acid, and (+)-catechin) at a concentration of 0.6 mM was used. The quinones were formed by adding 0.4 ppm of Cu^{2+} in the form of copper sulfate pentahydrate, and 7.5 ppm of Fe^{2+} in the form of ferrous sulfate. Then, the respective amino acids (phenylalanine or methionine) were added in a concentration 4 times higher than the respective phenolic compounds (2.4 mM). Control flasks with no phenolic compounds were also employed (Control_Phe and Control_Met, Figure 6.29). The evolution of "Strecker aldehydes" was monitoring during 10 days by GC-MS (Chapter 3; 3.10.2. Solid Phase Micro Extraction (SPME) extraction).

Results have showed that the formation of phenylacetaldehyde and methional were achieved in all the four flaks (Figure 6.30). The presence of gallic acid, caffeic acid, and (+)-catechin with reactive oxygen species (ROS) formed quinones, that have reacted with phenyalanine to produce phenylacetaldehyde (Figure 6.30), while a small increase in this aldehyde was observed by direct degradation of phenylalanine (Control_Phe) in the presence of ROS (Figure 6.30). Furthermore, (+)-catechin was the phenolic that had promote higher levels of phenylacetaldehyde, follow by gallic acid and caffeic acid (Figure 6.30).

The analogous reaction with methionine has also produce the "Strecker aldehyde" methional (Figure 6.30), but a similar increase in this aldehyde was observed by the direct degradation of methionine (Control_Met) in the presence of ROS (Figure 6.30). Methionine is very sensitive to oxygen, and readily oxidized to the sulfoxide and sulfone (Figure 6.9). This fact could have limited the reaction with quinones. These results suggest that "Strecker aldehydes" can be formed by quinones intermediates at wine pH. The reaction products between the *ortho-quinones*, formed from gallic acid, caffeic acid, and

(+)-catechin, with phenylalanine were tentatively determined by MS analysis at this wine-model system conditions. Samples were analysed after 1 hour of reaction.

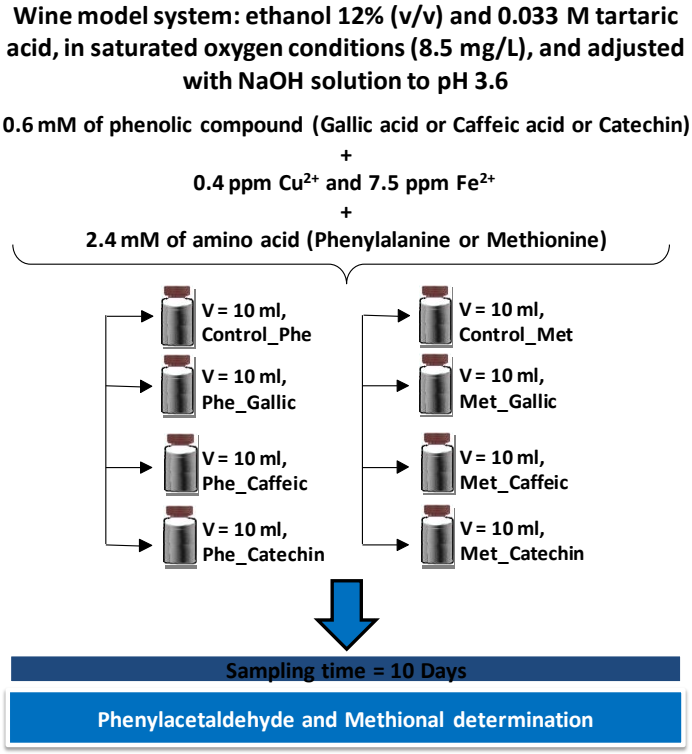

Figure 6.29. Wine-model system used for the study of "Strecker aldehydes".

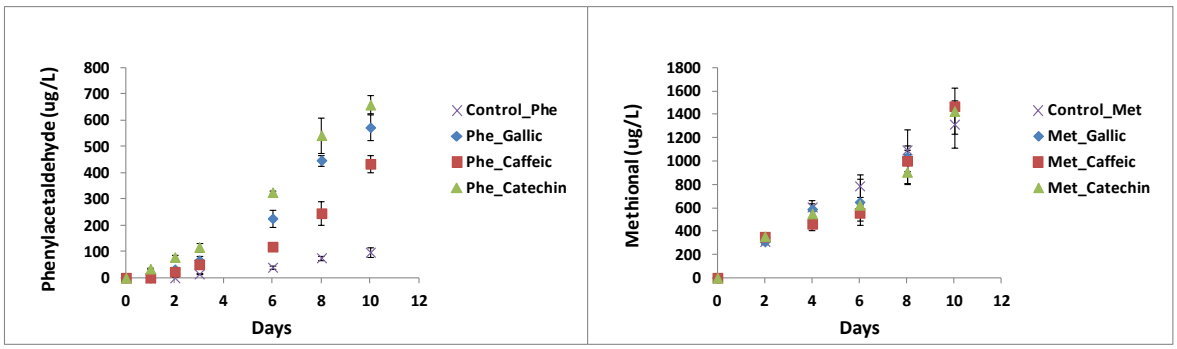

Figure 6.30. Evolution of phenylacetaldehyde and methional under the wine-model system used for the study of "Strecker aldehydes"; N=2.

Reaction products between gallic acid, caffeic acid, and (+)-catechin ortho-quinones and phenylalanine.

A LCQ Fleet ion trap mass spectrometer (ThermoFinnigan, San Jose, CA, USA), equipped with an electrospray ionization source and operating in negative mode was used. The nitrogen sheath gas was 10 (arbitrary units). The spray voltage was 5 kV and the capillary temperature was 275 ºC. The capillary and tune lens voltages were set at -28 V and -115 V, respectively. CID-MS^n experiments were performed on mass-selected precursor ions in the range of m/z 150-2000. The isolation width of precursor ions was 1.0 mass units.
The scan time was equal to 100 ms and the collision energy was optimized between 20 and 35 (arbitrary units), using helium as collision gas. The data acquisition was carried out by using Xcalibur® data system (ThermoFinnigan, San Jose, CA, USA).
The proposed Rizzi reaction products, formed during the first steps of Strecker degradation of phenylalanine with gallic acid, caffeic acid, and (+)-catechin *ortho*-quinones, were screened by full MS. Table 6.5 represents the mass-selected precursor ions (negative mode) of the proposed Michael addition products of the respective quinones with phenylalanine (adapted from Rizzi, 2006) (Chapter 2; Figure 2.23). The extracted m/z 332.3, 342.3, and 452.5 corresponding respectively, to phenylalanine adducts to gallic acid, caffeic acid, and (+)-catechin quinones moieties, $C_{16}H_{15}NO_7$, $C_{18}H_{17}NO_6$, and $C_{24}H_{23}NO_8$ (Chapter 2; 1; Figure 2.23) were not observed. This result indicates that these compounds do not result from the nucleophilic addition of phenylalanine onto the quinones in a similar manner as that recently reported by Nikolantonaki and Waterhouse (2012) or Rizzi (2006). In the same way, the structure types 2 to 5 (Table 6.5) were also not found. Nevertheless, a similar reaction of that reported by Strecker (1862) to effect decarboxylation/deamination of amino acids is proposed.
Figure 6.31 and Table 6.6 represents respectively the formation of "Strecker aldehydes" from *ortho*-quinones and the corresponding mass-selected precursor ions (negative mode) of the proposed reaction products. Results have shown that, for gallic acid, structures 2 and 3 were attained with m/z of respectively, 270.3, and 168.1 (Figure 6.31 and Table 6.6). For caffeic acid, structures 1, 2 and 3 were found with m/z of respectively, 324.3, 280.3, and 178.1 (Figure 6.31 and Table 6.6). Finally, for (+)-catechin, the corresponding m/z 434.4, 390.4, and 288.3 (Figure 6.31 and Table 6.6) were not attained. These results could be

explained by the different phenolic reactivities. Because (+)-catechin was the phenolic that had promoted higher levels of phenylacetaldehyde (Figure 6.30), it is suppose that the formation of "Strecker aldehydes" from this phenolic is faster than that of gallic or caffeic acids, and so the intermediary products were not observed. This fact could be related with a faster quinone formation, i.e., a faster phenolic oxidation.

Follow by (+)-catechin, gallic acid was the phenolic that had promoted higher levels of phenylacetaldehyde (Figure 6.30). In the same way, only structures 2 and 3 were achieved with this phenolic (Figure 6.31). The reason for not finding the structure 1 may be related with its faster reactivity as well. Finally, caffeic acid was the phenolic that had generate less phenylacetaldehyde (Figure 6.30). Conversely, all the three structures 1, 2 and 3 (Figure 6.31) were found in the medium reaction with caffeic acid, transitions metal ions, and phenylalanine. Furthermore, all reactions moieties have a product ion at m/z = 163 ([M − H]¯). This compound is phenylpyruvic acid (Figure 6.32), the α-keto acid derived from phenylalanine oxidative deamination. This compound was quantified (Chapter 3; 3.8.), in the end of the protocol (after 10 days) in all the four reaction media (Control_Phe, Phe_Gallic, Phe_Caffeic, and Phe_Catechin). Results have showed similar concentrations of phenylpyruvic acid in the four reaction media, indicating that this compound is a result of phenylalanine oxidative deamination and had contributed to certain level of phenylacetahldehyde in all samples (Figure 6.30).

MS/MS fragments were attempted for the precursor ions of respectively, gallic and caffeic acids quinone moieties. Figure 6.33a and Figure 6.33b represents the MS/MS fragments occurred for gallic and caffeic acids quionone products with phenylalanine.

Table 6.5. Mass-selected precursor ions (negative mode) of the proposed Michael addition reaction products of *ortho*-quinones with phenylalanine (adapted from Rizzi, 2006).

[M-H]⁻ m/z			
Structure type	**0.6 mM Gallic acid**	**0.6 mM Caffeic acid**	**0.6 mM (+)-Catechin**
	2.4 mM Phe	***2.4 mM Phe***	***2.4 mM Phe***
1	332.3	342.3	452.5
2	330.3	340.3	450.4
3	477.5	487.5	597.6
4	433.5	443.5	553.6
5	331.3	341.3	451.5

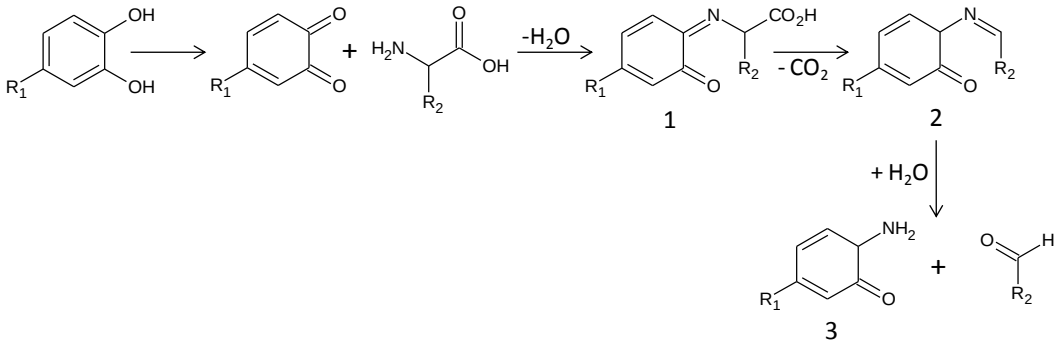

Figure 6.31. Formation of Strecker aldehydes from *ortho*-quinones assisted decarboxylation/deamination of amino acids.

Table 6.6. Mass-selected precursor ions (negative mode) of the proposed Strecker aldehyde reaction products formation through assisted *ortho*-quinones (adapted from Strecker, 1862).

[M-H]⁻ m/z			
Structure type	**0.6 mM Gallic**	**0.6 mM Caffeic**	**0.6 mM Catechin**
	2.4 mM Phe	***2.4 mM Phe***	***2.4 mM Phe***
1	314.3	324.3	434.4
2	270.3	280.3	390.4
3	168.1	178.1	288.3

Phenylpyruvic acid

163 - 91 (-72)

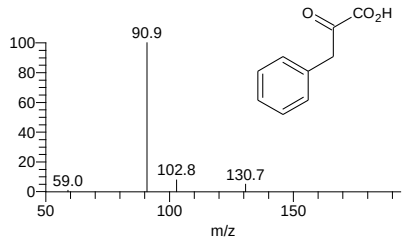

Figure 6.32. MS/MS fragments of phenylpyruvic acid.

Gallic acid

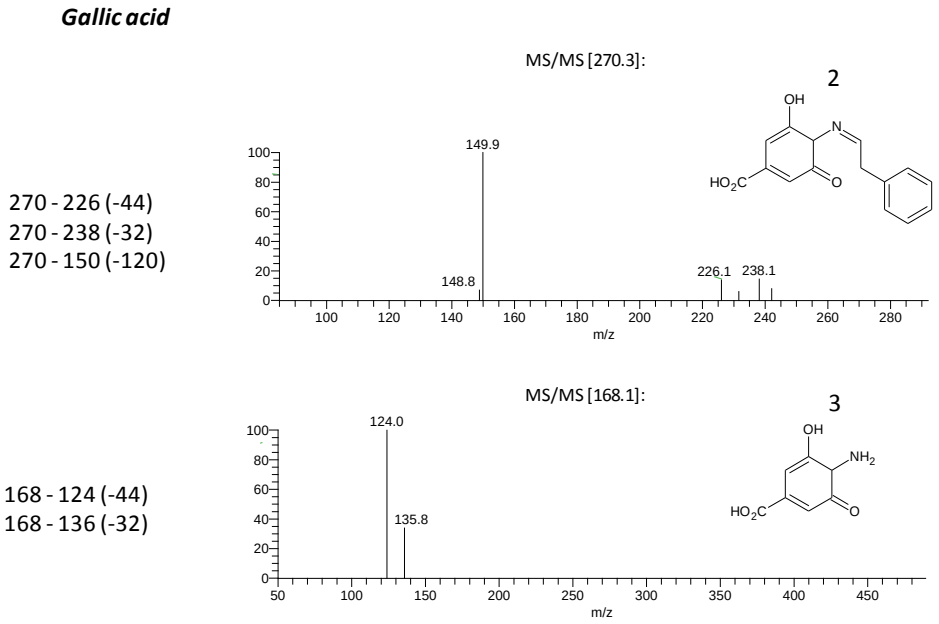

Figure 6.33a. MS/MS fragments occurred for gallic acid quionone products with phenylalanine.

Caffeic acid

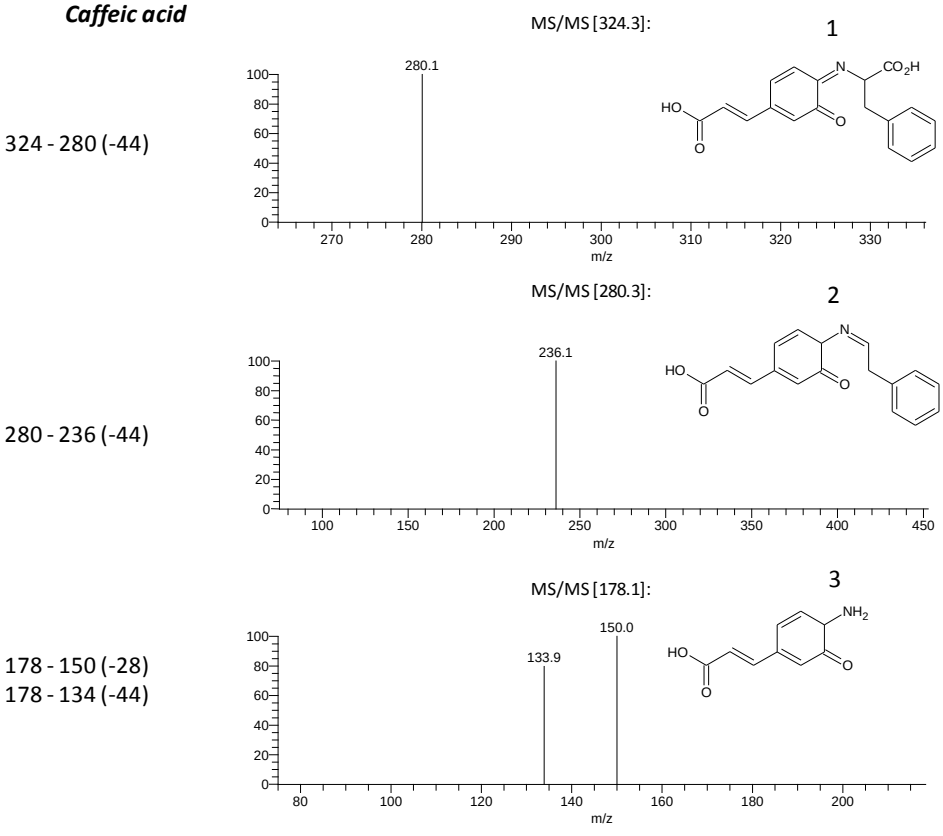

Figure 6.33b. MS/MS fragments occurred for caffeic acid quinone products with phenylalanine.

6.5. Conclusions

White wine amino acid levels (435.1 mg/L) are 4 times higher than the red Port wine (99.6 mg/L). Among the fifteen amino acids analysed, variations higher than the method error, were only observed for glutamic acid, cysteine, asparagine, glutamine, arginine, alanine, methionine, and phenylalanine. All these amino acids have been depleted with temperature and oxygen exposure. Among these, methionine was the amino acid that suffers the faster depletion with oxygen treatment, which can be explained by its conversion to the corresponding sulfoxide and sulfone. These results suggest that amino acids do not have equal reactivity in the same matrix, and the reaction rates, involved on the different mechanisms responsible for their degradation, namely Maillard degradation and oxidation, seem to be dependent on the amino acid nature and concentration. Generally, the higher depletion of amino acids with oxygen treatment could be related with the possible formation of α-dicarbonyl compounds from oxidation reactions, which will react with amino acids by the "Strecker reaction".

White wine has higher levels of "Strecker aldehydes" than the red Port wine. Higher levels of amino acids induce higher levels of these aldehydes.

Even in wines with lower concentration of sugar like the analysed dry white wine with residual reducing sugars (1.6 g/L, for both glucose and fructose), Maillard reaction occurs.

The furanic compounds, 2-furfural, 5-(hydroxymethyl)furfural, and 5-methylfurfural are not affected by oxygen consumption and have higher formation rates in both white and red Port wines. The formation of these compounds is about 10 times higher in the white wine forced aging than the red Port wine forced aging. This fact could be related with the reactivity of these aldehydes with anthocyanins or flavan-3-ols in the red Port wine forced aging protocol. In this study, the red Port wine linked to a rapid and at the same time complete depletion of anthocyanins or flavan-3-ols.

The furanic compounds, 2-acetylfuran, 2-(2-hydroxyacetyl)furan, ethyl 2-furoate, and furfuryl alcohol have similar formation or depletion (furfuryl alcohol) rates in both white and red Port wines forced aging protocols. 2-(2-Hydroxyacetyl)furan seems to be affected by oxygen exposure. Higher values of this compound are found with lower oxygen regimes. This could be related with the possible oxidation of the hydroxyl group with

oxygen exposure. Also, the depletion of furfuryl alcohol is affected by oxygen exposure. This fact could be related with the oxidation of furfuryl alcohol into 2-furfural or other reactions like the addition of hydrogen sulfide to form 2-furfurylthiol.

Sotolon, maltol, and 5-hydroxymaltol were only found in the red Port wine forced aging protocol. Sotolon is clearly related to temperature and to the presence of oxygen. This fact could be explained by the fact that, during oxidative aging, ethanol is converted into acetaldehyde, thus allowing the formation of sotolon. Higher values of maltol and 5-hydroxymaltol are found in experiments with lower oxygen regimes. This could be related with the possible oxidation, of the respectively one and two hydroxyl groups with higher oxygen treatments. Furthermore, 5-hydroxymaltol is highly dependent on temperature regimes.

Degradation pathway of the Amadori product through enolization, can lead to either 3-deoxyosone (3-deoxyglucosone; 3DG) from 1,2-enaminol, and 1-deoxyosone (1-deoxyglucosone; 1DG) or 4-deoxyosone (4-deoxyglucosone; 4DG) from 2,3-enaminol. At lower pH, 1,2-enolization is believed to be favored and therefore a higher yield of 3DG is expected, and therefore higher values of HMF [5-(hydroxymethyl)furfural] or 2-furfural are found. Nevertheless, degradation compounds from Amadori product 2,3-enolization, that are favorable at pH higher than 7, were also found like maltol, 5-hydroxymaltol, 2-acetylfuran, and 2-(2-hydroxyacetyl)furan.

For the same level of amino acids content, higher concentration of sugars induced higher concentration of 3DG, 2-furfural, HMF, and 5-methylfurfural. Furthermore, fructose is the major source of 3DG and these furanic compounds.

The formation of 3DG, in both white and red Pot wines, is not affected by oxygen consumption. For the white wine, 3DG have decreased during the forced aging protocol, while for the red Port wine this compound have increased. The same trend was observed for normal aged wines.

“Strecker aldehydes” can be formed by quinones intermediates at wine pH. Follow by (+)-catechin, gallic acid was the phenolic that had promoted higher levels of phenylacetaldehyde. A similar reaction of that reported by Strecker (1862) to effect decarboxylation/deamination of amino acids is proposed to explain “Strecker aldehydes” formation.

6.6. References

Ames, J. M., Guy, R. C. E., & Kipping, G. J. (2001). Effect of pH, temperature, and moisture on the formation of volatile compounds in glycine/glucose model systems. *Journal of Agricultural and Food Chemistry, 49,* 4315-4323.

Antal, M. J., Mok, W. S. L., & Richards, G. N. (1990). Mechanism of formation of 5-hydroxymethy)-2-furaldehyde from D-fructose and sucrose. *Carbohydrate Research, 199,* 91-109.

Belitz, H.-D., Grosch, W., & Schieberle, P. (2009). Food Chemistry. In 4th revised and extended (Ed.), Springer Verlag Publishers, Berlin Heidelberg.

Blank, I., Lin, J., Fumeaux, R., Welti, D. H., & Fay, L. B. (1996). Formation of 3-Hydroxy-4,5-dimethyl-2(5H)-furanone (Sotolone) from 4-Hydroxy-L-isoleucine and 3-Amino-4,5-dimethyl-3,4-dihydro-2(5H)-furanone. *Journal of Agricultural and Food Chemistry, 44,* 1851-1856.

Câmara, J. S., Marques, J. C., Alves, M. A., & Silva Ferreira, A. C. (2004). 3-Hydroxy-4,5-dimethyl-2(5H)-furanone levels in fortified Madeira wines: relationship to sugar content. *Journal of Agricultural and Food Chemistry, 52,* 6765-6769.

Câmara, J. S., Alves, M. A., & Marques, J. C. (2006). Changes in volatile composition of Madeira wines during their oxidative ageing. *Analytica Chimica Acta 563,* 188-197.

Cerny, C., & Davidek, T. (2003). Formation of aroma compounds from ribose and cysteine during the Maillard reaction. *Journal of Agricultural and Food Chemistry, 51,* 2714-2721.

Chen, Y., & Ho, C. T. (1999). Comparison of volatile generation in serine/threonine/glutamine-ribose/glucose/fructose model systems. *Journal of Agricultural and Food Chemistry,* 47, 643-647.

Cutzach, I., Chatonnet, P., & Dubourdieu, D. (1999). Study of the formation mechanisms of some volatile compounds during the aging of sweet fortified wines. *Journal of Agricultural and Food Chemistry, 47,* 2837-2846.

Davidek, T., Nathalie, C., Aubin, S., & Blank, I. (2002). Degradation of the Amadori compound *N*-(1-Deoxy-d-fructos-1-yl)glycine in aqueous model systems. *Journal of Agricultural and Food Chemistry, 50,* 5472-5479.

De Revel, G., Marchand, S., & Bertrand, A. (2004). Identification of Maillard-Type Aroma Compounds in Wine-like Model Systems of Cysteine-Carbonyls: Occurrence in Wine. *ACS Symposium Series, 871,* 353-364.

Dubois, P., Rigaud, J., & Dekimpe, J. (1976). Identification of 4,5-dimethyltetrahydrofuran-2,3-dione in a Flor sherry wine. *Lebensmittel-Wissenschaft und -Technologie, 9,* 366-368.

Escudero, A., Cacho, J., & Ferreira, V. (2000a). Isolation and identification of odorants generated in wine during its oxidation: a gas chromatography-olfactometry study. *European Food Research and Technology, 211,* 105-110.

Escudero, A., Hernandez-Orte, P., Cacho, J., & Ferreira, V. (2000b). Clues about the role of methional as a character impact odorant of some oxidized wines. *Journal of Agricultural and Food Chemistry, 48,* 4268-4272.

Escudero, A., Asensio, E., Cacho, J., & Ferreira, V. (2002). Sensory and chemical changes of young white wines stored under oxygen. An assessment of the role played by aldehydes and some other important odorants. *Food Chemistry, 77,* 325-331.

Es-Safi, N. E., Cheynier, V., & Moutounet, M. (2000). Study of the reactions between (+)-catechin and furfural derivatives in the presence or absence of anthocyanins and their

implication in food colour change. *Journal of the Science of Food and Agriculture, 48,* 5946-5954.

Es-Safi, N. E., Cheynier, V., & Moutounet, M. (2002). Role of aldehydic derivatives in the condensation of phenolic compounds with emphasis on the sensorial properties of fruit-derived foods. *Journal of Agricultural and Food Chemistry, 50,* 5571-5585.

Ghiron, A. F., Quack, B., Mahinney, T. P., & Feather, M. S. (1988). Studies on the role of 3-deoxy-Derythro-glucosulose (3-glucosone) in nonenzymatic browning. Evidence for involvement in a Strecker degradation. *Journal of Agricultural and Food Chemistry*, 36, 677-680.

Guichard, E., Pham, T. T., & Etievant, P. X. (1993). Quantitative determination of sotolon in wines by high-performance liquid chromatography. *Chromatographia, 37,* 539-542.

Guichard, E., Pham, T. T., & Charpentier, C. (1997). Le sotolon, marqueur de la typicité de l'arome des vins du Jura. *Reviews Oenologie, 82,* 32-34.

Hashiba, H. (1978). Isolation and identification of Amadori compounds from miso, white wine and sake. *Agricultural and Biological Chemistry, 42*, 1727-1731.

Hofmann, T., & Schieberle, P. (1996). Identification of the key odorants in processed ribose-cysteine Maillard mixtures by instrumental analysis and sensory studies. *Special Publication - Royal Society of Chemistry, 197* (Flavour Science), 175-181.

Hofmann, T., & Schieberle, P. (1997). Identification of potent aroma compounds in thermally treated mixtures of glucose/cysteine and rhamnose/cysteine using aroma extract dilution techniques. *Journal of Agricultural and Food Chemistry, 45,* 898-906.

Hofmann, T., Münch, P., & Schieberle, P. (2000). Quantitative model studies on the formation of aroma-active aldehydes and acids by Strecker-type reactions. *Journal of Agricultural and Food Chemistry, 48,* 434-440.

Hofmann, T., & Schieberle, P. (2000). Formation of aroma-active Strecker-aldehydes by a direct oxidative degradation of Amadori compounds. *Journal of Agricultural and Food Chemistry, 48,* 4301-4305.

Huber, B., & Ledl, F. (1990). Formation of 1-amino-1,4-dideoxy-2,3-hexodiulose and 2-aminoacetylfurans in the Maillard reaction. *Carbohydrate Research, 204,* 215-220.

Keim, H., De Revel, G., Marchand, S., & Bertrand, A. (2002). Method for determining nitrogenous heterocycle compounds in wine. *Journal of Agricultural and Food Chemistry, 50,* 5803-5807.

King, H., & Wilken, D. R. (1972). Separation and preliminary studies on 2-ketopantoyl lactone and 2-ketopantoic acid reductases of yeast. *The Journal of Biological Chemistry, 247,* 4096-4098.

Konig, T., Gutsche, B., Hartl, M., Hubscher, R., Schreier, P., & Schwab, W. (1999). 3-Hydroxy-4,5-dimethyl-2(5H)-furanone (sotolon) causing an off-flavor. Elucidation of its formation pathways during storage of citrus soft drinks. *Journal of Agricultural and Food Chemistry, 47,* 3288-3291.

Kroh, L.W. (1994). Caramelisation in food and beverages. *Food Chemistry, 51,* 373-379.

Lee, H. S., & Nagy, S. (1990). Relative reactivities of sugars in the formation of 5-hydroxymethyl furfural in sugar-catalyst model systems. *Journal of Food Processing and Preservation 14,* 171-178.

Lerk, K., & Ambuhl, M. (1995). Biotechnological production of 4,5-diméthyl-3-hydroxy-2(5H)-furanone. in: Bioflavor 95. Analysis-Precursor Studies-Biotechnology; Etiévant, P.; Schreier, P., Eds.; Les Colloques no.75, INRA: Paris, 381-384.

Loscos, N., Hernandez-Orte, P., Cacho, J, & Ferreira V. (2010). Evolution of the aroma composition of wines supplemented with grape flavour precursors from different varietals during accelerated wine ageing. *Food Chemistry, 120,* 205-216.

Maga, J.A. (1979): Furan in foods. *Critical Reviews in Food Science and Nutrition, 11,* 35-400.

Marchand, S, De Revel, G., & Bertrand, A. (2000). Approaches to wine aroma: Release of aroma compounds from reactions between cysteine and carbonyl compounds in wine. *Journal of Agricultural and Food Chemistry, 48,* 4890-4895.

Marchand, S.; De Revel, G., & Bertrand, A. (2002). Possible mechanism for involvement of cysteine in aroma production in wine. *Journal of Agricultural and Food Chemistry, 50,* 6160-6164.

Marchand, S., Almy, J., & De Revel, G. (2011). The cysteine reaction with diacetyl under wine-like conditions: proposed mechanisms for mixed origins of 2-methylthiazole, 2-methyl-3-thiazoline, 2-methylthiazolidine, and 2,4,5-trimethyloxazole. *Journal of Food Science, 76,* C861-8.

Martin B., & Etievant, P. X. (1991). Quantitative determination of solerone and Sotolon in Flor Sherries by Two-Dimensional-Capillary GC. *Journal of High Resolution Chromatography & Chromatography Communications, 14,* 133-135.

Martin, B., Etiévant, P. X., Le Quéré, J. L., & Schlich, P. (1992). More clues about the sensory impact of Sotolon in flor sherry wines. *Journal of Agricultural and Food Chemistry, 40,* 475-478.

Martins, R. C., Monforte, A. R., & Silva Ferreira, A. C. (2013). Port wine oxidation management: a multiparametric kinetic approach. *Journal of Agricultural and Food Chemistry, 61,* 5371-5379.

Masuda, M., Okawa, E., Nishimura, K., & Yunome, H. (1984). Identification of 4,5-dimethyl-3-Hydroxy-2(5H)-furanone (Sotolon) and ethyl 9-hydroxynonanoate in Botrytised wine and evaluation of the roles of compounds characteristic. *Agricultural and Biological Chemistry, 48,* 2707-2710.

Moreno, J. A., Zea, L., Moyano, L., & Medina, M. (2005). Aroma compounds as markers of the changes in sherry wines subjected to biological ageing. *Food Control, 16,* 333-338.

Nikolantonaki, M., & Waterhouse, A. L. (2012). A Method to quantify quinone reaction rates with wine relevant nucleophiles: A key to the understanding of oxidative loss of varietal thiols. *Journal of Agricultural and Food Chemistry, 60,* 8484-8491.

Niquet, C., & Tessier, F. J. (2007). Free glutamine as a major precursor of brown products and fluorophores in Maillard reaction systems. *Amino Acids, 33,* 165-171.

Oliveira e Silva, H., Guedes de Pinho, P., Machado, B., Hogg, T., Marques, J. C., Câmara, J. S., Albuquerque, F., & Silva Ferreira, A. C. (2008). Impact of forced-aging process on Madeira wine flavour. *Journal of Agricultural and Food Chemistry, 56,* 11989-11996.

Perez, L. C., & Yaylayan, V. A. (2004). Origin and mechanistic pathways of formation of the parent furan - A food toxicant. *Journal of Agricultural and Food Chemistry, 52,* 6830-6836.

Pham, T. T., Guichard, E., Schlich, P., & Charpentier, C. (1995). Optimal conditions for the formation of sotolon from α-ketobutyric acid in the french "Vin Jaune". *Journal of Agricultural and Food Chemistry, 43,* 2616-2619.

Pons, A., Lavigne, V., Landais, Y., Darriet, P., & Dubourdieu, D. (2010). Identification of a sotolon pathway in dry white wines. *Journal of Agricultural and Food Chemistry, 58,* 7273-7279.

Pripis-Nicolau, L., Revel, G., Bertrand, A., & Maujean, A. (2000). Formation of flavor components by the reaction of amino acid and carbonyl compounds in mild conditions. *Journal of Agricultural and Food Chemistry, 48,* 3761-3766.

Radler, F. (1993). Yeasts - metabolism of organic acids. In G. H. Fleet (Ed.), Wine Microbiology and Biotechnology: Harwood Academic Publishers, Singapore.

Rapp, A., & Guntert, M. (1986). Charalambous G (Ed.). The shelf life of foods and beverages. Elsevier, Amsterdam, 141-165.

Rizzi, G. P. (2006). Formation of strecker aldehydes from polyphenol-derived quinones and α-amino acids in a nonenzymic model system. *Journal of Agricultural and Food Chemistry*, *54*, 1893-1897.

Rizzi, G. P. (2008). The strecker degradation of amino acids: Newer avenues for flavor formation. *Food Reviews International, 24,* 416-435.

Schirlekeller, J. P., & Reineccius, G. A. (1992). Reaction-kinetics for the formation of oxygen-containing heterocyclic-compounds in model systems. *ACS Symposium Series, 490,* 244-258.

Shaw, P. E., Tatum, J. H., Berry, R. E. (1971). 2,3-dihydro-3,5-dihydroxy-6-methyl-4H-pyran-4-one, a degradation product of a hexose. *Carbohydrate Research, 16,* 207-211.

Shneider, R., Baumes, R., Bayonove, C., & Razungles, A. (1998). Volatiles compounds involved in the aroma of sweet fortified wines (vins doux naturels) from Grenache Noir. *Journal of Agricultural and Food Chemistry, 46,* 3230-3237.

Shonberg, A., & Moubacher, R. (1952). The Strecker degradation of α-amino acids. *Chemical Reviews, 50,* 261-277.

Silva Ferreira, A. C., Guedes de Pinho, P., Rodrigues, P., & Hogg, T. (2002). Kinetics of oxidative degradation of white wines and how they are affected by selected technological parameters. *Journal of Agricultural and Food Chemistry, 50,* 5919-5924.

Silva Ferreira, A. C., Barbe, J. C., & Bertrand, A. (2003). 3-Hydroxy-4,5-dimethyl-2(5H)-furanone: a key odorant of the typical aroma of oxidative aged Port wine. *Journal of Agricultural and Food Chemistry, 51,* 4356-4363.

Silva Ferreira, A. C., Avila, I. M. L. B., Guedes de Pinho, P. (2005). Sensorial Impact of Sotolon as the "Perceived Age" of Aged Port Wine. *Natural Flavors and Fragrances, 10,* 141-159.

Silva Ferreira, A. C., Reis, S., Rodrigues, C., Oliveira, C., & Guedes de Pinho, P. (2007). Simultaneous determination of ketoacids and dicarbonyl compounds, key Maillard intermediates on the generation of aged wine aroma. *Journal of Food Science, 72 (5),* S314-S318.

Sousa, A., Mateus, N., Silva, A. M. S., Vivas, N., Nonier, M. F., Pianet, I., et al. (2010). Isolation and structural characterization of anthocyanin-furfuryl pigments. *Journal of the Science of Food and Agriculture, 58,* 5664-5669.

Sulser, H., Depizzol, J., & Buchi, W. (1967). A probable flavoring principle in vegetable-protein hydrolysates. *Trends in Food Science, 32,* 611-615.

Tominaga, T., Guimbertau, G., & Dubourdieu, D. (2003). Role of certain volatile thiols in the bouquet of aged champagne wines. *Journal of Agricultural and Food Chemistry, 51,* 1016-1020.

Tressl, R., Kersten, E., & Rewicki, D. (1993). Formation of 4-aminobutyric acid-specific Maillard products from 1-C-13-D-glucose, 1-C-13-D-arabinose, and 1-C-13-D-fructose. *Journal of Agricultural and Food Chemistry, 41,* 2278-2285.

Tressl, R., Nittka, C., & Kersten, E. (1995). Formation of isoleucine-specific Maillard products from [1-^{13}C]-D-glucose and [1-^{13}C]-D-fructose. *Journal of Agricultural and Food Chemistry, 43,* 1163-1169.

Vernin, G., & Parkanyi, C. (1982). Mechanisms of formation of heterocyclic compounds in Maillard and pyrolysis reactions. Chemistry of Heterocyclic Aroma Compounds in Flavours and Aromas; Vernin, G. (Ed). Ellis Horwood, Chichester, U.K., Chapter 3, 151-207.

Vivas, N., Bourden Nonier, M. F., Absalon, C., Lizama Abad, V., Jamet, F., Vivas de Gaulejac, N., Vitry, C. & Fouquet, É. (2008). Formation of flavanol-aldehyde adducts in barrel-aged white wine - possible contribution of these products to colour. *South African Journal of Enology & Viticulture,* 29, 98-108.

Wang, Yu, & Ho, Chi-Tang. (2008). Comparison of 2-acetylfuran formation between ribose and glucose in the Maillard reaction. *Journal of Agricultural and Food Chemistry,* 56, 11997-12001.

Wang, Yu (2009). Roles of reactve carbonyl species in health and flavor generation. A PhD Dissertation submitted to the Graduate School–New Brunswick Rutgers, The State University of New Jersey.

Webb, A. D., Kepner, R. E., & Maggiora, L. (1967). Sherry aroma. VI. Some volatile components of flor sherry of spanish origin. Neutral substances. *American Journal of Enology and Viticulture, 18,* 190-199.

Wildenradt, H. L., & Singleton, V. L. (1974). The production of aldehydes as a result of oxidation of polyphenolic compounds and its relation to wine aging. *American Journal of Enology and Viticulture, 25,* 119-126.

Wnorowski, A., & Yaylayan, V. A. (2000). Influence of pyrolytic and aqueous-phase reactions on the mechanism of formation of Maillard products. *Journal of Agricultural and Food Chemistry, 48,* 3549-3554.

Yaylayan, V. A., & Mandeville, S. (1994). Stereochemical control of maltol formation in Maillard reaction. *Journal of Agricultural and Food Chemistry*, *42*, 771-775.

Yaylayan, V. A., & Keyhani, A. (2000). Origin of carbohydrate degradation products in L-alanine/D-C-13 glucose model systems. *Journal of Agricultural and Food Chemistry, 48,* 2415-2419.

Yaylayan, V.A. (2006). Precursors, formation and determination of furan in food. *Journal für Verbraucherschutz und Lebensmittelsicherheit, 1,* 5-9.

Yeo, H., & Shibamoto, T. (1991). Effects of moisture content on the maillard browning model system upon microwave irradiation. *Journal of Agricultural and Food Chemistry*. *39,* 1860-1862.

7. Chapter 7 - Conclusions and future work

7.1. Conclusions

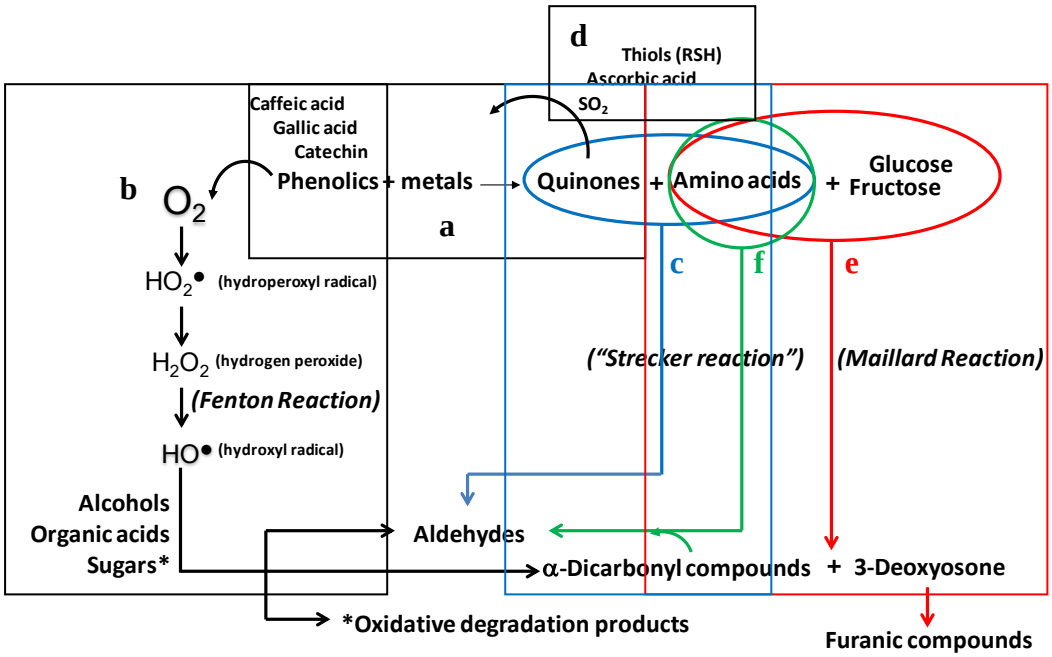

Figure 7.1. Pathways of different interaction reactions of color/flavor compounds.

The production of color/flavor compounds in wine is the result of different interrelated mechanism reactions. Among these, the oxidation phenomenon and the Maillard reaction stands out with particular relevance due to their large impact on the sensory quality of wines and consequently on the product shelf-life. For this reason, the mechanisms explaining the key color/flavor formation through temperature and oxygen are of main importance. Results clearly demonstrate a "convolution" of chemical mechanisms. The presence of oxygen combined with temperature had a synergistic effect on the formation of several key odorant compounds like sotolon, in red Port wines or phenylacetaldehyde and methional, in white wine.

Although phenolics are recognized to be related with health benefits by limiting lipid oxidation, in wine, they are the primary substrates for oxidation resulting in the by-products quinones with the participation of transition metal ions (Figure 7.1a). In this way, oxygen is progressively depleted and becomes unavailable to oxidize other wine compounds (Figure 7.1b). On the other hand, in this process, phenolics oxidation generates

hydrogen peroxide and the hydroxyl radical (Figure 7.1b) that undergoes further oxidation reactions with major wine compounds like alcohols, organic acids or sugars (Figure 7.1b).

Cyclic voltammetry was used to access the "degradation status" of wines based on their electroactive phenolic oxidation. Cyclic voltammograms of the white wine had two main anodic peak potentials Ep,a (0.45 and 0.85 V), while cyclic voltammograms of the red Port wine had three main peak potentials Ep,a (0.35, 0.55 and 0.75 V). The most relevant white wine phenolic oxidation markers were *trans*-GRP, *trans*- and *cis*-caftaric acid, and catechin-type flavonoids [(+)-catechin and (-)-epicatechin], which had the highest decreases during the thermal and oxidative white wine process. Considering red Port wine, the most relevant phenolic oxidation markers were anthocyanins and catechin-type flavonoids, which had the highest decreases during the thermal and oxidative red Port wine process. Both temperature and oxygen treatments affected the rate of phenolic degradation. In addition, temperature seems to affect mostly the phenolics kinetic degradation. In this way, the previous identified phenolics could be used as oxidation markers, and their modulation may well be used for the optimization of wine processing and/or storage conditions.

A nucleophilicity scale, promoted by cyclic voltammetry, related to the reaction of quinones with amino acids (Figure 7.1c), thiols (Figure 7.1d), ascorbic acid (Figure 7.1d) and sulfur dioxide (Figure 7.1d) was attempted. Concerning thiols, 4-methyl-4-sulfanylpentan-2-one was more reactive with quinones than 3-sulfanylhexan-1-ol, but the highest reactivity was attributed to furan-2-ylmethanethiol. Sulfur dioxide and ascorbic acid had higher and similar reactivity with quinones. Concerning amino acids, results have showed that these class of nucleophiles had the lowest reactivity toward quinones. Nevertheless, this observation suggested that an interaction of wine phenolic compounds, in the oxidized form of quinones, with Maillard reaction (Figure 7.1e) could occur. In fact, quinones acted as "Strecker degradation" (SD) reagents (Figure 7.1f). In a wine-model solution, gallic acid, caffeic acid, and (+)-catechin quinones had promoted higher levels of phenylacetaldehyde, in the presence of phenylalanine (Figure 7.1f). A similar reaction of that reported by Strecker (1862) to affect decarboxylation/deamination of amino acids is proposed in this thesis to explain these "Strecker aldehydes" formation. This mechanism has been described for the first time at wine conditions.

Amino acids do not have equal reactivity in wine matrix, and the reaction rates, involved on the different mechanism responsible for their degradation, namely Maillard degradation and oxidation, seem to be dependent on the amino acid nature and its concentration. Generally, the higher observed depletion of amino acids with oxygen treatment could be related with the formation of α-dicarbonyl compounds from oxidation reactions (Figure 7.1b), which will react with amino acids in the "Strecker reaction" (Figure 7.1f) to give "Strecker aldehydes".

In Maillard reaction (Figure 7.1e), at wine pH, 1,2-enolization is believed to be favored and therefore a higher yield of 3DG (Figure 7.1e) is expected. For this reason, higher values of the furanic compounds, HMF [5-(hydroxymethyl)furfural] and 2-furfural were found. Nevertheless, degradation compounds from Amadori product 2,3-enolization, that are favorable at pH higher than 7, were also found, like maltol, 5-hydroxymaltol, 2-acetylfuran, and 2-(2-hydroxyacetyl)furan. For the same level of amino acids content, higher concentration of sugars induced higher concentration of 3DG and furanic compounds (HMF, 2-furfural, and 5-methylfurfural). Furthermore, fructose was found to be the major source for 3DG and these furanic compounds in wines. In this thesis, and for the first time, an attempt to quantified 3DG in dry white wines and red Port wines has been made. 3DG quantification was conducted in the forced aging wines, and in natural aging wines. For the white wine, 3DG have decreased during the forced aging protocol, while for the red Port wine this compound have increased. The same trend was observed for normal aged wines. We can hypothesize that the 3DG accumulation in red Port wine is due to its higher sugar concentration and also to a lower nucleophilic compounds available in this wine, which could be related with the lower amino acids content, 99.6 mg/L in contrast with the 435.1 mg/L in the white wine.

The results of this work could be translated to the wine-making and wine-storage environment from the modelling of the analysed compounds. The temperature and oxygen conditions could be calculated and the rate and the extent of each reaction could be used to model them.

7.2. Future work

1. The annotation and identification of interesting compounds accounting for white wine and red Port wine metabolic variability, by the analysis of the non-target GC/MS approach.
2. The kinetic modeling of relevant oxidation compounds in white wine similar to that found for anthocyanins in red Port wine.
3. The application of cyclic voltammetry for the study of more polyphenols with wine antioxidants and other nucleophilic compounds that could react with quinones.
4. The NMR characterization of "Strecker degradation products".

8. Appendix

8.1. Data

Data in appendix for **Figure 5.26**. Phenolics formation or depletion during the forced aging protocols in white wines. I - no oxygen addition; II - oxygen addition.

White wine (mg/L/day)	Treatment I				Treatment II			
	20ºC	**30ºC**	**40ºC**	**50ºC**	**20ºC**	**30ºC**	**40ºC**	**50ºC**
trans-GRP	-0.0045	-0.0337	-0.0272	-0.0365	-0.0070	-0.0456	-0.0428	-0.0620
cis-caftaric acid	-0.0087	-0.0191	-0.0241	-0.0355	-0.0116	-0.0183	-0.0261	-0.0440
trans-caftaric acid	-0.0033	-0.0308	-0.0286	-0.0465	-0.0155	-0.0313	-0.0325	-0.0587
cis-coutaric acid	-0.0021	-0.0045	-0.0044	-0.0064	-0.0035	-0.0048	-0.0042	-0.0165
trans-coutaric acid	-0.0168	-0.0165	-0.0158	-0.0184	-0.0136	-0.0109	-0.0152	-0.0233
trans-fertaric	-0.0157	-0.0183	-0.0134	-0.0194	-0.0127	-0.0083	-0.0136	-0.0325
caffeic acid	0.0136	0.0205	0.0303	0.0402	0.0091	0.0199	0.0304	0.0413
para-coumaric acid	0.0003	0.0028	0.0042	0.0100	0.0048	0.0034	0.0062	0.0087
ferulic acid	-0.0014	-0.0021	-0.0040	-0.0042	-0.0017	-0.0049	-0.0062	-0.0055
gallic acid	-0.0091	-0.0108	-0.0143	-0.0210	-0.0148	-0.0202	-0.0206	-0.0240
protocatechuic acid	-0.0047	-0.0080	-0.0119	-0.0128	-0.0096	-0.0091	-0.0100	-0.0150
(+)-catechin	-0.0575	-0.0738	-0.0693	-0.1049	-0.0689	-0.0802	-0.0906	-0.1511
(-)-epicatechin	-0.0126	-0.0202	-0.0245	-0.0306	-0.0217	-0.0241	-0.0306	-0.0423

Data in appendix for **Figure 5.27**. Phenolics formation or depletion during the forced aging protocols in red Port wines. I - no oxygen addition; II - oxygen addition.

Red Port wine (mg/L/day)	Treatment I				Treatment II			
	20ºC	**30ºC**	**35ºC**	**40ºC**	**20ºC**	**30ºC**	**35ºC**	**40ºC**
trans-caftaric acid	-0.0669	-0.1021	-0.1170	-0.1839	-0.0695	-0.1078	-0.1204	-0.1723
trans-coutaric acid	-0.0276	-0.0484	-0.0819	-0.0926	-0.0357	-0.0487	-0.0711	-0.1102
trans-fertaric	-0.0035	-0.0022	-0.0034	-0.0160	-0.0071	-0.0072	-0.0083	-0.0202
caffeic acid	0.0028	0.0054	0.0070	0.0099	0.0018	0.0048	0.0070	0.0106
para-coumaric acid	0.0017	0.0023	0.0025	0.0023	0.0033	0.0045	0.0044	0.0046
ferulic acid	-0.0017	-0.0018	-0.0024	-0.0029	-0.0015	-0.0019	-0.0026	-0.0029
gallic acid	0.0197	0.0261	0.0441	0.0722	0.0433	0.0452	0.0570	0.0736
protocatechuic acid	0.0011	0.0039	0.0073	0.0081	0.0010	0.0030	0.0057	0.0083
syringic acid	0.0443	0.0649	0.0772	0.1125	0.0386	0.0639	0.0732	0.1229
(+)-catechin	-0.1156	-0.1252	-0.1447	-0.1453	-0.1185	-0.1500	-0.1542	-0.1578
(-)-epicatechin	-0.0565	-0.0666	-0.0862	-0.1042	-0.0564	-0.0788	-0.0932	-0.1115

Data in appendix for **Figure 6.3**. Amino acids content of both white and red Port untreated wines (P0).

Amino acids content (mg/L)	White wine	Red Port wine
Asp	28.7 ± 2.1	4.9 ± 0.2
Glu	55.8 ± 4.1	24.1 ± 0.1
Cys	2.4 ± 0.1	1.2 ± 0.1
Asn	7.8 ± 0.2	5.6 ± 0.2
Ser	41.7 ± 3.0	14.5 ± 0.1
Gln	nd	4.3 ± 0.1
Thr	9.1 ± 0.2	2.9 ± 01
Arg	165.0 ± 5.2	14.3 ± 0.1
Ala	47.0 ± 3.2	12.0 ± 0.5
Tyr	13.9 ± 0.6	2.8 ± 0.1
Val	12.6 ± 0.2	1.9 ± 0.2
Met	4.3 ± 0.2	0.9 ± 0.1
Phe	18.6 ± 0.3	4.4 ± 0.1
Ile	6.8 ± 0.3	1.9 ± 0.1
Leu	21.4 ± 2.1	3.9 ± 0.1
Total	***435.1***	***99.6***

Data in appendix for **Figure 6.4**. Amino acids depletion during the forced aging protocols in white wines (mg/L/day). I - no oxygen addition; II - oxygen addition.

	Treatment I				**Treatment II**			
White wine (mg/L/day)	**20ºC**	**30ºC**	**40ºC**	**50ºC**	**20ºC**	**30ºC**	**40ºC**	**50ºC**
Glutamic acid	-0.4243	-0.4897	-0.4685	-0.5446	-0.4437	-0.4114	-0.4791	-0.6809
Cysteine	-0.0119	-0.0152	-0.0153	-0.0185	-0.0192	-0.0155	-0.0158	-0.0199
Asparagine	-0.0232	-0.0233	-0.0341	-0.0470	-0.0221	-0.0309	-0.0404	-0.0467
Arginine	-0.8917	-1.0973	-0.8721	-1.5977	-1.0076	-1.2745	-1.7911	-1.7587
Alanine	-0.2893	-0.2529	-0.2430	-0.2559	-0.3344	-0.2703	-0.2715	-0.3449
Methionine	-0.0183	-0.0206	-0.0136	-0.0289	-0.0198	-0.0276	-0.0270	-0.0428
Phenylalanine	-0.1133	-0.0887	-0.0778	-0.0953	-0.0997	-0.1076	-0.0974	-0.0987

Data in appendix for **Figure 6.5**. Amino acids depletion during the forced aging protocols in red Port wines (mg/L/day). I - no oxygen addition; II - oxygen addition.

	Treatment I				**Treatment II**			
Red Port wine (mg/L/day)	**20ºC**	**30ºC**	**35ºC**	**40ºC**	**20ºC**	**30ºC**	**35ºC**	**40ºC**
Glutamic acid	-0.0303	-0.0401	-0.0690	-0.0696	-0.0533	-0.0544	-0.0760	-0.0798
Cysteine	-0.0029	-0.0043	-0.0063	-0.0135	-0.0071	-0.0050	-0.0131	-0.0168
Asparagine	-0.0162	-0.0167	-0.0172	-0.0175	-0.0058	-0.0132	-0.0135	-0.0194
Glutamine	-0.0333	-0.0641	-0.0613	-0.0659	-0.0412	-0.1162	-0.1386	-0.1397
Methionine	-0.0003	-0.0036	-0.0021	-0.0071	-0.0080	-0.0145	-0.0144	-0.0148
Phenylalanine	-0.0137	-0.0086	-0.0097	-0.0141	-0.0134	-0.0140	-0.0168	-0.0154

Data in appendix for **Figure 6.12**. Amino acids content of the applied wine-model system.

Amino acids content (mg/L)	**100**	**400**
Asp	5.4	31.8
Glu	25.0	50.5
Cys	3.1	6.5
Asn	5.1	8.2
Ser	15.0	50.3
Gln	5.2	7.8
Thr	3.2	10.6
Arg	16.0	150.8
Ala	16.9	40.9
Tyr	3.0	15.3
Val	2.2	15.2
Met	1.3	5.2
Phe	5.2	19.8
Ile	2.5	8.3
Leu	4.0	25.1
Total	**113.1**	**446.3**

Data in appendix for **Figure 6.13**. 3DG quantification in a wine-model system.

Wine-model system	
35 days at 40ºC	**3DG (mg/L)**
(ia) Glucose 50 g/L + 100 mg/L aa	nd
(ib) Fructose 50 g/L + 100 mg/L aa	16.7 ± 0.7
(ic) Glucose 2 g/L + 100 mg/L aa	nd
(id) Fructose 2 g/L + 100 mg/L aa	1.4 ± 0.0
(iia) Glucose 50 g/L + 400 mg/L aa	2.2 ± 0.0
(iib) Fructose 50 g/L + 400 mg/L aa	16.7 ± 0.7
(iic) Glucose 2 g/L + 400 mg/L aa	nd
(iid) Fructose 2 g/L + 400 mg/L aa	1.3 ± 0.0

Data in appendix for **Figure 6.14**. Furan derivatives formation or depletion (furfuryl alcohol) during the forced aging protocol of white wines. I - no oxygen addition; II - oxygen addition.

White wine	**Treatment I**				**Treatment II**			
	20ºC	**30ºC**	**40ºC**	**50ºC**	**20ºC**	**30ºC**	**40ºC**	**50ºC**
2-furfural *	0.0013	0.0344	0.0561	0.1461	0.0009	0.0329	0.0588	0.1434
5-(hydroxymethyl)furfural *	0.0410	0.2641	0.3972	1.0792	0.0372	0.3158	0.4401	1.1146
5-methylfurfural **	0.0842	0.6895	1.1882	1.4057	0.0408	0.6421	1.0748	1.3281
2-acetylfuran **	0.0345	0.1040	0.1710	0.7400	0.0538	0.1087	0.2130	0.7152
2-(2-hydroxyacetyl)furan **	0.6450	0.5160	0.7702	0.5184	0.5430	0.3593	0.5206	0.1849
ethyl 2-furoate **	0.0190	0.1029	0.1766	0.4105	0.0127	0.0971	0.1504	0.3673
furfuryl alcohol **	-0.1334	-0.3857	-0.4927	-0.5899	-0.0335	-0.4287	-0.5212	-0.6229

Data in appendix for **Figure 6.15**. Furan derivatives formation or depletion (furfuryl alcohol) during the forced aging protocol of red Port wines. I - no oxygen addition; II - oxygen addition.

Red Port wine	**Treatment I**				**Treatment II**			
	20ºC	**30ºC**	**35ºC**	**40ºC**	**20ºC**	**30ºC**	**35ºC**	**40ºC**
2-furfural *	0.0004	0.0012	0.0020	0.0037	0.0004	0.0010	0.0018	0.0037
5-(hydroxymethyl)furfural *	0.0110	0.0174	0.0277	0.0520	0.0084	0.0125	0.0290	0.0495
5-methylfurfural **	0.0250	0.0495	0.0900	0.1707	0.0206	0.0605	0.0840	0.1774
2-acetylfuran **	0.0216	0.0846	0.1252	0.2137	0.0244	0.0827	0.1309	0.1890
2-(2-hydroxyacetyl)furan **	0.1832	0.4871	0.8030	0.9605	0.2057	0.4683	0.7749	0.9115
ethyl 2-furoate **	0.0276	0.0197	0.0477	0.0593	0.0186	0.0276	0.0365	0.0607
furfuryl alcohol **	-0.0968	-0.1093	-0.1223	-0.1412	-0.1048	-0.1400	-0.1677	-0.1890

(mg/L/day)*; (µg/L/day)**

Data in appendix for **Figure 6.20**. 2-Furfural, HMF, and 5-methylfurfural quantification in a wine-model system.

Wine-model system	Concentration (µg/L)		
35 days at 40ºC	2-Furfural	HMF	5- Methyl-2-furfural
(ia) Glucose 50 g/L + 100 mg/L aa	39.9 ± 2.8	129.2 ± 11.7	nd
(ib) Fructose 50 g/L + 100 mg/L aa	391.7 ± 26.9	2108 ± 52.4	2.87 ± 0.7
(ic) Glucose 2 g/L + 100 mg/L aa	3.5 ± 0.4	6.2 ± 2.3	nd
(id) Fructose 2 g/L + 100 mg/L aa	19.1 ± 0.9	168.7 ± 2.8	nd
(iia) Glucose 50 g/L + 400 mg/L aa	54.9 ± 6.7	280.4 ± 15.1	nd
(iib) Fructose 50 g/L + 400 mg/L aa	330.7 ± 27.7	2420 ± 55.9	3.23 ± 0.7
(iic) Glucose 2 g/L + 400 mg/L aa	3.0 ± 0.1	13.9 ± 1.7	nd
(iid) Fructose 2 g/L + 400 mg/L aa	23.4 ± 6.7	118.3 ± 8.7	nd

8.2. Expressions

The regression equation (Y = ax + b) was calculated by the follow equations:

a - slope; b - y - intercept; Sa - standard deviation of the slope; Sb - standard deviation of the y -intercept; r - coefficient of correlation; Sy/x - instrumental signal values dispersion around calibration curve.

$$a = \frac{\sum_i \left[(x_i - \bar{x})(y_i - \bar{y}) \right]}{\sum_i (x_i - \bar{x})^2}$$

$$b = \bar{y} - a\bar{x}$$

$$sa = \frac{s_{y/x}}{\sqrt{\sum_i (x_i - \bar{x})^2}}$$

$$sb = s_{y/x} \sqrt{\frac{\sum_i x_i^{\,2}}{n \sum_i (x_i - \bar{x})^2}}$$

$$r = \frac{\sum_i \left[(x_i - \bar{x})(y_i - \bar{y}) \right]}{\sqrt{[\sum_i (x_i - \bar{x})^2][\sum_i (y_i - \bar{y})^2]}}$$

$$S_{y/x} = \sqrt{\frac{\sum_{i=1}^{N} [y_i - (ax_i + b)]^2}{n-2}}$$

Kinetic of compound depletion:

zero order [$c = c_0 + kt$]

first order [$c = c_0 e^{(kt)}$]

second order [$1/c = 1/c_0 + kt$]

c - concentration

c_0 - initial concentration

k - rate constant

t - time

Rate expression for oxygen consumption: $r = -d[DO]/dt = k[A][DO]$

DO - dissolved oxygen

t - time

A - oxidizable matter

k - rate constant

$[DO]t = [DO]_0 e^{(-Kox\ t)}$

DO - dissolved oxygen

t - time

K_{ox} - oxidation rate constant

Arrhenius equation: $k = k_0 e^{-Ea/RT}$

k - rate constant

k_0 - pre-exponential factor

E_a - activation energy

R - gas constant equal to 8.314 J/mol.K

T - temperatute

$\ln(K_{ox}) = \ln(k_0) - E_a/RT$

ln - natural logarithm

K_{ox} - oxidation rate constant

k_0 - pre-exponential factor

E_a - activation energy

R - gas constant equal to 8.314 J/mol·K

T - temperatute